The University Of Sheffield.

Rapid assessment method to predict the failure modes of laminated bamboo composites

by

Olivia Espinosa Trujillo

Submitted to the School of Architecture
in partial fulfilment of the requirements for the degree of
Doctor of Philosophy in Architecture

The University of Sheffield
Faculty of Social Science

February 2022

A thesis supervised by:

Dr. Wen-Shao Chang	- Senior Lecturer in Architectural Structure
Dr. Hassan Ghadbeigi	- Senior Lecturer in Mechanical Engineering
Prof. Fionn Stevenson	- Professor of Sustainable Design

Acknowledgements |

I am grateful for the people that walked with me these years and helped me complete this project. In no particular order, I would like to thank:

Ana Lamy | Patito Esquivel Soto | José Luis Amury | Magda | Dr. Wen-Shao Chang | Luke Jones | Louis Chen | Sofia González Games | Cathryn Klasto | Don Jenkins | Stuart Moran | Sini Klasto | Prof. Yu-Lin Chun | Richard Kay | Faith Ng'eno | Dr. Tsung-Hsien Wang | Prof. Fionn Stevenson | Itzel San Román Pineda | Alfredo Sánchez Andalco | The Hoyland family | Nourhan Eid | Dr. Hassan Ghadbeigi | Niveen & Omar | Mahsa Mohajer | Angélica Álvarez Quiñones | Meng Le Zhang | Andira Hernández Monzoy | Diana Bolaina Trujillo | Saydi | Esra Can | Ana Méndez |

Finally, special thanks to my beautiful family, Maria, Antonio, Natalia & Leo.

To complete this project, I was funded by the National Council of Science and Technology (CONACyT, Mexican government agency) and the Council of Science and Technology of the State of Queretaro (CONCyTEQ).

Abstract |

Laminated bamboo is a promising material with mechanical properties comparable to structural timber. The lack of technologies available to assess its structural integrity limits the use of laminated bamboo as a reliable building material. Modelling failure is of specific importance to guarantee the structural preservation of any material. Currently, no methods are developed to assess the deformation and failure of laminated bamboo rapidly. Attempts have been made at modelling the mechanical behaviour of laminated bamboo using numerical methods. However, these methods require a considerable number of computational resources and time. Moreover, they do not acknowledge how the cellular structure of bamboo strips affects the material's behaviour. The use of geometric methods can help overcome these limitations. The present study focuses on developing a geometric-based method to assess and predict laminated bamboo composites' failure rapidly. A series of tensile, compressive and shear experiments were carried out on small-sized pieces to achieve this objective. The original configuration of the specimens, as well as their deformation and failure, were recorded with a High-Resolution Camera. Simultaneously, deformation fields were determined using Digital Image Correlation. The experiments suggest that the distribution of bamboo fibres and their geometric arrangement are the features that will determine the failure mechanisms of the composites. As such, a series of geometric relationships and algorithms were developed to predict the deformation and failure of laminated bamboo by acknowledging the physical features of the pieces before loading. The primary input of the algorithms is a picture of the un-deformed specimens where the areas with fewer bamboo fibres are highlighted. Then, an array of points is used to describe the original and deformed states of the pieces. Finally, a tracking algorithm determines the most likely fracture geometry. The mathematical parameters that define the displacement of points and the fracture geometry are based on a geometric analysis of the findings of the experimental program. The study results suggest that the proposed methodology does approximate the actual behaviour of laminated bamboo. Moreover, it strongly suggests that the application of geometric methods is a novel approach that could signal new avenues to understand and predict the behaviour of laminated bamboo as a structural element.

Table of contents |

List of Figures |

List of Tables |

Chapter 1 | Introduction

| This chapter introduces the topic of research. In the first section, the need to promote alternative structural materials is discussed. In the second part, the advantages, and disadvantages of using laminated bamboo as a construction material are analysed. In the third section, the need to develop reliable methods to predict the mechanical response of structural materials is outlined. The fourth section describes the statement of the problem. The research question, aim and objectives are stated in section five. Finally, the sixth section lists the reason why the research is relevant. Lastly, section seven provides an overview of the thesis structure. |

1.1 Alternative structural materials

There is an increasing need in the building industry to embrace the use of structural materials with lower environmental impact. In this regard, various practitioners – such as architects and engineers, believe that it is essential to challenge the status quo of the modern building industry by pushing the structural limits of non-conventional materials (Schuler, 2016). Most importantly, Harries, Sharma, and Richard (2012) and Broto (2015) believe that there is an increasing need for architects and engineers to re-consider locally available resources as viable building materials.

Bamboo is a widely available natural resource with excellent mechanical properties. From small to mid-sized buildings, bamboo culms have been successfully used for a long time - predominantly in the tropics, where it is vastly available (Escamilla et al., 2019). However, every bamboo pole is different in terms of shape and mechanical performance. Such irregularities make building with bamboo a challenge. The successful use of bamboo as a reliable structural material requires a deep understanding of the material as well as the development of technologies to cope with its natural indeterminacy. Several authors agree that if bamboo is to be used as a reliable building material for large-scale projects, it is essential to foster the development of strategies to standardise its use (Janssen, 2005, Harries, Sharma, and Richard, 2012). In this regard, Sharma et al. (2014) argue that engineering bamboo into laminated composites is a technology that can help reduce the physical and mechanical variability of natural bamboo.

1.2 Laminated bamboo as a construction material

Laminated bamboo is a manufactured composite made with bamboo strips glued together using different types of adhesives. Laminating bamboo enables the creation of multiple products with regular sections (Harries, Sharma, and Richard, 2012). The objective of laminating bamboo is to reduce the number of irregularities by splitting bamboo into thinner strips with a rectangular cross-section. Overall, the following steps are needed to manufacture laminated bamboo: (1) material selection, (2) splitting bamboo into strips, (3) treating bamboo strips, (4) arranging the location of bamboo strips, and (5) applying adhesive and pressure to laminate the composites. Research carried out by Sharma, Gatóo, and Ramage (2015b) suggests that every step and decision taken during the manufacturing process could affect the material's mechanical performance. Moreover, the physical characteristics of bamboo strips are expected to impact the structural performance of laminated bamboo critically. Estrada, Linero, and Takeuchi (2019) and Xiao, Yang, and Shan (2014) argue that the successful use of laminated bamboo relies on understanding how the physical characteristics of bamboo strips affect the macroscopic behaviour of the material.

Bamboo strips are composed of a series of bamboo fibres running along the longitudinal direction of the cane. The fibres are embedded in a soft matrix made of parenchyma cells. The fibres act as the main elements providing stiffness to the material, while the parenchyma cells are weaker and act as a medium to transmit efforts among the fibres (Mannan, Knox, and Basu, 2017, Osorio et al., 2018). The structure of bamboo fibres is functionally graded, which means that the number and distribution of bamboo fibres changes across the entire culm's length. As shown in Figure 1.1-**a**, the distribution of bamboo fibres changes in the transversal section of the culm. Bamboo fibres become smaller and densely packed towards the exterior face of the culm. Additionally, bamboo fibres will have internodal and nodal sections. Fibres run uninterrupted at internodal regions. However, fibres' size, shape, and arrangement become irregular and discontinuous at nodal regions (Figure 1.1-**b**). Research carried out by Chen et al. (2015) and Shao and Wang 2018, suggests that the irregular distribution of fibres are likely to determine and influence the material's performance. Moreover, the irregularity of fibres is exacerbated by the process used to mill the strips into regular sections. As seen in Figure 1.1-**c**, the volume of fibres – in the transversal section – will be reduced after milling. Nodal regions are also affected by the milling process. Fibres at nodal regions bend in and out to support the vertical growth of the culm. After milling, the fibres become discontinuous (Figure 1.1-**d**). Bamboo strips are the main components of laminated bamboo. It can be concluded, then, that their physical characteristics and arrangement are likely to determine the structural capabilities of laminated bamboo.

Laminated bamboo has mechanical properties comparable to structural timber. Its use has a promising future in the Architecture, Engineering, and Construction (AEC) industries. However, it is essential to identify the factors that can affect the material's structural soundness before considering it a reliable structural material. The manufacturing process and the quality and characteristics of bamboo strips are the main factors determining the structural integrity of laminated composites. From these two, manufacturing factors are hard to predict. Efforts to standardise manufacturing processes can help prevent failures due to manufacturing errors. On the other hand, an in-depth analysis of how the physical characteristics and arrangement of bamboo strips compromise the mechanical performance of laminated bamboo composites is an effort that can boost the development of methods that use these characteristics as the primary input to predict the behaviour of the material. The characteristics of bamboo strips are visible on a macroscopic level. Hence, their identification can potentially shed some light on the material's response when loads are applied.

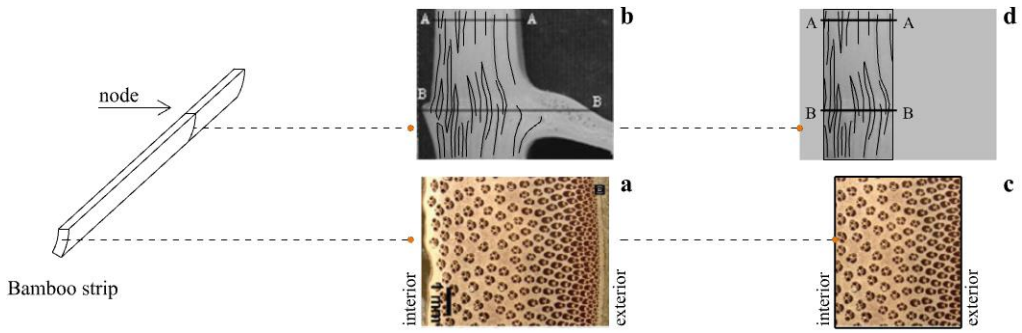

Figure 1. 1: The arrangement of fibres in bamboo strips.

1.3 Predicting the deformation and failure of laminated bamboo composites

Being able to predict the response of a material when loads are applied can help prevent accidents, preserve the life of structural components, and optimise the inherent attributes of a material. Laminated bamboo is a new material compared to highly commercial materials, such as timber, steel, and concrete. The mechanical response of these materials has been studied for years. Such knowledge has enabled the development of methodologies that can predict the materials' behaviour with a satisfying degree of reliability. In the case of laminated bamboo, more research is needed to start building solid methodologies that accurately predict the material's behaviour.

Currently, the most common approach to model the behaviour of bamboo and bamboo-based composites is the use of numerical modelling techniques. However, the complexity

of the material is usually simplified when using numerical methods. Attempts have been made to model the material's behaviour using two-dimensional, three-dimensional, and structural models. Reynolds et al. (2016), Khoshbakht et al. (2018), and Estrada, Linero, and Takeuchi (2019) have used the Finite Element Method to characterise the two-dimensional response of dowelled connections and determine the shear and tensile strength of small-sized specimens. Laminated bamboo is an orthotropic material with different properties in three directions: longitudinal, radial, and tangential. The radial and tangential directions are assumed to have the same properties in the developed models. Hence, the material is modelled as a transversely isotropic material, having different properties only in two directions – the parallel (longitudinal) and the perpendicular (radial and tangential).

Three-dimensional models have only been used to characterise the mechanical response of full culm bamboo. Full culm bamboo, unlike laminated bamboo, is a transversely isotropic material. Godina and Lorenzo (2015) did acknowledge the change in properties as the fibres become denser, close to the outer layer of the culm. Akinbade et al. (2020) also acknowledged the different properties of bamboo fibres along the radial direction. Three-dimensional models have been developed to model the behaviour of full culm bamboos, and the radial distribution of bamboo fibres has been acknowledged. However, the three-dimensional models did not acknowledge the mechanical behaviour of bamboo at nodal regions. Finally, Fang et al. (2015) and Ngudiyono et al. (2019) developed numerical models to investigate the structural response of assemblies made with bamboo-based components.

Overall, it can be concluded that efforts to develop methods to simulate and predict the mechanical behaviour of laminated bamboo are still limited and scattered. Further investigations are needed to develop robust strategies that successfully acknowledge how the inherent characteristics of bamboo strips affect the material's mechanical performance. The lack of a comprehensive understanding of how laminated bamboo behaves in the longitudinal, radial, and tangential directions prevent the development of strategies to predict the mechanical response of laminated bamboo composites accurately. Additional analysis and testing are needed to identify how the hierarchical structure of bamboo fibres and their subsequent arrangement influence the onset and evolution of damage in the bamboo laminates.

Contemporary research shows that using numerical approaches is the preferred method to predict the mechanical response of natural and engineered bamboo elements. However, such an approach fails to capture the material's complexity fully. Often, the orthotropic

nature of the material is simplified. Moreover, the impact that the cellular distribution of fibres has on the material's behaviour is usually dismissed. As suggested by Habibi and Lu (2014), Chen et al. (2015), and Shao and Wang (2018), the uneven distribution of fibres in the transversal direction and the discontinuous distribution of fibres factors that have a clear impact on the performance of the material. Hence, predicting the performance of laminated bamboo relies on acknowledging these factors. The development of modelling approaches that use the physical characteristics of bamboo strips as indicators of the material's behaviour can potentially provide a better approximation of how the material behaves.

1.4 Statement of the problem

Laminated bamboo is a material with promising applications in the Architecture, Engineering and Construction (AEC) industries. However, the promotion of laminated bamboo as a reliable material relies on identifying the factors that can compromise its structural integrity. As with any other engineered material, manufacturing factors can hinder the structural performance of laminated bamboo. There are different methods used to laminate bamboo composites. Efforts to standardise the processes used to manufacture laminated bamboo are essential to guarantee to minimise structural failure due to manufacturing errors. Such errors are hard to detect, and when predicting the failure of materials, it is usually assumed that small imperfections – due to manufacturing processes – are not likely to hinder the performance of the bulk material. In the case of laminated bamboo, instead, the quality and characteristics of bamboo strips are expected to be the main features affecting the structural performance of the material. Bamboo strips are the main constituents of laminated bamboo composites. Coming from a natural material, the strips have physical irregularities. To begin with, bamboo culms have a hierarchical cellular structure, which means that the properties of the material are highly heterogeneous. Hence, bamboo strips have a different distribution of fibres in the transversal direction and a different distribution of fibres at internodal and nodal regions. It can be concluded, thus, that the physical characteristics of bamboo strips and their arrangement are factors that will play a vital role in the mechanical performance of laminated bamboo.

The characteristics of bamboo strips and their arrangement make bamboo a material with different properties and behaviours in three directions: longitudinal, radial, and tangential. Contemporary research has focused on identifying the mechanical behaviour of laminated bamboo composites and the most common types of failure. However, the current literature has not focused on understanding the role that the characteristics of bamboo

strips play in the deformation and failure of laminated bamboo. Moreover, the mechanical differences between the radial and tangential directions have not been fully characterised. Research carried out by Habibi and Lu (2014), Chen et al. (2015), and Shao and Wang (2018) suggest that the characteristics of bamboo strips are crucial to understanding the mechanical and structural response of laminated bamboo. Identifying how the features of bamboo strips affect the structural capabilities of laminated bamboo can help develop strategies to predict how the material will behave as a structural element.

Presently, numerical modelling is the most common approach used to model the behaviour of laminated bamboo. As reported by Estrada, Linero, and Takeuchi (2019) currently there are no constitutive models that describe the complex behaviour of bamboo and bamboo-based composites. When using numerical models to approximate the behaviour of laminated bamboo, the inherent variation of the material is simplified. Hence, the models can misrepresent the mechanical behaviour of the laminates. In the case of laminated bamboo, current models simplify the orthotropic nature of the material and fail to acknowledge the different properties of the material along the perpendicular direction and at nodal regions. The properties of bamboo strips, such as fibre distribution, fibre arrangement and nodes, are likely to orchestrate the ultimate response of laminated bamboo when loads are applied. Such properties are visible at a macroscopic level, which means that it is possible to visually identify the sections of the laminates that have a different distribution of fibres. Suppose the effect that the physical characteristics of bamboo strips have on the mechanical performance of the laminates is identified. In that case, there is a potential that such characteristics can be used as visual input to predict the likely deformation and failure of the material. Such methodologies can help prevent the unexpected failure of structures made with laminated bamboo composites. Moreover, the methods can also help preserve the service life of laminated bamboo structures.

1.5 Research question, aim, and objectives

1.5.1 The research question

Based on the previous analysis, the following research question was outlined:

Can one use the physical characteristics of bamboo strips to predict the deformation and failure patterns of laminated bamboo composites?

1.5.2 Research aim

The overall aim of this study is to identify how the physical characteristics of bamboo affect the mechanical performance of laminated bamboo and determine how can these be used as parameters to predict the deformation and failure modes of the material.

1.5.3 Research objectives

[1] To identify, through literature review, what are the features of bamboo strips that can affect the mechanical performance of laminated bamboo.

[2] To identify, through literature review, what is the mechanical behaviour of laminated bamboo composites.

[3] To identify, through literature review, what methods have been used to model and predict the deformation and failure of laminated bamboo composites.

[4] To design a testing program to identify how the physical characteristics of bamboo strips determine the mechanical behaviour, deformation, and failure modes of the material.

[5] To analyse the results of the experimental program and map out the patterns that determine the deformation and failure modes of laminated bamboo composites.

[6] To establish a methodology that uses the physical characteristics of bamboo as an input to predict the deformation and failure of laminated bamboo composites.

1.6 Significance of the research

Currently, no methods have been developed to predict the mechanical behaviour of laminated bamboo using the physical characteristics of the material as the primary predictive input. As it was previously outlined, the main components that make up the physical characteristics of the laminates are bamboo strips. The strips have an inherent heterogeneous arrangement of fibres that can be visually identified at a macroscopic level. Recent literature suggests that the uneven distribution of bamboo fibres in the transversal direction and at nodes are likely to play a crucial role in the material's mechanical performance (Habibi and Lu, 2014, Chen et al., 2015, and Shao and Wang, 2018). The present study aims to develop a methodology that uses these characteristics as the primary input to determine how the material will deform and eventually fail under static loading. The development of such methods can positively impact the Architecture, Engineering and Construction (AEC) industries. Notably, it can help to quickly identify the areas of a component that are likely to fail when loads are applied or increased. This can be useful to preserve the life service of existing buildings. Furthermore, it can be used as a way of

planning reinforcement strategies for structural members at the early stages of the design process.

1.7 Thesis structure

The thesis provides a novel methodology to predict the deformation and failure of laminated bamboo by using the physical characteristics of bamboo strips as a visual input to determine the expected behaviour of the material. The thesis is divided in eight chapters:

Chapter 1 provides a general overview of the research topic, and it outlines the main aims and objectives of the present study.

Chapter 2 reviews the literature available on laminated bamboo, its mechanical behaviour and the methods developed to predict its behaviour. The chapter also highlights the gaps in the literature, and it discusses future considerations to address these gaps. The first section of the chapter focuses on identifying the features that are likely to impact the performance of laminated bamboo. The second section summarises the research that has been carried out to characterise the mechanical behaviour of laminated bamboo. The third section reviews the methods that have been developed to predict the mechanical behaviour of bamboo laminated. Finally, the fourth section summarises the key findings of the literature.

Chapter 3 outlines the framework used to develop a methodology to predict the mechanical performance of laminated bamboo using the characteristics of bamboo strips as the primary input. First, the chapter outlines the objectives and assumptions of the methodology. Second, it describes a series of experiments aimed at determining how the physical features of bamboo strips influence the response of the material under uniaxial static loading. Lastly, the chapter describes the steps taken to use the physical characteristics of laminated bamboo as the main input to predict the behaviour of the material.

Chapter 4 describes how the physical characteristics of bamboo strips influence the behaviour, deformation, and failure of laminated composites under uniaxial tensile loading. The first section describes the results of the tensile experiments carried out in the longitudinal direction. The results of the sample submitted to radial tension are outlined

in the second section. The third section describes the results of the sample under tangential tension. Finally, the fourth section compares tensile behaviour in the three directions.

Chapter 5 describes how the physical characteristics of bamboo strips impact the response of laminated bamboo under uniaxial compressive loads. The first section summarises the results of the sample under longitudinal compression. The second section analyses the results of the tests that were carried out in the radial direction. The third section describes the behaviour of the sample under tangential compression. Lastly, the fourth section compares the results of the sample under longitudinal, radial, and tangential compression.

Chapter 6 describes how the physical characteristics of bamboo strips determine the failure modes of laminated bamboo when uniaxial shear loads are applied. As Chapters 5 and 6, the first part of the chapter describes the results of the sample under longitudinal shear. The second part describes the deformation and failure of laminated bamboo under radial shear, and the third part describes the behaviour of laminated bamboo under tangential shear. The final section of the chapter compares the different responses of the material in the longitudinal, radial, and tangential directions.

Chapter 7 presents the development of a methodology that uses the findings of Chapters 4, 5 and 6 to predict the mechanical behaviour, deformation and failure of laminated bamboo composites submitted to uniaxial static loading. The first section describes the general approach used to estimate the deformation and fracture of laminated bamboo. The second part summarises algorithms developed to predict tensile deformation and fracture. The third section describes the algorithms developed to predict compressive failure. The fourth section describes the algorithms designed to predict shear failure. Finally, the fifth section discusses the applicability and limitations of the method.

Chapter 8 provides general conclusions and outlines the future work that can be carried out to optimise the proposed methodology.

Chapter 2 | Literature Review

| The first part of this chapter focuses on identifying which are the factors that can compromise the structural performance of laminated bamboo. The second part summarises the research that has been carried out to characterise the mechanical behaviour, deformation, and failure of laminated bamboo. The third part is a summary of the methods that have been developed to simulate and predict the mechanical responses of laminated bamboo. The summary includes methods used to describe the mechanical behaviour of raw bamboo and bamboo-based engineered components. Finally, the fourth section recaps the key findings of the literature review. |

2.1 Laminated bamboo composites

2.1.1 Raw bamboo as a structural material

Bamboo is a natural resource that can become a prominent sustainable building material if technologies are developed to overcome its limitations. Bamboos are a subfamily of grasses that, over a long period, evolved to thrive in the climatic conditions of the tropical and sub-tropical forests. The physical shape of bamboo is tuned to withstand the lateral action of the wind. Its hollowness and longitudinal nodes give the plant the lightness and reinforcement needed to act as a natural oscillator (Broto, 2015). Bamboo's cellular structure provides a system to supply food and nutrients to the plant and protects it from natural threats. The microscopic structure of bamboo reveals a network of cellulose fibres embedded in a soft and ductile lignin matrix. The fibres are distributed along the longitudinal direction of the cane. Transversely, the number of fibres increases towards the exterior face of the cane, where a thick silica layer protects the plant from any external damage. This arrangement explains why bamboo is a strong material when loads are applied in the direction of its fibres, whilst it becomes brittle when loads are applied in the opposite direction (Figure 2.1).

Bamboos are classified into herbaceous and woody plants with more than 1,400 species (Gibson, 2009, Liese and Köhl, 2015). From such variety, only woody or giant bamboos have the dimensions and mechanical properties needed for construction or industrial use. The highest diversity of woody bamboo has been recorded in the tropics, particularly in

the Asia Pacific region, followed by America, Madagascar, and Africa (Bystriakova, Kapos and Lysenko, 2004). Due to its geographical availability and remarkable mechanical properties, tropical regions have long embraced bamboo to construct small to mid-sized projects. From local buildings, like the METI handmade school (Figure 2.2-**left**) to complex structures like the ZERI pavilion (Figure 2.2-**centre**) and the Children's Activity and Learning Centre (Figure 2.2-**right**), bamboo poles have been used for a considerable amount of time as structural elements. However, every bamboo pole is different in shape and mechanical performance. Such irregularities make using bamboo in projects with more demanding structural requirements challenging. Building with bamboo at a large scale requires a deep understanding of the material and the development of technologies to cope with its natural irregularities.

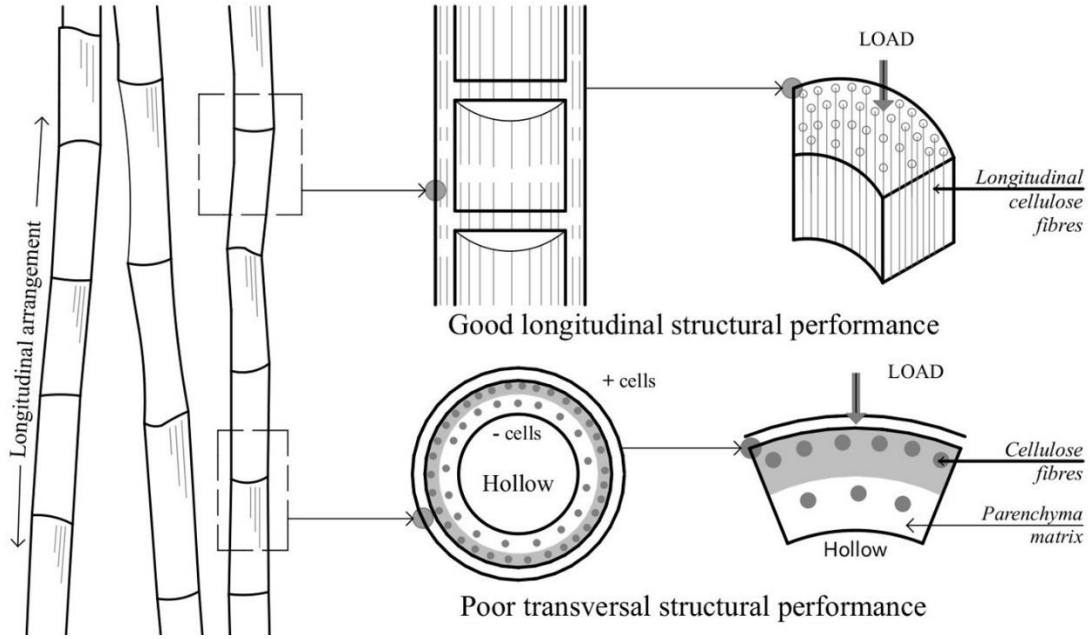

Figure 2. 1 – The mechanical properties of bamboo culm.

Figure 2. 2: **left** - METI handmade school, Anna Heringer + Eike Roswag, 2005. **centre** – ZERI pavilion, Simon Vélez, 2005. **right** – Children's activity and learning centre, 24H-Architecture, 2007.

Janssen (2005), Jayanetti and Follet (2008) and Harries, Sharma, and Richard (2012) believe that the transition of bamboo from a local resource to a mainstream structural material can only be achieved if efforts are made to standardise its irregularities and efficiently evaluate its structural limitations. In this regard, Sharma et al. (2014) and Xiao, Yang and Shan (2013) argue that engineering bamboo-based composites can help regulate the use of bamboo in terms of design, shape regularity, mechanical testing, structural performance, and manufacturing processes.

2.1.2 Engineered bamboo as a structural material

Engineering bamboo is a technology developed in the 1970s in China (Sharma et al., 2014). The production of bamboo-based composites utilises different sections of the whole culm for various manufacturing techniques. The methods used to engineer bamboo have been extensively drawn from the techniques developed to manufacture engineered timber products. However, the interest in using engineered bamboo as a reliable building material has only spiked in the past 15 to 20 years. Dauletbek et al. (2022) reported that the present need to identify and embrace sustainable building materials in the Architecture, Engineering and Construction (AEC) industries has made designers, engineers and researchers focus on investigating the potential of using bamboo as a mainstream building material

Liu et al. (2016) recorded an extensive list of engineered bamboo products that are currently used as primary (structural framing and sheathing) and secondary (panels, sheets, and floorboards) building materials. Most of these products are manufactured in Asia, where special equipment and techniques have been developed to transform raw bamboo into engineered products with standard sizes. Of particularly interest is the development of bamboo-based products with the potential to be used as reliable structural materials for large-scale buildings. The production of structural members requires the use of facilities where the bamboo culms can be properly treated to increase their durability. Additionally, specialised machinery and tools are needed to eliminate the rounded shape of bamboo culms and shape beams into regular and customised cross-sections. Sharma et al. (2014) reported that laminated bamboo and bamboo scrimber are the structural products mostly distributed by Asian companies. Laminated bamboo composites are produced by hot or cold pressing regular bamboo strips (Liu et al., 2016). To achieve a regular section, the strips are milled or planned into rectangular shapes (Figure 2.3-**left**). Unlike laminated bamboo, bamboo scrimber is manufactured without processing bamboo strips into regular sections. Instead, the strips are roughly planned and then arranged into bundles that will be later glued together (Figure 2.3-**centre**) (Liu et al., 2016). Alternative

to these commercial products, Xiao, Yang and Shan (2013) reported the development of a process to manufacture Glue Laminated Bamboo (GluBAM) for structural applications. In this case, the structural sections are formed by pressing together bamboo curtains made with slender and thin bamboo strips. The strips are arranged in an interlocking orthogonal pattern (Figure 2.3-**right**).

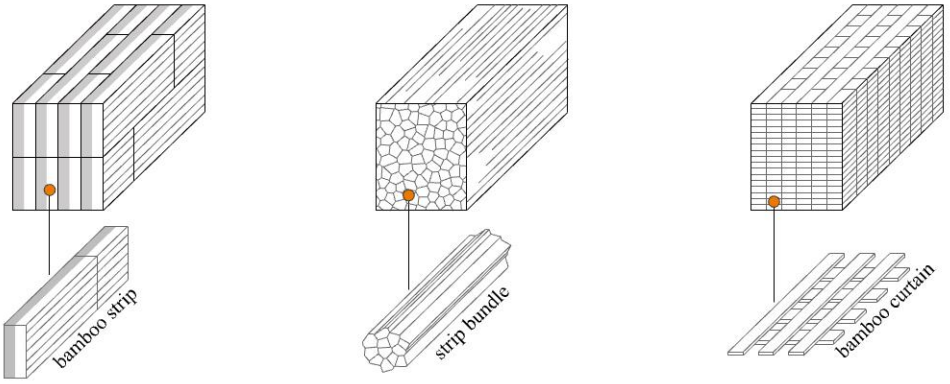

Figure 2. 3: left – laminated bamboo composite **centre** – bamboo scrimber **right** – Glue Laminated Bamboo (GluBAM).

From the three manufacturing processes, laminating bamboo is the process that requires more steps to produce strips with a regular cross-section. Additionally, production costs are affected by the acquisition and maintenance of specialised machinery and equipment. Despite these limitations, laminated bamboo is the product with a higher commercial outreach. Furthermore, recent research and experimental results suggest that laminated bamboo composites can be structurally compared to timber and can potentially play a bigger role in the future of the building industry (Xiao, Yang and Shan, 2013, Zea Escamilla and Habert, 2014, and Sharma et. al. 2017).

2.1.3 Manufacturing laminated bamboo composites

The objective of manufacturing composites is to enhance the macroscopic properties of a material by having more control over the arrangement of its physical properties. It is generally assumed that "*the number of microscopic flaws which act as fracture initiation sites in bulk materials are reduced when the material is drawn into a thinner section*" (Staab, and Pearson, 2017, p. 3). This is the principle that guides the design and fabrication of laminated bamboo composites. Engineering bamboo eliminates the round section of bamboo poles by creating bundles of longitudinal strips, which can be laminated together to produce a composite. Several authors agree that engineering bamboo is a manufacturing process that, by reducing physical variability and re-distributing material defects, enhances the mechanical and structural properties of natural

bamboo (Sharma et al., 2014, Xiao et al. 2013, Ni et al., 2016 and Sun, He, and Li, 2020). As can be seen in Figure 2.4, the production of laminated bamboo composites can be summarised in five steps consisting of (1) natural bamboo selection, (2) splitting or flattening bamboo's rounded shape, (3) treating bamboo strips before being laminated, (4) laminating the strips or bundles and, finally, (5) post-processing to increase the strength of the final product.

Figure 2. 4: Process to manufacture laminated bamboo composites.

Not all bamboo species are suitable to manufacture laminated composites. A wall thickness of 10 to 20mm and a height of 15 to 30m are required to maximise the use of bamboo as the primary constituent material (Semple, 2015a, Liu et al., 2016). Only a few species like Moso and Guadua bamboo possess the size and mechanical properties needed to guarantee structural integrity. After selecting bamboo specimens with the required size and shape, the culms are cut into smaller pieces, being 1, 2 ,3 and 4 meters the most commercially available length sizes (Moso ® International, 2018). The round shape of bamboo culms is then eliminated by splitting the culms into slender strips using manual or mechanised splitters (Mahdavi, Clouston, and Arwade, 2011, Sharma et al. 2014). The strips can have a 15 to 30mm width and a 10 to 20mm thickness (Liu et al., 2016). After splitting bamboo culms, the strips go through a process of rough planning to remove the outer and inner layers. The strips are then treated to prevent biological degradation and maximise durability. Leaching, smoking, chemical bleaching, and hygro-thermal caramelisation are some of the most used treatment techniques (NMBA, 2006 and Shah, Sharma, and Ramage, 2018).

The treated strips are finely planed into rectangular shapes with the use of a four-sided planing tool. The final average size of the planed strips ranges from 15 to 20mm in width and 5 to 8mm in thickness (Ni et al. 2016). After treating and processing the strips into regular shapes, the strips are air-dried, and those with a moisture content of 12% or less are selected to form the laminated composites (Sun, He, and Li, 2020). Experiments

carried by Nugroho and Ando (2001) and Mahdavi, Clouston, and Arwade (2011) demonstrated that the optimal strategy to align bamboo strips is to use inner – outer and inner – inner face contact and to avoid, as much as possible, outer – outer face contact (Figure 2.5-**left**). Following this criterion, bamboo strips can be arranged horizontally (flatwise) or vertically (edgewise) (Sharma et al., 2015a and Moso ® International, 2018).

After planing, bamboo strips go through a process of visual strength grading to determine which are suitable for lamination and which are not (Xiao, Yang, and Shan, 2013, and Sun, He and Li, 2020). Before glueing the strips together, the location of nodes is randomized, as much as possible, to avoid concentration of zones with weaker cellular arrangement (Figure 2.5-**centre**). For longer beams, butt, finger, and scarf joints are used. It is standard practice to use only one type of joint to laminate beams (Bodig and Jayne, 1993). As with nodes, the location of joints is spaced and randomized. Generally, the re-arrangement of material defects or weak zones is a strategy that successfully improves the mechanical optimisation of laminated composites (Vasiliev and Morozov, 2013 and Staab, and Pearson, 2017). According to Ansell (2015), laminations with higher strength should be positioned at the outer zone of the beam to resist higher stresses, while lower strength elements should be placed at interior layups (Figure 2.5-**right**).

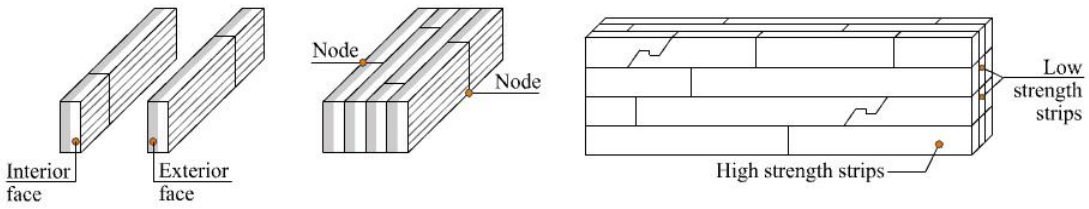

Figure 2. 5: Strip arrangement, **centre** – Location of nodes, **right** – Beam arrangement.

After processing and arranging bamboo strips, these are glued together with adhesives that have been successfully used in the timber industry and that are mechanically stronger than wood itself. Research carried out by Sharma et al. (2014) states that even though the use of bio-based resins is becoming a priority, the use of phenol resins continues to be the norm due to cost efficiency. As shown in Table 2.1, laminated bamboo products have an adhesive content ranging from 1% to 7%, depending on the manufacturing procedure. On this regard, experiments performed by Correal and Ramirez (2010) and Ogunsanwo, Adenaiva, and Adedeji (2019) suggest that adhesive selection and glue quantity have no significant impact on the mechanical properties of laminated bamboo. Finally, the strips are hot or cold pressed together to form the laminated composite. The applied pressure force and time of application are variables determined by the adhesive's specifications.

Product	Adhesive content	Reference
Strand woven bamboo	4 – 5%	Ambient Bamboo Floors (2021)
Laminated bamboo beams	3 %	Moso International BV (2017)
Bamboo plywood	1 – 3%	Smith & Fong company (2011)
Bamboo scrimber	7 %	Zhang et al. (2011)

Table 2. 1: Adhesive content of different laminated bamboo products.

Despite the strategies used to optimise the production and performance of laminated bamboo, decisions taken in every step of the process can impact the mechanical performance of the product. For example, Sharma, Gatóo, and Ramage (2015b) demonstrated that processing methods can have a significant impact in the resulting mechanical properties of the laminated boards. For this reason, it is essential to regulate the manufacturing process of laminated bamboo before the material can have a solid presence in the construction industry. Furthermore, Xiao, Yang, and Shan (2014) argue that the quality of bamboo strips, the predominant constituents of laminated bamboo, is essential to guarantee the mechanical and structural performance of the laminated products. Understanding the structure of bamboo strips is, therefore, necessary to characterise and enhance the mechanical behaviour of laminated-bamboo composites.

2.1.4 Bamboo, a functionally graded material

To understand how bamboo strips affect the mechanical performance of laminated bamboo, first it is essential to understand the cellular structure of raw bamboo. Bamboo is a natural composite with a complex arrangement of functionally graded structures that work together to provide food, support, and protection to the living organism (Amada et al. 1997, Ghavami, Rodrigues, and Paciornik 2003, Mannan, Knox, and Basu, 2016). The hierarchical structure of bamboo explains why bamboo is a lightweight material with considerable strength in the direction of its fibres and a brittle behaviour when loads are applied perpendicularly. To clearly map out the mechanical response of laminated bamboo as a building material, it is necessary to understand how the interactions occurring at different length scales will affect the material's behaviour and strength (LeMaître, 2001, Youssefian and Rahbar, 2015). The hierarchical structures of laminated bamboo, from the nanoscale to the macroscale, are briefly outlined here (Figure 2.6):

Nanoscale: At this level, bamboo is made of cellulose hexagonal or rectangular nanofibrils formed by chains of glucose molecules and regular or irregular hydrogen bonds (Youssefian and Rahbar 2015, Mannan, Knox, and Basu, 2019). Depending on the nature of the hydrogen bonds, the nanofibrils will have orderly crystalline regions or

random and amorphous regions. Cellulose nanofibrils are the basic building blocks of bamboo.

Sub-microscale: In this level, bamboo fibres are assembled by combining thin and thick layers made of a hemicellulose-lignin matrix reinforced with cellulose nanofibrils oriented at different angles (Gritsch, Kleist, and Moveh, 2004, Mannan, Knox, and Basu, 2019). Bamboo fibres have a hexagonal or pentagonal shape with an opening or lumen right at the middle (Osorio et al. 2018). The fibres assemble in bundles that resemble a beehive honeycomb pattern, except that the size of bamboo fibres varies depending on the location of the fibres and the characteristics of the vascular bundles (Gritsch, Kleist, and Moveh, 2004).

Microscale: An assembly of tube-like structures gives rise to a system of vascular bundles in charge of transporting water and nutrients along the full length of the culm. The vascular bundles are composed of vessels, phloem, and tracheids surrounded by bundles of bamboo fibres that provide mechanical strength and protection to the plant's vascular system (Smith, 2010). Bamboo fibres are distributed following a monotonic arrangement, which means that they are smaller near the edge of vessels and increase in size as they are further away from the edge of the vessels. Vascular bundles are surrounded by supportive ground tissue formed with simple parenchyma cells. This tissue is often referred to as the parenchyma matrix, in which the vascular bundles are embedded (Habibi and Lu, 2014, Mannan, Knox, and Basu, 2019, Deniz et al., 2017).

Mesoscale: This scale, also known as the Representative Volume Element (RVE) represents the smallest section of the material that can be used to characterise the mechanical response of the bulk material within a reasonable tolerance (LeMaître 2001, Moussady, Lévesque, and Therriault, 2013). At this level, bamboo's wall is formed by a series of vascular bundles that increase in size and volume as they approach the outer face of the culm (Mannan, Knox, and Basu, 2019, Shao and Wang, 2018). A parenchyma matrix surrounds these vessels and acts as a mechanical buffer. The outer skin of the culm is a hard silica shell that protects the interior structure of the plant. The RVE of laminated composites differs from that of raw bamboo, since the outer skin of bamboo's wall is often removed to guarantee strong bonding joints between different bamboo layers (Mahdavi, Clouston and Arwade, 2011, Sharma et al. 2014). It is important to consider that the arrangement of the vascular bundles becomes irregular and discontinuous at the nodal section. For this reason, research is still under development to determine the impact that nodal sections have in the mechanical behaviour of the bulk material (Cui et al. 2020, Ramful and Sakuma 2020).

Macroscale: This level represents the whole bamboo culm or the whole laminated bamboo assembly.

As mentioned earlier, the main constituents of laminated bamboo composites are bamboo strips. Roughly speaking, bamboo strips are composed of vascular fibre bundles embedded in a matrix made of parenchyma cells. The distribution, density and interaction of these components will impact the overall performance of laminated bamboo. The following section, therefore, discusses how the cellular structure of bamboo fibres affects the physical properties of laminated bamboo composites.

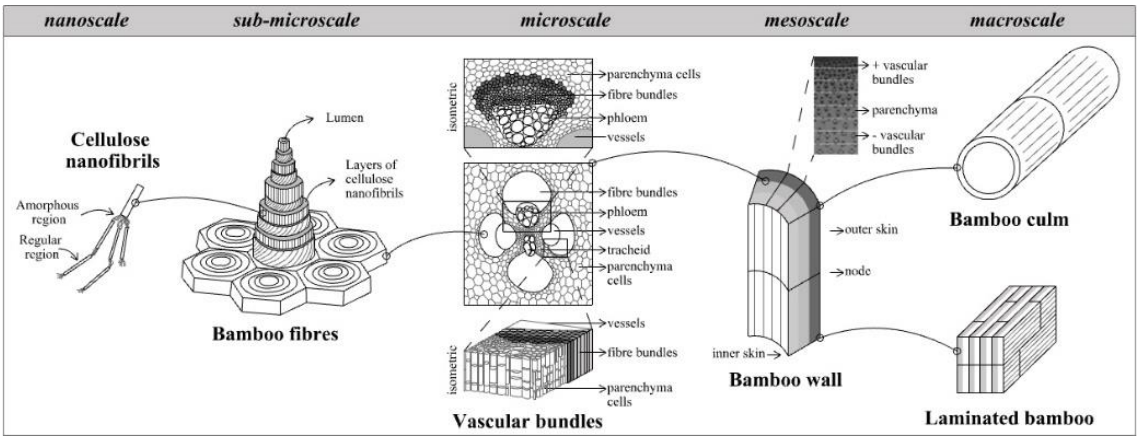

Figure 2. 6: Hierarchical structure of laminated bamboo, spanning from the nanoscale to the macroscale. Change image – only laminated bamboo.

2.1.5 The cellular structure of bamboo strips

Bamboo is a naturally fibre-reinforced composite formed by longitudinal vascular bundles embedded in a soft parenchyma matrix (Liese, 1985). The vascular fibre bundles are the elements that provide strength to the material (Osorio et al., 2018). At the same time, the parenchyma cells are weaker and only act as a matrix to diffuse the forces acting on the material (Dixon and Gibson, 2014, Mannan, Knox, and Basu 2017). Several microscopy methods have been used to characterise the shape of fibre bundles and parenchyma cells (Gritsch and Murphy, 2005, Habibi and Lu, 2014, Mannan, Knox and Basu, 2017). Transversally, both elements are polygonal shapes that change in size depending on their location within the culm's wall. However, bamboo fibres are continuous along the longitudinal direction, while parenchyma cells retain the same polygonal distribution.

As can be seen in Figure 2.7 – **left**, the size, shape, number, and density of vascular bundles vary according to their location along the culm wall. (Gritsch, Kleist, and Murphy 2004, Trujillo, and López, 2016, Osorio et al., 2018). Vascular bundles become smaller

and densely packed towards the exterior face of bamboo. Given this cellular arrangement, the outer layer of bamboo is a thick and waxy layer that acts as a protective shell. Experiments carried out by Chen et al. 2015, and Shao and Wang 2018 have proven that the density of vascular fibre bundles will directly impact the material's performance. In other words, the sections with a higher volume of fibres will be stronger than the sections with a lower volume of fibres. Bamboo strips undergo a process of rough and fine planing to eliminate their original curved cross-sections. As shown in Figure 2.7-**right**, planing the strips will decrease the volume of bamboo fibres. Depending on the initial configuration of the bamboo plus the process used to sand the strips, the fibre-to-parenchyma ratio will vary, meaning that some strips will have better mechanical performance than others. Further research is needed to understand how fibre distribution affects the overall performance of laminated bamboo composites.

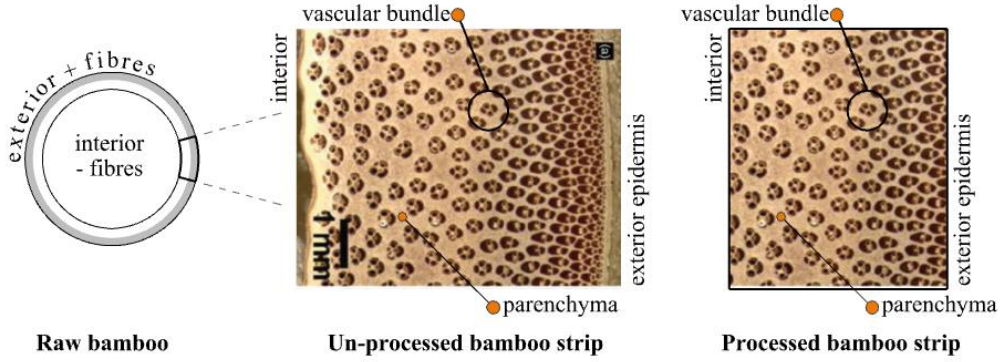

Figure 2. 7: **left –** Bamboo's cross section, **centre –** Cellular arrangement of vascular bundles (Osorio et. al. 2018), **right –** Components of vascular bundles: (a) hollow vessels, (b) sclerenchyma fibres and (c) parenchyma matrix (Deniz et. al 2017).

Bamboo culms are formed by internodal and nodal sections. Internodal sections consist of bamboo outer skin, middle section, and interior tissue. At these sections, vascular bundles run unchanged and uninterrupted along the longitudinal direction of the cane (Figure 2.8-**left**). Nodal regions, being fundamental to support upward growth, are formed by a sheath scar, a nodal ridge, and a diaphragm. At these regions, the shape, size, and arrangement of vascular bundles are disrupted to support the structural changes of the cane (Amada et. al, 1997, Lybeer, 2006, and Osorio et al., 2018). As can be seen in Figure 2.8-**centre**, the vascular tissue of the outer layers is broken to support leaf and sheath lateral growth. The fibres located in the middle part of the wall are curved and thickened when passing nodes. At the same time, some fibres will bend inward or outward to support the radial structure of the node and will eventually spread back along the longitudinal direction (Amada et. al, 1997 and Shao et. al 2010). Shao and Wang (2018) carried out a series of experiments to determine to what extent nodal regions affect the mechanical performance of bamboo strips. The results suggests that the discontinuity and variation of vascular bundles at nodal sections will have a clear impact in the mechanical performance of bamboo strips.

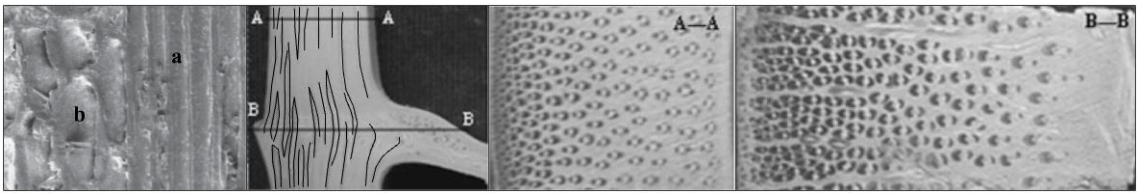

Figure 2. 8: Longitudinal section of vascular bundle (a) and parenchyma matrix (b) (Mannan, Knox and Basu 2017) – **centre –** Longitudinal section of bamboo culm at internodal and nodal regions, and cross section of bamboo internode (A-A), **right –** Cross-section of bamboo node (B-B) (Shao and Wang, 2018).

The process of planing or milling bamboo strips can exacerbate the weakness of the strips, particularly at nodal regions. The areas along the nodes are particularly affected as many of the fibres turning inward or outward will become discontinuous after planing (Figure 2.9). Additionally, microcracks can be formed in the outmost layer of the machined surface (Astakhov, 2009). Further studies are needed to clearly understand the behaviour of nodal regions as the material deforms and eventually fails. Such understanding can generate valuable information to reinforce and prevent failure of the weakest areas of laminated bamboo composites.

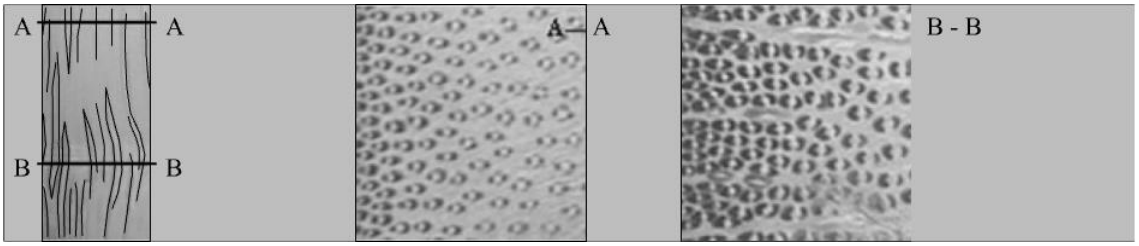

Figure 2. 9: **left** – Longitudinal section of planed strip at internodal and nodal sections, **centre –** Cross-section of planed strip at internode (A-A), **right –** Cross-section of planed strip at node (B-B) (Original image from Shao and Wang 2018 – Modified by author).

Bamboo strips have an irregular distribution of fibres. Hence, it is expected that the arrangements of fibres – during the manufacturing process – will also influence the mechanical performance of the material. The physical characteristics of bamboo fibres and the arrangement of these will determine the physical characteristics of laminated bamboo. The following section describes the physical characteristics of the laminated material.

2.1.6 The mechanical behaviour of layered composite systems

Laminated bamboo composites are formed by gluing together unidirectionally arranged bamboo strips. As can be seen in Figure 2.10-**left**, the resulting composite has three contact surfaces, interior contact face, adhesive surface, and exterior contact face. The simplest unit of a layered composites is a lamina, composed of a series of bamboo strips

glued together (Figure 2.10-**centre**). A series of laminas are glued together to form a laminate (Figure 2.10-**right**) (Staab and Pearson, 2015). For the analysis of laminates, however, it is assumed that glue bonds are perfectly rigid, accounting for less than 1% of the total volume, making its impact on the material's performance negligible (Bodig and Jayne 1993). Hence, it can be assumed that the behaviour of laminated bamboo is exclusively affected by the quality, physical characteristics and arrangement of the bamboo strips forming the laminate.

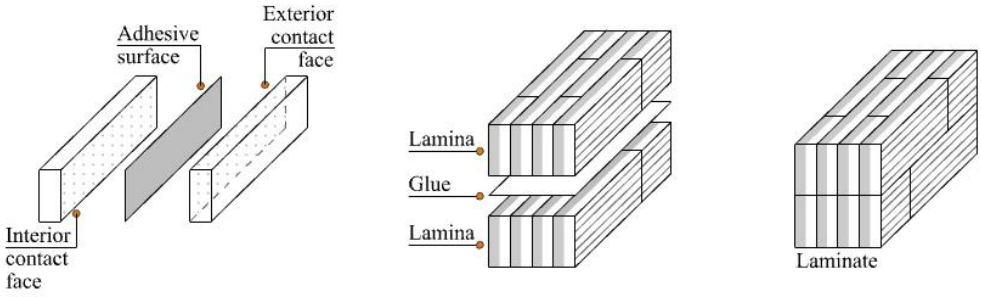

Figure 2. 10: **left** – Contact surfaces, **centre** – Lamina arrangement, **right** – Laminate.

Bamboo strips are orthotropic, meaning that they exhibit different characteristics on three mutually perpendicular axes (Bodig and Jayne 1993). As shown in Figure 2.11-**a**, bamboo strips have a longitudinal, radial, and tangential sections. As such, laminated bamboo composites are also orthotropic. If we place a small cube of laminated bamboo on a three-dimensional Cartesian system, it is possible to observe that the material has different properties along the longitudinal, radial, and tangential direction (Silva, Walters, and Paulino, 2006). Slicing a piece of laminated bamboo into three mutually perpendicular planes reveals three planes of symmetry, the x-z plane, the x-y plane, and the y-z plane. A closer look at the strips, however, reveals that laminated bamboo is not symmetric when the piece is equally divided along the radial direction (the x-z plane) (Figure 2.11-**b, c, and d**).

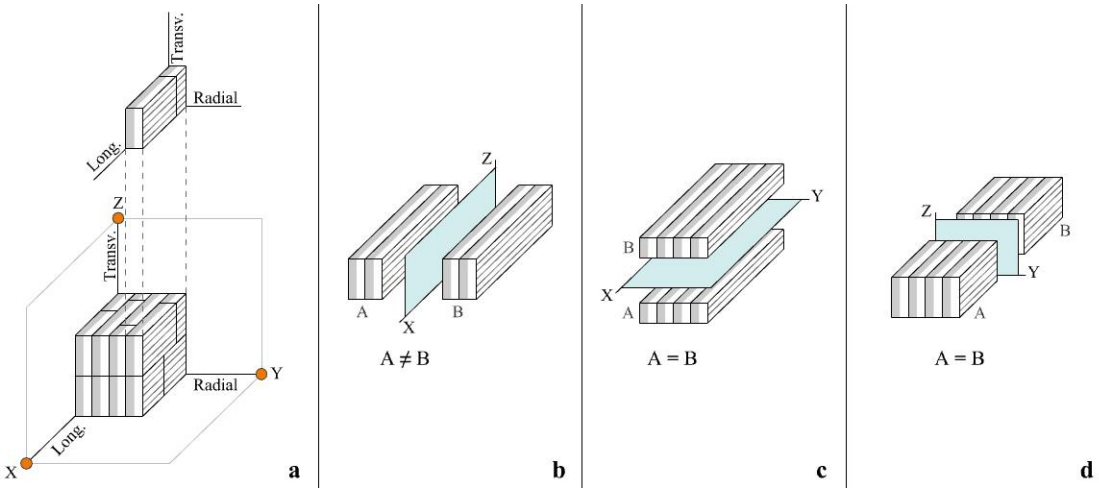

Figure 2. 11: **a-** The three directions of laminated bamboo, **b** – Material asymmetry along the x-z plane, **c** - Material symmetry along the x-y plane, **d** – Material symmetry along the y-z plane.

The arrangement of bamboo strips disrupts radial symmetry in terms of cellular arrangement but not in terms of the fibres' volume fraction. Although laminated composites are non-homogeneous, to reduce the complexity of modelling and predicting their behaviour, the composites are assumed "*to be an orthotropic material with transversal isotropy in the radial-tangential plane*" (Ramírez et al. 2012, p. 1382). Such approach reduces the complexity of laminated bamboo by assuming that the behaviour of the tangential and radial directions is the same. Additional research is needed to validate the applicability of using this approach. Finally, since laminated bamboo is a relatively new material, Estrada, Linero, and Takeuchi (2019) argue that further research is essential to have a comprehensive understanding of how strip arrangement and cellular structure affects the macroscopic behaviour of the material. Such knowledge is particularly useful to develop strategies aimed at guaranteeing and preserving the structural soundness of structures made with laminated bamboo.

2.1.7 Considerations for future research

Given the natural properties of bamboo, it is possible to assume that bamboo can be used as a reliable structural material. However, before bamboo can have a solid presence in the construction industry, it is important to identify strategies to overcome the irregularities that come from working with natural materials. Engineering bamboo is a solution that can help standardise and promote bamboo as a reliable structural material.

Laminated bamboo, bamboo scrimber, and GluBAM are some of the products that have been developed as structural bamboo-based materials. Recent research suggests that laminated bamboo has a mechanical performance comparable to structural timber. Additionally, laminated bamboo is a product with more commercial availability. Therefore, it can be concluded that if the technologies to produce laminated bamboo and assess its structural performance are developed, laminated bamboo could soon become a serious alternative to structural timber.

The process to manufacture laminated bamboo composites consists of five steps: (1) material selection, (2) splitting and planning bamboo strips, (3) treatment to preserve bamboo strips, (4) applying adhesive and laminating the strips, and (5) post-processing. The decisions taken in every step of the process can impact the mechanical performance of the product. Efforts to regulate the manufacturing process and guarantee manufacturing quality are essential to promote the use of laminated bamboo as a reliable building material. Finally, since bamboo strips are the main components of laminated bamboo composites, understanding how their cellular structure affects the mechanical

performance of the composites is crucial to develop strategies aimed at structurally reinforcing the material.

Bamboo strips are the primary construction blocks of laminated bamboo. The cellular structure and arrangement of bamboo strips are likely to impact the mechanical response of laminated bamboo. Of particular importance is the understanding of how the fibre-to-parenchyma ratio affects the macroscopic behaviour of laminated bamboo composites. Also, it is vital to determine how bamboo's nodes impact the performance of laminated bamboo. Nodal regions are regions where the fibres become discontinuous and irregular. These zones are weaker than other regions and can play a crucial role in the onset of failure and material deformation. Understanding how nodal regions affect the performance of laminated bamboo is essential to develop strategies to prevent failure efficiently.

Given natural bamboo characteristics, the laminated composites have different properties along the longitudinal, radial, and tangential directions. To simplify the material's complexity, it is usually assumed that the differences between the radial and tangential direction are negligible and, therefore, should not be acknowledged when studying the behaviour of laminated bamboo. However, the validity of this assumption is yet to be proven. Further research is needed to fully characterise the differences between the longitudinal, radial, and tangential directions of laminated bamboo.

2.2 The deformation and failure of laminated bamboo

2.2.1 Deformable solids

The observable universe is composed of matter, forces, space, and time. Forces create motion and affect the way in which matter interacts and eventually deforms. Forces moving through space and time can either push objects away from each other or pull them closer. As a result of these interactions, all objects are exposed to external and internal forces (Figure 2.12-**a**). The pressure of the wind and friction are examples of external forces acting outside the boundary of defined matter. Internal forces, on the other hand, are the dynamic laws that regulate the microscopic interactions of the atoms and molecules that form an object (Hrabovsky and Susskind, 2020). Gravity and electric fields are examples of such forces. The intensity of a force or system of forces acting on the unit area of an object is known as stress. In mechanics, stresses are classified into normal and shear stresses (Gupta, 2013). Normal stresses act normal to a plane and can either cause elongation (tension) or shortening (compression) (Figure 2.12-**b, c**). Shear stress occurs

when an object is submitted to opposite forces running parallel to each other (Figure 2.12-**d**). Applied forces cause material deformations and eventually, they can deform the material to appoint where it is not capable of sustaining any more forces. Strain is a physical quantity that measures the degree of change that a material experiences when exposed to different forces. Stress–strain systems, hence, are an effective way of describing the constitutive nature of deformable solids.

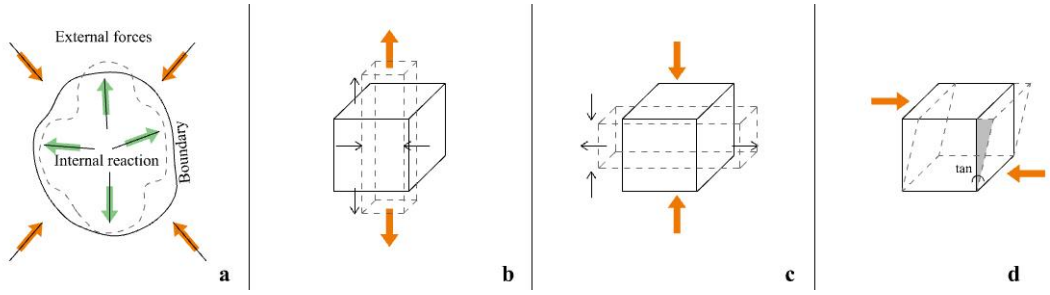

Figure 2. 12: **a-** Internal and external forces, **b** – deformation of a body under tension, **c** – deformation of a body under compression, **d** – deformation of a body under shear.

Understanding how laminated bamboo deforms and eventually fails is essential to understand the structural capabilities of the material and efficiently minimise structural weaknesses. The following sections, therefore, summarise the research done to characterise the mechanical properties and response of laminated bamboo composites.

2.2.2 Determining mechanical properties

The mechanical behaviour of any material must be determined experimentally since there are no theoretical equations to predict the behaviour of most materials, particularly if these are relatively new, as it is the case of laminated bamboo. The mechanical parameters of materials are determined by deforming differently sized pieces and simultaneously measuring their reactive performance. Determining the properties of bamboo is necessary to predict and simulate the mechanical behaviour of bamboo-based products and standardise their use as reliable construction materials. Even though a series of standards have been developed to regulate the use of raw bamboo (Gatóo et al. 2014, Liu et al. 2016), the standardisation of engineered bamboo products is still under development. Being an orthotropic material, the performance of laminated bamboo can be compared to the performance of timber products. For this reason, laminated bamboo has borrowed the standards and terminology commonly used to test timber products as a way of determining its mechanical properties with a degree of reliability. However, further research is needed to assess the validity of using timber standards to determine the mechanical behaviour of laminated bamboo (Sharma et al., 2017).

Recent publications, utilised ASTM-D143 and BS-373:1957 to characterise the properties of small clear specimens (Xiao, Yang, and Shan, 2013, Sinha, Way, and Mlasko, 2014 and Sharma et al., 2015a). Sharma et al. (2017) utilised BS EN 408: Timber structures to characterise the mechanical properties of structural sized pieces. Frequently, testing is carried out in the parallel direction (*longitudinal*) of bamboo fibres or along the perpendicular (*radial* and *tangential*) direction. It is important to note that most of these studies do not acknowledge the differences between the radial and tangential direction. Instead, it is generally assumed that the differences between both directions are negligible. Additional research is needed to fully characterise the mechanical response of laminated bamboo in all the directions.

The results of these experiments are plotted in a stress-strain curve., from which it is possible to calculate the strength and mechanical properties of the material. Values such as the tensile strength, compressive strength, shear strength, Modulus of Elasticity, and Modulus of Rigidity are used to mathematically describe the deformation of a body and can only be determined experimentally. As can be seen in Figure 2.13, this curve gives the relationship between stress and strain of a given material. The first region of the curve (**a**) is caused by specimen misalignment and can be ignored when analysing the data. The second region of the curve (**b**) represents the linear elastic behaviour of the material, which means that during this phase, stress and strain are proportional. In the third stage (**c**), the relationship between stress and strain is no longer proportional and the curve deviates from a straight line. The point from which the material transitions from linear elastic behaviour to non-linear elastic behaviour is known as the proportional limit (**pl**). Beyond the proportional limit, strain will increase at a faster rate until achieving a maximum load (**u**). After this point, the material fails and the loading can decrease gradually or abruptly, depending on the physical properties of the material. This region of the curve is known as the post-failure region (**d**).

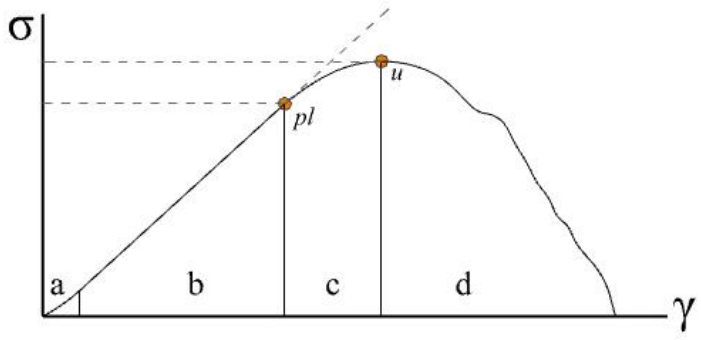

Figure 2. 13: Mechanical values of the stress-strain curve.

Sections **a**, **b**, and c are used to understand how the material deforms as the loading increases. On the other hand, section **d** provides information about the mechanism by which a material fails. Failure is reached either by sudden fracture or prolonged deformation. In any case, failure is assumed once the material is unable to fulfil its original design purpose. The stress-strain curve, the mechanical properties derived from the curve and the analysis of the broken specimens will provide a comprehensive idea of the mechanical response of a material.

2.2.3 Tensile loading

Tensile tests are used to measure the strength and elongation of materials when submitted to uniaxial tension. This test method is used to determine the Ultimate Tensile Strength and the Modulus of Elasticity of natural and engineered bamboo at different scales.

Parallel tension:

The tension method along the parallel direction requires a test specimen with a so-called dog bone shape (Fig. 2.14-**left**). The shoulders of the piece are enlarged for gripping, and the cross-section of the gauge is reduced to localise failure within this region (Davis, 2004). The size of the specimens varies depending on the purpose of the testing program. Kariuki (2018), Chen et al. (2015), and Shao and Wang (2018) have used specimens with a cross-section of no more than 8 mm^2 to determine the tensile properties of bamboo strips. Xiao, Yang, and Shan (2013), Sharma et al. (2015a), Sharma, Gatóo, and Ramage (2015b), and Khoshbakht et al. (2018) have used specimens with a cross-section ranging from 45 mm^2 to 150 mm^2 to determine the tensile properties of laminated bamboo products. Structural sized specimens with a cross-section greater than 2,000 mm^2 have also been tested by Xiao et al., 2014, and Sharma et al. (2017). Depending on the standard, specimens are loaded at constant rates of 1mm/min (ASTM-D143 and BS-373:1957), 2mm/min (GB/T 15780 1995) and 4-5mm/min (BS-EN 408). Table 2.1 shows a summary of the tensile strength and Modulus of Elasticity of pieces with different sizes. The Ultimate Tensile strength, as well as the Modulus of Elasticity are values that seem to be reduced as the bamboo strips are further processed to form laminated composites (Chen et. al. 2015).

Product type	Ultimate Tensile Strength	Modulus of Elasticity	Source
Bamboo fibre	581.70 MPa	40, 400 MPa	Shao and Wang, 2018

Unprocessed bamboo strip	300.00 MPa	19, 850 MPa	Cheng et al. 2015
Laminated bamboo (planned strips)	95.00 MPa	9, 219 MPa	Khoshbakht et al., 2018

Table 2. 2: Tensile strength and Modulus of Elasticity of bamboo products.

The stress-strain curve of parallel tension tests reveals a linear or elastic behaviour prior to failure (Figure 2.14-**centre**). Such stress-strain curve is characteristic of brittle materials. Figure 2.14-**right** shows the most common types of parallel tension failures: (a) fibre pull-out with combined tension and shear, (b) fibre pull-out with splintering failure, (c) shear failure and, (d) trimmed failure. Habibi and Lu (2014) explained that bamboo's failure is likely to start when cracks propagate across the interface of parenchyma cells and find a path through the longitudinal interface between bamboo fibres and the parenchyma cells. The mechanical behaviour and posterior failure of laminated composites under tension along the parallel direction can be explained by analysing the hierarchical composition of bamboo fibres. The different failures of bamboo can be explained by the distribution of bamboo cells along the radial section of a single strips. Research by Shao and Wang (2018) and Chen et al. (2015) have found that sections of the bamboo strip with higher volume fraction will be stronger than sections with lower volume fraction. As a result, failure is likely to start in the areas with the least concentration of vascular bundles.

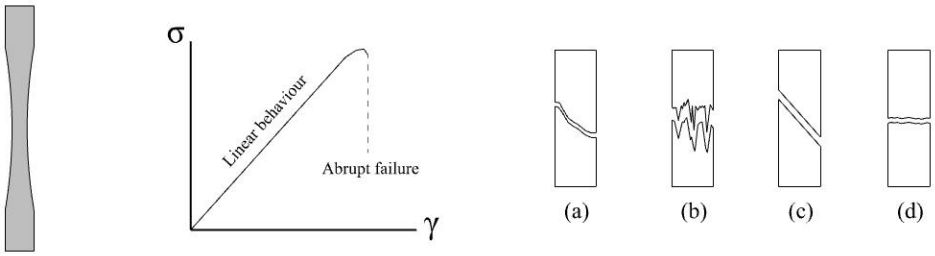

Figure 2. 14: left – test specimen for parallel tension, **centre**- stress-strain curve of specimens subjected to parallel tension, **right** – failure modes of specimens subjected to parallel tension

Perpendicular tension:

The tension test along the perpendicular direction, requires special attention to guarantee that failure occurs in the fibres and not in the grips or in the glue lines. The design of effective perpendicular tension specimens has been the focus of many investigations, particularly for timber-based laminated products. However, the most common geometry used to test the perpendicular tensile properties of laminated bamboo is the specimen described in the ASTM-143 standard (Figure 2.15-**left**). Such specimen has proven to be quite successful due to its easiness to fabricate. However, it has some limitations. For example, the tensile stress is not always distributed along the anvil or tensile area and the

grips can cause additional stress near the curved section of the specimen (Bodig and Jayne 1993). The standard cross section of the test specimen is 25 mm * 50 mm. The maximum tensile strength varies depending on the process used to manufacture the laminated bamboo composites. Sharma et al. (2015a) reported an Ultimate Tensile Strength of 2MPa for caramelised laminated bamboo, while the Ultimate Tensile Strength of bamboo scrimber is superior to that of caramelised laminated bamboo with a value of 3MPa (Sharma, Gatóo, and Ramage, 2015b). Similarly, Khoshbakht et al. (2018) reported an Ultimate Tensile strength of 5.38MPa for laminated bamboo veneer. The standard loading rate of the specimens is 2.5mm/min. Current studies tend to assume that the mechanical properties of the tangential and radial directions are equal. For this reason, researchers only carry out tests in one of the directions. However, research carried out by Sharma et al. (2017) suggests that laminated composites manufactured with strips arranged in the radial direction or flatwise have a superior Ultimate Tensile Strength of 4.20MPa, while laminated composites with strips arranged in the tangential direction or edgewise have an Ultimate Tensile Strength of 3.80 MPa. Further research is needed to fully understand how strip arrangement affects the structural performance of bamboo-based components.

The stress-strain curve of specimens under perpendicular tension shows a linear behaviour prior to failure (Figure 2.15-**centre**). As can be seen in Figure 2.15-**right**, the most common types of failure happen along the reduced section of the specimen and usually start in the strips and not in the glue lines. Delamination is the observable failure of specimens under perpendicular tension. Based on bamboo's hierarchical arrangement, fracture is likely to begin when the interface of the parenchyma cell breaks or the matrix embedding the cellulose nanofibrils breaks, creating fibre delamination.

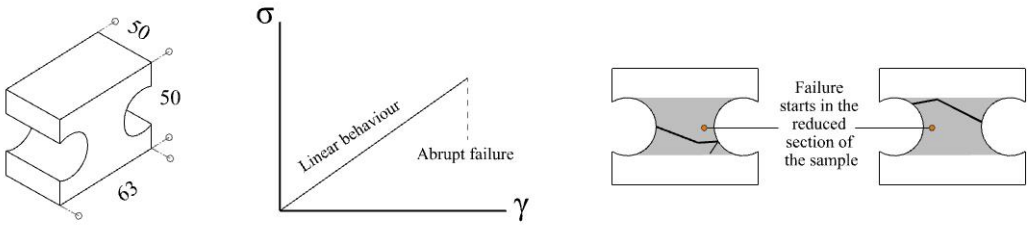

Figure 2. 15: left- test specimen for perpendicular tension, **centre**- stress-strain curve of specimens subjected to perpendicular tension, **right-** failure modes of specimens subjected to perpendicular tension.

2.2.4 Compressive loading

Compression tests are used to determine the behaviour of a material subjected to crushing loads. The results of the test method can be used to calculate Poisson's ratio, Compressive Ultimate Strength, Compressive Yield strength and the Compressive Module of Elasticity of natural and engineered bamboo at different scales.

Parallel compression:

Compression tests along the parallel direction are usually done using a rectangular geometry. The length-to-width ratio of the specimens ranges from 2 to 4. Specimens with higher ratios are not advisable since the test piece will undergo buckling deformation instead of producing a compressive failure (Bodig and Jayne 1993). As shown in Figure 2.16-**left**, the most common dimensions of the test pieces are 50x50x200 mm or 20x20x60 mm, as stated in ASTMD-143 and BS 373-1957. The average loading rate of the specimens is 0.6 mm/min. Previous research has been conducted to characterise the mechanical behaviour of bamboo under compressive loading. The studies have reported compressive values ranging from 34.40MPa (Sharma et al., 2017) to 86MPa (Sharma et al., 2015a), being 55MPa to 65MPa the average range (Sharma, Gatóo, and Ramage, 2015b, Takeuchi, Linero, and Estrada, 2016, Khoshbakht et al. 2017). Research carried out by Li et al. (2013) demonstrated that the compressive strength of bamboo increases as the wall thickness of the material decreases. Hence, the lower section of bamboo culms has a compressive strength of 57.90 MPa, the middle section 61.20 MPa, and the upper section 62.70 MPa. The results of the compressive test can also be used to calculate Poisson's ratio. However, little information can be found of the subject, being Takeuchi, Linero, and Estrada (2016), the only investigation that calculated Poisson's ratios of 0.811 and 0.981 when carrying out compression tests along the parallel direction. Overall, further research is needed to minimise the buckling effect on the tested specimens and establish Poisson's ratios that accurately describe the deformation of bamboo-based components.

The stress-strain curve of specimens under parallel compressive loading shows elastic behaviour follow by a phase on non-linearity and plastic plateau (Figure 2.16-**centre**). Failure of unidirectionally reinforced composites, as it is the case of laminated bamboo, is a mix of complex failure modes due to the heterogeneous nature of the material. Depending on the fibre and matrix interface bonding and the discontinuity of fibres along nodal regions, a mix of failure mechanisms are likely to appear on the specimens until complete failure occurs. As reported by Bodig and Jayne (1993) and Thomsen and Kratmann (2010), some of the most common failures are: (a) fibre kinking, (b) fibre crushing, (c) shear band formation, (d) matrix cracking, (e) splitting, and (f) buckle delamination (Figure 2.16-**right**).

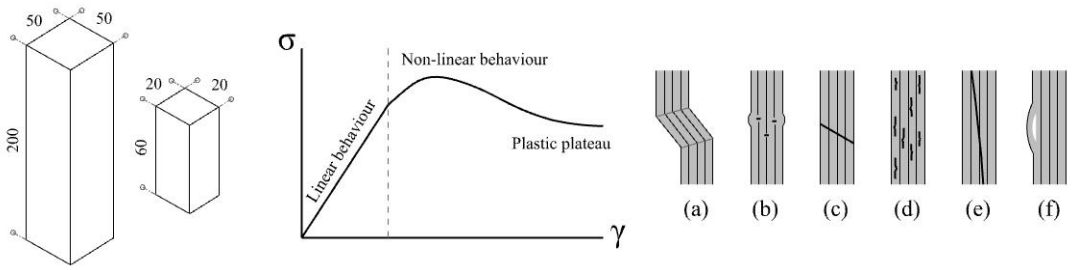

Figure 2. 16: **left-** Test specimens for parallel compression, **centre-** stress-strain curve of specimens subjected to parallel compression, **right-** failure modes of specimens subjected to parallel compression.

Perpendicular compression:

Compression tests along the perpendicular direction are done with specimens shaped as rectangles or cubes. As shown in Figure 2.17-**left**, the common dimensions of the test specimens are 50x50x100-150 mm or 50x50x50 mm. The average length-to-width ratio ranges from 1 to 3. Standards, such as ASTMD-143 and BS 373-1957, are typically used to set up the experimental program, with loading rates ranging from 0.31 to 0.60 mm/min. Even though the graded distribution of bamboo provides different mechanical characteristics along the radial and tangential direction, little research has been done to determine how the graded nature of bamboo affects its mechanical performance. In this regard, Takeuchi, Linero, and Estrada (2016), carried out compression tests along the radial and tangential directions on small-scale specimens with a length-to-width ratio of two. The research suggests that components with strips aligned in the radial direction have a higher compressive strength with a value of 9.28MPa. On the other hand, components with strips arranged tangentially have a value of 7.20 MPa. Contrary to this finding, research on structural-sized specimens suggests a similar compressive strength of 12MPa in both radial and tangential directions (Sharma et al. 2017). Such findings suggest that manufacturing parameters need to be closely documented and controlled to establish a reliable comparison between the compressive behaviour along the radial and tangential directions. Other studies have investigated the compressive strength of laminated bamboo along the perpendicular direction (Sharma et al. 2015a, Sharma, Gatóo, and Ramage, 2015b, Khoshbakht et al. 2017). However, these studies do not specify which direction was tested. Based on these studies, the compressive perpendicular strength of laminated bamboo ranges from 18 MPa to 37 MPa.

As seen in Figure 2.17-**centre**, the stress-strain curve of components under perpendicular compressive loading shows a bilinear mechanical behaviour. Along the radial direction, failure is a mix of parenchyma and fibre fracture mechanisms that create cracking patterns in the tested pieces (Takeuchi, Linero, and Estrada, 2016, Sharma et al. 2015a). Such patterns release energy and displace cell components towards the boundaries of the pieces, which causes buckling in the outer faces (Figure 2.17-**right**). Failure along the tangential direction exhibits a different type of failure. In this case, Takeuchi, Linero, and Estrada (2016), recorded the occurrence of elastic-micro buckling (Figure 2.17-**right**). The representative sinuous geometry of the deformed specimens likely results from cells being displaced towards the path with less resistance. In other words, vascular bundles will re-accommodate in the area that parenchyma cells were previously occupying. However, these conclusions are speculative, and further research is needed to fully characterise the failure development of members under perpendicular compressive loading of the tangential and radial directions of bamboo.

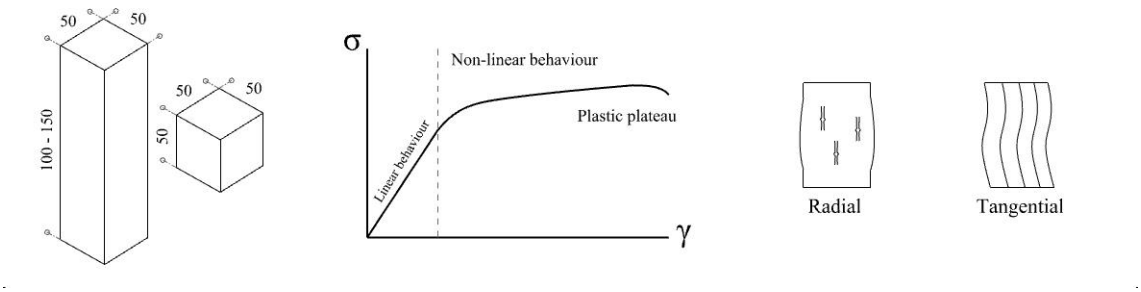

Figure 2. 17: left- test specimens for perpendicular compression, **centre-** stress-strain curve of specimens subjected to perpendicular compression, **right**– compressive failure mode along the radial and tangential directions.

2.2.5 Shear loading

Shear tests are used to determine the mechanical behaviour of a material subjected to a pair of forces acting on opposite directions, creating a sliding failure in the material. The results of the test method can be used to calculate Shear Strength and the Shear Modulus of natural and engineered bamboo at different scales.

Parallel shear:

As shown in Figure 2.18-**left**, shear tests along the parallel direction of the grain are done with two common types of geometry: a 50x50x50 mm cube or a 50x50x63 rectangle with a notched end. Bodig and Jayne (1993) stated that obtaining pure shear stress is difficult to achieve experimentally since the test piece will have to remain in complete equilibrium. Applying two opposite loads induces orthogonal shear stress and additional forces to resist the rotation. Despite the limitations, few innovations and investigations have been done to propose new geometries or testing setups. The standards used to test parallel shear on small-scale specimens are ASTM D143 and BS 373:1957. The average loading rate is 0.6 mm/min. Tests on structural specimens have also been carried out by Sharma et al. (2017), with a loading rate ranging from 0.7 to 0.9 mm/min. Kariuki (2018) reported shear strength values lower than 10MPa. On the other hand, Sharma et al. (2015a), Sharma, Gatóo, and Ramage (2015b), Khoshbakht et al. (2017) and Chen et al. (2019), reported shear strength values ranging from 10 MPa to 20 MPa. These results suggest that bamboo is a brittle material with low strength values when forces are applied against the direction of the vascular bundles.

The stress-strain curve of components subjected to parallel shear loading show a brittle behaviour. The beginning of the curve has a linear section, then non-linearity sets in until abrupt failure occurs (Figure 2.18-**centre**). The typical failure of specimens under parallel shear is fibre splitting (Figure 2.18-**right**). The unidirectional arrangement of the fibres

can explain such failure. If a force is applied against the direction of the fibres, the fibre bonds will break, and fibre splitting will ensue. Once the fibres split, the fracture will quickly follow a linear path until the test piece breaks into two sections.

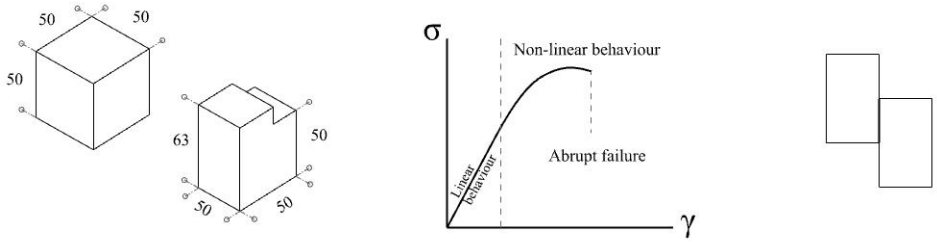

Figure 2. 18: **left**- test specimens for parallel shear, **centre**- stress-strain curve of specimens subjected to parallel shear, **right** – failure mode of specimens subjected to parallel shear.

Perpendicular shear:

Few studies have been carried out to characterise the shear strength of laminated bamboo along the perpendicular direction. For example, Kariuki (2018) used the BS 373:1957 to test the perpendicular shear behaviour of 20x20x20 cubical bamboo pieces. More recently, Estrada, Linero, and Takeuchi (2019) used the ASTM D143 standard to test the perpendicular shear response of 50x50x63 notched rectangular specimens made with laminated Guadua bamboo. However, as can be seen in Figure 2.19, both did not obtain pure shear fracture responses. Instead, the fibres were compressed perpendicularly, resulting in a mix of failures, such as fibre splitting and diagonal cracking – a consequence of the pieces resisting rotation after the load was applied. Bodig and Jayne, in 1993, reported the limitations of using standard test setups to calculate the shear strength of wood-based composites perpendicularly. They stated that **"***because of the extremely high shear resistance across the grain, shear testing of wood is restricted to failure in the longitudinal direction only. Attempts to introduce shear forces in the tangential and radial directions nearly always induce failure in compression***"** (p. 427).

Figure 2. 19: **left** – perpendicular shear failure reported by Kariuki (2018), **centre and right** – perpendicular shear failures reported by Estrada, Linero and Takeuchi (2019).

Bamboo testing is based on wood testing standards. Since little research has been done to identify or develop suitable tests to characterise the perpendicular shear performance of wood-based components, the number of investigations to characterise the perpendicular shear performance of laminated bamboo is scarce. However, recent research has focused on transferring ceramic, metal, or composite testing techniques to characterise the perpendicular shear performance of wood and bamboo-based materials. For example, Archila, Ansell, and Walker (2015) used the Iosipescu test method to calculate the in-plane shear modulus of Guadua bamboo. Like this research, Zhang, and Yang (2017) use the Iosipescu shear test method to determine the shear properties of clear wood. Finally, Bilko et al. (2021) used the Arcan test method to determine the shear properties of pine wood. Further research and experiments are needed to find efficient ways of determining the shear properties of laminated bamboo. Moreover, research should also focus on analysing how the strength along the tangential and radial directions differs. Using methods to test other materials can be a good way of developing shear tests that measure the shear performance accurately along the perpendicular direction.

2.2.6 Considerations for future research

A bamboo-based component subjected to stress will have a maximum stress value. After reaching that value, abrupt failure or prolonged deformation can occur. Once any of these states is attained, the material is considered to have failed. Based on Bodig and Jayne (1993), Figure 2.20 illustrates the stress-strain curves of both conditions. As discussed in the previous sections, members under tensile and shear loading – both in the parallel and perpendicular directions – will break abruptly after reaching a maximum load. On the other hand, members subjected to compressive loading – both in the parallel and perpendicular directions – will fail after experiencing considerable deformation. Determining these stress-strain relationships is essential to establish the failure behaviour of any material. Moreover, mapping out the stress values that trigger failure in different settings and investigating failure onset and its subsequent development is essential to guarantee the structural reliability of laminated bamboo composites.

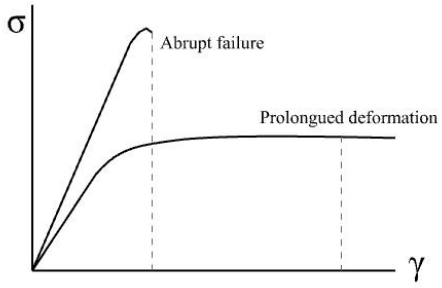

Figure 2. 20: Stress-strain curves defining the failure modes of laminated bamboo.

Many studies have been carried out to determine the mechanical properties of laminated bamboo, particularly on samples subjected to tensile and compressive loading along the parallel direction. Most of the available literature classifies the different failure types of laminated bamboo. Additionally, lateral research done on the cellular structure of bamboo can shed some light on the underlying failure mechanisms of the material. However, no current study has provided a detailed description of how damage starts and propagate. Moreover, no study has focus on identifying how the physical characteristics of bamboo strips and arrangement influence the deformation and failure of laminated bamboo. A comprehensive analysis of how laminated bamboo deforms, fails, and eventually fractures in the three directions (longitudinal, radial, and tangential) is yet to be completed. Such analysis can provide valuable insights to develop tools to assess the structural integrity of existing buildings, as well as optimising the design of structural members made with laminated bamboo. One of the main limitations towards developing robust designing such tools is the lack of information on the mechanical performance of laminated bamboo along its perpendicular direction. Particularly the scarcity of studies that distinguish the mechanical performance of the tangential direction from the radial direction. Additionally, the characterisation of mechanical properties of elements under perpendicular shear is usually overlooked by researchers since it is assumed that the member will undergo other types of failures before reaching perpendicular shear failure. Overall, laminated bamboo is an engineered material that became commercially available recently. As such, more experimental studies are needed to fully characterise the material's mechanical response and improve its use as a structural material.

2.3 Predicting material behaviour and failure

2.3.1 General considerations

A material fails once it can no longer fulfil its primary purpose (Huda, Bulpett, and Lee, 2010). Predicting failure is essential to preserve the life of a building, prevent accidents and optimise the attributes of a material (Eberhart, 2007) As mentioned in the previous section, laminated bamboo can fail by undergoing brittle fracture or plastic deformation. Predicting how a material deforms and eventually fails is essential to assess the integrity of structural members and design strategies to enhance their mechanical response. Models to predict material behaviour are developed with real observations later synthesised into analytical and computational frameworks simulating the observed phenomena (LeMaître, 2001). Currently, computational, and numerical modelling techniques are the most widely used to understand and predict the behaviour of materials. However, the numerical models simplify the complexity of natural material such as bamboo and bamboo composites.

The number of available publications on models used to predict bamboo composites' mechanical response and failure is limited. For this reason, the following section summarises the modelling techniques that have been developed to simulate the mechanical response of both natural bamboo and laminated bamboo composites. Researchers have used two-dimensional, three-dimensional, and structural models to investigate the macro-mechanical response of raw bamboo and laminated bamboo composites under different loading scenarios. Finally, this section discusses how geometric methods can be used, instead of numerical methods, to create user-friendly tools that predict material failure with an acceptable degree of accuracy.

2.3.2 Two-dimensional models

Two-dimensional modelling requires the input of fewer parameters and simplifies mechanical behaviour to only two dimensions. Because of this, researchers use this approach to investigate how the surfaces of a given material deform under different loading settings. Such approach has only been applied to model the response of small pieces of laminated bamboo. Reynolds et al. (2016) used a numerical model to characterise the mechanical performance of bamboo dowelled connections. The authors used the Lekhnitskii function to determine the stress distribution around holes. This function has been successfully used to model stress distribution in orthotropic plates loaded by a dowel, both in timber and fibre-reinforced composites. The model is two-dimensional and based on a state of plane stress. The model was calibrated and validated with experimental data. The results suggest a good correlation between the experimental data and the Finite Element analysis. Like this research, Khoshbakht et al. (2018) used a two-dimensional plane strain Finite Element model to simulate and predict the mechanical behaviour of laminated bamboo veneer dowel connections under compression. The model was calibrated with data obtained from compression, tension, shear, and embedment tests. The model was developed using ADINA software. To optimise the model's reliability, the authors trialled different mesh configurations, contact parameters, and load settings. The calibrated model examined the stress distribution and progressive development of failure in the region located under the dowel. The study suggests that friction between the laminated bamboo veneer and the dowel significantly impacts the progressive development of structural failure.

On the other hand, research at the National University of Colombia has focused on exploring the development of two-dimensional constitutive models that accurately describe the mechanical behaviour of Guadua bamboo. Takeuchi, Estrada, and Linero. (2018) used a numerical model of Finite Elements to study the shear strength and crack

pattern of laminated Guadua bamboo. The authors used Experimental data to calculate the shear strength values. The model is based on the Continuum Strong Discontinuity Approach for composite materials and the Weibull probability model to describe the progressive failure process on the parallel fibre bundles. The crack direction obtained in the numerical simulations is approximately equal to that observed in the experimental data, regardless of the fibre orientation. Based on the previous research, Estrada, Linero, and Takeuchi (2019) used a numerical model to predict the appearance of cracks and calculate their propagation in elements made with Laminated Guadua Bamboo (LGB). The material was modelled as a unidirectional fibre-reinforced composite. The two-dimensional damage constitutive model was used to describe the behaviour of the parenchyma cells (the matrix), while the one-dimensional constitutive model was used to describe the macroscopic behaviour of the vascular bamboo bundles (unidirectional fibres). The homogenisation method used in the formulation is the Mori-Tanaka Scheme. The authors used the Continuum Strong Discontinuity Approach (CSDA) to simulate the fracture mechanics of laminated bamboo. The code was written with Fortran and implemented in COMET; a FE-based open-source software used to solve non-linear mechanical problems. Tension and shear small-scale tests were performed to validate the reliability of the model. The developed model represents with a high degree of accuracy the two-dimensional crack patterns of LGB specimens subjected to tensile and shear static loading. For the shear pieces, the model accurately predicts the different failure modes of different fibre orientations. The research is still under development, and it is not clear if the researchers will adjust the current investigations to account for the three-dimensional behaviour of the material.

Even though two-dimensional models fail to describe how stress and strain fields propagate in three-dimensional bodies, their implementation requires fewer variables. Also, they need less computational and time resources, which makes them ideal to quickly gather information on the behaviour of materials with complex mechanical responses.

2.3.3 Three-dimensional models

Even though the orthotropic nature of bamboo is widely acknowledged, the lack of information to characterise the transverse properties of bamboo has promoted a tendency to model bamboo as a simplified transversely isotropic material. García, Rangel, and Ghavami (2012) developed a Finite Element model to determine the elastic constants of full culm Guadua bamboo along the transverse axes. The authors carried out dynamic loading tests on rings obtained from three and five years old Guadua culms. The tests measured the radial circumferential Poisson's ratio and the elastic constants. The values

were later used as the material properties of a transversely isotropic model implemented in ABAQUS. The material was assumed to be a cylinder with wall-thickness variations along its length. For this study, the transverse plane is assumed to be isotropic in nature and the constants are the same in both the radial and tangential directions. Chand, Shukla, and Sharma (2008) built a finite element model, in ABAQUS, to determine the stress and strain values of bamboo under tension. The authors modelled bamboo as an isotropic material and used the nine engineering constants to run the simulations. Godina and Lorenzo (2015) used a composite material model to describe the macroscopic behaviour of bamboo culms. This study modelled bamboo as an orthotropic material with transversely isotropic properties along the transverse plane. Compressive small-scale tests and volume fraction analyses were carried out to build a hollow cylindrical beam with three layers. The mechanical properties of each layer resemble the properties of the wall culm as the percentage of vascular bundles increases toward the outer layer. The model considers variation along the transverse plane, yet it fails to address how node discontinuity affects the mechanical performance of bamboo. Ramful and Sakuma (2020) also used a transversely isotropic approach to model the fracture mechanics of bamboo culms. The material parameters of the model were experimentally determined with a series of small-scale specimens. To develop the model, the radial and tangential properties of bamboo were considered equal. The model was developed in a Finite Element software called FEMAP.

With the aim of acknowledging the graded nature of bamboo along the transverse axis, Akinbade et al. (2021) used the results of a series of circumferential ring tests to develop four models to simulate the mechanical behaviour of full culm bamboo. The authors used the standard ISO 22157:2019: Bamboo structures to conduct the tests. Like the previous studies, bamboo is assumed to behave as a transversely isotropic material. However, in this study, the transverse or radial plane is assumed to have functionally graded properties. The models were developed in ABAQUS. The first model was based on Castigliano's equations for thin-walled rings under diametrically oriented compression. In this model, bamboo is assumed to have homogeneous radial properties. The second model is a Finite Element model where the orthotropic mechanical properties of the material are calculated using a gross section fibre volume factor and the rule of mixtures equations; however, the graded nature of the culm is not considered in the model. The third model is a Finite Element model. The culm of the bamboo is divided into ten concentric annular rings with distinctive orthotropic mechanical properties calculated with the rule of mixtures. The fourth model is a user-defined constitutive Finite Element model developed using a customised ABAQUS User Subroutine (UMAT). The subroutine automatically calculates and predicts the changing parameters of the material at different integrations points of the mesh. Model four is the one with a higher degree of accuracy compared to the test specimens' performance. This suggests that the graded distribution of cells along the

radial direction should not be omitted when developing models that accurately capture the nature of bamboo. Further research is needed to explore how reliable it is to dismiss the hierarchical structure of bamboo and simplify it using a transversely isotropic approach.

2.3.4 Structural models

Recent studies are also focusing on exploring strategies to model the behaviour of structural assemblies made with bamboo or bamboo-based components. For example, Fang et al. (2015) used a Finite Element model to simulate and predict the load deflection-response of GFRP-bamboo-wood-sandwich beams. Shear bonding tests between wood and bamboo, and 4-point full-size static tests were performed to obtain the mechanical properties for the model, as well as validating the model. The authors used a simplified model based on Timoshenko beam theory and the sandwich beam theory to simulate the 3-dimensional behaviour of full-size beams. MATLAB and ANSYS were the platforms selected to run the simulations. Each material was modelled with lamina properties along the three axes, hence, the 9 engineering constants of each material were used for the model. The results showed a significant correlation between the numerical simulations and the experimental data. Ngudiyono et al. (2019) developed a UMAT–ABAQUS subroutine to approximate the long-term behaviour of Glued-Laminated bamboo (GLUBAM) structural components. The authors employed a rheological creep model for viscoelastic materials. The model considers time, loading, temperature, and humidity as the inputs needed to determine long-term creep. Two approaches were used to develop the model: the power law approach and the Maxwell approach. The study suggests that the power law approach is more effective when modelling structural laminated components.

The structural models are developed with pre-determined functions available in software used to solve linear and non-linear problems. However, without a clear understanding of the three-dimensional behaviour of bamboo, the models can only be considered exploratory. Further research is needed to fully characterise, predict, and simulate the mechanical response of structural components manufactured with bamboo.

2.3.5 Numerical vs. geometric methods

As can be seen in the previous review, numerical techniques are the go-to approaches used to model complex physical problems, such as the deformation of materials. Overall, the Finite Element Method is the preferred method to simulate the performance of either

natural or laminated bamboo. The material's mechanical properties are used as input to solve a series of differential equations that approximate the behaviour of real-life phenomena. Although highly used in physics and engineering, the method has some drawbacks. For example, the most noticeable disadvantage is that approximation is less accurate as the shapes/systems become more complex. For this reason, physical problems are usually simplified, and oversimplification can result in misrepresenting real-life problems.

Coolidge (2003) argues that non-traditional approaches, such as geometric methods, can be successfully applied to study materials' behaviour. Geometric methods focus on reducing the complexity of a figure to its basic geometric units such as points, lines, vectors, geometric shapes, etc. (Needman, 2021). By assigning a coordinate system to different geometric units, it is possible to track their transformation. Their advantage lies in the fact that these methods require less computer power and complexity, can be implemented in different geometry-based software, and have the potential to be scalable. Examples of successful implementation of geometric methods can be found in the following disciplines: geometric modelling, computer graphics, computer vision, robotics, machine learning, etc. (Gallier 20011, Peters, 2020). The most common application of geometric principles is the analysis of visual mediums, such as images, and the digital representation of solids or objects using computer graphic techniques (Klette and Rosenfield, 2004).

The literature review suggests that a limited number of attempts have been made to explore the use of geometric methods and graphic means to approximate the behaviour and representation of materials. In 2010, Kapko et al. used geometric methods to investigate the flexibility of zeolite frameworks. In their work, they discovered that the zeolite framework joints are flexible and not rigid, as thought before. In 2011, Rudnev, Semukhin, and Klishin used elliptic Riemannian geometry to model crystal structures. In 2015, Setaluri et al. used image deformation techniques and grid-based geometric methods to simulate the two-dimensional deformation of elastic membranes. More recently, Semenova et al. (2021) used geometric methods to investigate how the structure of crystals changes as composites are formed. These publications demonstrate that geometric methods can be applied to analyse material behaviour, determine materials' properties, and simulate material deformation.

Material deformation and failure are problems related to how an object's shape changes over time as a load is applied. Hence, it is possible to assume that the deformation of a material can be explained and modelled using geometric methods. These methods have

not been used to model the behaviour of laminated bamboo composites, but exploring their application is a novel approach that could signal new avenues to understand and predict the material's behaviour when used as a structural element.

2.3.6 Considerations for future research

Overall, models used to simulate the mechanical response of bamboo and bamboo-based components at different length scales are recent, scattered throughout the literature and lack continuity. The reality is that the lack of robust knowledge about the mechanical behaviour of bamboo along the longitudinal, radial, and tangential directions prevents the construction of comprehensive tools able to predict the mechanical response of the material. Additional testing and additional understanding of damage propagation and failure criteria are needed to fully analyse and capture how the functionally graded properties of bamboo fibres and their arrangement affect the macro mechanical behaviour of bamboo-based components.

Current research shows a trend of using the Finite Element Method to simulate and predict the mechanical behaviour of natural and laminated bamboo. The models fail to properly acknowledge the orthotropic nature of laminated bamboo, the impact that the cellular distribution of fibres has on the material's performance and how to accurately represent the fibre discontinuity of nodal sections. When using the Finite Element Method, the variability of heterogeneous materials – such as laminated bamboo – is usually simplified. For this reason, the cellular and mechanical complexity of laminated bamboo is usually simplified. Using other modelling approaches, such as geometric methods, can help bridge that gap since they require less computational complexity and resources. Moreover, the hierarchical structure of laminated bamboo can be synthesised into an array of geometric units, such as points, lines, vectors, tessellations, etc. Doing this can be a novel approach to model and predict the mechanical response of laminated bamboo composites when used as structural elements.

2.4 Summary of key findings

The previous sections provided an overview of the advantages and challenges of using laminated bamboo as a reliable building material. In the first section, the factors that can influence the mechanical performance of laminated bamboo were identified. The second section of the review summarised the research that has been carried out to characterise the mechanical behaviour, deformation, and subsequent failure of laminated bamboo

composites. Finally, the third section of the review provided a summary of the research that has been done to create models that accurately simulate and predict the mechanical behaviour of laminated bamboo. The efficient development of strategies to predict and assess the structural behaviour of bamboo rely on an accurate characterisation of the mechanical behaviour of the material. Overall, the main observations and findings of the literature review are summarised as follow:

- Engineering bamboo is a technology that can help regulate and promote the use of laminated bamboo as a serious alternative to structural timber.

- The process of manufacturing laminated bamboo composites requires different steps, including, material selection, processing raw bamboo into regular bamboo strips, treating bamboo strips, selecting, and applying adhesive and pressing the strips into regular sections. Every step of the process can have an impact in the mechanical performance of the material. Efforts to regulate the manufacturing process are essential to promote the use of laminated bamboo as a reliable structural material.

- The main constituents of laminated bamboo composites are bamboo strips. The cellular arrangement of vascular fibre bundles and the location of nodes will affect the mechanical properties of bamboo strips. It is important to determine how the characteristics of bamboo fibres affect the behaviour of laminated bamboo.

- The characteristics of bamboo strips and their arrangement, make laminated bamboo and orthotropic material. Hence, the material has different properties along the longitudinal, radial, and tangential direction. To simplify the material's complexity, the radial and tangential directions are assumed to have similar properties. Additional research is needed to validate this assumption.

- Current research has focused on determining the mechanical properties and common failures of laminated bamboo under tensile, compressive and shear loads. However, none of these studies provide a detailed description of how damage propagates as the material deforms and eventually fails. Additionally, the studies do not address how the role that the physical characteristics of bamboo strips play in the behaviour of the material. A comprehensive atlas of how laminated bamboo's failure mechanisms evolve – in the longitudinal, radial, and tangential directions - can help develop tools to guide the design and reinforcement of structural elements made with laminated bamboo.

- Numerical methods are currently being used to model and predict the mechanical responses of both natural and laminated bamboo. These methods often fail to accurately represent the complexity of heterogeneous materials. In the case of

modelling bamboo, current models do not acknowledge the orthotropic nature of bamboo, nor do they acknowledge the cellular distribution of bamboo fibres and fibre discontinuity in nodal regions. The use of geometric methods can help overcome these limitations.

Chapter 3 | Methodology

| This chapter summarises the methods used to achieve the objectives of the research. The first part outlines the objectives of the investigation. The second part describes the constraints of the project. The third part describes the methods used to design and carry out the experimental program. The fourth part described the methods used to analyse the experiments' results. Finally, the fifth section outlines the methods used to establish a procedure to predict laminated bamboo's deformation and failure modes. |

3.1 General objectives

As stated in Chapter 1 - section 1.5.2 – this study aims to identify how the physical characteristics of bamboo strips influence the mechanical response of laminated bamboo composites and establish a methodology to use these characteristics as parameters to predict the deformation and failure modes of the material. The following objectives were outlined to achieve the aim of the research:

Objective 1 – To design an experimental program to identify how the physical characteristics of bamboo strips determine the mechanical behaviour, deformation, and failure modes of the material.

Objective 2 - To analyse the results of the experimental program and map out the patterns that determine the deformation and failure modes of laminated bamboo composites.

Objective 3 - To establish a methodology that uses the physical characteristics of bamboo as an input to predict the deformation and failure of laminated bamboo composites.

The literature review findings suggest that the physical features of bamboo strips and the process used to manufacture bamboo laminates determine the material's structural performance. However, bamboo strips are the main constituents of the laminates, and their impact on performance is expected to be more significant. Failure due to poor manufacturing practices can be minimised or prevented through manufacturing

optimisation. Contrary to this, failure due to material characteristics can only be prevented through developing a deep understanding of how the natural irregularities of bamboo strips affect the materials' performance. For this reason, this research is mainly concerned with analysing how the physical characteristics of bamboo strips influence the deformation and failure of bamboo laminates.

The following sections outline the methods that were used to achieve the objectives of the research.

3.2 General constraints

The experimental program and subsequent analysis were carried out during the outbreak of the COVID-19 pandemic. Consequently, the process of preparing and testing the test pieces was severely disrupted. Initially, the manufacturing and test program were planned to be carried out at the facilities of the University of Sheffield. However, the facilities remained close from March 2020 to October 2020. After this date, access to the facilities remained limited. Part of the experimental program was carried out at the National Cheng Kung University in Taiwan to account for these constraints. The other part of the testing program was carried out in the Lea Lab at the University of Sheffield.

3.3 Experimental program

3.3.1 Static testing

The properties and behaviours of materials can only be determined experimentally. Static tests are frequently used to map out the behaviour of various materials. Static testing is used to determine materials' strength and deformation behaviour when a load is applied slowly and constantly. Uniaxial tension, uniaxial compression and uniaxial shear are the tests more commonly used to characterise the mechanical properties of materials. A series of static tests were designed to identify how the physical characteristics of bamboo strips affect the deformation and fracture of laminated bamboo. The objective of the tests was to record the deformation and evolution of damage in the three directions of the material. Hence, tensile, compressive and shear tests were carried out in the longitudinal, radial, and tangential directions of laminated bamboo composites.

Even though there are no test standards developed exclusively for determining the properties of bamboo and bamboo-based products, laminated bamboo is assumed to have properties similar to engineered timber products. Recent publications have characterised the mechanical properties of laminated bamboo using standards published by the American Society for Testing and Materials (ASTM) and the British Standards Institution (BSI) (Xiao, Yang, and Shan, 2013, Sinha, Way, and Mlasko, 2014 and Sharma et al., 2015a). To compare and validate results with the available literature, the experiments of this research were also carried out following ASTM and BSI procedures. The material and mechanical properties of laminated bamboo were obtained with tension, compression and shear tests based on ASTM D3500-20 – *Standard Test Methods for Wood Structural Panels in tension*, ASTM-D143-14 – *Standard Test Method for Small Clear Specimens of Timber*, and BS 373:1957 – *Methods of testing small clear specimens of timber*. The radial and shear properties were obtained with modified three-point short-beam tests. These standards were selected because the literature review suggested an agreement – in the research community – that the methods are reliable to determine the mechanical properties of laminated bamboo composites. Moreover, the standards use small-sized specimens, which can be manufactured using fewer materials and resources.

For this research, the size of the samples was calculated by determining the average sample size of previous publications. Authors have used samples ranging from 10 to 20 specimens to investigate laminated bamboo's mechanical behaviour (Sharma et al., 2015-a, Sharma, Gatóo, and Ramage, 2015-b, Chen et al., 2019). Based on this analysis, an average sample size of 12 specimens is sufficient to determine the mechanical properties of laminated bamboo. Hence, for this study, 12 specimens were tested for each variable. In the case of tensile tests – in the longitudinal direction – the specimens broke at different sections. For this reason, the sample size was increased to 15 specimens to augment the probability of mapping out the reasons why the material broke at different locations. In total, 111 pieces were used to identify the deformation and failure patterns of laminated bamboo:

- 15 specimens for tensile testing in the longitudinal direction
- 12 specimens for tensile testing in the radial direction
- 12 specimens for tensile testing in the tangential direction
- 12 specimens for compressive testing in the longitudinal direction
- 12 specimens for compressive testing in the radial direction
- 12 specimens for compressive testing in the tangential direction
- 12 specimens for shear testing in the longitudinal direction
- 12 specimens for shear testing in the radial direction
- 12 specimens for shear testing in the tangential direction

3.3.2 Materials

The pieces for the experimental program were fabricated using three materials. The pieces for longitudinal tension were fabricated with 600x600x19mm solid bamboo panels. In contrast, the specimens for radial tension, tangential tension, longitudinal compression, radial compression, tangential compression, and longitudinal shear were manufactured with 50X200X2000 and 50X36X2000 N-Finity beams. Moso bamboo surfaces, UK supplied both materials. The beams and the panels were made with side-pressed Moso bamboo strips glued together with Phenol-Formaldehyde resin (PF). The recorded moisture content of both materials was 2%. The physical and mechanical properties of the materials were provided by the supplier and are outlined below in Table 3.1:

Density	**Tensile strength**		**Compression strength**		**Shear strength**		**Elastic module**
	Parallel	Perpend.	Parallel	Perpend.	Parallel	Perpend.	
kg/m3	N/mm2	N/mm2	N/mm2	N/mm2	N/mm2	N/mm2	N/mm2
700	39.90	2.80	34.40	9.20	6.50	-	8866

Table 3. 1: Physical and mechanical properties of N-Finity Moso bamboo beams and panels.

On the other hand, the fabrication of the radial and tangential shear pieces was done with 10x10x1600mm Moso bamboo strips shipped by a local seller from Tianjin, China. The supplier did not provide the physical and mechanical properties of the strips. However, upon arrival, the moisture content of the strips was measured and recorded to be 3%.The moisture content of all materials were measured with a digital wood moisture meter.

3.3.3 Tension tests

Longitudinal tension

The specimens for longitudinal tension were fabricated with 600X600X19mm solid bamboo panels. The pieces were manufactured according to the geometry specified in ASTM-D3500-20. Figure 3.1-**a** shows the final geometry of the test pieces. The pieces were tested at a load rate of 0.9mm/min. The pieces were pulled apart using self-aligning wedge-type grips, as specified in the test standard. Figure 3.1-**b** shows the final test set-up. The sample was tested at the Lea Lab in the University of Sheffield. The machine used to carry out the tests was a Tinius Olsen universal testing machine with a load capacity of 25kN.

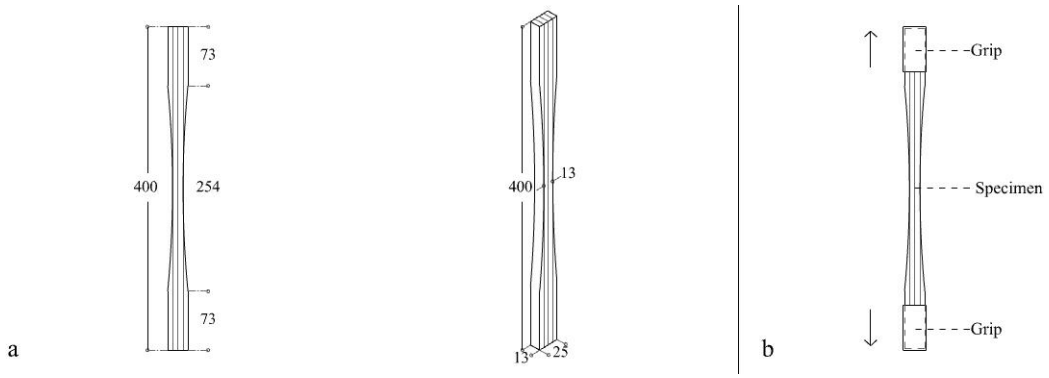

Figure 3. 1: Configuration of tensile tests in the longitudinal direction.

Radial and tangential tension

The specimens for radial and tangential tension were fabricated with 50X36X2000 mm N-Finity bamboo beams. The pieces were manufactured according to the geometry specified in ASTM-D143-14. However, due to the dimensions of the beams available in the UK, the thickness of the pieces was reduced to 36mm, instead of 50mm. Figure 3.2-**a** shows the final geometry of the test pieces. The pieces were tested at a load rate of 2.5mm/min. Special steel grips were manufactured to fasten the pieces. Figure 3.2-**b** shows the final test setup. The sample was tested at the Lea Lab in the University of Sheffield. The machine used to carry out the tests was a Tinius Olsen universal testing machine with a load capacity of 25kN.

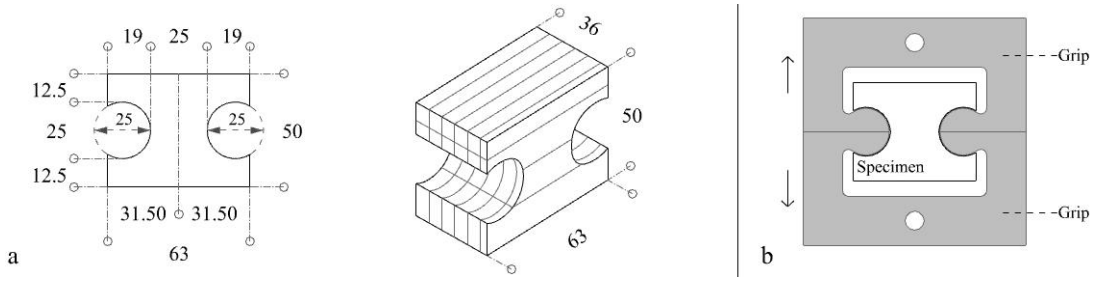

Figure 3. 2: Configuration of tensile tests in the radial and tangential directions.

3.3.4 Compression tests

Longitudinal, radial, and tangential compression

The compression specimens were fabricated with 50x200x2000 mm N-Finity bamboo beams. All the pieces under compressive loading were tested at the National Cheng Kung University in Taiwan. The specimens of the compression tests were the only pieces sent to Taiwan for testing. This happened because the testing facilities in Sheffield (the Lea

lab) did not allow students to use testing machines with loading capacities greater than 25 kN, and the compression pieces were expected to break at a higher loading rate. The specimens were cut and prepared for testing in Sheffield. Then, all the pieces were shipped and carefully packed using protective plastic wrap.

All the test pieces were manufactured following the guidelines outlined in BS 373-1957. As shown in Figure 3.3-**a**, the final geometry of the specimens was a 50x50x50mm cube. The pieces were tested at a load speed of 1mm/min. The pieces were crushed using standard compression plates. Figure 3.3-**b** shows the final test set-up. The machine used to test the sample was a Mayes hydraulic machine with a load capacity of 100kN.

One of the limitations of testing the samples in Taiwan was that it became challenging to ship them back to the UK, given the ongoing COVID-19 shipping restrictions. Due to this, I could not examine the broken specimens and relied only on the digital data sent from the researchers at National Cheng Kung University.

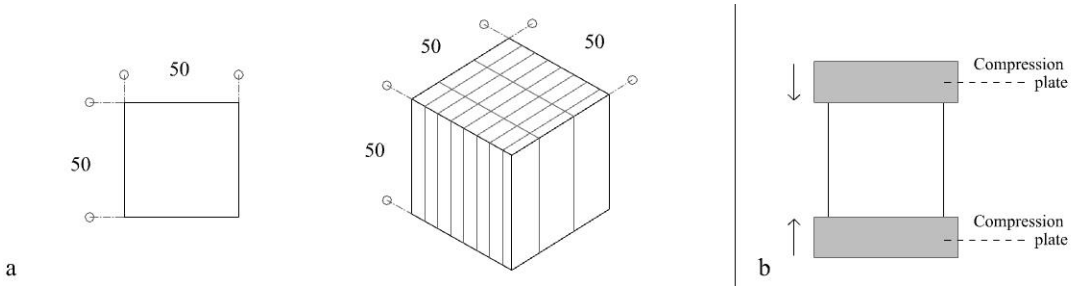

Figure 3. 3: Configuration of compressive tests in the longitudinal, radial, and tangential directions.

3.3.5 Shear tests

Longitudinal shear

The specimens for longitudinal shear were manufactured with 50X36X2000 mm N-Finity bamboo beams. The test pieces were manufactured according to the specifications outlined in ASTM-D143-14. However, due to the dimensions of the beams available in the UK, the thickness of the pieces was reduced to 36mm, instead of 50mm. Figure 3.4-**a** shows the final geometry of the specimens. The pieces were tested at a load rate of 3mm/min. Special steel grips were manufactured to carry out the experiment. The final set up of the test is shown in Figure 3.4-**b**. The sample was tested at the Lea Lab in the University of Sheffield. The machine used to carry out the tests was a Tinius Olsen universal testing machine with a load capacity of 25kN.

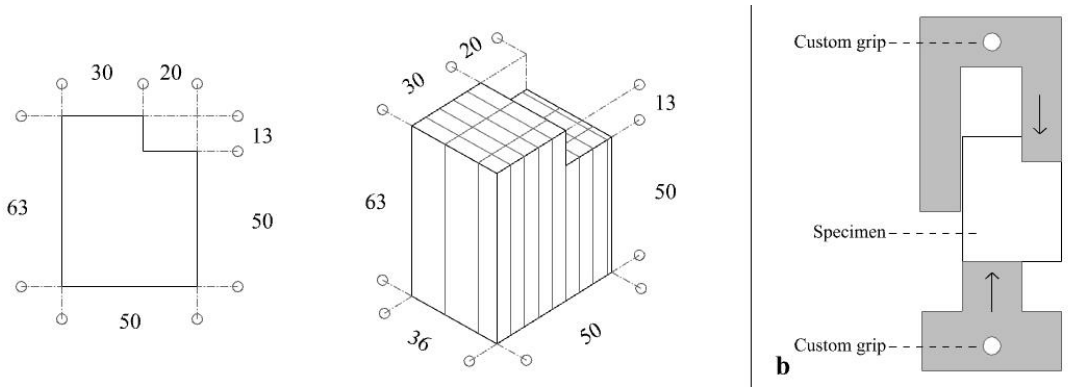

Figure 3. 4: Configuration of shear tests in the longitudinal direction.

Radial and tangential shear

Bodig and Jayne (1993) state that the shear strength of fibres across the radial and tangential directions makes it challenging to induce shear forces in experimental setups. Initially, the radial and tangential shear pieces were manufactured the same way as the longitudinal sample. However, as shown in Figure 3.5-**a**, the shape of the pilot specimen was not altered as the load neared 25kN (the maximum loading capacity of the test machine). Figures 3.5 **b** to **c** show the state of the test piece after loading. The piece only had a slight indentation in the bottom face. The pilot test results demonstrated that the shear strength across the grain is high, and shear failure across the grain is likely to happen at later stages of the deformation process. Hence, predicting shear failure across the grain is not a priority since the piece is expected to fail by other mechanisms before perpendicular shear occurs.

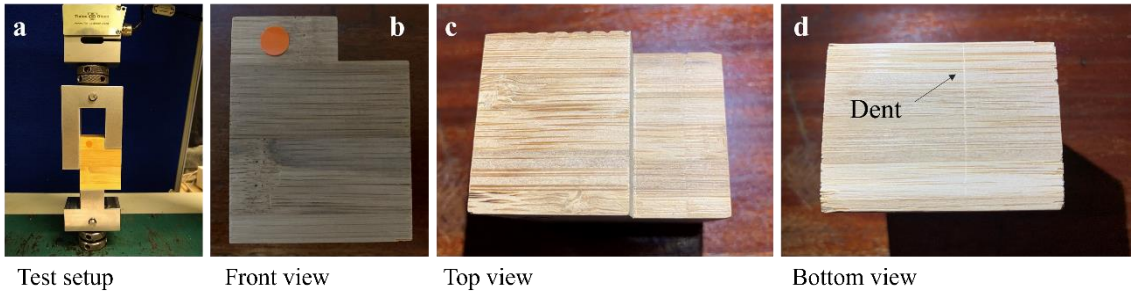

Figure 3. 5: Initial configuration of perpendicular shear tests.

The outcome of the pilot test opened avenues to explore the use of alternative shear tests to investigate the shear response of bamboo fibres. In chats with my supervisor - from the Mechanical Engineering department - it was discussed the possibility of using a modified three-point short beam test to induce shear forces in small-sized bamboo specimens. This

setup has been successfully used - at the Lea lab - to characterize the mechanical shear response of different alloys. At this point, the aim of the radial and tangential shear tests was to explore the applicability of using a modified three-point short beam shear test to characterize the shear response of bamboo fibres across the grain.

The selected setup required the production of small specimens with a maximum size of 10x15x50mm. As seen in Figure 3.6, the fixture used to carry out the tests had three components. The upper part is a steel block used to apply the force in the mid-section of the specimen (Figure 3.6-**a**). The middle part is a steel plate to fix the specimen (Figure 3.6-**b**). Finally, the lower part of the fixture is the base where the small-sized specimens sit (Figure 3.6-**c**). Due to the size constraints of the test setup, it was decided to use strips to produce the specimens. The radial and tangential shear specimens were the only ones done with strips and not bamboo laminates. The main aim of this experiment was not to characterise the radial and tangential shear mechanical properties. Instead, this setup aimed to explore whether alternative shear tests could be applied to bamboo. This is why the use of bamboo strips was considered acceptable.

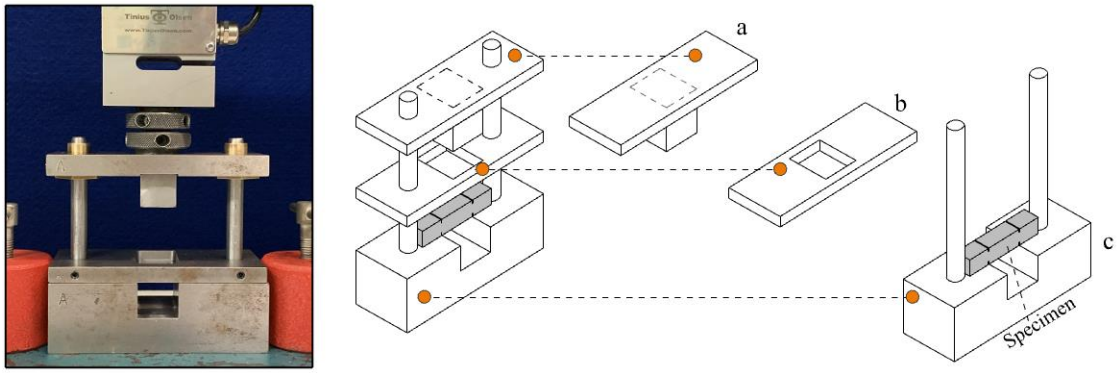

Figure 3. 6: Fixture for the modified three-point short beam tests.

The new radial and tangential shear test pieces were fabricated with 10x10x1600 mm Moso bamboo strips. The final geometry of the reduced pieces is shown in Figure 3.7-**a**. The pieces were tested at the same load rate as those subjected to longitudinal shear, i.e., 3mm/min. The final setup of the test is shown in Figure 3.7-**b**. The samples were tested at the Lea Lab at the University of Sheffield. The machine used to carry out the tests was a Tinius Olsen universal testing machine with a load capacity of 25kN. The final test pieces did not have nodal regions. Due to the fragility of nodal areas and the reduced size of the specimens, the bandsaw blade kept breaking apart the strip nodes. For this reason, it was decided to manufacture and test only specimens without nodes.

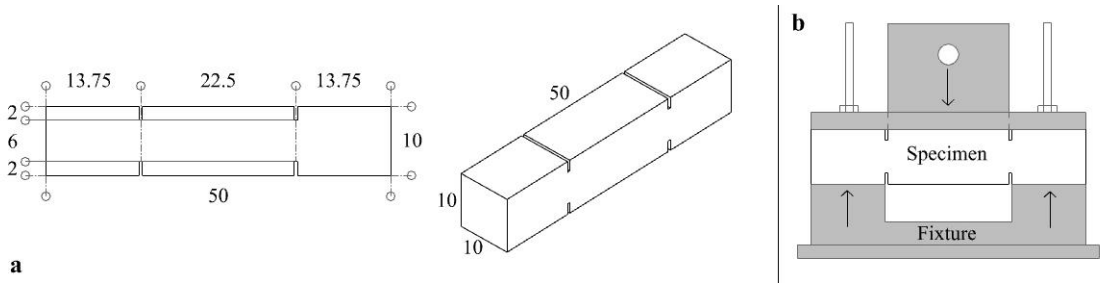

Figure 3. 7: Configuration of shear tests in the radial and tangential directions.

3.3.6 Full-field strain measurement

The main aim of the research was to identify how the physical features of bamboo strips affected the mechanical response of bamboo laminates. All the specimens had different physical characteristics across the tested surfaces. To achieve the purpose of this research, it was necessary to record and analyse the deformation of the entire tested surfaces. Doing this enabled the establishment of a clear link between bamboo strips' physical features and the deformation process. Conventional strain measurement techniques, such as extensometers and strain gauges, only measure deformation in selected points and directions (Górszczyk, Malicki, and Zych, 2019). In comparison, the Digital Image Correlation (DIC) technique can measure full-field deformation in all directions. For this reason, the use of DIC was prioritised over the use of conventional strain measurement methods.

Various authors have successfully used the DIC method to investigate the strength and mechanical properties of laminated bamboo composites (Archila et al., 2014, Tinkler-Davies and Shah, 2021, Wang et al., 2021). The method is a non-contact technique and has proven to be a reliable strategy to characterise the mechanical behaviour of bamboo laminates. Given the aim of this research and the recorded reliability of the method, it was decided not to use standard strain measurement techniques to complement the data collected by the DIC equipment.

The DIC technique aims to track patterns in a series of images. As stated by Jones and Iadicola (2018), the method follows three steps: (1) apply a speckle pattern on a specimen, (2) capture images of the specimen as it deforms, and (3) use correlation algorithms to compute displacement or deformation. Figure 3.8 illustrates the steps of the technique.

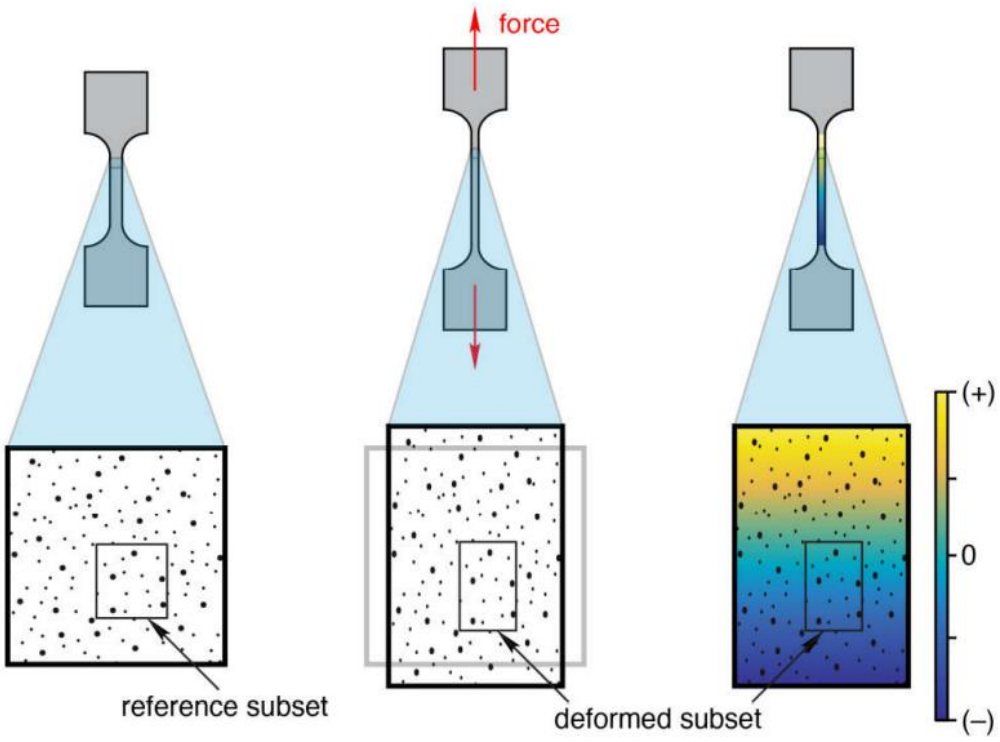

Figure 3. 8: DIC steps. Source: LePage, (2020)

For this research, the following procedure was used to apply the Digital Image Correlation technique on the tested pieces:

Applying the speckle patterns: a speckle pattern was applied in all the samples to track the deformation of the pieces. First, a thin layer of White Matt aerosol paint was applied on one of the faces of the pieces. Then, a speckle pattern was applied using black acrylic paint and an airbrush. Figure 3.9-**a** shows the speckles applied on one of the tested specimens.

Capture deformation: The StrainMaster system from LaVision was used to record and process the deformation of the specimens as the load was applied. The system uses a high-resolution digital camera to record the deformation of the pieces. The data were stored and processed by a device control unit with an integrated AD converter. Figure 3.9-**b** shows the DIC setup.

Compute displacement: Finally, the captured images were processed in Davis 8.0 – an image correlation software from LaVision. The software contains a set of pre-set correlation algorithms that track the displacement of a subset of the speckle pattern as an

object deforms. The outcome of the correlation process is a strain map superimposed in the recorded images (Figure 3.9-**c**).

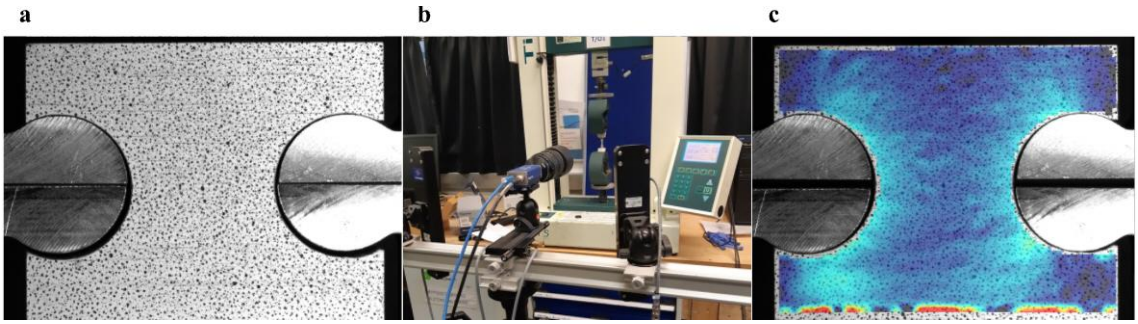

Figure 3. 9: Procedure to apply DIC technique.

3.4 Deformation and fracture analysis

3.4.1 Mapping physical characteristics

Before the tests were performed, the physical characteristics of all pieces were recorded using a high-resolution digital camera. As shown in Figure 3.10, six flat faces form the boundary of the specimens. For this research, the characteristics of the six faces of each specimen were recorded by taking photographs of each face.

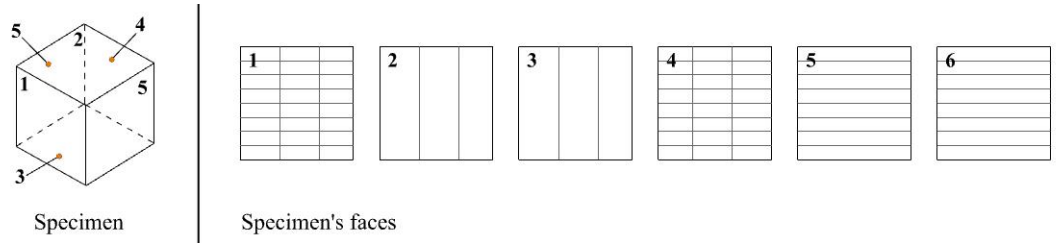

Figure 3. 10: Method to record the specimen's external features.

After taking the pictures, the physical characteristics of the bamboo strips were identified. As Amada et al. (1997) demonstrated, bamboo's functionally graded macroscopic structure can be analysed by taking pictures of the material and transforming these into binary-processed images - images with only two colours: black and white. In these images, the areas with more fibres will be black, and those with fewer fibres will be white. Following this approach, the pictures of the specimens were transformed into binary-processed images using Photoshop. First, the original photographs were converted to grayscale, and the exposure and brightness levels were adjusted (Figure 3.11-**a**). Then, the white and black thresholds of the images were adjusted to create the binary-processed images (Figure 3.11-**b**).

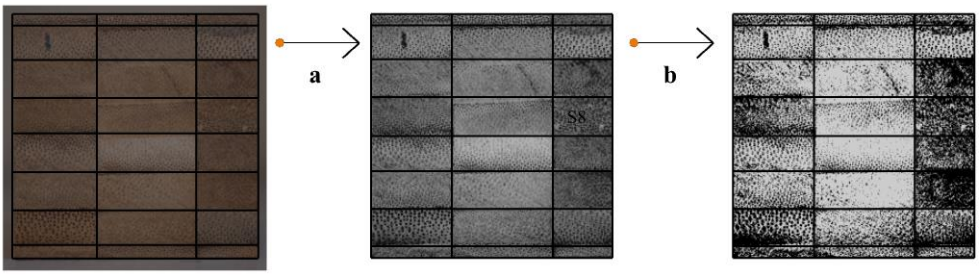

Figure 3. 11: Transforming original pictures into binary processed images.

The analysed surface of the specimens was either formed by end-grain strips or by the view of the longitudinally arranged fibres. Depending on the case, the following criteria were used to identify strips with irregularities after processing the binary images. The main goal was to identify areas with fewer fibres and areas with nodes:

- In the specimens where the end-grain of the strips is facing front, regions with more withe saturation are considered strips with fewer fibres. Conversely, areas with black saturation are considered strips with a higher concentration of fibres (Figure 3.12-**right**). For these specimens, it is not easy to identify nodal regions given the distribution of fibres displayed at the end-grain of the strips.

- In the case of specimens where the longitudinally distributed fibres are facing the front, the same criteria apply to identify strips with fewer and more fibres. White regions are considered areas with fewer fibres, whereas black parts are considered strips with more fibres. Contrary to the other specimens, it is possible to identify nodal regions in these specimens. As shown in Figure 3.12-**left**, node regions create fibre discontinuity that is easily identifiable by looking for continuous white patches in the strips.

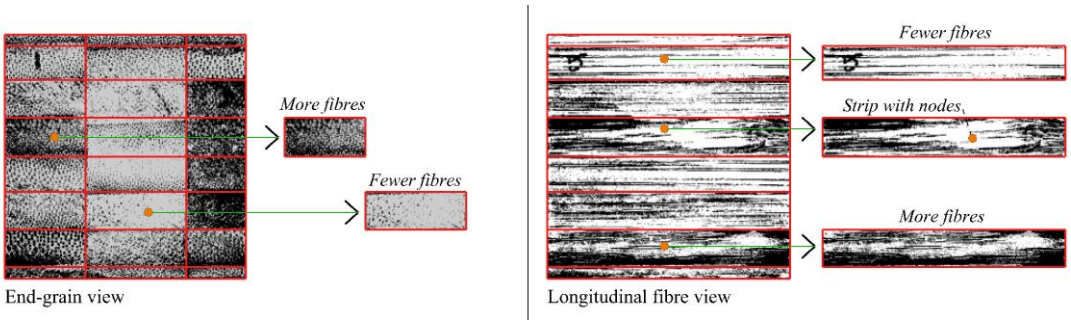

Figure 3. 12: Criteria to identify strip irregularities.

The reason for recording the physical characteristics of the pieces was to later identify how the characteristics influenced the behaviour of the material as the loads were applied.

3.4.2 Defining mechanical behaviour

For every test, the force and displacement of the test pieces were recorded. The force and displacement were converted to stress and strain to calculate the strength and mechanical properties of the material, respectively. The results of the experiments, thus, were plotted in stress-strain curves. In this thesis, the term elastic describes the linear section of the stress-strain curves. In contrast, the term plastic describes the areas of the stress-strain curves that follow a non-linear distribution. Based on the analysis of the stress-strain curves, three types of mechanical behaviours were found:

Elastic-brittle (Figure 3.13-**a**): This term is used to describe the specimens that only exhibited linear behaviour until reaching their Ultimate Strength. After this point, the pieces fractured abruptly.

Elastic-plastic brittle (Figure 3.13-**b**): This term describes the behaviour of the specimens that underwent linear deformation followed by a short period of non-linear deformation until reaching their Ultimate Strength. After this, the material fractured rapidly.

Elastic-plastic (Figure 3.13-**c**): This term is used to describe the behaviour of the specimens that exhibited a small region of elastic behaviour followed by a longer region of non-linear or plastic deformation.

The stress-strain curves were also used to identify critical moments in the deformation process of the tested pieces. For this reason, the following values were calculated for all specimens:

Proportional Limit (PL): The point at which the material transitioned from elastic to plastic deformation. This value was only calculated for the pieces that exhibited plastic behaviour.

Ultimate Strength (US): The maximum stress that the material can withstand.

Fracture Strength (FS): The point at which the material physically breaks, and the loading capacity drops abruptly.

Finally, the Moduli of Elasticity and Rigidity were also retrieved from the stress-strain curves. These values were used to compare the stiffness of the material in all directions and validate the accuracy of the results. Both Moduli were calculated using the linear equation of the elastic regime (Figure 3.13-**d**). The average behaviour of the material – in the three directions – was determined by calculating the average and characteristic values of the strength and mechanical properties. According to BS-EN 384-2004, the characteristic values of all samples were defined as the 5-percentile of the statistical distribution of the strength and mechanical properties.

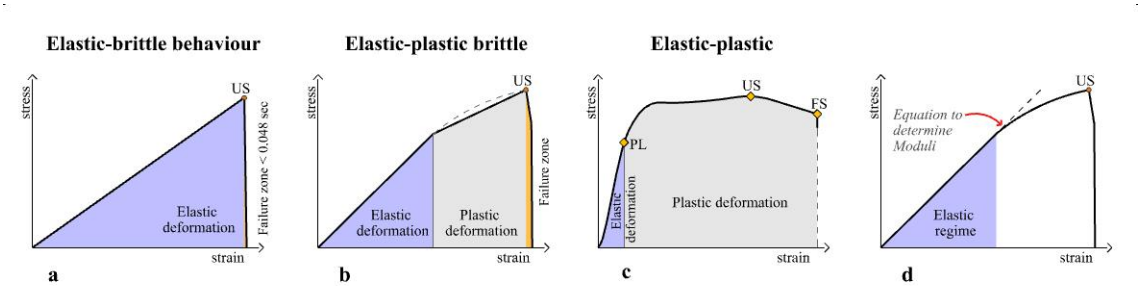

Figure 3. 13: Process to define mechanical behaviour and properties.

3.4.3 Initial vs deformed states

The image of the piece before loading, the DIC analysis and the stress-strain curves were the elements used to identify how the physical characteristics of the bamboo strips influenced the deformation and failure of the material. The following steps outline how these elements were analysed to determine the role that the physical characteristics of bamboo strips play in the deformation and failure of laminated bamboo:

Step 1: The images of the specimens before loading were used to identify the physical characteristics of the strips forming the laminates. As explained in section 3.4.1, strips with fewer fibres and with nodes were identified. The outlines describing the test piece and the physical characteristics of bamboo strips were used as templates to track the behaviour of the physical characteristics as the load was applied. As seen in Figure 3.14, the outlines of the specimens - where the longitudinal arrangement of fibres was facing the front - were created using the grayscale images. The lines of the fibres were traced using the grayscale images as reference. This process was achieved using a computer graphics software called Rhinoceros 3D. On the other hand, the outlines of the specimens - where the end-grain of the strips was facing the front - were created using the binary processed image (Figure 3.15). Both Figure 3.14 and Figure 3.53 show examples of the templates used to track deformation.

Figure 3. 14: Method to trace the geometry of fibres in specimens where the longitudinal arrangement of fibres is facing front.

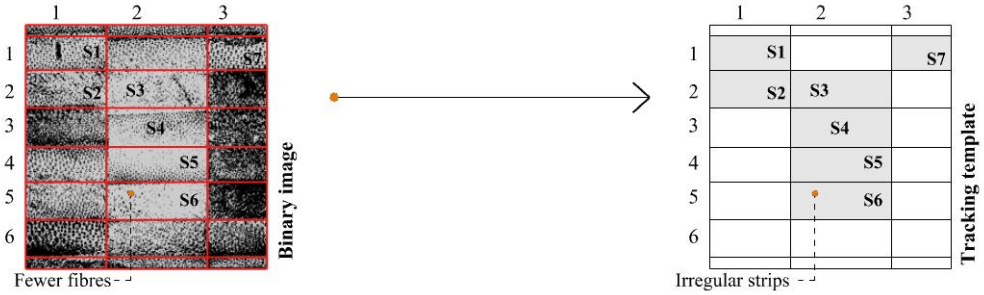

Figure 3. 15: Method to identify fibre density in specimens where the end grain of the strips is facing front.

Step 2: The stress-strain curves were used to select critical moments within the deformation process. For example, the Proportional Limit and the Ultimate Strength were always considered key moments to understand how the samples behaved as the loads were applied. Then, the strain maps – calculated with the DIC technique - of these critical moments were used to analyse the distribution of strain in all the tested pieces. Figure 3.16 shows an example of how the key moments were selected.

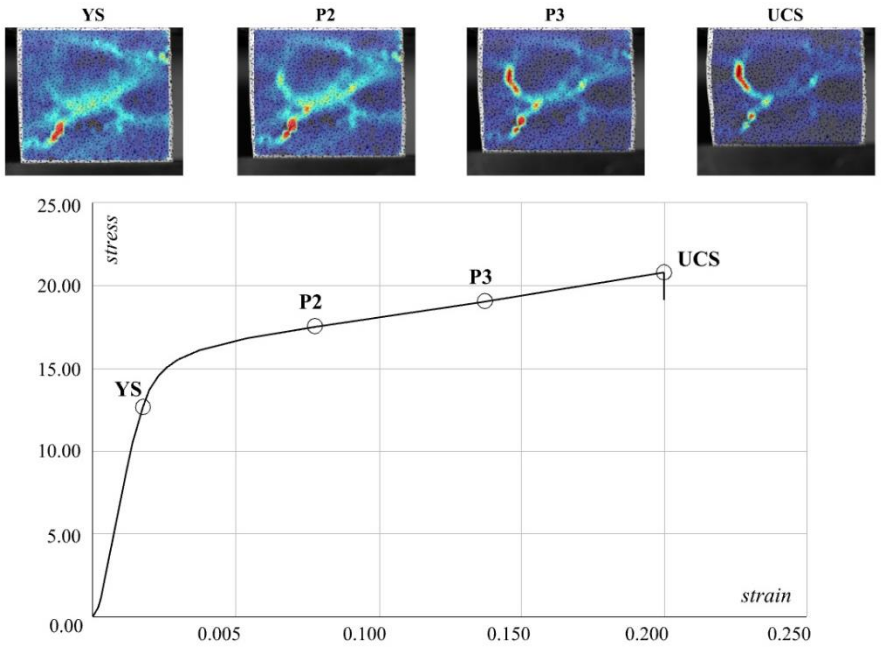

Figure 3. 16: Mapping the critical moments of the deformation process.

Step 3: The characteristics defined in Step 1 were superimposed in the DIC images of the critical moments defined in Step 2. As shown in Figure 3.17, once the characteristics of the pieces were placed on the DIC images, it became possible to observe if strain concentrations formed due to the physical features of the material.

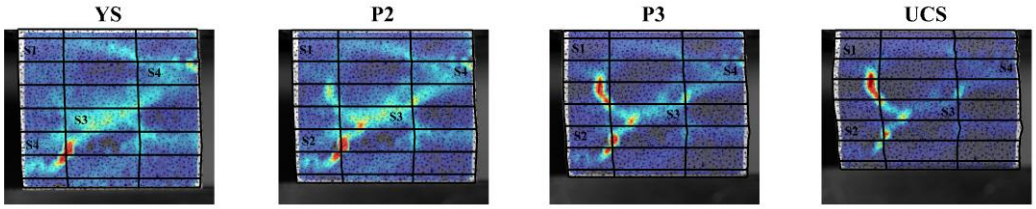

Figure 3. 17: Physical characteristics and the deformation process.

Step 4: The specimens' geometric representation was used to understand further how fracture developed and propagated. To achieve this, the characteristics of bamboo elements were represented with lines and polygons. Then, based on the analysis done in Step 3, the development of fracture was mapped on the geometric representation of the pieces. For example, in Figure 3.18, bamboo fibres were represented by lines and the parenchyma cells by polygons. The areas with no lines where the sections were fractured started. Then, the fracture propagated following the arrangement of the fibres. In all the analysed cases, fracture always began in the regions with no fibres, while fibres always served as channels to direct the energy released by the initial crack.

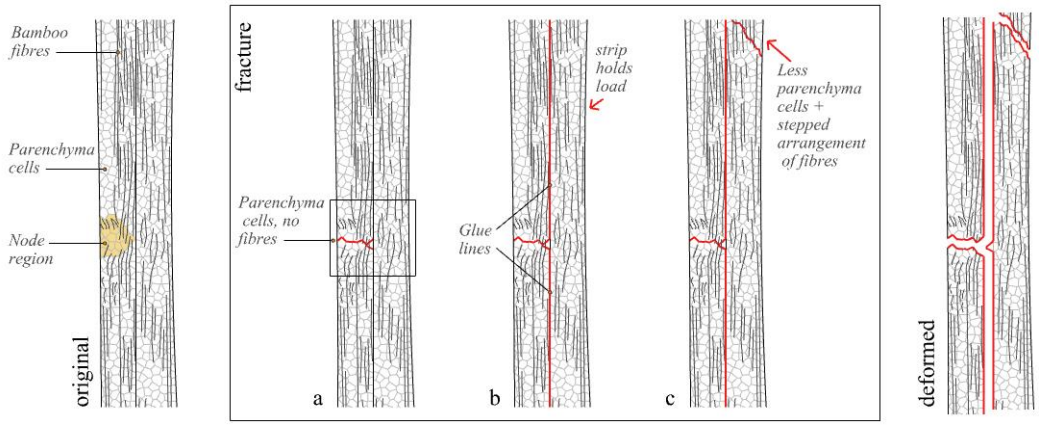

Figure 3. 18: Process to map the onset and development of fracture.

3.4.4 Mapping failure patterns

The steps outlined in the previous section were used to define the fracture patterns in the longitudinal, radial, and tangential directions. The same procedure was applied to the samples submitted to tensile, compressive and shear loads. The results of the analyses are described in Chapters 4, 5, and 6.

3.5 Predicting deformation and failure

3.5.1 Geometric methods

Based on the results of the experiments, the following conclusions were drawn:

Conclusion 1: In all the samples, fractures began after the samples reached their Ultimate Strength. The change in shape and size of the specimens before fracture can be determined by mapping out the deformation of the pieces in the x and y directions.

Conclusion 2: In all samples, fracture always started in or close to the regions of the strips that had fewer fibres or nodes. Furthermore, the final fracture geometry was defined by the geometric arrangement of bamboo fibres. The final geometry of the material can be represented by a polyline or by a set of polygons. The shape of the fracture polyline or polygons can be predicted if the areas with fewer fibres, the nodes and the geometric arrangement of fibres are identified before loading begins.

As explained in the lines above, deformation can be predicted if the x and y transformations are mapped. On the other hand, fracture geometry can be predicted if the characteristics of bamboo strips – listed above – are used as the generative input to define the geometry of fracture polylines and polygons. For these reasons, geometric methods were selected to predict laminated bamboo's deformation and failure patterns.

3.5.2 Predicting X and Y deformation

Vector fields were used to determine the deformation of the tested pieces in the x and y directions. The steps outlined below were followed to retrieve the deformation vectors of the pieces:

Step 1: An image of a specimen - before loading - was used to create an outline of the piece before deformation.

Step 2: An image of a specimen - at the moment it reached its Ultimate Strength – was used to create an outline of the piece right before the onset of fracture. The image was retrieved from the sequence of images captured by the camera of the DIC system.

Step 3: The outlines of the specimen before loading and before the onset of fracture were subdivided into equal segments and the centroids of each segment were retrieved.

Step 4: The centroids of the tested pieces before loading and before the onset of fracture were superimposed. Then, a set of lines were used to connect the original points with the deformed points. These lines represented the transformation vectors of the pieces and were used to calculate a set of equations to predict the deformation of the material. The process to calculate the equations is outlined in Chapter 7. Figure 3.19 shows an example of how the vector fields were retrieved.

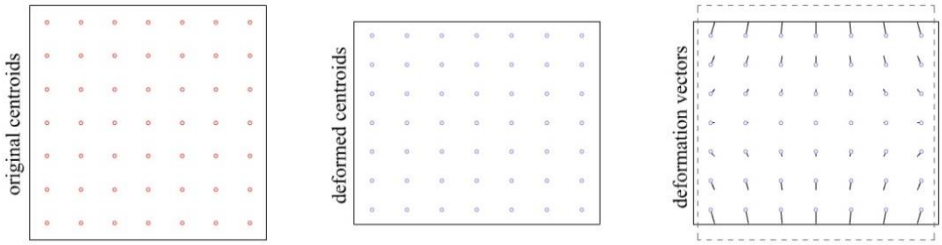

Figure 3. 19: Process to analyse deformation vectors.

3.5.3 Predicting fracture geometry

A set of parametric algorithms were developed to determine the fracture geometry of the samples. Images of the pieces before loading were used as a template to identify areas of the strips with fewer fibres, nodes, and the geometric arrangement of fibres. The specimens' pictures were edited to highlight the arrangement of fibres and the areas with fewer fibres. These characteristics were identified with points, lines, and polygons. The geometric representations of the regions where the fracture was likely to develop, were used as the generative input to define the final geometry of the material. Figure 3.20 shows an example of an algorithm designed to determine the fracture polyline of specimens under longitudinal tension. The algorithms used to determine the fracture geometries of pieces subjected to tensile, compressive and shear forces are further described in Chapter 7.

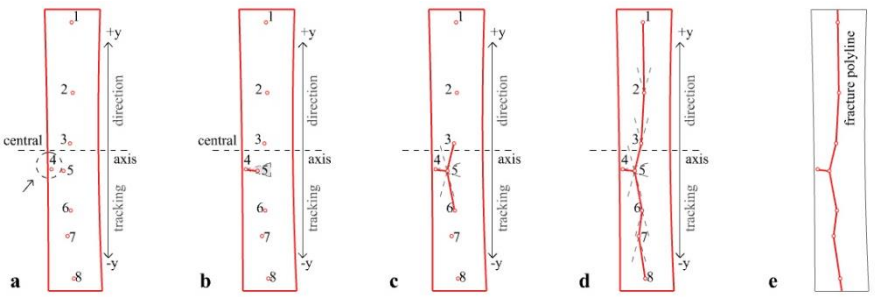

Figure 3. 20: Example of an algorithm designed to predict fracture.

3.5.4 Visualising fracture

The centroids representing the deformed pieces and the fracture geometries were used as the main inputs to visualise fracture. The next steps were followed to visualise fracture:

Step 1: Polygons were placed in the centroids representing the deformed pieces. Then, the radius of the polygons was adjusted to describe the solid-state of the deformed piece (Figure 3.21-**a**).

Step 2: The fracture geometries were used as attractor points to change the scale of the polygons defined in the previous steps (Figure 3.21-**b**). The purpose of using the fracture geometries as attractor points was to reduce the scale of the polygons closer to the geometries while increasing the size of the polygons placed further away. Visually, this change in scale approximated the deformed and fractured states of the material (Figure 3.21-**c**).

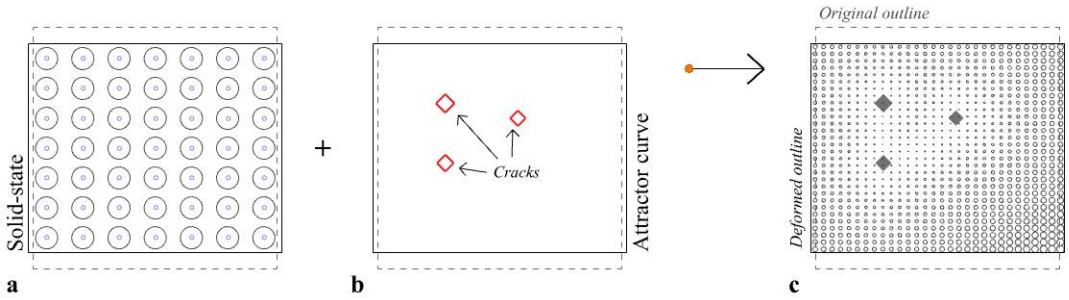

Figure 3. 21: Process to visualise fracture.

The methods described in this chapter provided a novel procedure to use the characteristics of bamboo strips as generative inputs to predict fracture. The technique is not a precise tool to estimate mechanical properties or map out different scales' behaviour. However, it offers a rapid method to assess the potential failure of the material. It can be a valuable approach to prevent the sudden failure of structures made with laminated bamboo. The limitations and advantages of the method are further discussed in Chapter 7.

3.5.5 Geometric generative software

All the geometric analyses and algorithms were developed in Grasshopper – a generative and parametric geometric plugin embedded in Rhino-3D. The algorithms used to define the fracture lines of pieces under tensile loading were developed by editing a VB script

created by Rutten (2011). The original algorithm finds the closest points by following rules to navigate the X-Y-Z coordinate system. I edited the original script to set the rules outlined in section 7.2. In contrast, the algorithms used to define the fracture geometry of pieces subjected to compressive loading were developed from scratch using the default functions of Grasshopper.

Chapter 4 | Uniaxial tension

| This chapter describes the deformation and failure modes of laminated bamboo when tensile forces are applied. The first, second and third sections summarise the findings of the tensile tests that were carried out in the longitudinal, radial, and tangential directions. The fourth section of the chapter compares the performance of the three directions. |

4.1 Longitudinal deformation and failure

4.1.1 Mechanical properties and behaviour

The analysed sample showed two types of behaviours: elastic-brittle and elastic-plastic brittle behaviour (Figure 4.1). Nine of the fifteen specimens showed elastic-brittle behaviour. This mechanical behaviour is characterised by a lack of plastic deformation, sudden fracture, and rapid damage evolution. These specimens had an average Ultimate Strength of 88.55 MPa. The remaining six specimens showed an elastic-plastic brittle behaviour. This behaviour is characterised by an elastic region followed by a period of plastic deformation until reaching the Ultimate Tensile strength. Compared to the previous specimens, these specimens reached an average Ultimate Strength of 102.80 MPa. In both cases, the samples fractured abruptly after reaching the Ultimate strength. However, the difference in loading capacities suggests that the specimens with elastic-brittle behaviour are weaker than the pieces with elastic-plastic brittle behaviour.

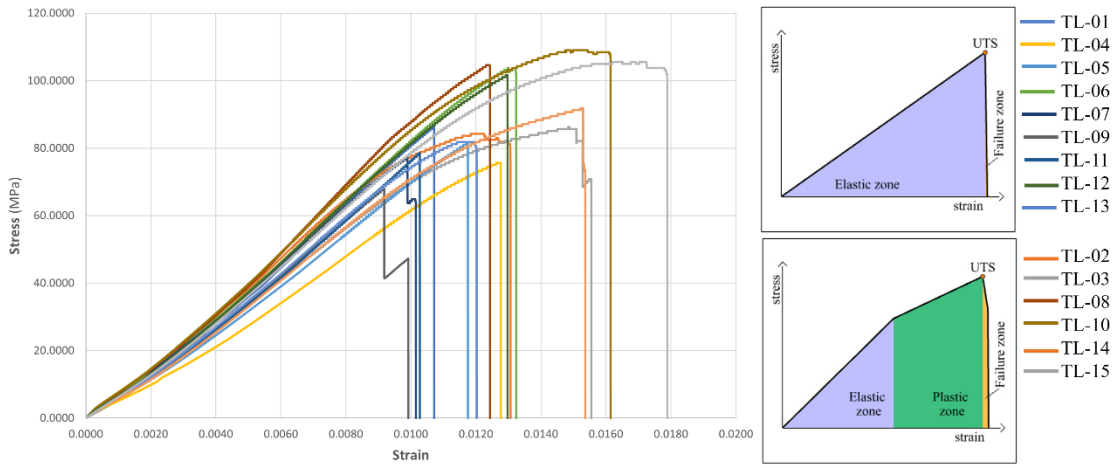

Figure 4. 1: Stress-strain curves and behaviour of specimens under longitudinal loading.

Table 4.1 summarises the strength and mechanical properties of the population. The average Ultimate Tensile Strength of the population is 89.10 MPa, and the average Modulus of Elasticity is 8,177.27 MPa. The values of the experiments are consistent with those reported in the available literature. Sharma et al. (2015a) reported an average Tensile Strength of 90 MPa. Khoshbakht et al. (2018) reported an average Tensile Strength of 95 MPa, and an average Modulus of Elasticity of 9,219MPa. The average maximum displacement of the population was 6.40 mm.

	Average	SD value	Characteristic value
Ultimate Tensile Strength (MPa)	89.10	12.85	73.39
COV	0.14		
Modulus of Elasticity (MPa)	8,177.27	756.39	7,185.37
COV	0.09		

Table 4. 1: Strength and mechanical properties of the sample under longitudinal tension.

4.1.2 Deformation and failure modes

Four types of failure modes were found in the specimens that exhibited elastic-brittle behaviour: trimmed tension (Figure 4.2-**Mode 1**), splintering tension with delamination along the glue lines (Figure 4.2-**Mode 2**), trimmed tension with delamination (Figure 4.2-**Mode 3**), and trimmed tension with splintering (Figure 4.2-**Mode 4**). The specimens of the failure modes' one, two and three had a loading capacity lower than the average tensile strength, while the specimens of mode four had higher loading capacities.

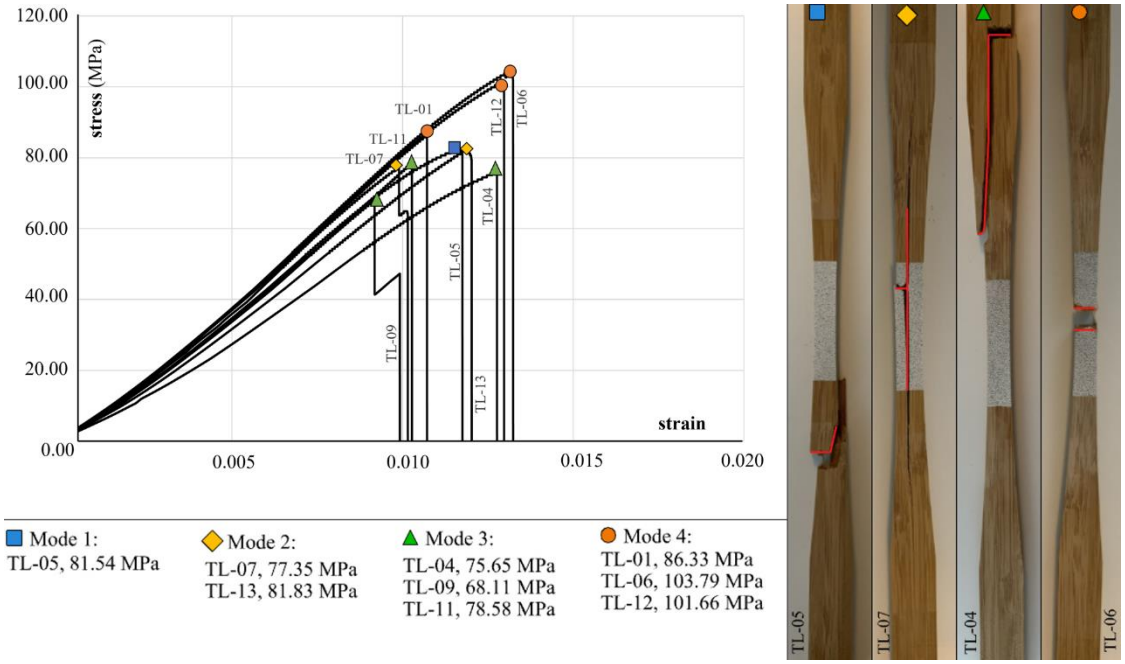

Figure 4. 2: Stress-strain curves and fracture modes of specimens with elastic-brittle behaviour.

Splintering tension was the only fracture mode that was found in the specimens with elastic-plastic behaviour (Figure 4.3-**Mode 5**). Contrary to the other pieces, these specimens had a loading capacity close to or higher than the average tensile strength of the population.

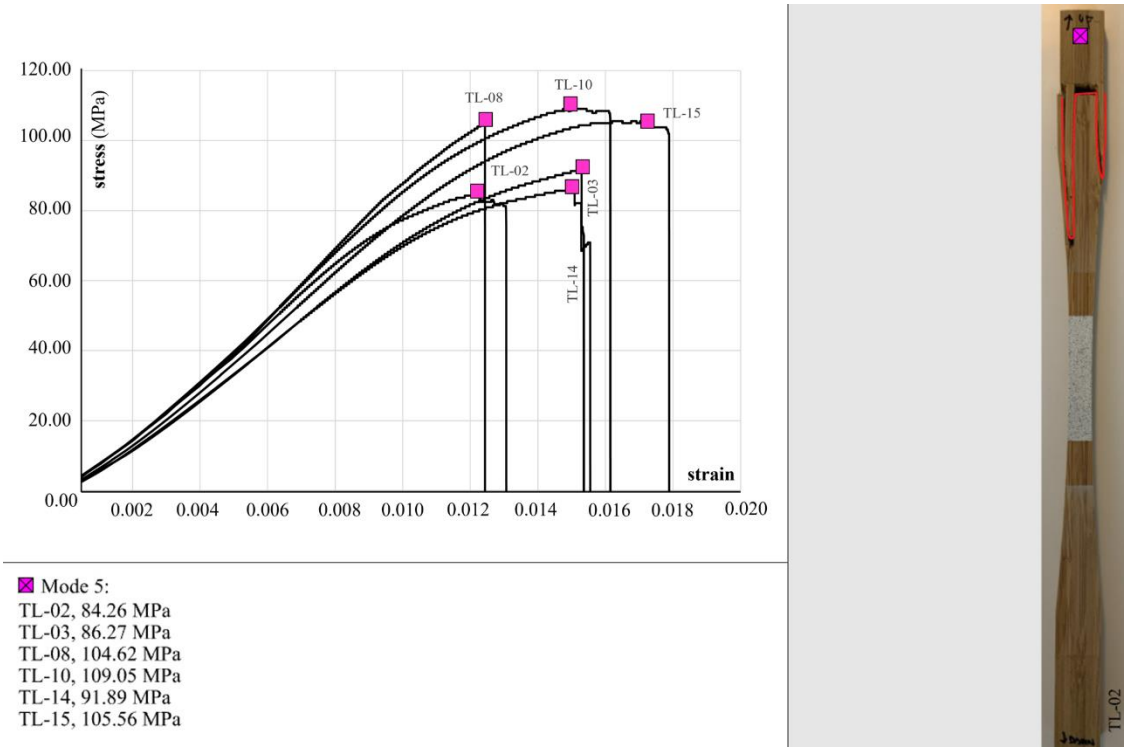

Figure 4. 3: Stress-strain curves and fracture modes of specimens with elastic-plastic brittle behaviour.

Failure Mode 1 or trimmed tension only occurred in specimen TL-05. As shown in Figure 4.4-**left**, the test area of the specimen had no nodes, and the bamboo strips had a lower concentration of bamboo fibres, meaning that the cross-section of the tested piece had a higher percentage of parenchyma cells. Figure 4.4-**right** shows the deformation of specimen TL-05 as the loading increased. At 20MPa, barely noticeable strain lines appeared with a maximum normal strain distribution close to zero. As the stress increased from 40MPa to 60 and 80 MPa, the strain concentration increased along the strain lines. At the same time, new strain concentration dots appeared along the edges of the specimen. Once the Ultimate Tensile Stress was reached and right before the onset of fracture, the strain lines reached a maximum normal strain of 0.018 to 0.020. Fracture started in one of these strain lines - less than a second later, the crack propagated along the area with the minimum cross-section. The resulting geometry of the trimmed tension failure is a polygonal line following an almost horizontal path.

The strain distribution and subsequent fracture mechanism of specimen TL-05 can be explained by analysing the fibre arrangement of the bamboo strips forming the tested piece. The test area of specimen TL-05 was composed of a low volume of bamboo fibres

and a high volume of parenchyma cells (Figure 4.5-**left**). As reported by Dixon and Gibson, 2014 and Mannan et al. 2017, the bonding strength of parenchyma cells is weaker than the strength of bamboo fibres. Hence, it is possible to conclude that trimmed failure is likely to start at the bonding interface of parenchyma cells, as shown in Figure 4.5-**centre**. The lack of bamboo fibres acting as a mechanical reinforcement accelerates the debonding of parenchyma cells, resulting in sudden brittle fracture (Figure 4.5-**right**). The analysis of the fracture mechanism of specimen TL-05 suggests laminated bamboo built with strips with a lower concentration of fibres are prone to trimmed tensile failure, have an elastic-brittle mechanical behaviour, and withstand lower loading forces.

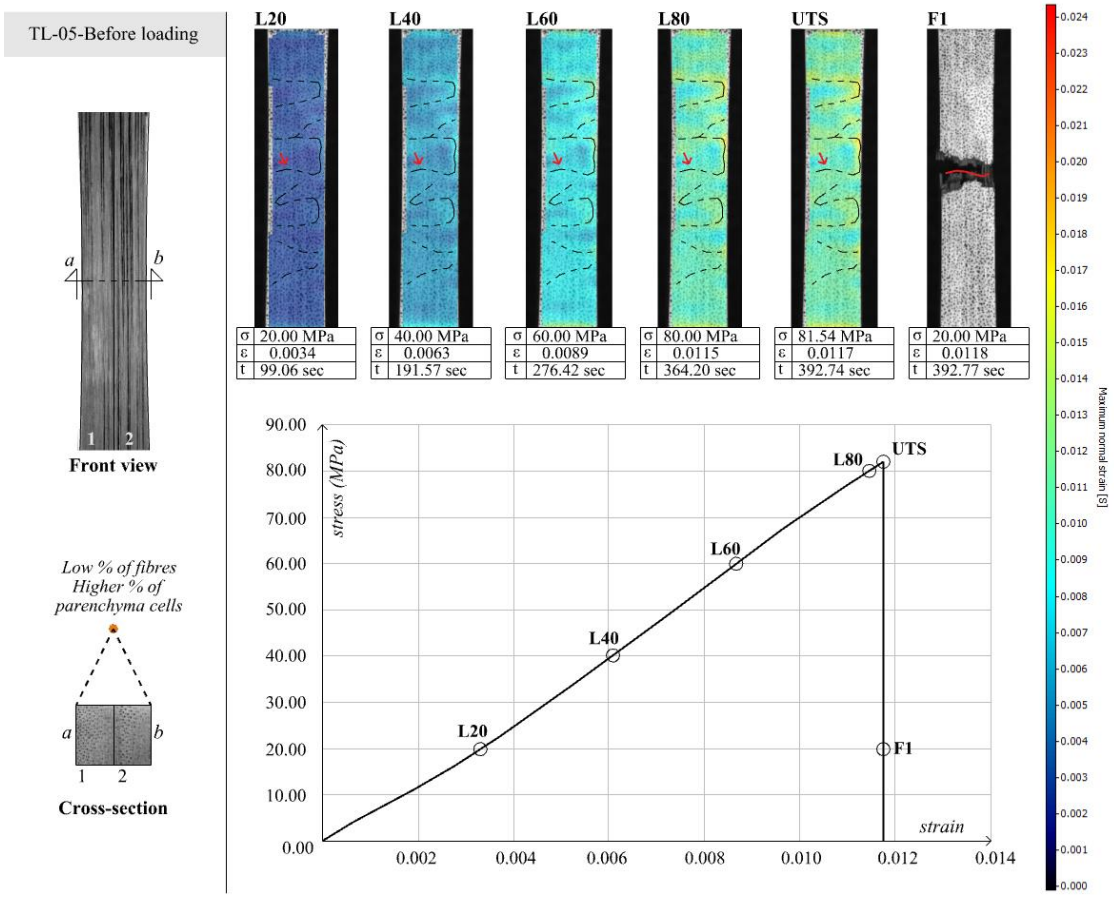

Figure 4. 4: left- Specimen TL-05 before loading, **right**- DIC analysis of specimen TL-05.

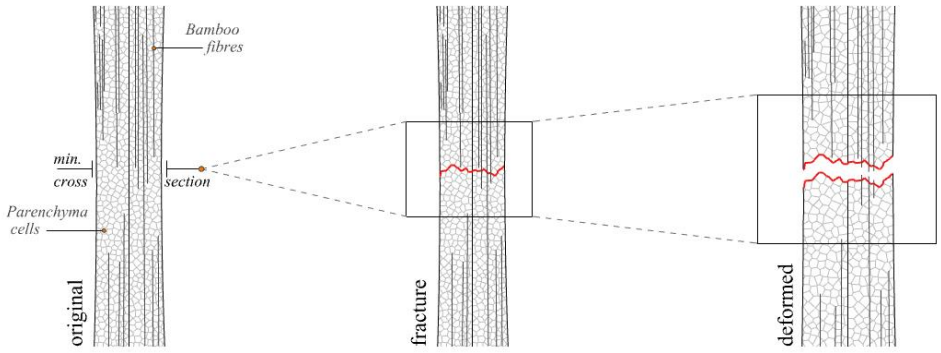

Figure 4. 5: Fracture analysis of trimmed tension.

Failure Mode 2 or failure or splintering tension with delamination along the glue lines was found in specimens TL-07 and TL-13. The specimens broke in the upper or lower regions close to the griping surfaces. As is shown in Figure 4.6-**left**, both tested pieces had nodal regions near the gripping zone. Even though the DIC analysis did not capture the sections near the grips, the analysis of the broken pieces suggests that the fracture started in the areas with a higher concentration of parenchyma cells and an irregular distribution of fibres. In other words, fracture is likely to have started in the nodal section of the laminates or bamboo strips. After reaching the Ultimate Tensile Strength, fracture started in the nodal regions, making the strength of the specimens drop to 64.32 MPa (Figure 4.6-**F1**). As damage continued, the specimens went through a brief period of increased strength as the crack travelled diagonally following the stepped pattern of the fibres located in the bamboo strip until reaching the glue line (Figure 4.6-**F2**). Then, the crack propagated vertically following the glue line. It is at this point where the loading integrity of the specimen dropped to 50.88 MPa (Figure 4.6-**F3**). It is probable that the presence of bamboo fibres delayed the abrupt fracture of the piece. Finally, the fracture travelled horizontally along the edge of the grips (Figure 4.6-**F4**). The resulting geometry of this type of fracture is a hook-like profile (Figure 4.6-**F5**). Considering the hierarchical structure of bamboo components, it is possible to map the onset of fracture in the regions that have more defects or weak points. The lack of fibre uniformity, the decrease of bamboo fibres and the high volume of parenchyma cells make nodal regions susceptible to fracture, particularly when tensile forces are applied.

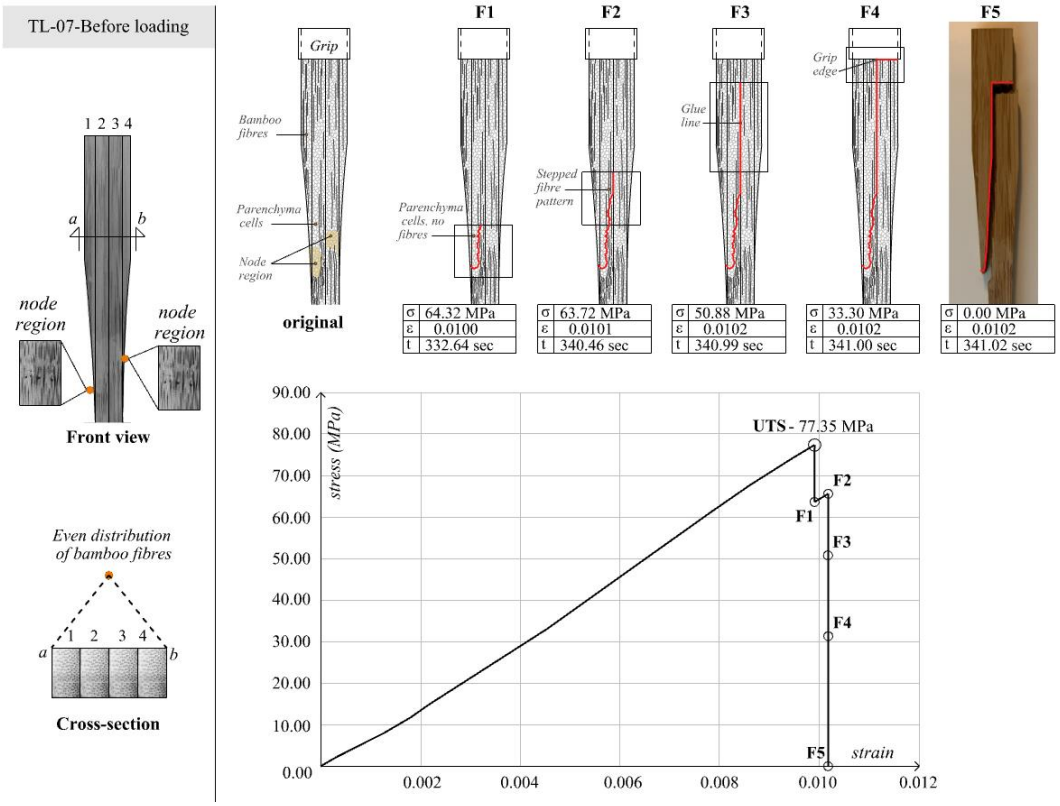

Figure 4. 6: left- Specimen TL-07 before loading, **right-** Fracture analysis of specimen TL-07.

Failure Mode 3 or trimmed tension with delamination happened in specimens TL-04, TL-09 and TL-11. As shown in Figure 4.7-**left**, there was at least one nodal region in the testing area or the reduced section of the specimens. As loading began, the specimens showed an even distribution of stress with minor strain deformation at 20 MPa, 40 MPa and 60 MPa (Figure 4.7-**L20**,**40** and **60**). As the Ultimate Tensile Strength was reached, a clear red spot appeared right in the area where the node was located. The maximum normal strain at this point was 0.024 (Figure 4.7-**UTS**). Fracture quickly set in by breaking the strip with the node into two parts. Then, in less than a quarter of a second, the crack travelled along the glue line of the tested piece (Figure 4.7-**F1**). As the crack travelled along the glue line, the specimen could still carry load since one of the strips remained unbroken. Hence, after the load dropped to 41.89 MPa, there was a brief period where the load increased to 46.92 MPa. As shown in Figure 4.7-**F2**, strain contours appeared on the right side of the strip that remained unbroken. On the upper side of the strain contours, another crack developed. At this point, the loading of the specimen finally dropped to zero. The initial geometry of this failure mode was a t-shaped profile formed by the breaking of one of the strips and the de-bonding along the glue lines (Figure 4.7-**F3**). Eventually, total fracture happened when the strips still carrying load broke at their weakest points.

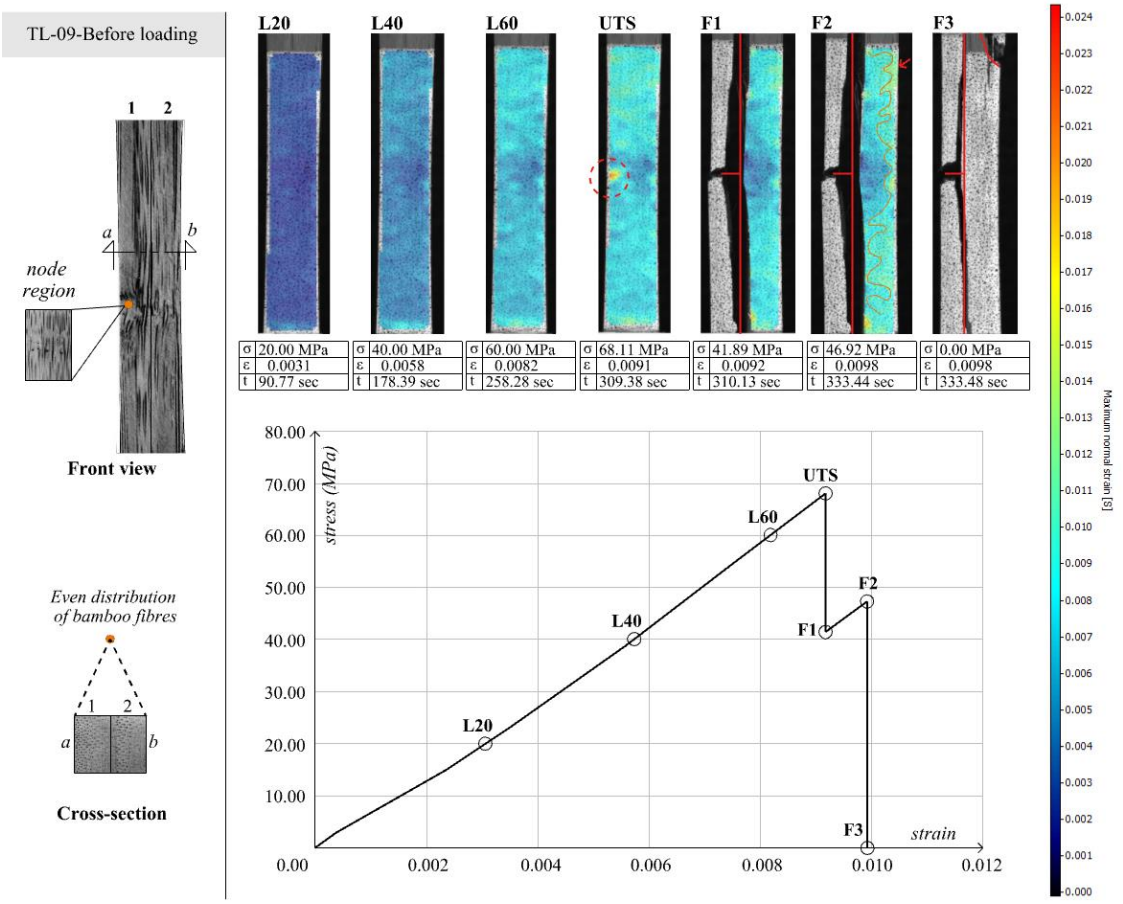

Figure 4. 7: left- Specimen TL-09 before loading, **right**- DIC analysis of specimen TL-09.

The fracture mechanism of Failure Mode 3f started in the nodal region of one of the strips of the tested pieces. Nodal regions have fewer bamboo fibres, and they are irregularly distributed. For this reason, fracture began by de-bonding the surface of the parenchyma cells located in the nodal region (Figure 4.8-**a**). Afterwards, the fracture propagated vertically, following the glued interface between the strips (Figure 4.8-**b**). As mentioned by Bodig and Jayne, 1982 and Sharma et al. 2014, glue lines should be rigid and ensure that the glued material behaves like a single unit. However, the presence of manufacturing irregularities (air gaps, uncleaned gluing surface, the irregular surface after planning bamboo strips, etc.) is likely to have weakened the bond between the glued surfaces. Even though one of the strips forming the laminate split into two, the unbroken strip continued carrying a load. In all the analysed pieces, the intact strips broke in the areas with a higher volume of physical irregularities (Figure 4.8-**c**). In other words, they failed in the regions with a higher concentration of parenchyma cells, less concentration of bamboo fibres or irregular arrangement of bamboo fibres.

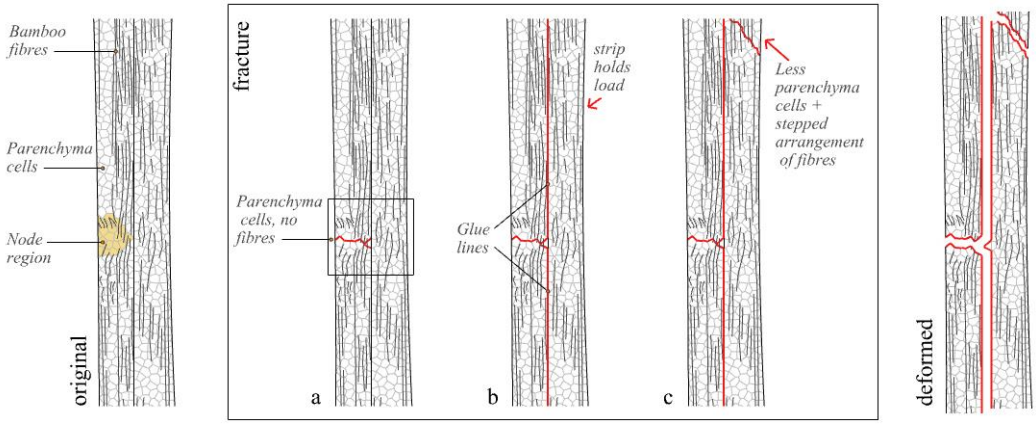

Figure 4. 8: Fracture analysis of trimmed tension with delamination along the glue lines.

Failure Mode 4 or trimmed tension with splintering was found in specimens TL-01, TL-06, and TL-12. The middle strips of all specimens had a typical configuration of one strip with no node and less concentration of bamboo fibres and another strip with nodes and a higher concentration of bamboo strips (Figure 4.9-**left**). Specimen TL-01 failed in the test area, but the splintering failure occurred in the back face of the specimen. On the other hand, the specimens TL-06 and TL-12 failed near the gripping zone. Regardless of the fracture area, all the tested pieces in this group had similar stress-strain curves and a similar fracture behaviour. Specimen TL-06 is used to illustrate Fracture Mode 4. Even though the DIC equipment did not record the strain deformation near the grip areas, an analysis of the broken pieces and the stress-strain curves were used to map out the on-set of fracture and the posterior evolution of damage. After reaching an Ultimate Tensile Strength of 103.79 MPa, the load dropped to 101.02 MPa. At this point, a crack developed in the strip with a minor concentration of bamboo fibres. Then in a matter of micro-

seconds, the damage extended towards the second strip by following the path of the bamboo fibres around the nodal region (Figure 4.9-**F1**). After the first strip broke, the second strip started its fracture process, and the high percentage of bamboo fibres produced a minor spike in the loading capacity of the specimen. For this reason, the stress increased from 101.02 MPa to 102.60 MPa. After the irregular pattern of the nodal region broke, the crack found its path by breaking the structure of the densely packed fibres located towards the edge of the specimen. At this point, the crack followed the stepped pattern of the fibres (Figure 4.9-**F2**). The final geometry of the fracture is the profile of an obtuse angle, a horizontal line created by the de-bonding of parenchyma cells and an inclined line created by the ripping of bamboo fibres (Figure 4.9-**F3**).

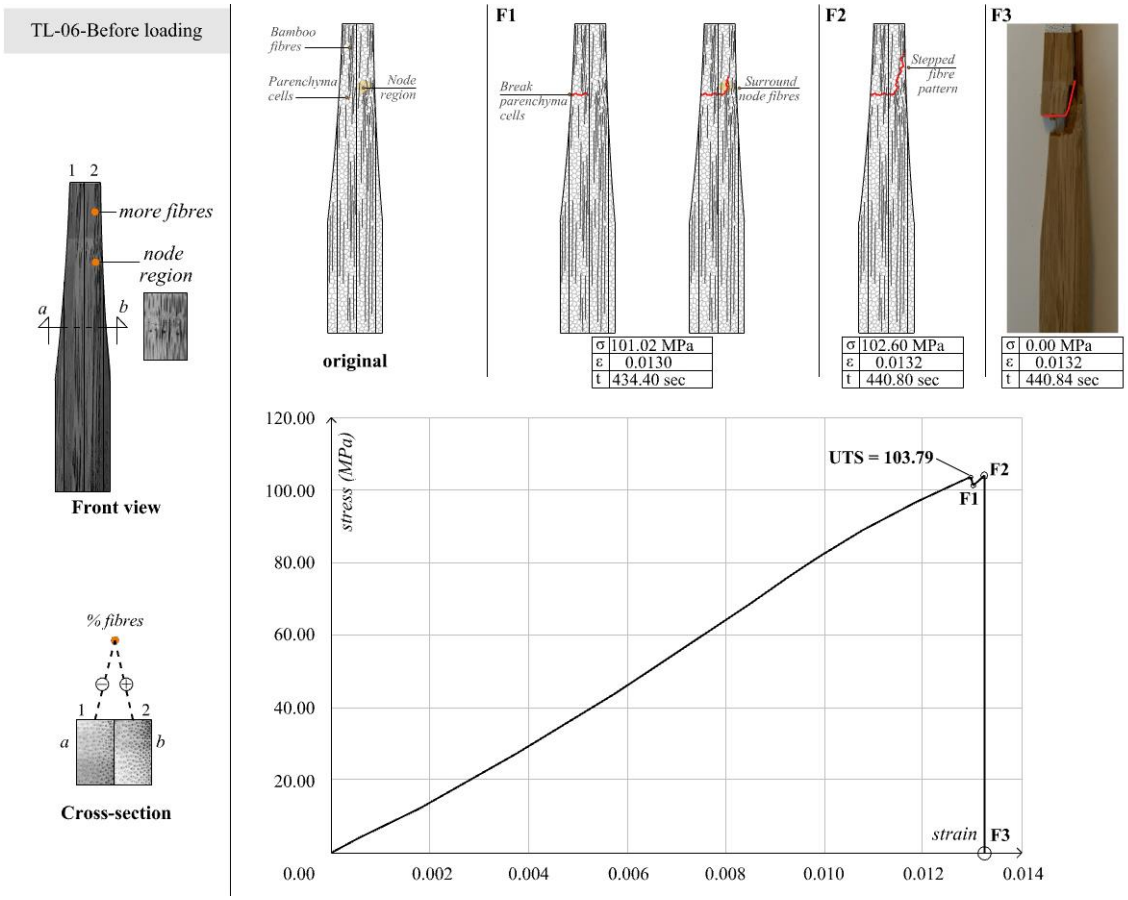

Figure 4. 9: left- Specimen TL-06 before loading, **right-** Fracture analysis of specimen TL-06.

Failure Mode 5, or splintering tension, was the most recurrent type of failure - with six pieces breaking this way. This type of failure occurred in the upper or lower sections of the specimens, and in all cases, the middle strips forming the specimen had at least one nodal region. Unlike the other groups, the specimens of Group 5 had a higher concentration of bamboo fibres (Figure 4.10-**left**). It is possible to conclude that the higher concentration of fibres is the reason why these pieces had higher tensile strength values. Even though the DIC analysis did not capture the sections near the grips, the analysis of

the broken pieces suggests that the fracture started in the areas with an irregular distribution of fibres. In other words, the fracture is likely to have begun in the nodal section of the laminates or bamboo strips (Figure 4.10-**F1**). After reaching an Ultimate Tensile Strength of 84.26 MPa, the load of the specimens dropped to 82.48 MPa once the de-bonding of the parenchyma cells around the nodal area began. Then, the fracture continued to travel upward, ripping the stepped arrangement of bamboo fibres. As the loading continued, another breakpoint started in the nodal area located in the other strip. At this point, the stress dropped to 80.72 MPa (Figure 4.10-**F2**). However, the specimen continued to carry some load as the bamboo fibres continued to be ripped apart as the cracks travelled towards the upper side of the tested piece. Once reaching the edge of the grips, the cracks travelled horizontally following the edge of the grips (Figure 4.10-**F3**). Finally, the pieces broke, producing a splintering fracture geometry (Figure 4.10-**F4**).

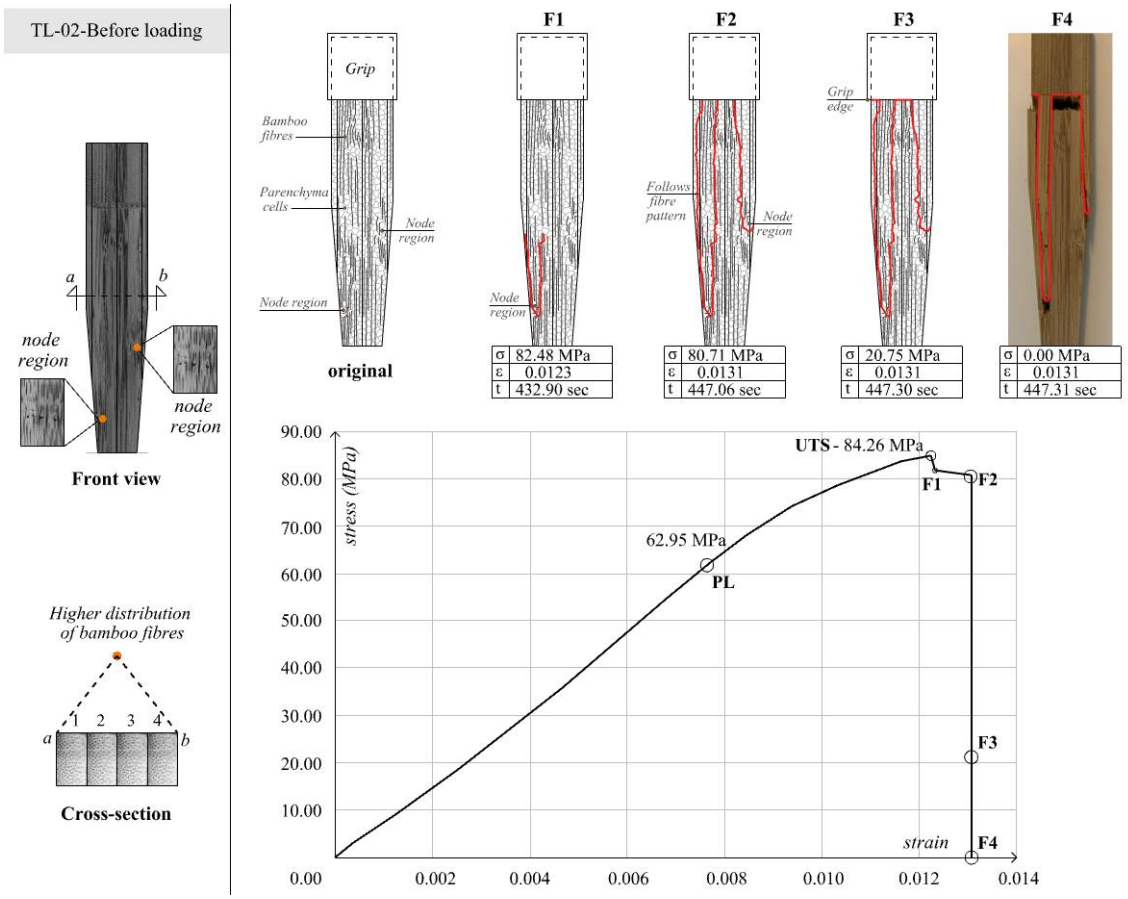

Figure 4. 10: left- Specimen TL-02 before loading, **right-** Fracture analysis of specimen TL-02.

4.1.3 Failure patterns in the longitudinal direction

The previous analysis demonstrated that the following features of bamboo strips had a direct impact on the mechanical strength and response of the tested sample:

Feature 1: The percentage and distribution of bamboo fibres directly influenced the strength of the material and determined the onset and evolution of damage. The radial distribution of fibres always increases towards the outer skin. However, the total density of the fibres depends on the characteristics of raw bamboo. Also, the transversal distribution of fibres can be affected after milling the strips. Some strips will have a cross-section with more parenchyma cells, while some will have more fibres. The strips with fewer fibres will have less longitudinal reinforcement when applying tensile forces (Figure 4.11-**a**). Hence, they will have a lower tensile strength. On the other hand, strips with more fibres have high longitudinal support and superior tensile strength (Figure 4.11-**b**).

Feature 2: The location and geometric arrangement of fibres in the nodal regions directly influenced the mechanical behaviour of laminated bamboo. Fibres at nodal regions have different configurations in the three directions of a strip (Figure 4.11-**c**). Longitudinally, the fibres become discontinuous. The discontinuity of bamboo fibres is also visible in the tangential face (Figure 4.11-**d**). When a longitudinal tensile force is applied, node areas become clear breakpoints since no continuous fibres reinforce this section. On the other hand, fibres bend in and out in the radial face, creating a curvilinear arrangement (Figure 4.11-**e**). Depending on the failure mode, the curvilinear fibres can change the direction of a crack.

Feature 3: Glue imperfections can also impact the development of damage. The fracture always started in areas with fewer fibres or nodes. However, if there were any glue irregularities, the crack would find a path in the bonded interface of two laminates. Delamination along the glue lines is hard to predict since there are no geometric cues that can help foresee the quality of the lamination.

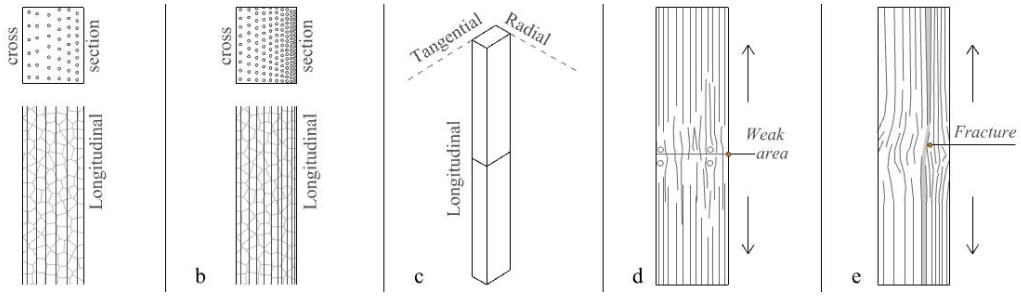

Figure 4. 11: Bamboo's features affecting tensile failure in the longitudinal direction.

All the factors mentioned above affected the material's mechanical properties and determined the failure mechanisms of laminated bamboo when subjected to longitudinal tensile loads. Overall, these are the characteristics of each failure mode:

Failure Mode 1, or trimmed tension, occurred in a specimen with a lower distribution of bamboo fibres and no nodes in the test region. In practice, elements without nodal areas are not likely to be found since larger pieces are bound to have multiple irregularities. As the load pulled the piece apart, the area with the least cross-section and fewer bamboo fibres became the weakest point. The crack travelled horizontally by breaking the bond between parenchyma cells in less than a second (Figure 4.12-**a**).

Failure Mode 2, or splintering tension with glue delamination, happened in specimens with an even concentration of bamboo fibres. The pieces had at least one nodal region close to the gripping area. As the load increased, fracture began in the area with the lowest concentration of fibres, i.e., the nodal region. Then, the crack propagated following the staggered arrangement of the bamboo fibres until reaching the glue line. It is possible that due to manufacturing errors, the glue line was not perfectly rigid. Hence, the crack travelled upward across the glue line (Figure 4.12-**b**).

Failure Mode 3, or trimmed tension with delamination, happened in specimens with at least one nodal region in the test section. Nodes were only found in one of the two strips that formed the test area of the specimens. As the load increased, the strip with the nodal region broke into two parts. As with the previous failure mode, the tested pieces likely had glueing imperfections. For this reason, the crack propagated along the glue lines. Total failure happened when the single strip carrying load finally broke. Complete fracture always occurred in the section with more irregularities (Figure 4.12-**c**).

Failure Mode 4, or trimmed tension with splintering, occurred in specimens that had one strip with less concentration of fibres and one strip with a higher concentration. Fracture began in the strip with the lower concentration of fibres. Then, the crack propagated to the other strip by breaking the staggered pattern of bamboo fibres (Figure 4.12-**d**).

Failure Mode 5, or splintering tension, was found in specimens with a higher bamboo fibres concentration. All the pieces had at least one nodal region. In all cases, fracture began in the nodal areas. Then, the crack propagated across the specimen by breaking the staggered pattern of bamboo fibres (Figure 4.12-**e**).

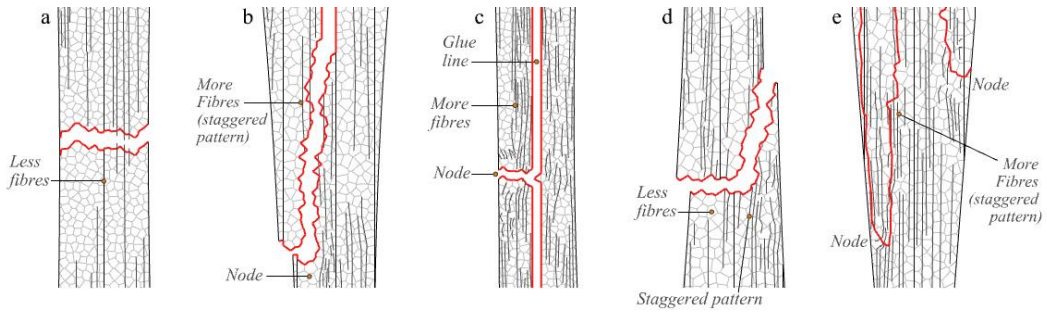

Figure 4. 12: Fracture patterns of laminated bamboo under longitudinal tension.

Even though the onset of failure and the failure modes might seem to be random at first, a closer look at the data revealed two clear patterns:

Pattern 1 - Fracture always started in the areas with fewer bamboo fibres. Naturally, bamboo strips have a monotonic arrangement of fibres. If the part of the strip with a higher volume of fibres is milled off during the manufacturing process, the milled strip will have a weaker configuration. Hence, strips with a lower percentage of fibres will also have a weaker mechanical response. Also, the irregular distribution of fibres - in nodal regions – behaved as the weakest link when tensile loads were applied in the longitudinal direction.

Pattern 2 – After the onset of fracture, the crack found the fastest and easiest path to release the energy in the weakest areas of the specimens. If the strips had a lower concentration of fibres, the crack found its path by de-bonding the interface of parenchyma cells. This process created a horizontal fracture. If the strips had a higher concentration of fibres, the crack found its path by breaking the staggered pattern of bamboo fibres. The existence of nodes also determined the resulting geometry of the damage. Finally, if there are any glue imperfections, the crack found an easy path by de-bonding the laminates along the glue line.

4.2 Radial deformation and failure

4.2.1 Mechanical properties and behaviour

Table 4.2 summarises the strength and mechanical properties of the sample submitted to radial tension. The average Ultimate Tensile Strength of the population was 4.85 MPa, and the average Modulus of Elasticity was 1,269.54 MPa. Most of the available literature reports an average tensile strength ranging from 2.00 MPa (Sharma et al., 2015a) to 5 MPa (Khoshbakht et al., 2018). However, these values describe the tensile strength along the perpendicular direction without specifying if the tests were done in the radial or tangential directions. In 2017, Sharma et al. conducted an experimental program on structural specimens. In this program, the values of the radial direction were recorded. The study reported an average Tensile Strength of 4.3 MPa and an average Modulus of Elasticity of 1,346 MPa. The values of this study are comparable to those found in the available literature. The average maximum displacement of the population was 0.20 mm. All the tested pieces exhibited a linear elastic behaviour before undergoing brittle and sudden failure (Figure 4.13-**left**). The specimens had a proportional increase of stress and strain until reaching the Ultimate Strength. Then, the pieces fractured abruptly (Figure 4.13-**right**).

	Average	SD value	Characteristic value
Ultimate Tensile Strength (MPa)	4.85	1.19	3.22
COV	0.25		
Modulus of Elasticity (MPa)	1,269.54	66.71	1,180.16
COV	0.05		

Table 4. 2: Strength and mechanical properties of the sample under radial tension.

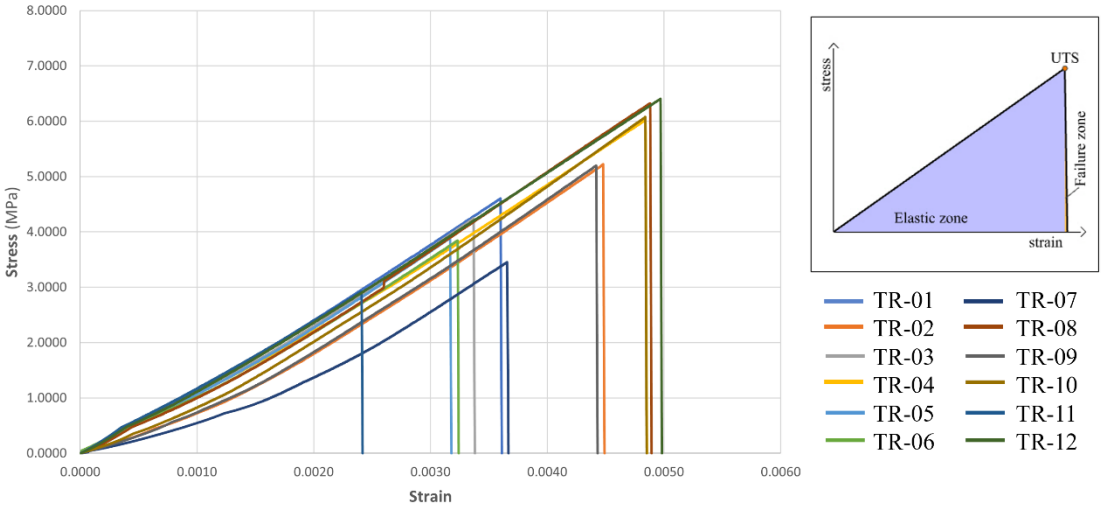

Figure 4. 13: left- Stress-strain curves of specimens under radial tension, **right**- Elastic-brittle behaviour.

4.2.2 Deformation and failure modes

All the tested pieces broke somewhere within the reduced section of the specimens. However, a closer look at the pieces revealed that the arrangement and physical characteristics of the strips - forming the test area of the specimen – were the underlying factors that determined the location of the fracture. Overall, three failure modes were identified. In Failure Mode 1, the fracture happened in the middle of the central strip (Figure 4.14-**Mode 1**). Conversely, in Failure Mode 2, the specimens broke in the upper or lower parts of the central strip (Figure 4.14-**Mode 2**). Lastly, the fractures of Failure Mode three occurred in the strips located above or below the central strip (Figure 4.14-**Mode 3**).

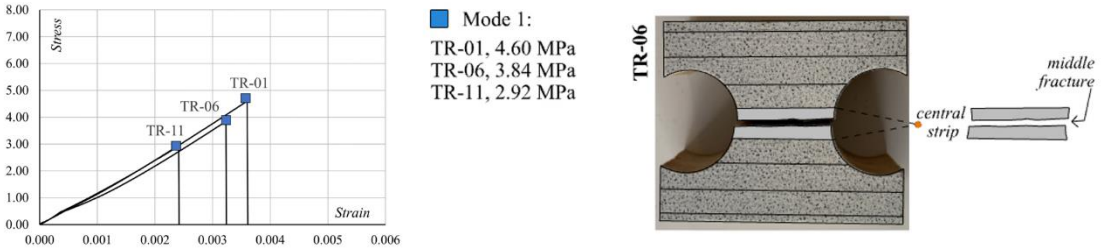

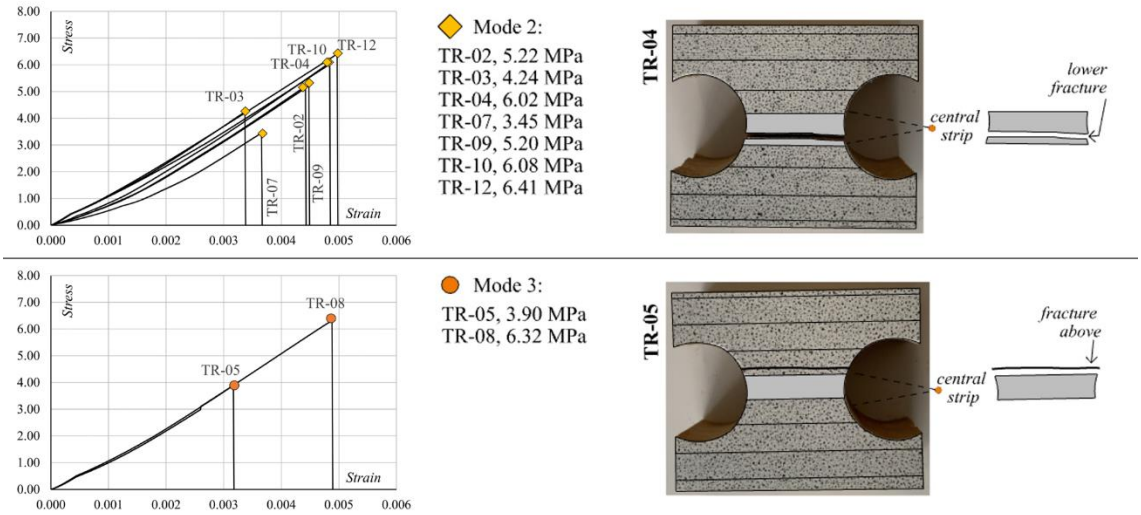

Figure 4. 14: Stress-strain curves and fracture modes of specimens under radial tension.

Fracture Mode 1 occurred in the specimens TR-01, TR-06 and TR-11. These pieces had a central strip with a low concentration of bamboo fibres. As shown in Figure 4.15-left, some pieces - like specimen TR-06 - had a node in the central strip. At 1.50 MPa, contours with a maximum normal strain of 0.0024 appeared at the edges of the specimen, particularly in the lateral sides– where the steel grips held the pieces (Figure 4.15-**L1.5**). At 3.00 MPa, patches with a maximum normal strain of 0.0048 appeared in the upper and lower areas of the specimen (Figure 4.15-**L3.0**). Once again, the regions with the higher deformation were located close to the gripping zone. At 3.84 MPa, the specimen reached its Ultimate Tensile Strength. At this stage, the maximum normal strain reached a peak value of 0.0052. Only at this point, it became possible to observe the appearance of strain fields forming in the central region of the tested piece. Figure 4.15-**UTS** shows the formation of a faint strain line crossing the specimen. It is along this line that the piece eventually broke into two parts. The resulting geometry of this failure mode was a horizontal line that crossed the middle section of the central strip (Figure 4.15-**F1**).

The onset of fracture and the subsequent damage evolution - in Failure Mode 1 - can be explained by analysing the specimen's frontal and side views. The uneven distribution of fibres in the radial direction determined the area prone to failure. Strip number one had an even distribution of fibres, and these were densely packed towards the bottom edge of the strip. On the other hand, strip number two had a lower allocation of fibres, and the fibres became less dense towards the lower part of the strip. Finally, strip number three had an even distribution of fibres. However, contrary to the first strip, the denser region of this strip was facing the upper part. As shown in Figure 4.16-**a**, the region with the lowest percentage of fibres was in the middle region of the central strip or strip number two. As loading increased, the lateral sides of the central strip began to break by de-bonding the interface of parenchyma cells (Figure 4.16-**b**). In a snap of a second, the

fracture travelled from both edges to the central axis of the specimen. Figure 4.16-**c** shows that the rupture propagated horizontally by breaking the parenchyma cells where the horizontally distributed fibres were embedded. For TL-06 – the fracture started in the mid-region of the central strip, and then it followed the arrangement of the fibres around the nodal region. In this case, the nodal region was not necessarily the weakest zone. Instead, the node provided an outline for the crack to quickly find its way to the central axis. Once the cracks of both edges met in the central region, total fracture happened, and the piece completely broke apart.

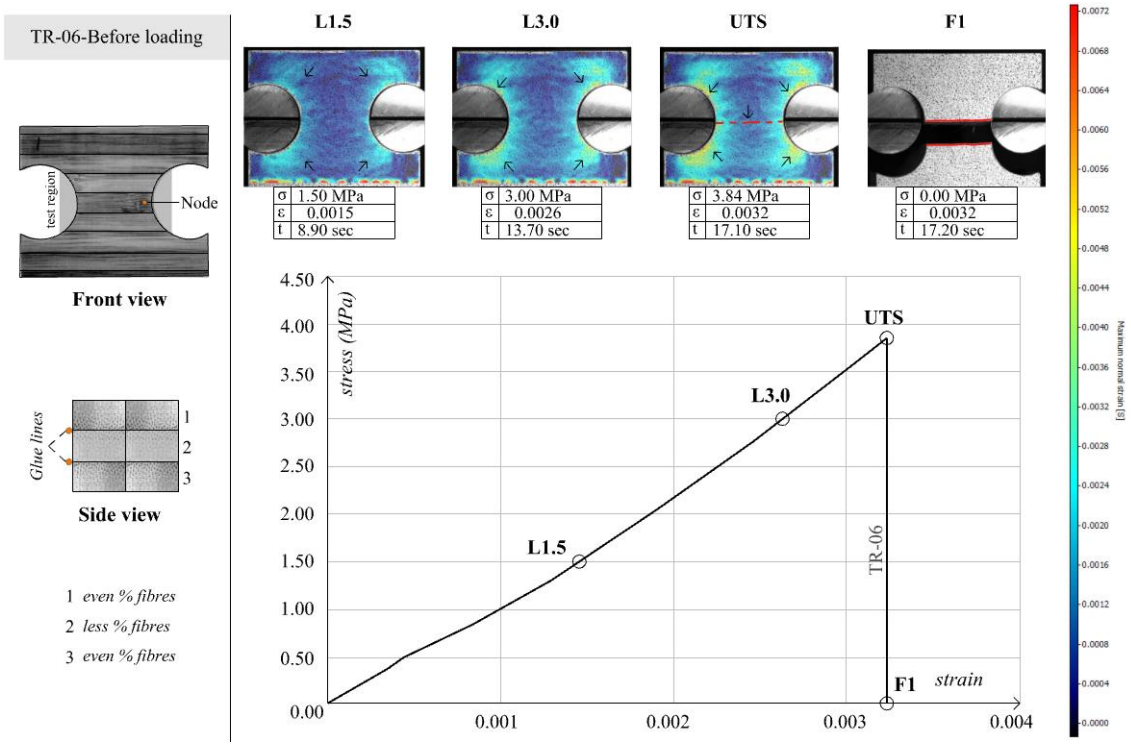

Figure 4. 15: left: Specimen TR-06 before loading, **right**: DIC analysis of specimen TR-06.

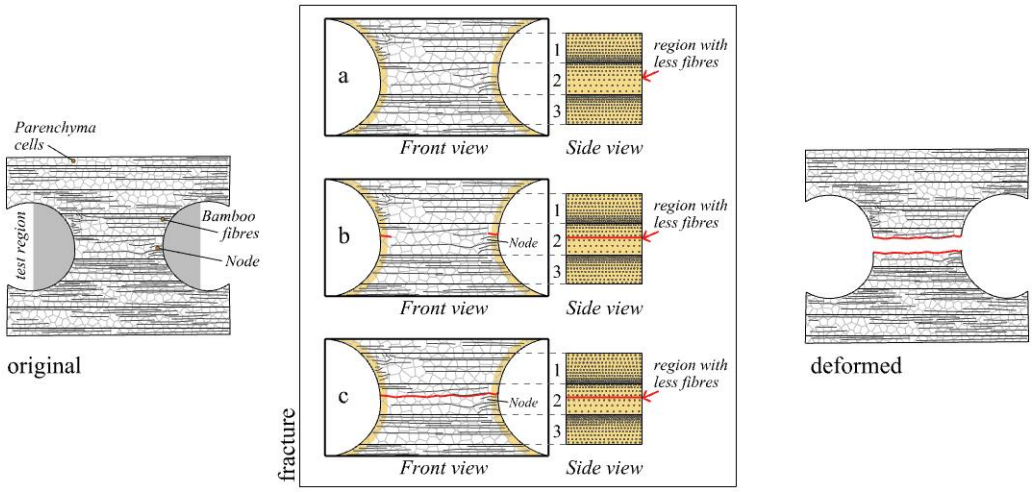

Figure 4. 16: Fracture analysis of Failure Mode 1.

Failure Mode 2 was the most recurrent failure mechanism. Specimens TR-02, TR-03, TR-04, TR-07, TR-09, TR-10, and TR 12 exhibited this type of failure. The specimens had an even distribution of fibres and parenchyma cells at the test region (Figure 4.17-**left**). As the load reached 1.50 MPa, light blue patches appeared in the upper and lower areas of the specimen (Figure 4.17-**L1.5**). The maximum normal strain at this point was no more than 0.0020. As the load increased, the strain also increased in the regions closer to the grips. At 3.00 MPa, yellow patches appeared in the areas that already had blue patches (Figure 4.17-**L3.0**). The maximum normal strain at this point was 0.0048. At 4.50 MPa, red spots appeared in the upper and bottom parts of the piece (Figure 4.17-**L4.5**). The maximum normal strain at these points was 0.0070. During this phase, light blue lines started to spread across the central axis of the tested piece. In other words, the entire test region began to be affected by the loading forces. These blue lines signalled the onset and subsequent path of fracture. The specimen reached its Ultimate Tensile Strength five seconds later at 6.02 MPa. Figure 4.17-**UTS** shows the strain field right before fracture. At this point, a light blue line was completely crossing the transversal section of the specimen. Immediately after reaching the Ultimate Tensile Strength, the piece broke along the blue line. The final geometry of this failure mode was a horizontal line in the upper or lower regions of the central strip (Figure 4.17-**F1**).

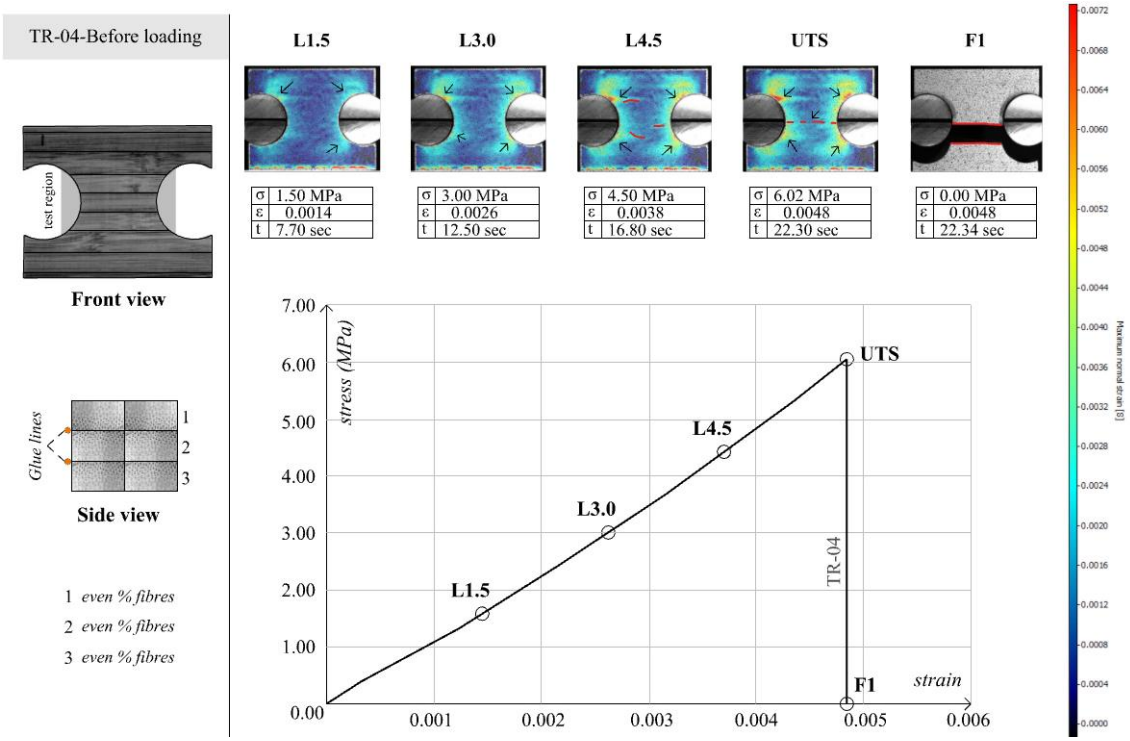

Figure 4. 17: **left**: Specimen TR-04 before loading, **right**: DIC analysis of specimen TR-04.

All the specimens that exhibited Failure Mode 2 had strips with an even or higher fibres distribution than the percentage of parenchyma cells. The densely packed fibres of strip

one were located in the bottom part of the strip. Contrary to this arrangement, the part of the strip with more fibres was facing the upper part. Strip number three had the same arrangement as strip number two. In other words, the part of the strip with more fibres was also facing the upper part. As can be seen in Figure 4.18-**a**, the lower section of the central axis was the area with the lowest percentage of fibres. Failure Mode 2 was found in the upper or lower regions of the central strip. The location varied depending on the arrangement of the central strip. However, all the strips located in the test region had an even fibre-to-parenchyma ratio in all cases. As the load increased, the fracture started in the lateral faces of the tested pieces (Figure 4.18-**b**). Specifically, the fracture began in the section of the central strip that had fewer fibres. The fracture started at the edges, and it quickly propagated across the mid-section of the specimens (Figure 4.18-**c**). In all cases, the path of the crack can be traced back by identifying the horizontal pattern formed by the strips closer to the area where the fracture began.

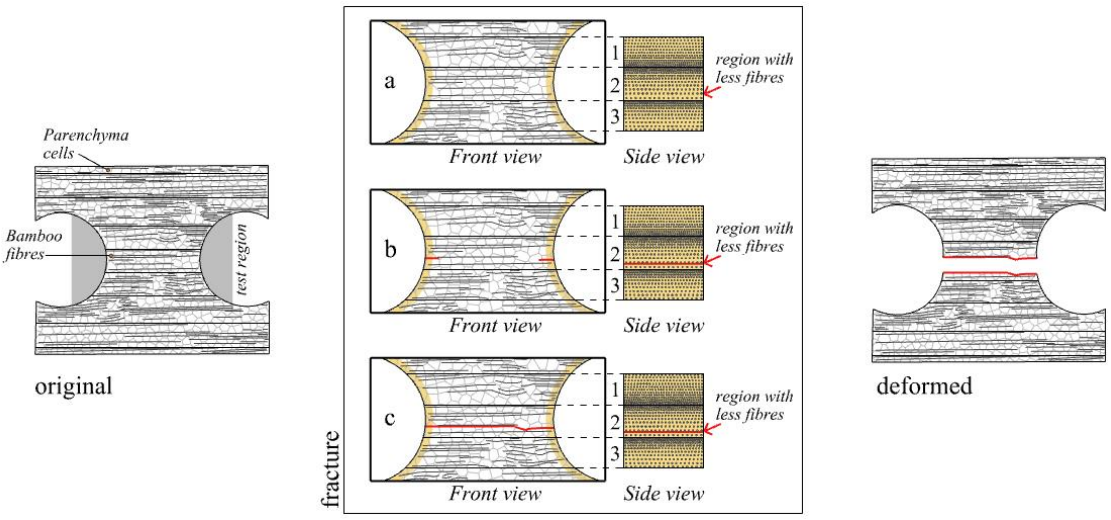

Figure 4. 18: Fracture analysis of Failure Mode 2.

Failure Mode 3 was the least frequent failure mechanism. Only specimens TR-05 and TR-08 exhibited this behaviour. The tested pieces had a central strip with a high percentage of bamboo fibres (Figure 4.19-**left**). Unlike the other Failure Modes, the strain distribution was faster in these specimens. As shown in Figure 4.9-**L1.5**, yellow patches were already visible at 1.50 MPa. The maximum normal strain at this point was 0.0048. As the load increased, the strain also increased in the upper and lower sections of the pieces. At 3.00 MPa, the maximum normal strain reached values higher than 0.0052 (Figure 4.19-**L3.0**). Also, at this point, blue lines started to stretch towards the central axis of the specimen. Three light blue lines began to find a path towards the centre of the piece. At 3.90 MPa, red dots appeared in the upper and lower sections (Figure 4.19-**UTS**). The maximum normal strain at these points was more than 0.0068. Also, at this point, one of

the blue lines completely crossed the test region of the specimen. After the piece reached its Ultimate Tensile Strength, the specimen quickly broke into two parts along the blue line crossing the specimen. The final geometry of this type of failure is a horizontal line in the strip located above or below the central strip (Figure 4.19-**F1**).

The pieces that underwent Failure Mode 3 had a strip arrangement where the central strip had a higher percentage of fibres than the upper and lower strips. Strip number one had an even distribution of fibres, and the area with more fibres was in the upper part. Strip number two or the central strip had a heavily packed number of bamboo fibres. Moreover, such density extended to the strip placed below. Strip number three had an even distribution of fibres, and like strip number one, the part of the strip with more fibres was facing upward. For this reason, strips two and three were densely reinforced by bamboo fibres, while the lower part of strip one became the weakest zone of the test region (Figure 4.20-**a**). Like the previous failure modes, the fracture started at the edges of the specimen, i.e., the lateral faces were the first to break (Figure 4.20-**b**). Then, the rupture propagated across the piece by breaking the parenchyma cells that supported the horizontally distributed bamboo fibres. Bamboo fibres became horizontal pathways for the crack to travel across the tested piece (Figure 4.20-**c**). As with the previous failure modes, fracture started in the area with fewer bamboo fibres, and it travelled horizontally - following the given outline of the bamboo fibres.

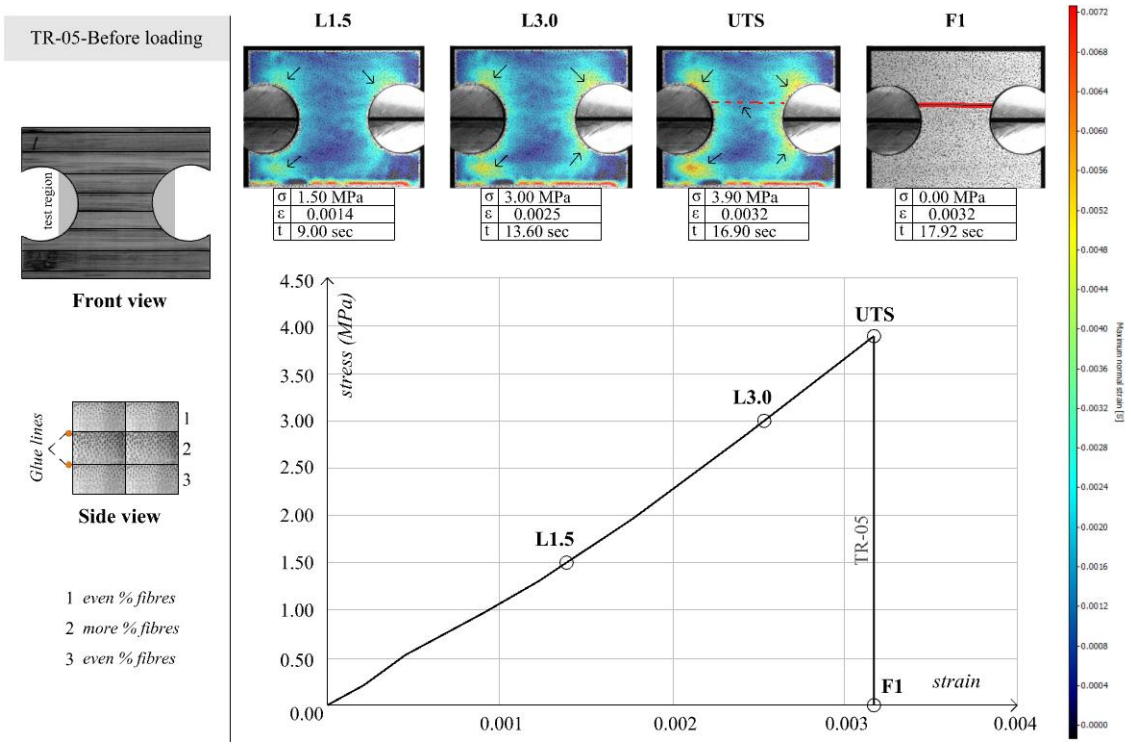

Figure 4. 19: **left**: Specimen TR-05 before loading, **right**: DIC analysis of specimen TR-05.

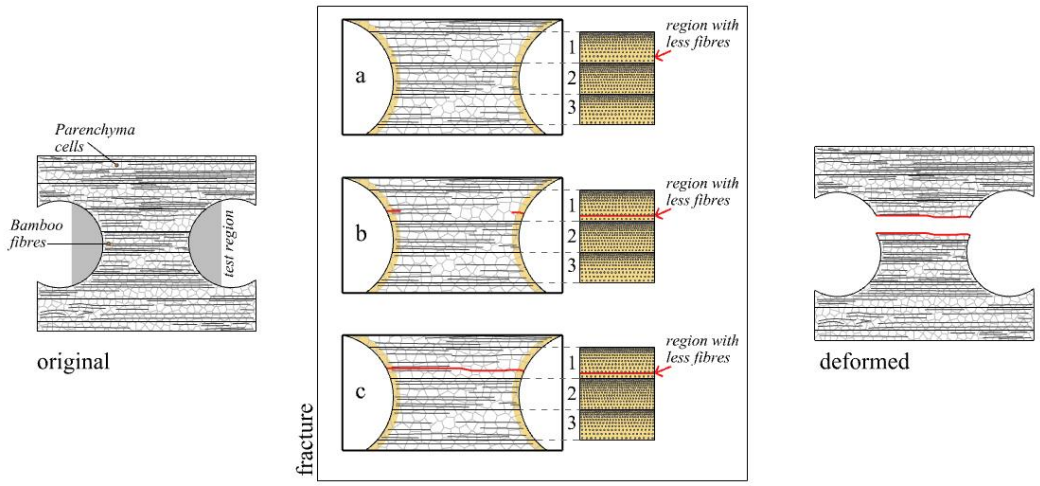

Figure 4. 20: Fracture analysis of Failure Mode 3.

4.2.3 Failure patterns in the radial direction

The analysis results suggest that fracture always started in the section of the test region that had the lesser reinforcement. The radial distribution of fibres, the location of nodes, and the arrangement of bamboo strips are the features that determined the mechanical response of the population. The section below describes how these features affected the onset of failure and the evolution of damage:

Feature 1: The cross-section of every bamboo strip has an area with more fibres and an area with fewer fibres. When tensile loads are applied along the radial direction, the area prone to failure will be the strip section with fewer fibres (Figure 4.21-**a**). It is in these areas where the parenchyma cells are not reinforced. Dixon and Gibson (2014) and Mannan et al. (2016) mentioned that the parenchyma cells are not as stiff as bamboo fibres. Hence, areas with a higher percentage of parenchyma cells will fail sooner.

Feature 2: As shown in Figure 4.21-**b**, in the radial face of the strip, bamboo fibres deviate from a unidirectional path to a curvilinear path. When pulling apart a strip in the radial direction, the fibres located near the nodes are not ripped apart. Instead, they provide a horizontal outline for the fracture to cut across the strip section with fewer fibres.

Feature 3: Strip arrangement becomes crucial when loads are applied in the radial direction. As shown in Figure 4.21-**a**, the amount of bamboo fibres increases towards the outer layer, decreasing near the inner layer. The experiments carried out by Xiao et al. (2013) suggest that the best way of arranging bamboo strips is by placing the interior

layer next to the outer layer. In practice, however, strips are arranged randomly. Areas with outer-to-outer arrangements will have a higher concentration of fibres (Figure 4.21-**c**). In comparison, areas with inner-to-inner arrangements will be weaker (Figure 4.21-**d**). In the case of the radial direction, the arrangement of strips creates material discontinuity. For this reason, some areas can become weaker spots.

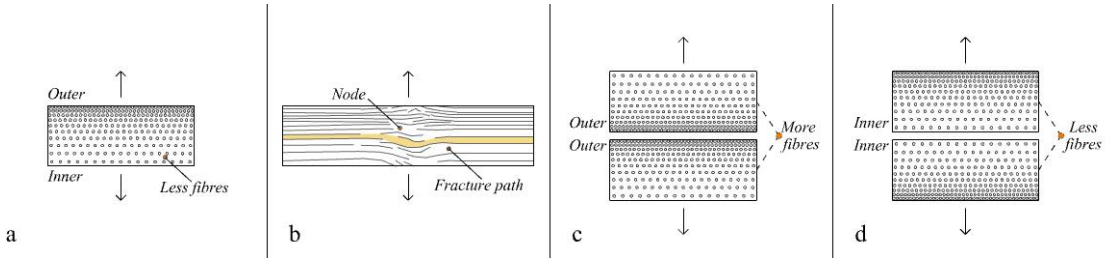

Figure 4. 21: Bamboo's features affecting tensile failure in the radial direction.

As described above, the physical features of bamboo - in the radial direction - were the factors that determined the beginning and evolution of damage. The main characteristics of the failure modes are outlined in the following section:

Failure Mode1 happened in the specimens with the lowest concentration of bamboo fibres in the mid-section of the central strip (Figure 4.22-**a**). As the tensile force pulled the piece apart, the edges of the tested pieces began to give way by de-bonding parenchyma cells. It is at the edges where the fracture started. Then, the crack travelled to the centre of the piece by following the outline of the fibres located close to the onset of failure. If nodes were found, the fracture followed the curvilinear profile of fibres surrounding the node.

Failure Mode 2 happened in the specimens with an even percentage of bamboo fibres in the test region. In this case, the dense part of the fibres occupied at least two-thirds of the cross-section of the strip (Figure 4.22-**b**). As such, as the loading increased, fracture started in the section of the central strip with the lowest concentration of fibres. It is in this place where the onset of fracture developed. Then, the fracture travelled horizontally following the fibres' linear patterns located in the strip's weakest region.

Failure Mode 3 happened in the specimens that had a central strip with a higher volume of bamboo fibres compared to the upper and lower strips forming the test region of the specimen (Figure 4.22-**c**). The high volume of fibres reinforced the central strip. Hence, fracture developed in the strip placed above or below the central strip - right in the less

reinforced area. As the force pulled the piece apart, fracture started in either the upper or lower strips. Then, like the previous failure modes, the fracture travelled horizontally following the linear patterns of the fibres located in the less reinforced section of the strip.

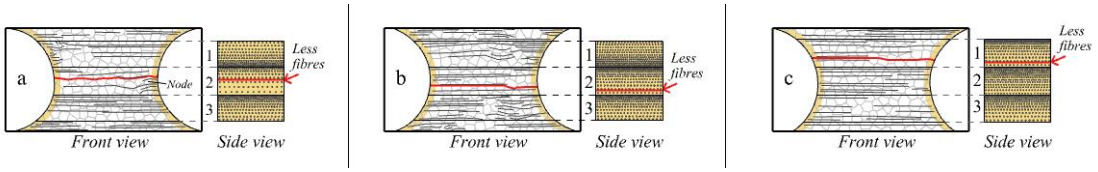

Figure 4. 22: Fracture patterns of laminated bamboo under radial tension.

Even though fracture happened in different sections of the test region, the onset of failure and posterior damage followed the same patterns:

Pattern 1 – Fracture always started in the regions with the lowest concentration of bamboo fibres. The inherent characteristics of the strips and the arrangement of the strip are factors that determined fracture's shape and location.

Pattern 2 – After the onset of failure, the crack always travelled horizontally - by following the pattern of the fibres located closer to the region with fewer fibres. If nodes were close to this region, the crack would follow the curvilinear outline of the fibres surrounding the nodes.

4.3 Tangential deformation and failure

4.3.1 Mechanical properties and behaviour

The sample under tangential tension broke at an average Ultimate Tensile Strength of 5.65 MPa. The average Modulus of Elasticity of the population was 1,487.44 MPa. Table 4.3 summarises the strength and the mechanical values of the tested sample. Sharma et al. (2015a) and Khoshbakht et al. (2018) and reported laminated bamboo's average perpendicular tensile strength as a value ranging from 2.00 MPa to 5.00 MPa. However, these studies do not distinguish between the radial and tangential directions. In 2017, Sharma et al. performed tests to determine the Tensile Strength of specimens submitted to tangential tension. The study reported an average Tensile Strength of 3.8 MPa and an average Modulus of Elasticity of 1,295 MPa. The values reported in this study are slightly higher than those reported in the available literature. Further investigations are needed to

fully characterise the tensile properties of laminated bamboo along the tangential direction. As shown in Figure 4.23, all the pieces exhibited an elastic-brittle behaviour. The stress-strain curves reveal a linear behaviour all the way up to the Ultimate Strength. After this point, the tested pieces broke abruptly. The average maximum displacement of the population was 0.52 mm.

	Average	SD value	Characteristic value
Ultimate Tensile Strength (MPa)	5.65	0.84	4.20
COV	0.15		
Modulus of Elasticity (MPa)	1,487.44	83.91	1339.17
COV	0.06		

Table 4. 3: Strength and mechanical properties of the sample under tangential tension.

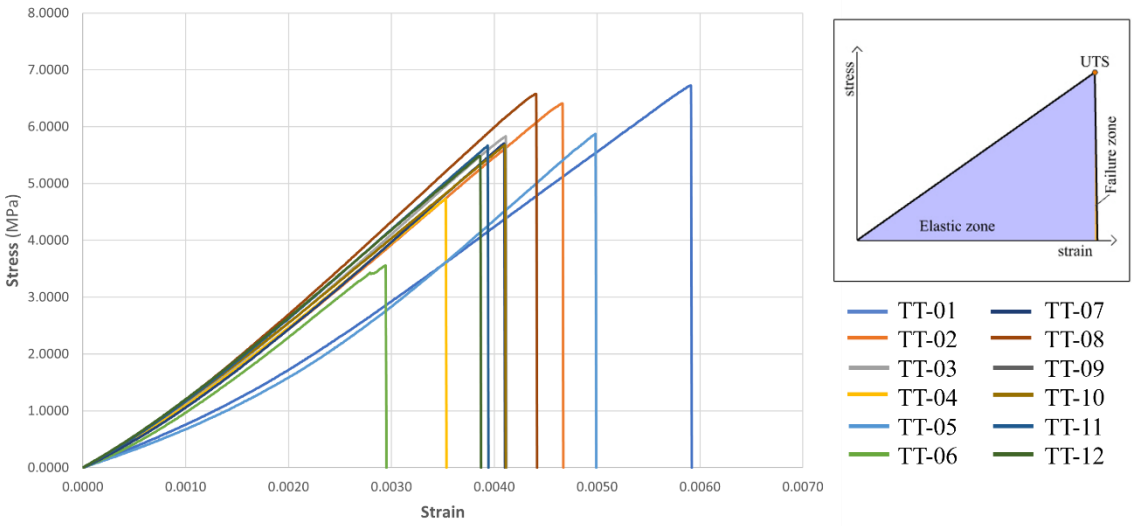

Figure 4. 23: Stress-strain curves of specimens under tangential tension.

4.3.2 Deformation and failure modes

The fracture of all pieces happened within the reduced section of the specimens. The density of bamboo fibres and the presence of node regions are the factors that determined the location of the fracture. Only two failure modes were found in the population. In failure Mode 1, the fracture occurred in the mid-section of the central strip (Figure 4.24-**Mode 1**). The tensile strength of these specimens ranged from 5.02 MPa to a maximum strength of 7.05 MPa. The difference in strength values can be explained by analysing the physical characteristics of the central strip. If the strip had fewer fibres, the strength would be lower than the average tensile strength. On the other hand, the fracture of Failure Mode

2 happened in the upper or lower sections of the central strip (Figure 4.24-**Mode 2**). As with the other specimens, the strength of the pieces - in Failure Mode 2 – was directly affected by the number of bamboo fibres. However, the presence of nodal regions created weaker regions in the upper or lower sections of the central strip.

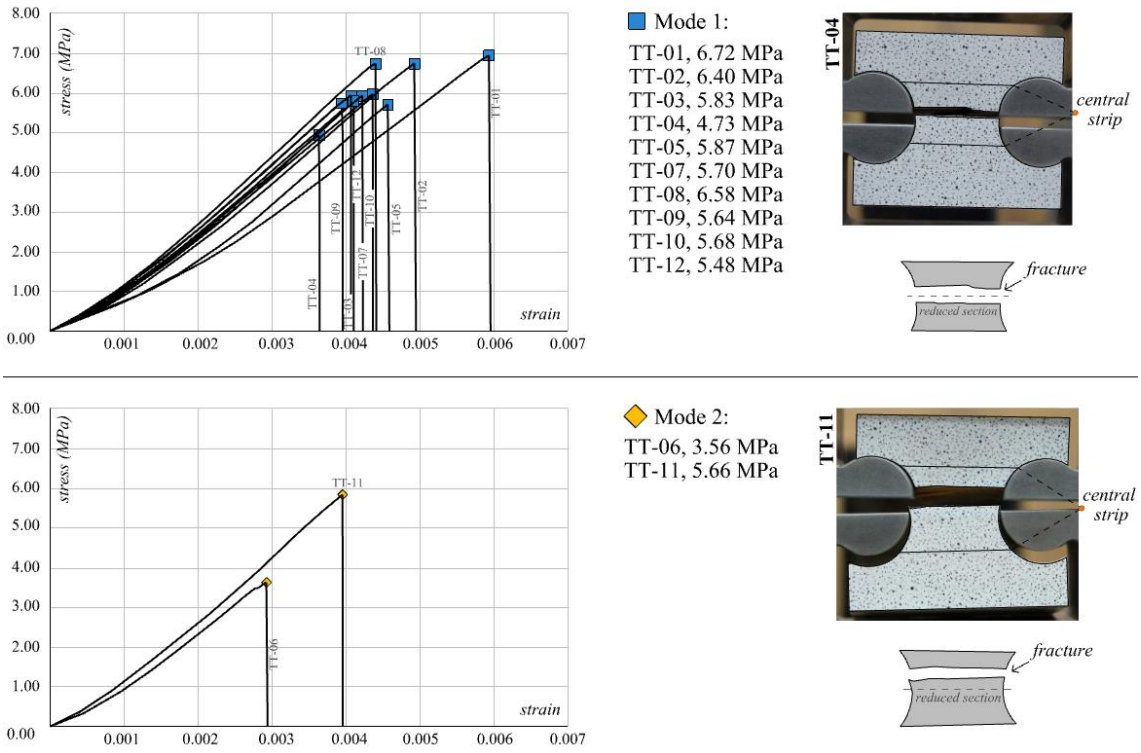

Figure 4. 24: Stress-strain curves and failure modes of the sample under tangential tension.

Failure Mode 1 was the most frequent type of failure. Specimens TT-01, TT-02, TT-03, TT-04, TT-05, TT-07, TT-08, TT-09, TT-10, and TT-12 exhibited this failure. As can be seen in Figure 4.25-**left**, the specimens had an even distribution of fibres with no nodal regions. At 1.50 MPa, strain fields were evenly distributed across the whole surface of the specimen (Figure 4.25-**L1.5**). The maximum normal strain at this stage did not exceed 0.002. At 3.0 MPa, the strain increased to 0.004. However, the strain remained equally distributed across the specimen's surface (Figure 4.25-**L3.0**). At 4.50 MPa, light yellow patches started to appear along the edges - close to the grips holding the specimen (Figure 4.25-**L4.5**). After 18.93 seconds, the specimen reached an Ultimate Tensile Strength of 4.73 MPa (Figure 4.25-**UTS**). At this point, the edges started to become more yellow, and a red spot appeared on one of the sides of the specimens. Simultaneously, light blue lines started to branch out from the edges towards the central axis of the tested pieces. The fracture happened in one of the blue lines—particularly the strain line within the specimen section that had the minimum cross-section. The final geometry of the fracture was a horizontal line in the mid-section of the central strip (Figure 4.25-**F1**).

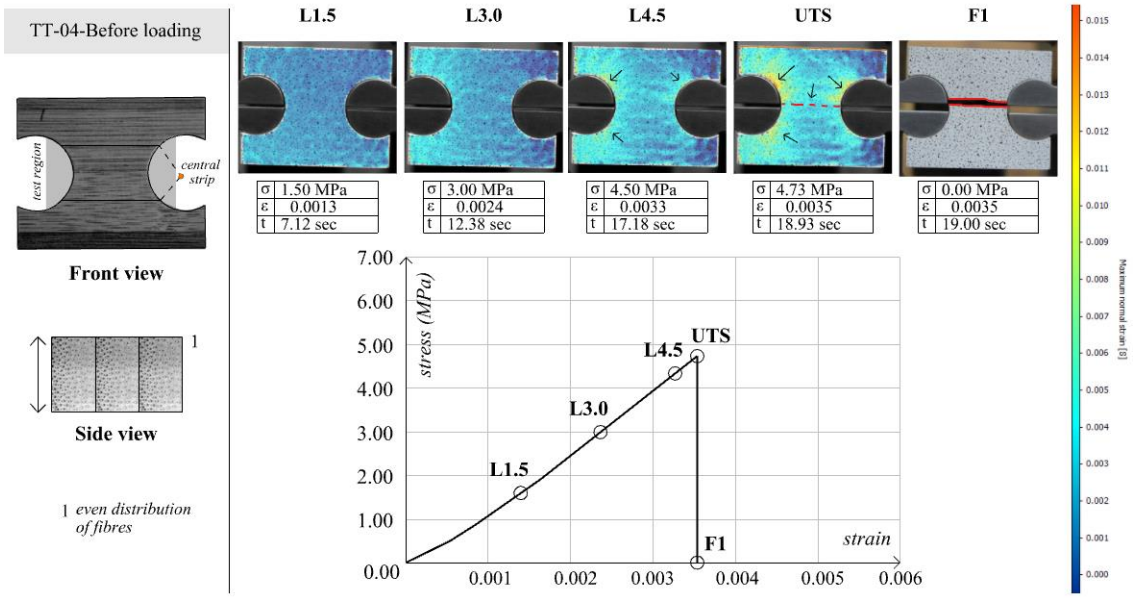

Figure 4. 25: left: Specimen TT-04 before loading, **right**- DIC analysis of specimen TT-04.

The fracture mechanism of Failure Mode 1 can be explained by analysing the frontal and side views of the tested pieces. As can be seen in Figure 2.26-**a**, the central strip is made of single strips arranged vertically. This means that the fibres are equally distributed along the tangential direction. The radial configuration of bamboo fibres does not affect the distribution of fibres in the tangential direction. Hence, it can be assumed that the central strip is equally reinforced across its cross-section. The reduced section of the main strip, thus, became the weaker section of the specimen (Figure 2.26-**b**). As shown in the DIC analysis, as the load increased, strain concentrations developed at the lateral faces of the specimen. Cracks likely formed at the middle of the lateral faces simultaneously. Then, the lateral cracks travelled to the middle of the central strip by following the horizontal arrangement of bamboo fibres (Figure 2.26-**c**). It is important to note that regardless of the percentage of bamboo fibres, the tangential distribution of bamboo fibres remains even. For this reason, the percentage of fibres affects the loading capabilities of the piece, but it did not trigger a failure mode different from the one described above.

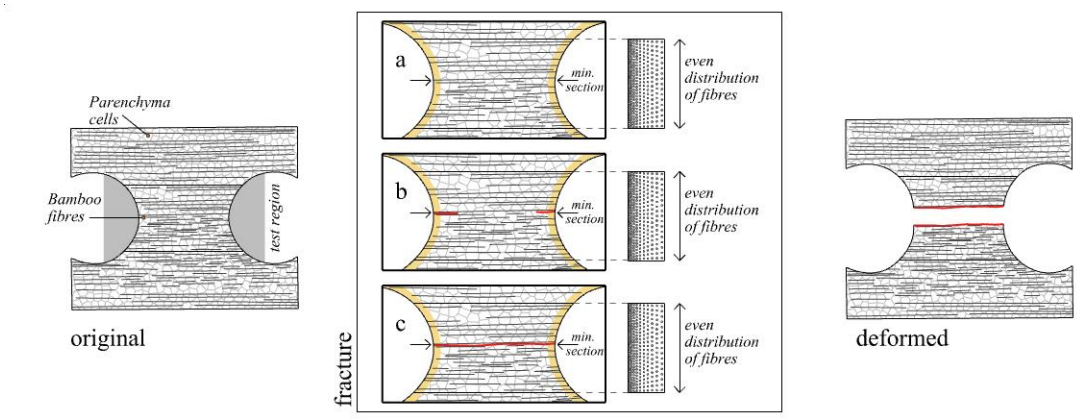

Figure 4. 26: Fracture analysis of Failure Mode 1

Failure Mode 2 was the least frequent type of fracture, and it only occurred in specimens TT-06 and TT-11. The presence of nodal regions - in the central strip - caused fibre discontinuity in some of the areas of the strip (Figure 2.27-**left**). Figure 2.27-L1.5 shows an evenly distributed strain field at 1.5MPa. The maximum normal strain at 1.50 MPa was 0.002. As the loading continued, the strain field increased gradually. At 3.00 MPa, the maximum normal strain values increased from 0.002 to 0.003 (Figure 2.27-**L3.0**). At 4.50 MPa, yellow patches appeared in the lateral edges of the specimen and in the upper and lower regions (Figure 2.27-**L4.5**). The values of the maximum normal strain at these regions ranged from 0.010 to 0.014. At this point, it became possible to notice that a myriad of blue lines was stretching out from the edges into the central axis of the piece. At 5.66 MPa, red spots are visible along the edges of the strip. The value of the maximum normal strain at these points is 0.0015. These red dots formed at the edges of the specimen. Specifically, they formed in the sections affected by the nodal region. Figure 4.27-**UTS** shows the strain distribution right before fracture. The fracture developed in the edges that had fewer to no fibres. These regions were found within or close to the nodal region of the strip. After lateral cracks developed, the fracture followed the path of one of the blue lines crossing the specimen. The final geometry of this failure mode is a horizontal line in the upper or lower sections of the central strip (Figure 4.27-**F1**).

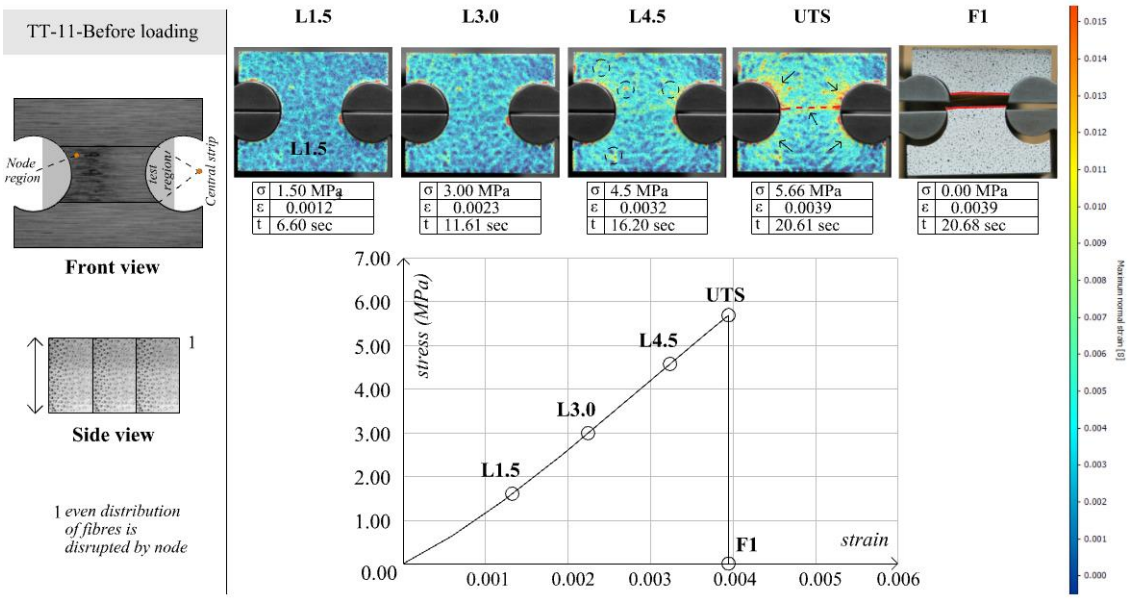

Figure 4. 27: **left**: Specimen TT-11 before loading, **right**- DIC analysis of specimen TT-11.

The fracture mechanism of Failure Mode 2 differs from Failure Mode 1 in that the existence of nodal regions created gaps of fibre discontinuity across the tangential direction (Figure 4.28-**a**). The irregular distribution of fibres along the nodal region created areas with fewer or no fibres. These areas happened to be located within the reduced section of the specimen - particularly in or close to the lateral edges. As the load increased, the lateral edges were submitted to higher strain concentrations – compared to

other parts of the specimen. Since the central region of the strip was reinforced with fibres, the fracture started in the area that had fewer fibres (Figure 4.28-**b**). This region was placed in the upper or lower sections of the strip – right in the node section. The sections of the edge with fewer or no fibres broke first. A fracture usually follows the fibres' path near the region where the initial cracks developed. For Failure Mode 2, the initial cracks formed in the nodal areas. Hence, after the onset of fracture, the cracks travelled to the centre of the specimen by following the arrangement of the fibres located in the nodal region (Figure 4.28-**c**). It can be concluded, thus, that nodes disrupted the even distribution of fibres in the tangential direction, which caused failure to happen off the central axis.

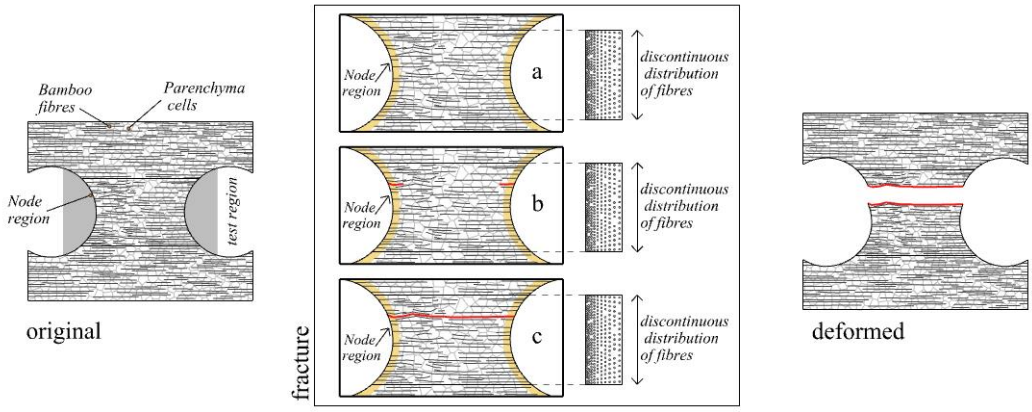

Figure 4. 28: Fracture analysis of Failure Mode 2.

4.3.3 Failure patterns in the tangential direction

The number of bamboo fibres and the location of nodes are the physical features of the strips that influenced the strength properties and mechanical response of the material when tangential tension was applied. Specifically, the number of fibres affected the loading capacity of the specimens, while the nodes created areas with less reinforcement. The section below explains the impact that each of these features had on the tested pieces:

Feature 1 – As shown in Figure 4.29-**left**, the distribution of bamboo fibres is constant in the tangential direction, whereas in the radial direction, the density of fibres changes horizontally. Such arrangement creates a section with equally distributed reinforcement along the tangential direction. In this case, the density of bamboo fibres affects the tensile strength of the material. In other words, strips with fewer fibres will have lower tensile strength compared to strips with more fibres. However, the results of the experiments suggest that changes in fibre density do not create different failure mechanisms.

Feature 2 – The location of nodes creates fibre discontinuity in all the strip directions (Figure 4.29-**right**). Nodal regions are the areas where the tangential reinforcement

decreases, or it might even become completely negligible. The presence of nodes disrupts the even distribution of fibres in the tangential direction. As tensile forces try to pull the strip apart, the strip will begin to break in the areas with less reinforcement, i.e., the nodal regions. Besides triggering fracture, nodal regions also act as pathways for the crack to cross the whole piece.

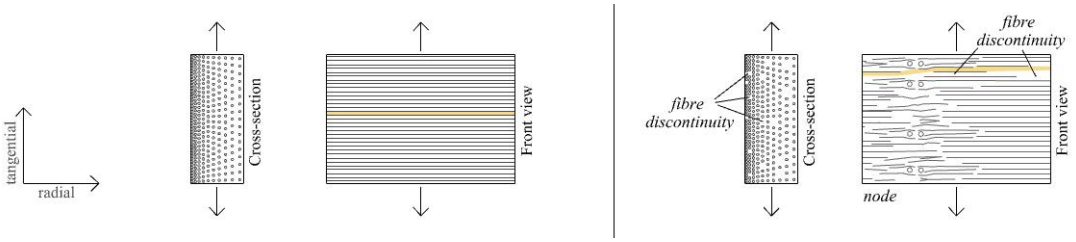

Figure 4. 29: Bamboo's features affecting tensile failure in the tangential direction.

Based on the analysis of the features that were previously outlined, laminated bamboo exhibited two failure modes when tensile forces were applied in the tangential direction:

Failure Mode 1 happened in the specimens with a constant fibre's distribution in the tangential direction. In other words, the pieces did not have nodes. The lack of areas with a lower concentration of fibres meant that the load was equally distributed across the lateral faces of the specimen (Figure 4.30-**a**). The weakest point of the specimen became the section of the strip with the minimum area, i.e., the middle of the central strip. As tensile loading increased, the fracture developed in the weakest section. After cracks formed in the lateral edges of the specimen, both cracks travelled to the central axis following the linear arrangement of bamboo fibres located in the mid-section.

Failure Mode 2 happened in the specimens that had one node in the central strip. The node disrupted the continuous distribution of fibres in the tangential direction, which created areas with a higher percentage of parenchyma cells. Because of this disruption, the areas with more parenchyma cells became the weakest points of the specimen (Figure 4.30-**b**). As the tensile load increased, cracks quickly developed near the node region - particularly in the part of the edges that had a lower percentage of fibres. After fracture ensued at both edges, the cracks quickly crossed the reduced section of the specimen by following the disrupted arrangement of the fibres located within the nodal region.

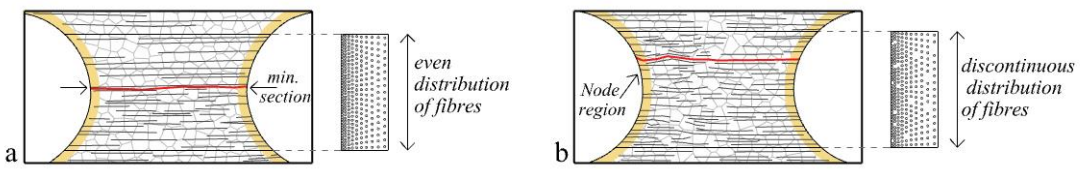

Figure 4. 30: Fracture patterns of laminated bamboo under tangential tension.

Overall, no matter the failure mode, two patterns were found in the population:

Pattern 1: The onset of failure always occurred in the areas where the even distribution of fibres was affected somehow. In the case of strips with no nodes, the reduced cross-section of the specimen became the weakest point. Contrary to this, the regions with fibre discontinuity became the sections prone to failure in the strips with nodes.

Pattern 2: After the fracture process began, the crack always travelled horizontally. If there were no nodes, the crack would simply follow the linear arrangement of bamboo fibres. Conversely, if there were node regions, the crack would follow the structure of the fibres located in the nodal area.

4.4 Longitudinal, radial, and tangential comparison

The unique physical and heterogeneous properties of raw bamboo are the factors that determine the mechanical response of laminated bamboo when tensile loads are applied in the longitudinal, radial, and tangential directions. First, it is essential to consider that the physical configuration of every bamboo culm is unique. This means that the density of bamboo's fibres inevitably varies from one strip to another. Second, the monotonic distribution of fibres across the radial direction naturally reinforces the outer layer of the culm, which means that a single strip has different mechanical properties along its cross-section. Third, the bamboo culm is divided by nodes that support its vertical growth. For this reason, bamboo fibres do not run continuously along the longitudinal direction. Instead, the distribution of fibres becomes highly irregular at nodes. This means that strips have different mechanical properties in node regions. Finally, given these discontinuities, the material's behaviour is directly impacted by how the strips are arranged during the manufacturing process.

The density of bamboo fibres directly impacted the tensile strength of the material. As can be seen in Figure 4.31-**a**, when loads are applied in the longitudinal direction, the force stretches the fibres. Since the fibres are the strongest elements of bamboo strips, the material has higher mechanical properties along the longitudinal direction. The average tensile strength - in the longitudinal direction - was 89.10 MPa. In the radial and tangential directions, the action of the force is not stretching the fibres. Instead, the force is pulling the parenchyma cells apart. The parenchyma cells are the first elements to fail as the load increases. The distribution of fibres – in the radial and tangential directions – explains why laminated bamboo a slightly higher tensile strength has when loads are applied in the tangential direction. As shown in Figure 4.31-**b**, the fibres are equally distributed

along the vertical direction when tangential tension is applied. When the force pulls the strip apart, the side of the strips with more fibres will act as a reinforcement. The average tensile strength – in the tangential direction – was 5.65 MPa. However, the radial direction has an uneven distribution of fibres when strips are placed horizontally. As shown in Figure 4.31-**c**, when tensile loads are applied in the radial direction, the strip section with fewer fibres will be prone to fail. For this reason, the tensile strength – in the radial direction – was the lowest, with an average value of 4.85 MPa. Overall, the main factors that determined the tensile strength of the laminates were fibre orientation, fibre density and fibre distribution.

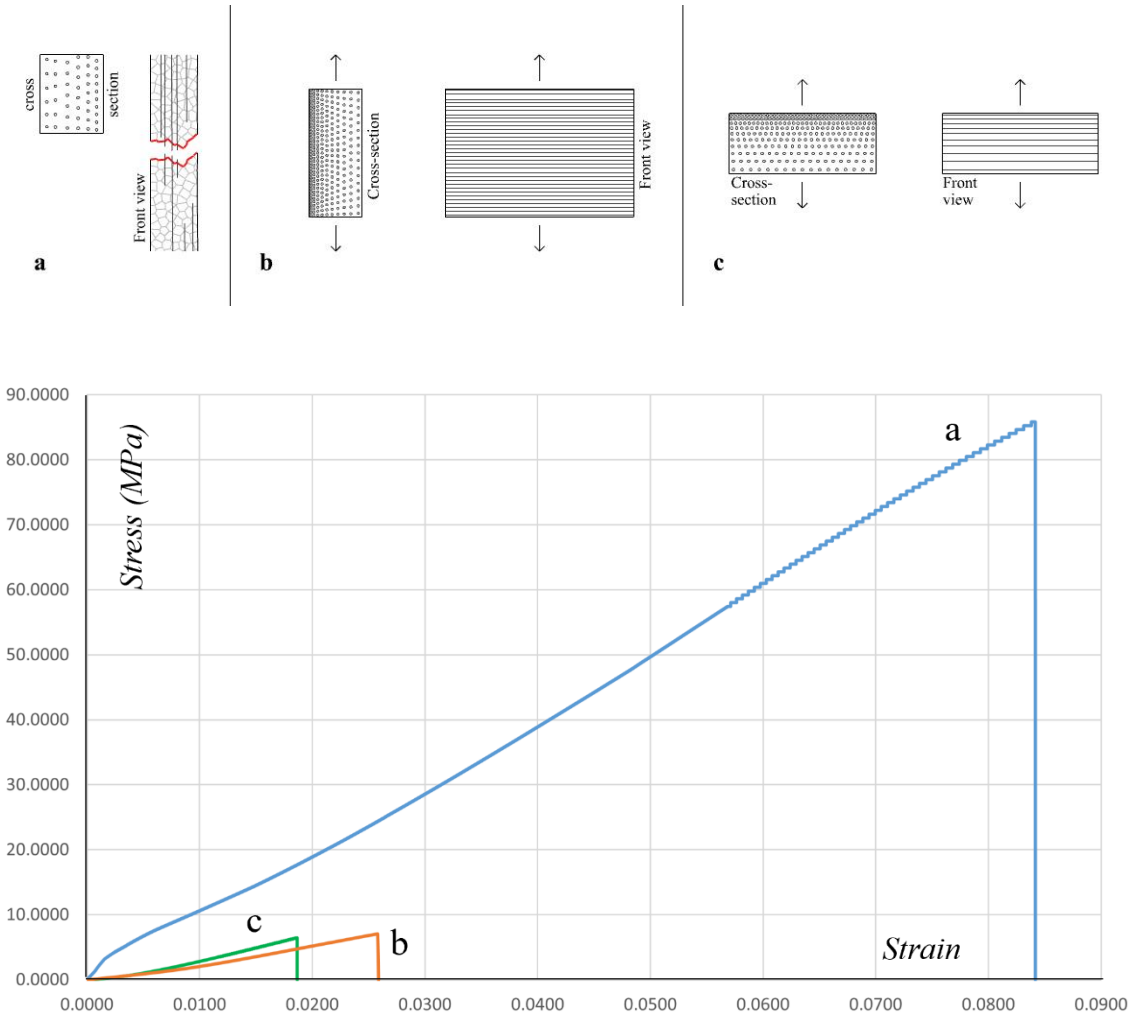

Figure 4. 31: The mechanical behaviour of samples under tensile loading.

The features that influenced the deformation and failure of the laminates under tension were the monotonic distribution of fibres – in the transversal section, the presence of nodes, and the arrangement of bamboo strips. The monotonic distribution of bamboo fibres in the transversal section affects the mechanical response of laminated bamboo in the longitudinal and radial directions. Specimens under tangential tension were not directly affected by this feature. When tensile loads are applied in the longitudinal

direction, the section with fewer fibres is usually more susceptible to fracture. Whenever a section with fewer fibres is pulled longitudinally, the load will break the parenchyma cells, and a linear crack appears (Figure 4.32- **a**). However, the section of the strip with a higher volume of fibres will have better performance, and the typical fracture is a staggered profile created as the force rips the fibres apart (Figure 4.32- **b**). The monotonic distribution of fibres plays a crucial role in the mechanical response of laminated bamboo in the radial direction. As can be seen in Figure 4.32- **c**, the section of the strip with fewer fibres is where the fracture is likely to start. In all the specimens under radial tension, fracture always began in the part of the strip that had fewer fibres. The tangential direction is not affected by the monotonic distribution of fibres. When strips are placed vertically, the increasing distribution of fibres is located horizontally. For this reason, when tensile loads are applied – in the tangential direction – the section of the strip that has more fibres is likely to act as reinforcement for the entire strip. In this case, failure is expected to happen in the part of the specimen that has a minimum cross-area (Figure 4.32- **d**).

Nodes have fewer fibres than internodal regions. Also, the fibres are irregularly distributed in these regions. Some fibres will curve around the node; some will change direction at the nodal region. Due to this arrangement, bamboo fibres become discontinuous in the nodal areas. Fibre discontinuity created spots with poor mechanical performance. In the longitudinal direction, nodes become breakpoints. When tensile loads are applied, nodes are the first elements to fail (Figure 4.33- **a**). The absence of fibres acting as reinforcement makes these areas quite fragile compared to other parts of the strip. In the radial direction, nodes do not seem to become breakpoints. Instead, they can change the path of the crack from linear to curvilinear (Figure 4.33- **b**). Finally, the tangential direction is affected by the presence of nodes since the irregular distribution of fibres disrupts the continuous arrangement of fibres along the longitudinal direction. Like in the longitudinal direction, nodes do become breakpoints in the tangential direction (Figure 4.33- **c**). And like in the radial direction, nodes also serve as pathways to direct the crack across the specimens. Overall, the direction mostly affected by nodes is the longitudinal direction since the applied load is directly pulling apart the poorly reinforced areas.

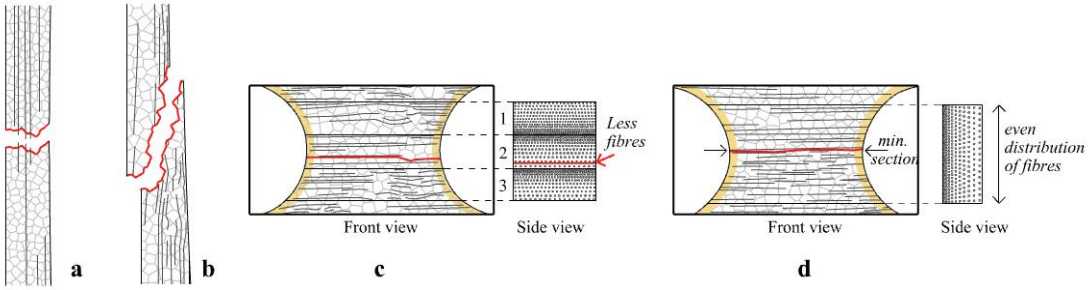

Figure 4. 32: Fibre distribution and its effect on tensile deformation.

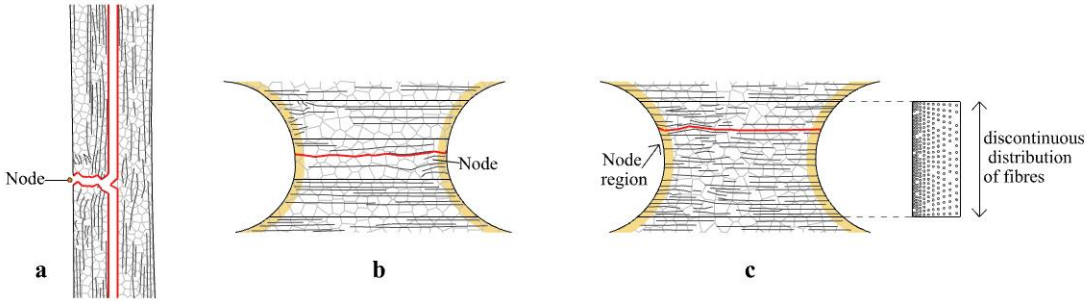

Figure 4. 33: Nodes and their effect on tensile deformation.

Finally, the arrangement of bamboo strips during the manufacturing process also affects the material's mechanical response. Nugroho and Ando (2001) and Mahdavi, Clouston, and Arwade (2011) mentioned that the optimal arrangement of fibres is to place inner-to-outer faces next to each other. However, in practice, this is not always achieved. In the longitudinal direction, the arrangement of strips can increase or decrease the density of fibres, making the laminate stronger or weaker (Figure 4.34-**a**). Also, strip arrangement determines the failure mode. If inner to outer layers are placed together, the distribution of fibres is more even, and the specimen is likely to fail due to other factors, such as the existence of nodes or in sections that have a smaller cross-section. On the other hand, if outer to outer or inner to inner arrangements are made, different fracture modes might be triggered. Overall, strip arrangement does not seem to impact the tensile strength of the tested pieces - in the radial and tangential directions. However, it can determine the type of fracture. In the radial direction, strip arrangement plays a crucial role in determining the mechanical response of the pieces. Outer to outer arrangements create areas with more fibre reinforcement (Figure 4.34-**b**), inner to inner arrangements create areas with less fibre reinforcement (Figure 4.34-**c**). From these two options, the less ideal is inner-to-inner since these areas become breakpoints. The ideal arrangement is outer to inner since this provides a balanced distribution of reinforced and less reinforced sections. Finally, the tangential direction does not seem to be highly impacted by strip arrangement. The fact that the fibre distribution does not increases or decreases means that the number of fibres remains constant despite the arrangement of the strips. Other factors such as the geometry of the specimen or the presence of nodes are the reasons likely to trigger fracture in the tangential direction.

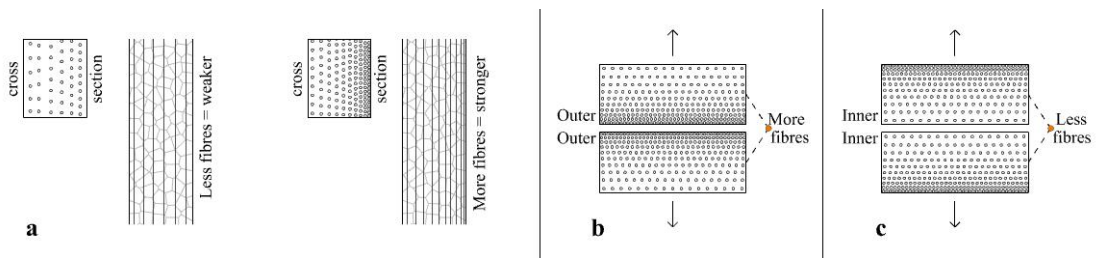

Figure 4. 34: Strip arrangements and its effect on tensile deformation.

Overall, it can be concluded that the characteristics of bamboo will have different levels of impact on the material's performance depending on the direction in which the load is applied. Node regions have a more significant influence on the specimens under longitudinal tension. On the other hand, the monotonic distribution of fibres and strip arrangement have a higher impact on the response of the material when radial tension is applied. To a lesser degree, nodes also affect the mechanical response of specimens under tangential tension since the irregular distribution of fibres also creates breakpoints. Knowledge of the different factors that affect the mechanical response of laminated bamboo in all directions is useful to develop strategies to reinforce structural elements submitted to uniaxial tensile loading.

Chapter 5 | Uniaxial compression

| This chapter describes the different failure modes of laminated bamboo when uniaxial compressive loads are applied. The first, second and third sections of the chapter describe the mechanical behaviour, deformation, and failure of laminated bamboo in the longitudinal, radial, and tangential directions. Finally, the fourth section compares the mechanical properties and behaviour of the three directions. |

5.1 Longitudinal deformation and failure

5.1.1 Mechanical properties and behaviour

The sample submitted to longitudinal compression exhibited an elastic-plastic behaviour. The sample had an average Proportional Limit (PL) of 38.84 MPa. After reaching this point, nonlinear plastic deformation set in, and the process of irrecoverable deformation began. As loading continued, the sample reached an average Ultimate Compressive Strength (UCS) of 58.43 MPa. Once reaching the Ultimate Compressive Strength, the strength of the sample started to decrease until reaching an average Fracture strength of 504.28 MPa. As shown in Figure 5.1, the stress-strain curves have a small elastic region and a wider plastic region, which means that the specimens underwent a considerable degree of deformation before fracture began. The average Modulus of Elasticity is 11,837.83 MPa. Table 5.1 summarises the strength and mechanical properties of the specimens under longitudinal compression.

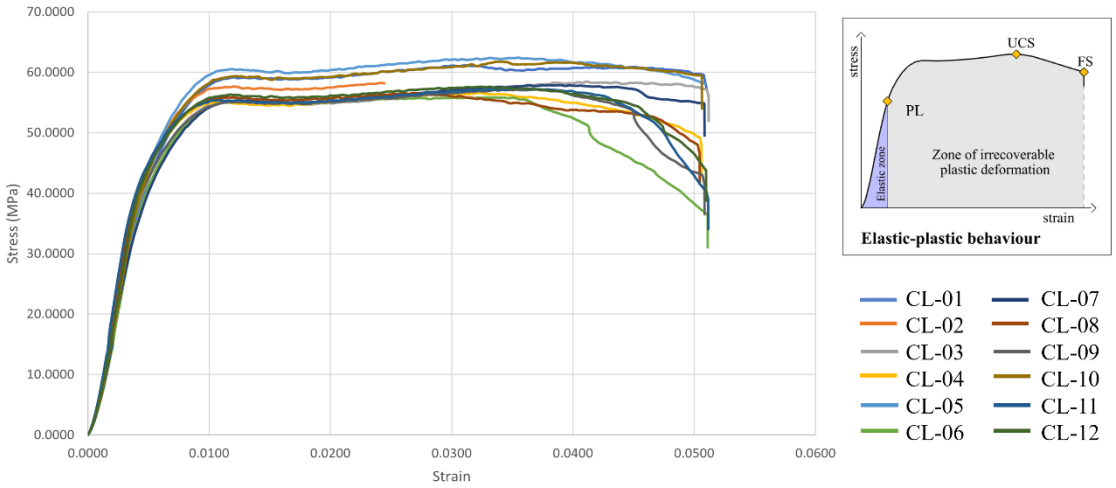

Figure 5. 1: Stress-strain curve of the sample under longitudinal compression.

	Average	SD value	Characteristic value
Proportional Limit (MPa)	38.84	1.85	35.67
COV	0.05		
Ultimate Compressive Strength (MPa)	58.43	2.17	56.25
COV	0.04		
Fracture Strength (MPa)	54.23	4.17	47.57
COV	0.16		
Modulus of elasticity (MPa)	11,837.83	739.59	11,006.25
COV	0.06		

Table 5. 1: Strength and mechanical properties of the sample under longitudinal compression

The strength and mechanical values reported in this study are within the range of those reported in the available literature. Khoshbakht et al. (2018) reported an average Compressive Strength of 62 MPa and an average Modulus of Elasticity of 9,219 MPa. Yang et al. (2020) registered an average Compressive Strength of 75.10 MPa - with a characteristic value of 69.90 MPa, and an average Modulus of Elasticity of 9,913 MPa - with a characteristic value of 8,915 MPa.

5.1.2 Deformation and failure modes

Matrix cracking, buckling, and crushing were the types of failures found in the population. The results suggest nodal regions played a critical role in determining the failure mechanisms of the specimens. Osorio et al. (2018) and Shao and Wang (2018a) noted that the irregularity of bamboo fibres at nodal regions creates areas with weaker mechanical properties. As shown in Figure 5.2, the distribution and arrangement of bamboo fibres are different along the radial and tangential directions. In the radial direction, the fibres bend in-and-out forming curvilinear profiles to support the upward growth of bamboo. Conversely, discontinuous fibres meet at the nodal ridge forming a horizontal line in the tangential direction. Based on the findings of the experimental program, it is possible to conclude that the number and location of bamboo nodes are factors that regulate the onset of failure and the posterior evolution of the material's damage.

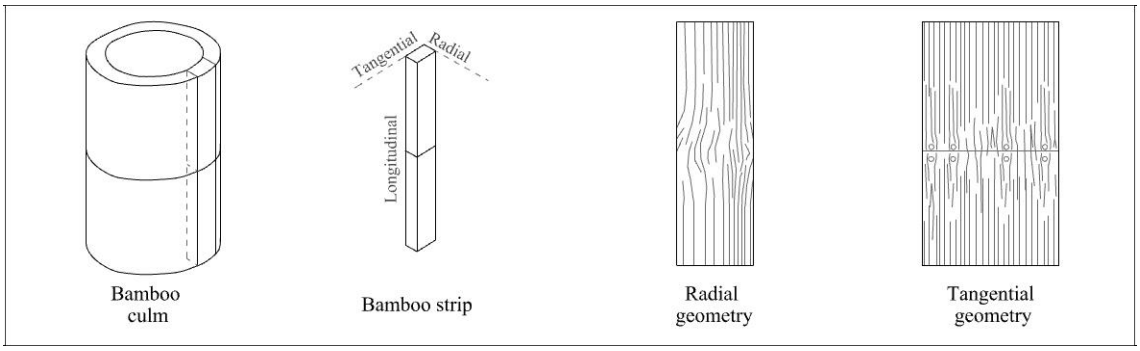

Figure 5. 2: The arrangement of bamboo fibres in nodal regions.

A higher concentration of nodal regions was found in five of the tested specimens. These specimens had compressive and fracture strengths higher than the average values. Failure started in the nodal regions where matrix cracking appeared. Simultaneously, lateral fibres began to buckle. This failure mechanism was classified as Failure Mode 1 (Figure 5.3-**up**). Some of these specimens presented crushing as secondary failure. However, crushing only appeared in the specimens that had tangential nodes in any of their faces. Contrary to the previous behaviour, the other six specimens had a lower concentration of nodal regions. These specimens had compressive and fracture strengths lower than the average values. For these specimens, no matrix cracking was found. Instead, as the load increased, the fibres started to bend, and buckling delamination happened in the external faces of the tested pieces. This failure mechanism was classified as Failure Mode 2 (Figure 5.3-**down**). As in Failure Mode 1, crushing developed later if any of the specimens had tangential nodes in their exterior faces.

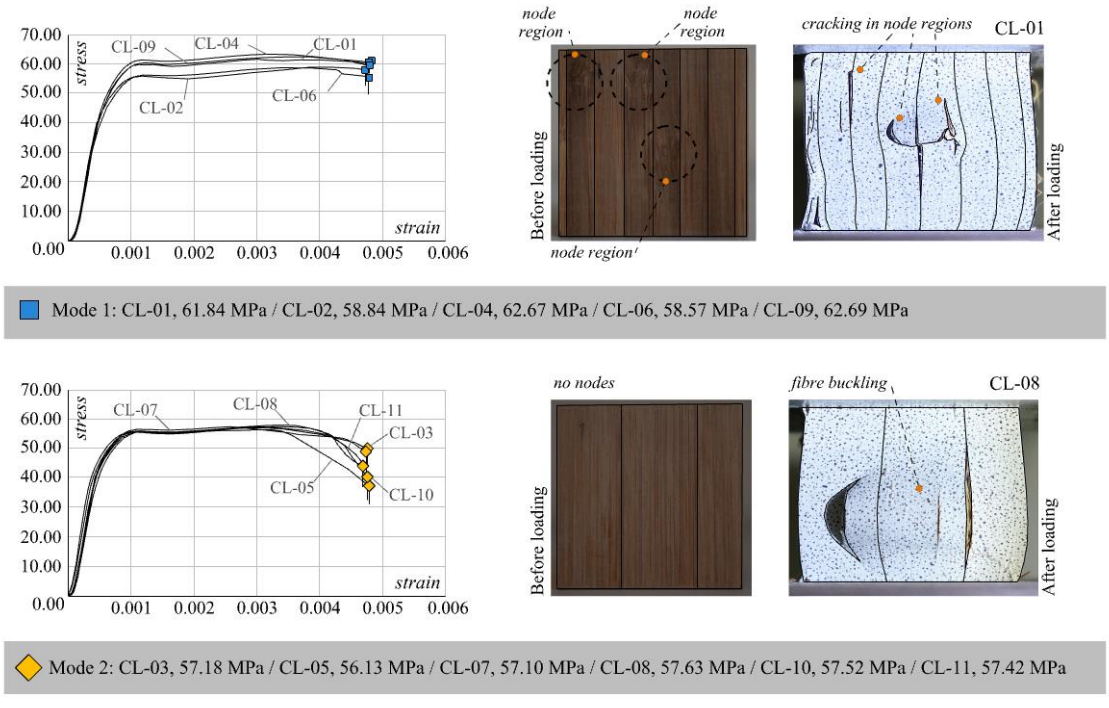

Figure 5. 3: **up**- Failure Mechanism 1, **down**- Failure Mechanism 2.

Failure Mode 1 occurred in specimens CL-01, CL-02, CL-04, CL-06, and CL-09. The pieces had more than two radial nodes in the face where the speckle pattern was applied. This is also the face recorded with the High-Resolution Camera and the DIC equipment. As shown in Figure 5.4-**up**, the lateral faces of the specimen had no nodes or one tangential node. In total, these specimens had more than five nodes. Some specimens had more nodes in the face that was not recorded with the camera. However, the existence of more nodes seemed to increase the strength of the samples. At 26.62 MPa, the strain distribution showed yellow and red patches across the middle section of the piece (Figure 5.4-**P1**). The most significant red spot was in the region between the central nodes. The maximum normal strain at these areas ranged from 0.325 to 0.425. When the specimen reached the Proportional Limit – at 40.37 MPa – the area covered by the yellow patches became smaller, and the area with the red patches became more defined (Figure 5.4-**PL**). The value of the maximum normal strain in the red zone was higher than 0.425. At 59.65 MPa, the maximum strain began to concentrate in the red spot. At this point, the yellow patches began to be less spread across the central region of the specimen (Figure 5.4-**P2**). When the specimen reached its Ultimate Tensile Strength – at 61.84 MPa – the yellow patches disappeared, and the area between the nodes showed the highest deformation. At this point, a crack appeared in the place where the red spot was located (Figure 5.4-**UCS**). After this moment, the stress decreased from 61.84 MPa to 60.63 MPa. As shown in Figure 5.4-**FS**, by the time the specimen reached the Fracture Strength, numerous cracks developed in the centre and upper regions of the tested piece. The cracks formed in or near the radial nodes.

The deformation of the specimens that exhibited Failure Mode 1 can be explained by looking at the arrangement of bamboo fibres in the frontal face of the tested piece. Figure 5.5-**a** shows the distribution of fibres before loading began. A closer look at the image revealed that the major disruption of fibres was located near the radial nodes. Parenchyma cells have a lower resistance when compared to bamboo fibres. For this reason, as the compressive load pushed the piece together, the parenchyma cells were crushed by the force. As the area of the parenchyma cells changed, the longitudinal fibres acted as lateral boundaries, resisting the push of the changing parenchyma cells. However, at some point, the lateral push created by the flattening of the parenchyma cells ended up bending the bamboo fibres. As shown in Figure 5.5 **b-c**, the lateral fibres began to buckle when the piece started to become shorter. However, around the nodes, the already curved fibres had less resistance than the longitudinal fibres. For this reason, the deformation was localised in the regions near the nodes. Additionally, the bending of the fibres near the radial nodes created pockets where the material was not reinforced. It is in these areas where cracks developed as the loading continued. Figure 5.5-**d** shows the deformed state of the specimen. At this point, the specimen completely lost its loading capabilities.

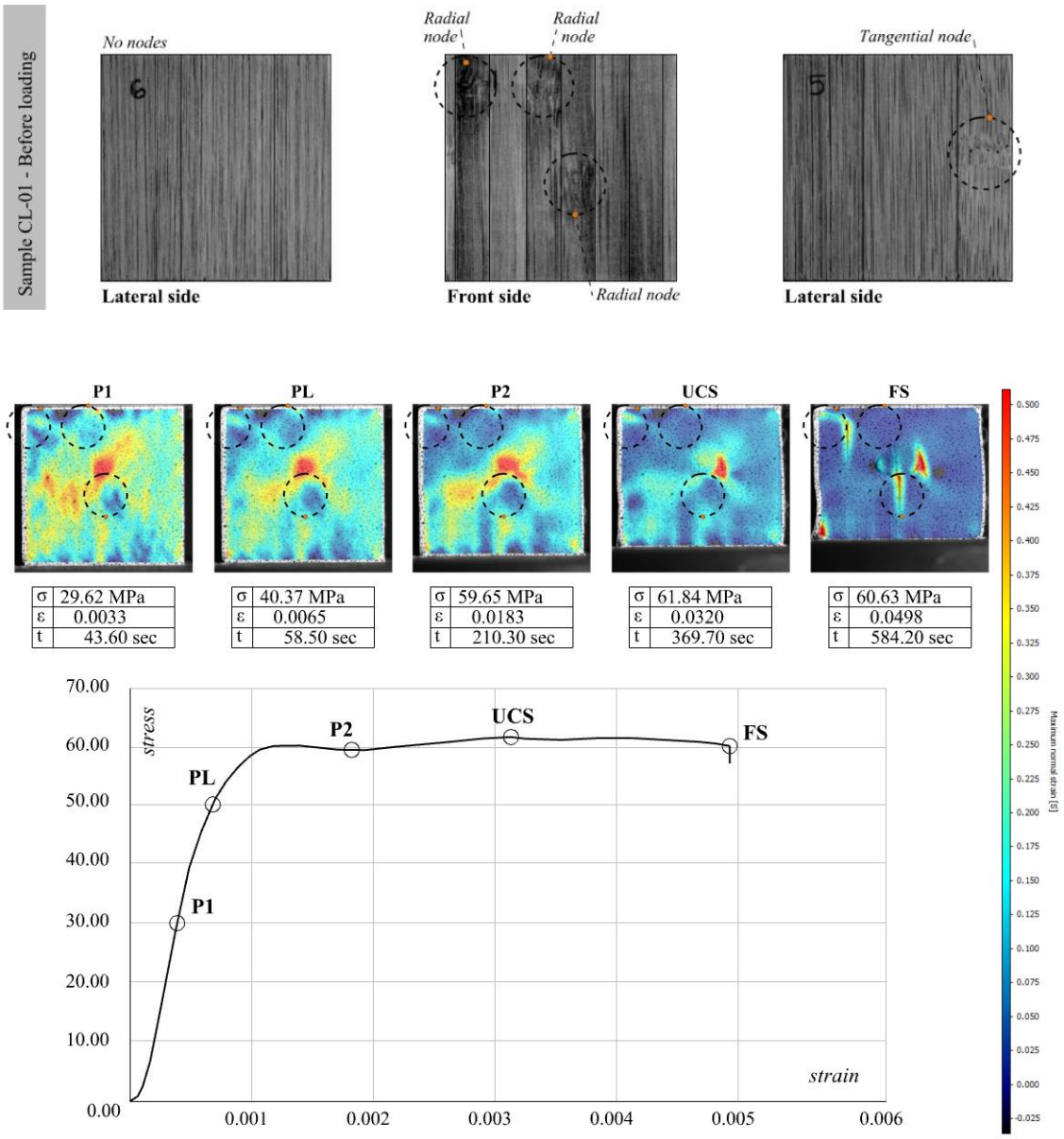

Figure 5. 4: **up**- Specimen CL-01 before loading, **down** – DIC analysis of specimen CL-01.

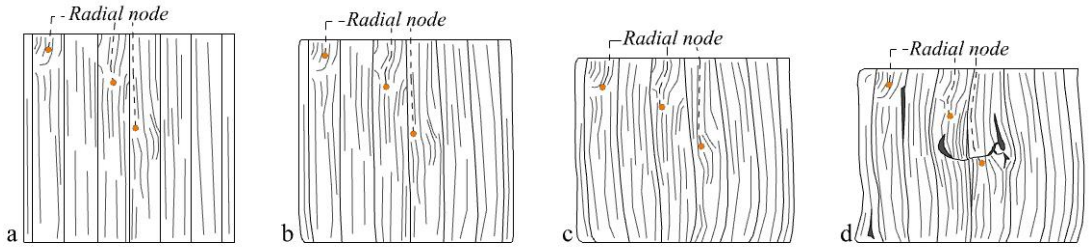

Figure 5. 5: Deformation and fracture analysis of Failure Mode 1.

Failure Mode 2 happened in specimens CL-03, CL-05, CL-07, CL-08, CL-10, and CL-11. Unlike the previous specimens, these specimens had a lower concentration of nodes.

As shown in Figure 5.6-**up**, the specimens had less than two nodes per face. At 20.12 MPa, it is possible to observe that the maximum deformation is concentrated on the right side of the tested piece (Figure 5.6-**P1**). The radial node located in the lateral face is likely the main driving force pushing the fibres towards the frontal face. Conversely, the other lateral side does not have any nodes. Hence, the deformation in the left section of the piece is lower. At 43.16 MPa, the fibres located on the right side of the specimen are the ones that continued to be pushed by the forces acting on the node placed in the lateral face (Figure 5.6-**PL**). The maximum normal strain at this point was 0.450. At 56.34 MPa, the maximum strain started to shift from the edge towards the middle strip of the specimen (Figure 5.6-**P2**). At this point, the fibres of the frontal face started to bend outwards. At 57.64 MPa, the piece reached its Ultimate Compressive Strength. Figure 5.6-**UCS** captured the strain distribution right before the loading decreased. As shown in the figure, two yellow and red patches are visible at the edges of the middle strip; these patches signalled the onset of fracture. After reaching the Ultimate Compressive Strength, the load decreased from 57.64 MPa to 43.40 MPa. At the same time, the middle strip continued to bend outwards, which created two cracks in the sides of the central strip. In this case, contrary to the previous Failure Mode, the crack appeared due to the delamination of the bamboo fibres, not due to the cracking of parenchyma cells in nodal regions. As seen in Figure 5.6-**FS**, the bending of the middle strip exceeded the bending of the other strips. At some point, the fibres of the middle strip created a buckle and separated from the strips with a lower bending curvature.

The process of damage of the specimens that exhibited Failure Mode 2 can be explained by analysing the fibres' physical arrangement located in the piece's frontal and lateral faces. Figure 5.7-**a** shows the original fibre arrangement before loading began. As seen in the figure, all the fibres were initially assembled linearly, and no curved fibres were found. However, there were areas in the strips that had a smaller number of fibres. Like the previous example, as the loading began, the parenchyma cells started to be crushed by the compressive force. As the area of the parenchyma cells changed, the flattening of the cells pushed the fibres outward. The right lateral face of the specimen had a node, which meant that more efforts were pushing the fibres outward on the right side of the specimen. As the loading continued, it was possible to see how the fibres began to bend. They went from a linear profile to a curvilinear shape (Figure 5.7 **b-c**). When the tested piece reached its fracture strength, the lines in the middle of the specimen experienced a greater degree of deformation. Also, the areas of the strips with a lower number of fibres were where fibre delamination happened. Figure 5.7-**d** shows the deformed geometry of the specimen. The middle strip is where the previously linear fibres became more curved. Also, delamination cracks were triggered in the regions with fewer fibres close to the central strip.

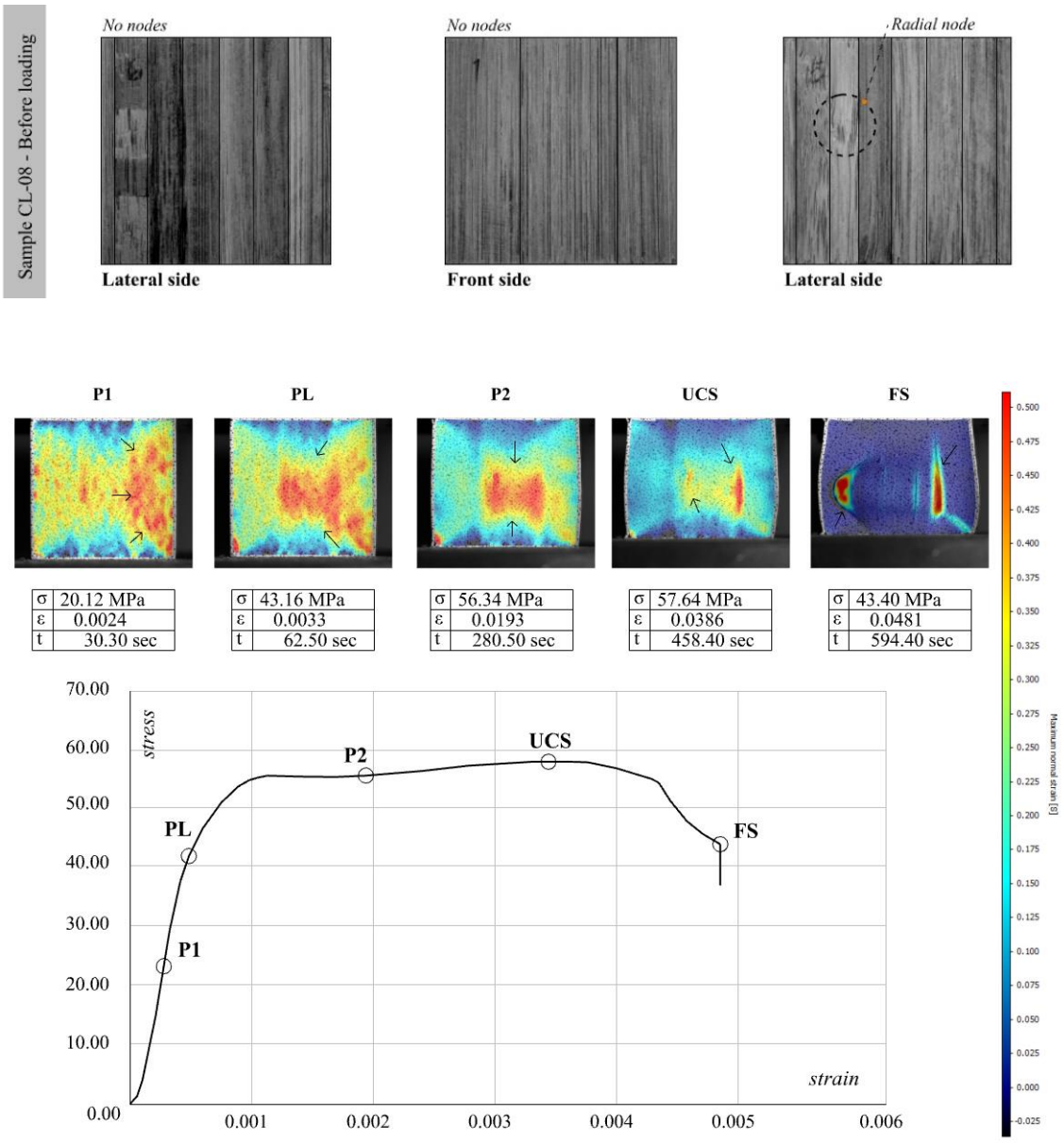

Figure 5. 6: **up**- Specimen CL-08 before loading, **down** – DIC analysis of specimen CL-08.

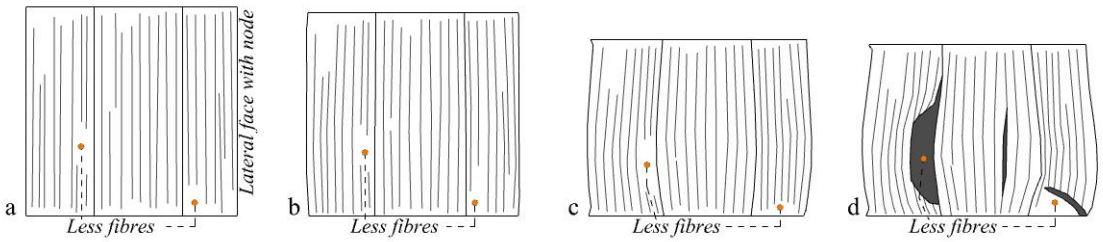

Figure 5. 7: Deformation and fracture analysis of Failure Mode 2.

As mentioned before, some specimens underwent crushing at later stages of the damage process. Specimen CL-07 is used to exemplify how crushing developed in these

specimens. As shown in Figure 5.8-**up**, the pieces that experienced crushing at some point had at least one nodal region in each of the specimen's faces. Specifically, crushing happened in the faces that had tangential nodes. At 26.21 MPa, most of the red patches are on the left side of the tested piece (Figure 5.8-**P1**). Like in the example of Failure Mode 2, the maximum strain concentration was found in the region close to the radial node located in the lateral faces. This confirms that the radial nodes are the areas that have a bigger impact in the process of deformation and failure of the sample under longitudinal compression. At 44.55 MPa, the red patches extended from the mid-left section of the specimen to the upper left section (Figure 5.8-**PL**). At 56.32 MPa, the strip on the middle began to bend more than the other sections of the specimen (Figure 5.8-**P2**). For this reason, the main concentration of strain shifted from the left side towards the middle section of the piece. From 56.32 to 57.10, the strain became localised in the lower regions of the specimen. In a matter of 104.5 seconds, the yellow patches disappeared, and the lower part of the specimen became the place where fracture began (Figure 5.8-**UCS**). At the early stages of the deformation, the strain field signalled failure by delamination. However, as the loading increased, the presence of a tangential node in the lower part of the specimen changed the distribution of strain. As soon as the Ultimate Compressive Strength was reached, the area of the tangential node became the weakest point of the specimen. When the specimen reached its Fracture Strength, cracks developed where the tangential node was located and, in the middle-low part of the specimen – right where the density of fibres decreased (Figure 5.8-**FS**). The tested piece lost its load capacity when crushing developed at the bottom part of the piece.

The crushing process can be explained by analysing the arrangement of fibres in the tangential nodes. As seen in Figure 5.9-**a**, the fibres of tangential nodes – before loading – are not curved, as is the case of radial nodes. Instead, the fibres are shorter, and they are not continuous. In tangential nodes, the discontinuous fibres leave a gap without any reinforcement. These characteristics played a crucial role in the development of failure. As the load increased, the fibres of the exterior face began to bend due to the flattening of parenchyma cells. However, it is important to notice that as bending increased, the small fibres located in the nodal region started to rotate outwardly (Figure 5.9 **b-c**). This rotation created a shift in the arrangement of the fibres. Particularly at the bottom of the central strip, where the section with fewer fibres began to crack. The rotation of fibres in the tangential node created a ripple effect where fibres stopped having a curvature with a single direction. Instead, multiple curvatures developed in single fibres. The rearrangement of fibres created a crushing pattern in the lower section of the specimen (Figure 5.9-**d**). The plates of the test machine likely stopped the energy released by the rearrangement of fibres, and for that reason, crushing developed close to the lower loading plate.

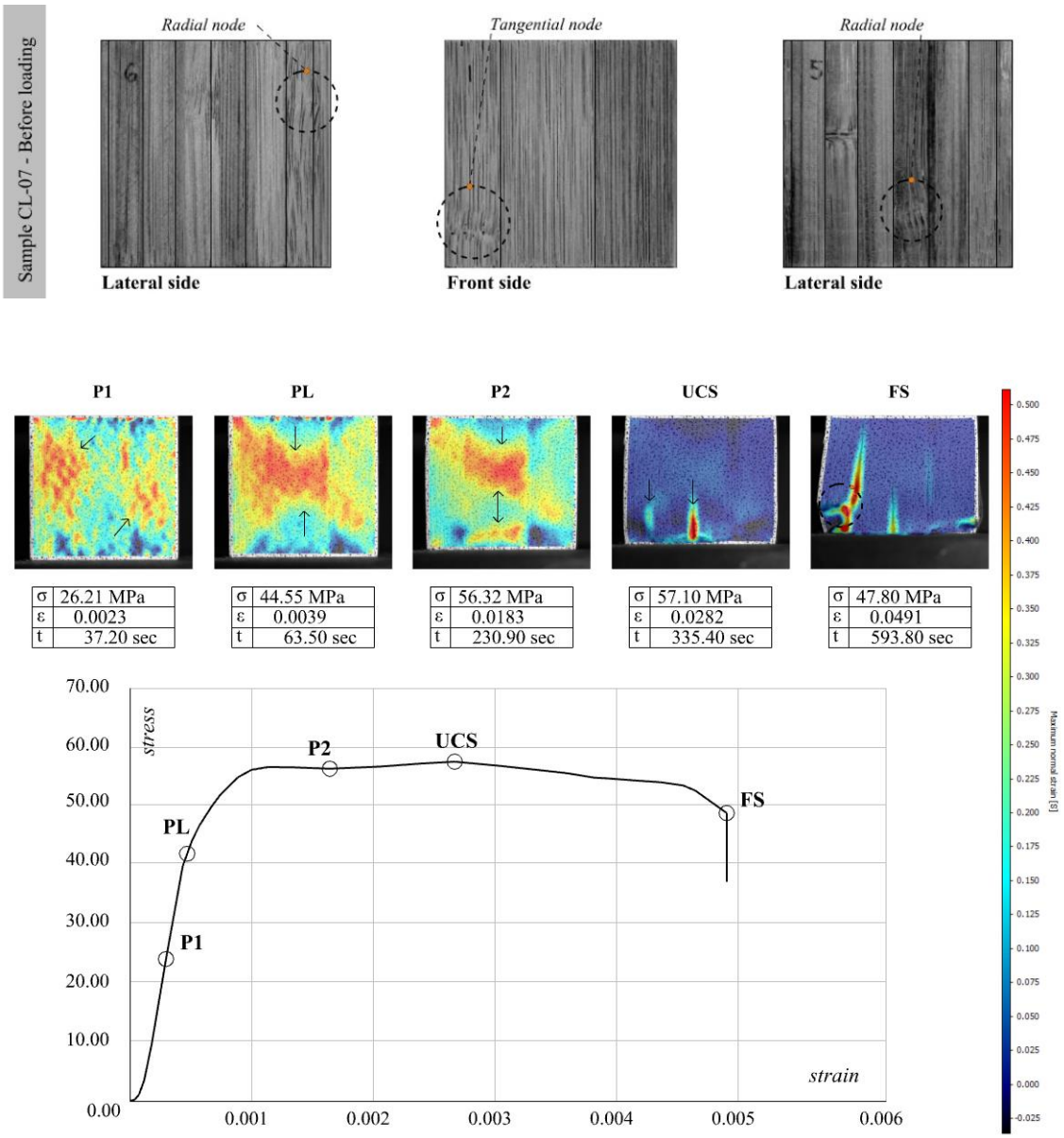

Figure 5. 8: **up**- Specimen CL-07 before loading, **down**: DIC analysis of specimen CL-07.

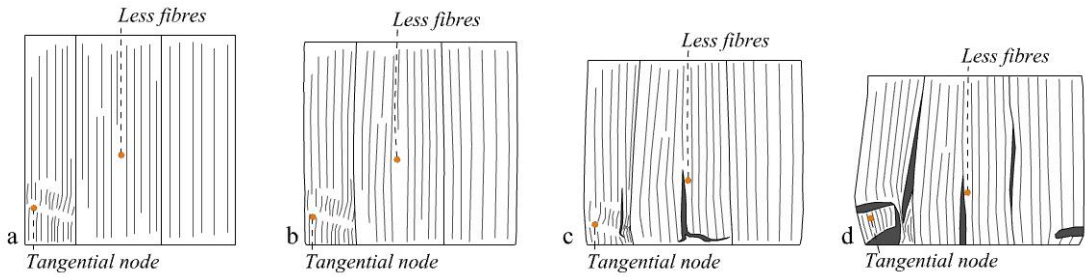

Figure 5. 9: Deformation and fracture analysis of the pieces that exhibited crushing.

5.1.3 Failure patterns in the longitudinal direction

The physical characteristics and the arrangement of bamboo fibres are the main features determining the mechanical properties and failure mechanisms of laminated bamboo under longitudinal compression. The role that these features had on the deformation and failure of the tested pieces is explained below:

Feature 1: Long and linearly arranged fibres deformed as the flattening of parenchyma cells increased. Their deformation resulted in a geometric transformation from straight to curved lines. The transformed lines had a single curvature (Figure 5.10-**a**). Shorter fibres also buckled, creating a single curvature profile like long fibres. However, if the length of the strip is short, as the fibres buckled, areas with no reinforcement developed (Figure 5.10-**b**). These areas became prone to failure.

Feature 2: The curved and short fibres located in the radial nodes accelerated the lateral push of bamboo fibres. Hence, the curvature of the neighbouring fibres was more pronounced than the curvature of the fibres located far from the radial node. Additionally, as the parenchyma cells pushed the curved and short fibres surrounding the nodes, the areas with no fibres became bigger. It is in these areas where cracking developed (Figure 5.10-**c**).

Feature 3: The short and discontinuous fibres of the tangential nodes affected the profile of the fibres as loading increased. Single curvature bending is the expected deformation of bamboo fibres when longitudinal compression is applied. However, if tangential nodes exist near the bottom or upper part of the specimen, the shorter fibres of the tangential nodes rotated. Such movement created a transformation in the profile of the fibres, which went from having a single curvature profile to having a multiple curvature profile (Figure 5.10-**d**).

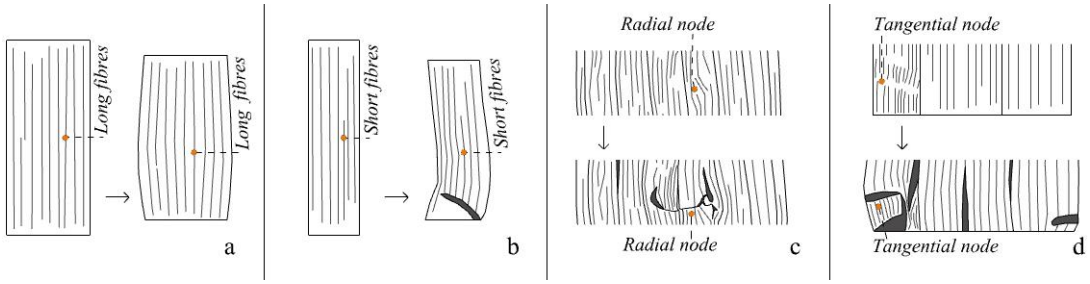

Figure 5. 10: Bamboo's features affecting compressive failure in the longitudinal direction.

The previously described features are the underlying forces that orchestrated the deformation and failure mechanisms of the population. Overall, these were the main characteristics found in the Failure Modes:

Failure Mode 1 happened in specimens with a higher concentration of radial nodes. As mentioned before, fibres' inherent curvilinear geometry around radial nodes increased the lateral push of parenchyma cells. As the force pushed the piece together, longitudinal fibres started to bend. Fracture happened in the regions with no reinforcement. These regions were located near the radial nodes (Figure 5.11-**a**).

Failure Mode 2 happened in the specimens with a lower concentration of radial and tangential nodes. The pieces had a regular distribution of fibres – compared to the pieces that exhibited Failure Mode 1. As the compressive load increased, the crushing of the parenchyma cells made the longitudinal fibres buckle outwardly. The fibres that underwent a higher degree of buckling became separated from the other fibres. Fracture began when the delamination of fibres happened. Cracks developed near the region where the fibres delaminated. The cracks usually occurred in areas with a lower concentration of fibres (Figure 5.11-**b**).

Crushing happened in all the specimens with a tangential node near the bottom or upper regions of the pieces. However, it is essential to note that tangential nodes do not play a vital role in the early stages of deformation. As the compressive load began, the fibres started to bend as expected. At some point, though, the push of the parenchyma cells forced the rotation of the short fibres located in the tangential nodes. This rotation released energy that changed the bending direction of the fibres across the specimen. As a result, fibres went from having one curvature to multiple curvatures. The changes in the profile of the fibres created a concentration of energy in the upper and lower sections of the specimen. As such, crushing happened in the bottom or upper parts of the tested pieces (Figure 5.11-**c**).

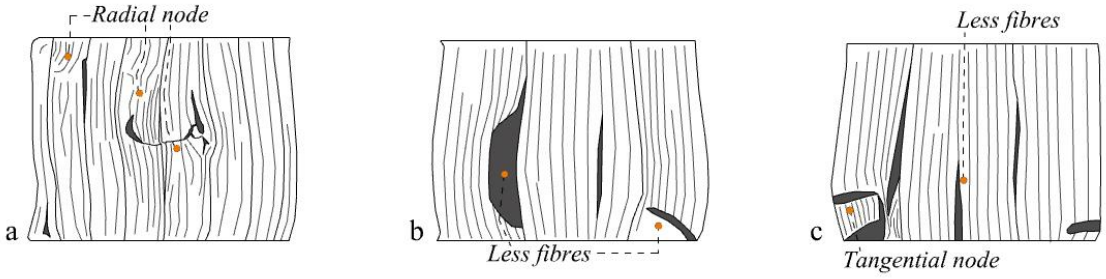

Figure 5. 11: The failure patterns of laminated bamboo under longitudinal compression.

Even though two Failure Modes were found, all specimens exhibited the following failure patterns:

Pattern 1: Fibres under longitudinal compression will always bend in the early stages of the deformation process. The fibres will go from straight lines to lines with a single curvature.

Pattern 2: If a specimen has a lower concentration of nodes, the size of the fibres can be used to determine the type of failure that the pieces will undergo at later stages. If the specimen has longer and linear fibres, the fibres will buckle, and delamination is likely to happen. If there are regions with shorter fibres, these will also buckle. However, their displacement will create pockets with no fibres as they buckle. Cracks are likely to appear in these regions.

Pattern 3: If a specimen has a higher concentration of nodes, the geometry of the fibres in the radial and tangential nodes can be used to determine the type of failure likely to happen at later stages. In radial nodes, the short and curved fibres will accelerate the lateral push of parenchyma cells. Also, the lateral displacement of the fibres surrounding the nodes will create a region with no nodes. Cracking is likely to happen in these areas. In tangential nodes, the short, discontinuous, and linear fibres in the node are likely to create a rotation movement that will disrupt the single-curved geometry of fibres. In this case, crushing is likely to happen.

5.2 Radial deformation and failure

5.2.1 Mechanical properties and behaviour

As shown in Figure 5.12, the sample submitted to radial compression exhibited an elastic-plastic behaviour. As the loading began, the stress and strain increased proportionally until reaching the Proportional Limit. After reaching the Proportional Limit, a zone of non-linearity began. However, soon after reaching the proportional limit, the stress increased linearly until reaching the Ultimate Compressive Strength (UCS). After this point, the tested pieces broke, and stress decreased. Overall, all the pieces had a small elastic region and a long plastic zone - where irrecoverable deformation ensued. The average Proportional Limit of the population was 10.00 MPa, and the average Ultimate Compressive Strength was 17.79 MPa. The average compressive Modulus of Elasticity was 1,062.82 MPa. Table 5.2 summarises the strength and mechanical properties of the sample subjected to radial compression.

The stiffness values reported in this study fall within the range of those reported in the available literature. Sharma et al. (2017) reported an average Compressive strength of

12.1 MPa and an average Modulus of Elasticity of 1,206 MPa. Khoshbakht et al. (2018) reported an average Compressive Strength of 28 MPa and an average Modulus of Elasticity of 1,440 MPa. Yang et al. (2020) registered an average Compressive Strength of 20.5 MPa - with a characteristic value of 17.50 and a Modulus of Elasticity of 1,853.90 MPa - with a characteristic value of 1,491,00 MPa.

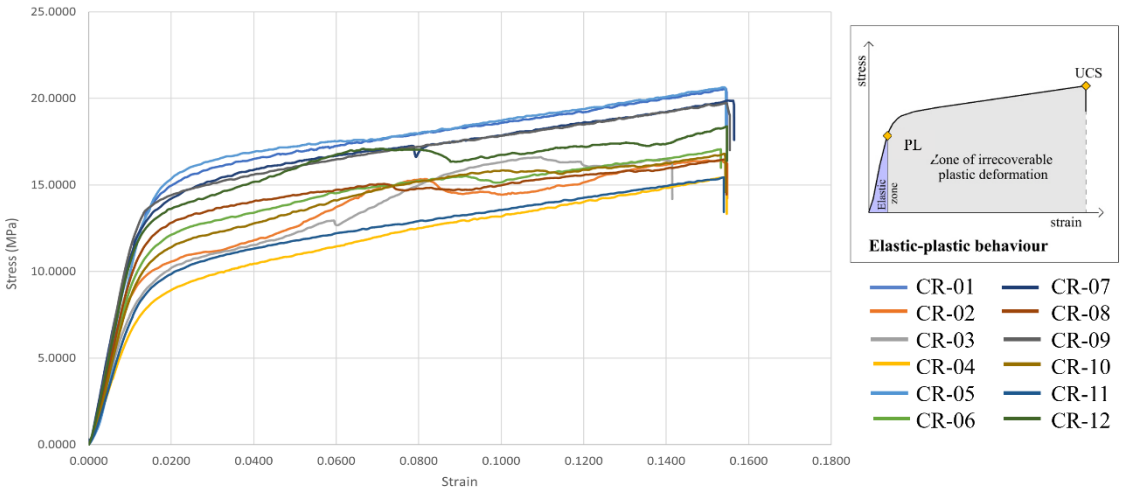

Figure 5. 12: Stress-strain curve of the sample under radial compression.

	Average	SD value	Characteristic value
Proportional Limit (MPa)	10.00	2.09	7.36
COV	0.21		
Ultimate Compressive Strength (MPa)	17.79	1.94	15.45
COV	0.11		
Modulus of elasticity (MPa)	1,062.82	166.32	779.02
COV	0.16		

Table 5. 2: Strength and mechanical properties of the sample under radial compression.

5.2.2 Deformation and failure modes

Cracking was the only type of fracture found in the population. The arrangement of fibres in the radial direction explains why cracks appeared in the specimens as the load increased. In the radial direction, fibres are distributed horizontally. The upper or lower parts of the strip have a higher concentration of fibres. However, the monotonic distribution of fibres -within a single strip – is a factor that did not affect the deformation of the sample under radial compression. Instead, the arrangement of strips with a different percentage of fibres and a different horizontal configuration are the factors that

determined the deformation of the pieces. The strips with more fibres took more time to deform, whereas those with fewer fibres deformed faster. As the load increased, the geometry of these strips transformed to a flattened rectangle (Figure 5.13 **a-b**). Finally, the strips with horizontal nodes deformed quicker and irregularly. In the case of the strips with nodes, the deformed geometry became a rhomboid rather than a flattened rectangle (Figure 5.13-**c**). The interplay among the different strips forming the laminate is the factor that determined the region where the cracks developed.

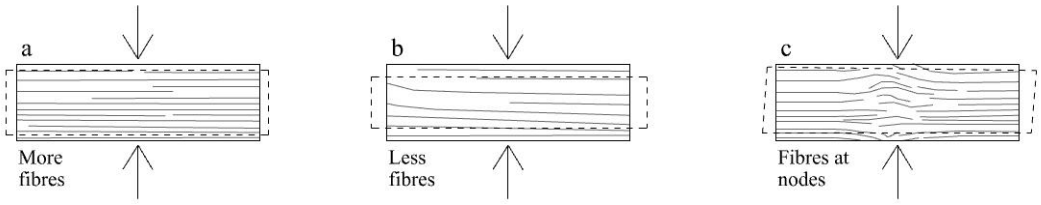

Figure 5. 13: The arrangement of fibres in the radial direction.

From the twelve specimens that were tested, seven specimens developed cracking patterns in the mid-section. All these pieces had a lower concentration of nodal regions. The average compressive strength of this group was higher than the average value of the whole population. Cracking in the middle of the specimen was classified as Failure Mode 1 (Figure 5.14-**up**). The remaining five specimens developed cracks in the mid-section and at the edges. Overall, these pieces had a higher concentration of nodes, and their average compressive strength is lower than the average strength of the population. Cracking in the mid-section and at the edges was classified as Failure Mode 2 (Figure 5.14-**down**).

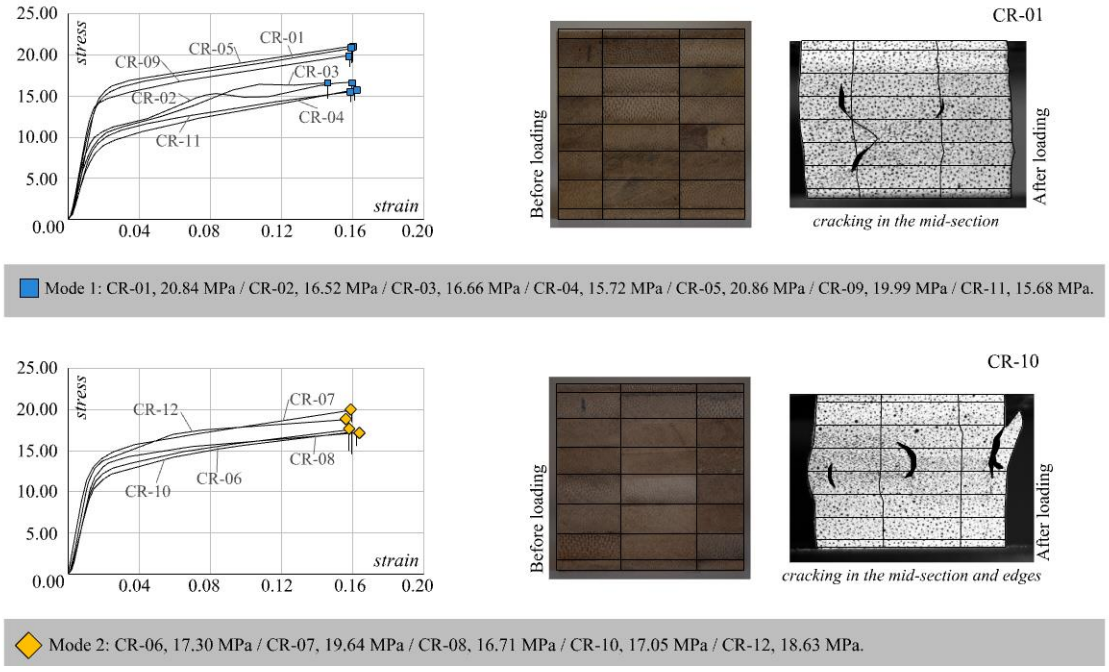

Figure 5. 14: up- Failure Mechanism 1, **down**- Failure Mechanism 2.

Failure Mode 1 occurred in the specimens CR-01, CR-02, CR-03, CR-04, CR-05, CR-09, and CR-11. The pieces had at least one radial node in each lateral face. Additionally, at least one of the strips in the mid-section had a lower distribution of bamboo fibres. Figure 5.15-**up** shows the state of the piece before loading. S1, S2, S3, and S4 are the strips with fewer fibres or nodes. AT 7.35 MPa, the strain concentrated in or near S2, S3, and S4 (Figure 5.15-**P1**). Red spots appeared in the region between S2 and S3 and in one of the edges of S4. Also, a yellow patch appeared in S3. The strain distribution did not change drastically as the tested piece reached its Proportional Limit (Figure 5.15-**PL**). The only difference was that the light blue patches became smaller and closer to the yellow and red patches. At 17.44 MPa, a red spot appeared in S3, and a yellow-blue line started to extend from S3 to S1 (Figure 5.15-**P2**). Also, the red dot in S4 became smaller, signalling the emergence of another weak spot in another region of the specimen. At 19.10 MPa, the yellow-blue line between S3 and S4 became red. At the same time, a yellow dot emerged in the region between S3 and S4 (Figure 5.15-**P3**). When the specimen reached its Ultimate Compressive Strength – at 20.85 MPa, the areas near S2, S3, and S4 became where the cracks developed. The region between S3 and S4 also showed a strain dot. Another crack would likely have appeared in this zone if the load had continued. As seen in Figure 5.15-**UCS**, the location of the cracks and the strain lines connect the strips that had more irregularities, i.e., S1, S2, S3, and S4.

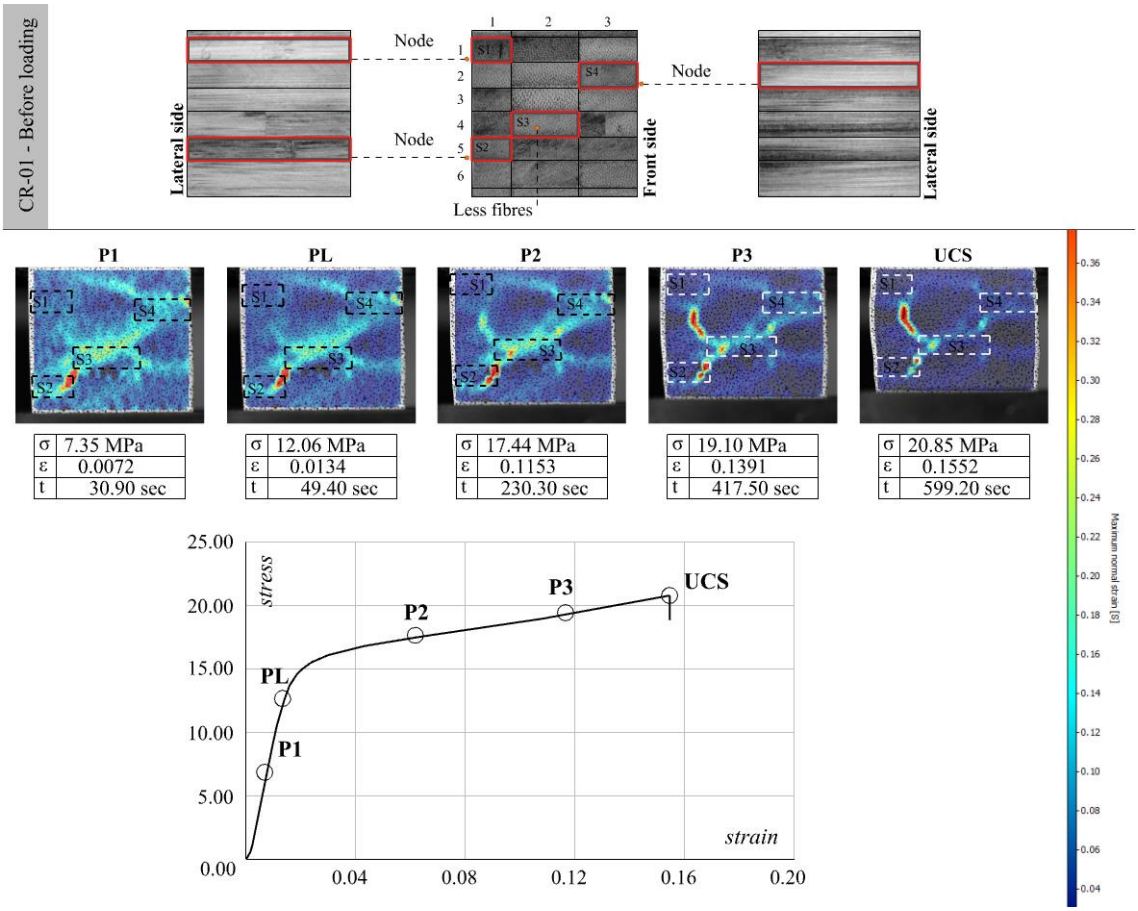

Figure 5. 15: **up**-Specimen CR-01, **down**- DIC analysis of specimen CR-01

The deformation of the specimens that exhibited Failure Mode 1 can be explained by identifying the location and number of strips with a lower concentration of fibres or nodes. During the first stages of loading, these strips underwent a higher degree of deformation than the other strips. As shown in Figure 5.16-**a**, the edges of the strips S1, S2, S3, and S4 are where a noticeable deformation began. Since the distribution of fibres is not uniform across the tested piece, compressive deformation is not distributed uniformly. Hence, some sections will be crushed faster than others. As the load increased, a crack appeared in the region at the intersection between S2 and S3 (Figure 5.16-**b**). These strips had a lower concentration of fibres and a higher concentration of parenchyma cells. Cracks developed as the parenchyma cells de-bonded. As the loading continued, another crack developed in the region located between strips S1 and S3. It is crucial to note that strips S1 and S3 were deforming faster, which inevitably created pressure in the area between them. In this region, a second crack developed (Figure 5.16-**c**). When the specimen reached its Ultimate Tensile strength, a third crack emerged. The crack was in the region between S3 and S4. Figure 5.16-**d** clearly shows that the primary deformation happened in the areas pushed by the accelerated deformation of the strips with less reinforcement. This finding suggests that the horizontal distribution of fibres directly impacts determining the location of cracks when radial compression is applied.

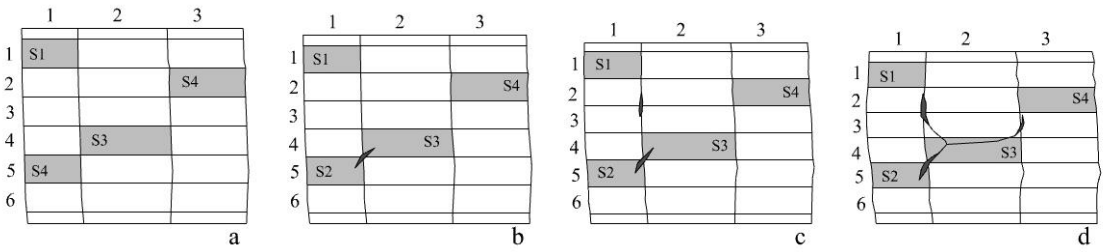

Figure 5. 16: Deformation and fracture analysis of Failure Mode 1.

Failure Mode 2 happened in specimens CR-06, CR-07, CR-08, CR-10, and CR-12. The pieces had more than two nodes in each of the lateral faces. Also, the mid-section of the piece had – at least – two strips with fewer fibres. Overall, these specimens had a higher number of strips with irregularities (Figure 5.17-**up**). As shown in Figure 5.17-**P1**, it was possible to see areas with yellow and red patches at the early stages of loading. These areas with the yellow and red patches were submitted to a higher degree of deformation than other regions. The areas with a higher degree of deformation were located in-between the strips that had more irregularities. At 9.94 MPa, the size of the yellow patches began to be reduced, and the red spots became more defined (Figure 5.17-**PL**). The uneven distribution of stress across the surface of the specimen created a staggered push at the middle of the piece. As a result, the maximum strain became focalised on the right side of the specimen, specifically in the region placed between S7 and S8. For this reason,

at 14.11 MPa, only three strain dots were visible, a small blue dot between S3 and S4, a mid-sized yellow dot between S5 and S6, and a big-sized red dot between S7 and S8 (Figure 5.17-**P2**). As the load increased to 15.88 MPa, the red dot became more prominent, and a crack appeared on the right edge of the specimen (Figure 5.17-**P3**). However, at this point, the stress in the tested piece continued to increase. When the specimen reached its Ultimate Compressive Strength – at 17. 05 MPa, the crack between S7 and S8 became bigger, and two more cracks appeared. One crack appeared in the area between S5 and S6, while the other crack emerged in-between S3 and S4 (Figure 5.17-**UCS**). The DIC analysis of specimen CR-10 clearly describes how radial deformation is not even across the tested piece. Bamboo strips with more irregularities created more pressure in some regions of the specimens. It is in these regions where cracks developed.

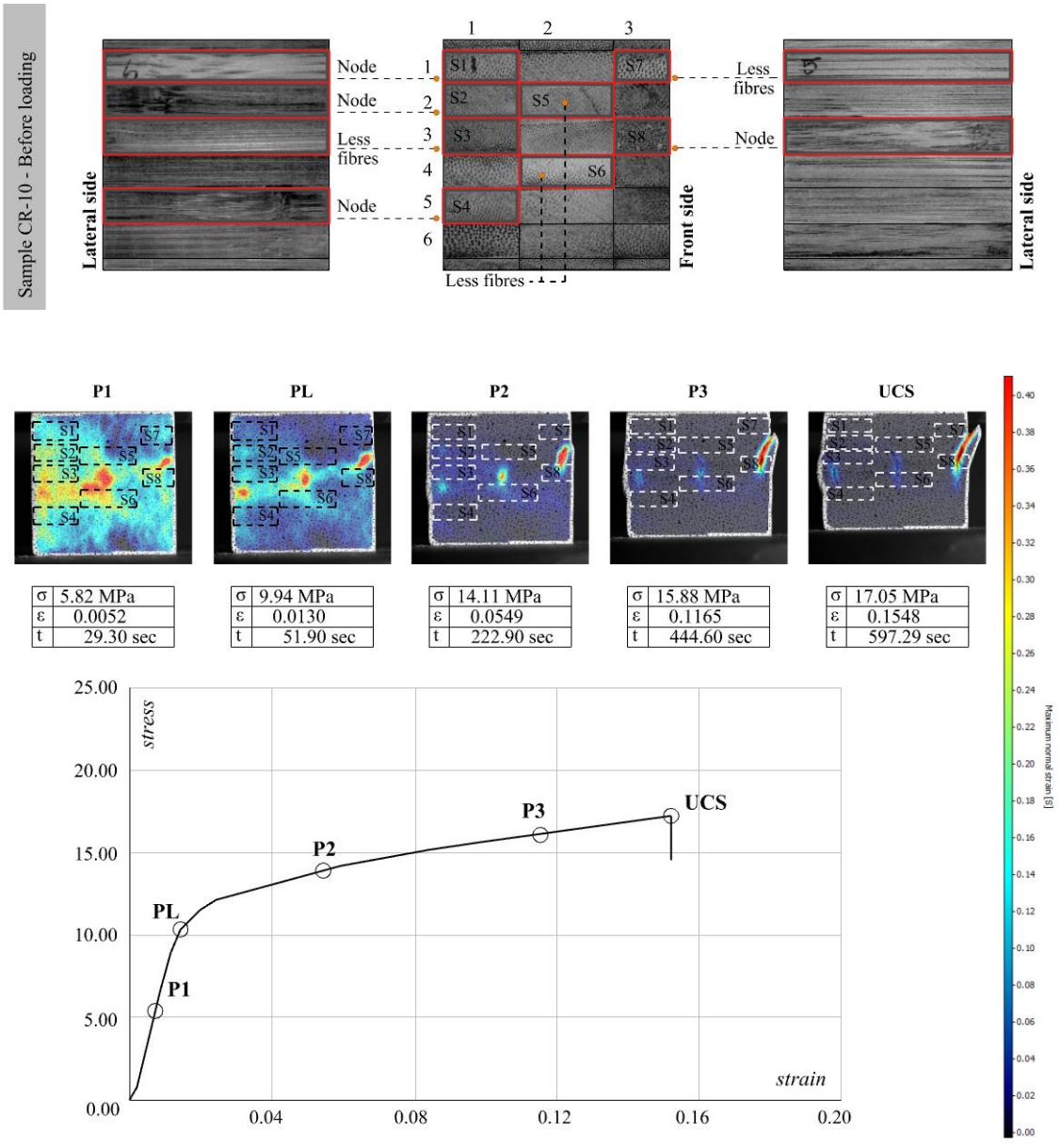

Figure 5. 17: **up**- Specimen CR-10, **down**- DIC analysis of specimen CR-10.

As with the previous failure mode, the underlying fracture mechanism of the specimens that exhibited Failure Mode 2 can be predicted if the strips with fewer fibres or with nodes are identified. As shown in Figure 5.18-**a**, the deformation of these pieces started in or near the strips with more irregularities. The right side of specimen CR-10 had a higher concentration of irregularities. As the load increased, the pressure was concentrated on the right side, creating a staggered distribution of energy. The pressure of the right side found release diagonally. For this reason, as shown in Figure 5.18-**b**, cracks appeared between S5 and S6 and between S7 and S8. Since one of the cracks was in the edges, the piece started to break apart in this region. As the loading continued, a third crack appeared between S3 and S4 (Figure 5.18-**c**). Even though the highest deformation started on the right side, the pressure was quickly redistributed across the specimen's surface and created a crack on the left side. When the tested piece reached the Ultimate Compressive Strength, all the cracks that emerged in previous stages became bigger (Figure 5.18-**d**). It is at this point that the loading of the tested piece dropped.

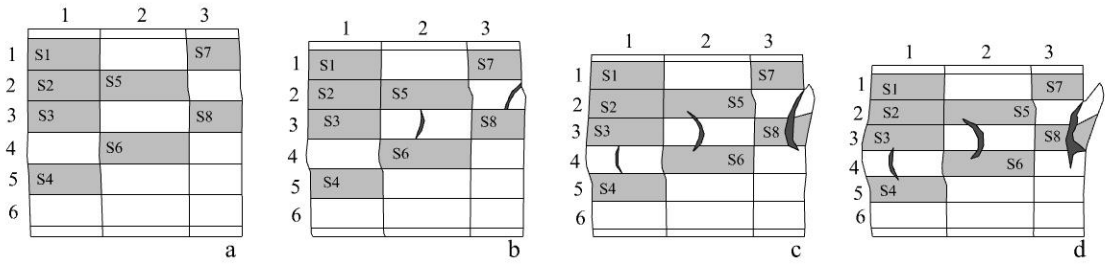

Figure 5. 18: Deformation and fracture analysis of Failure Mode 2.

5.2.3 Failure patterns in the radial direction

The cracks of Failure Mode 1 and Failure Mode 2 developed in different regions of the specimens because the pieces had a different number of strips with irregularities, and the distribution of those strips was also different. Hence, the main features that determined the deformation and failure of laminated bamboo under radial compression were the strips with an irregular distribution of fibres and the arrangement of these strips within the laminates. The following section explains how these features affected the mechanical behaviour of the sample under radial compression:

Feature 1: There are two reasons why the horizontal distribution of fibres can be affected. The first reason is the existence of nodes in the strips used to manufacture the laminates. The second reason is the existence of strips with a low distribution of fibres. A lower distribution of fibres can result from milling or due to the inherent characteristics of the bamboo species used to produce the laminates. In either case, however, the strips with any of these features are likely to deform faster than the strips with no irregularities.

Figure 5.19-**a** shows the deformation of strips with no irregularities. As the load increases, deformation is expected to be uniformly distributed, and the strips will deform into flattened rectangles. Instead, if a force is applied on the irregular strips, the deformation will not be uniformly distributed, and the strips would deform into rhomboid shapes (Figure 5.19-**b**). Based on the experiments, the strength of the material is also affected by the presence of strips with irregularities. Overall, the pieces with fewer irregularities had higher compressive strength than those with more irregularities.

Feature 2: If strips with irregularities create areas with higher deformation rates. It is expected that the placement of these strips will determine the region where the cracks are likely to develop. If a strip is placed between two irregular strips, the strips with irregularities will put more pressure on the strip in the middle (Figure 5.19-**c**). As the load increases, the strip with more pressure is bound to crack. The different arrangements of strips with and without irregularities created different crack patterns. Some of the patterns only developed in the mid regions, and some developed at the edges.

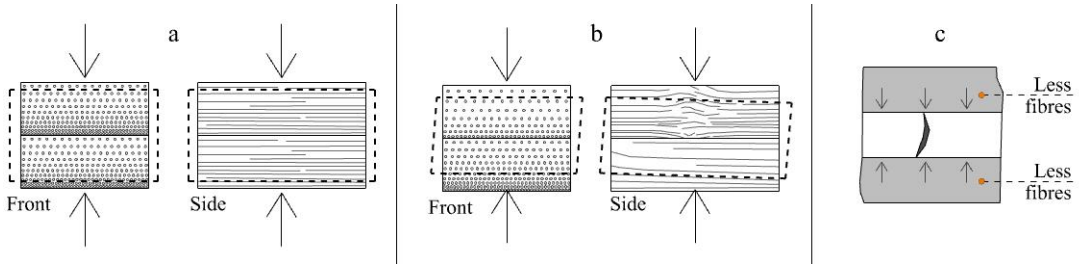

Figure 5. 19: Bamboo's features affecting compressive failure in the radial direction.

The features described above were the main reasons behind the deformation and subsequent fracture of the tested pieces. Overall, the failure modes had the following characteristics:

Failure Mode 1 happened in the specimens that had fewer fibres with irregularities. As the compressive load increased, the few strips with irregularities deformed faster than the other strips. As a result of this uneven deformation, cracks developed in the regions placed between the strips that had irregularities. As shown in Figure 5.20-**a**, the strips with irregularities were not concentrated in a single area. Instead, they were spread across the surface of the tested pieces. Hence, the cracks only emerged in the mid-section of the pieces.

Failure Mode 2 happened in the specimens that had more fibres with irregularities. These fibres were mainly concentrated on the right side of the piece. As the load began, the right

side began to deform faster. As the pressure increased on the right side, a crack appeared in the mid and left sections of the specimen. This cracking pattern happened as the pressure concentrated on the right side expanded across the whole surface of the specimen. As the loading continued, the crack on the left edge became bigger. At the same time, a third crack appeared on the right side of the specimen. As shown in Figure 5.20-**b**, the irregular strips were densely packed on the right side. The pressure concentrated in this area was released diagonally until reaching the left edge. Hence, cracks formed in the specimen's right, middle, and left sections.

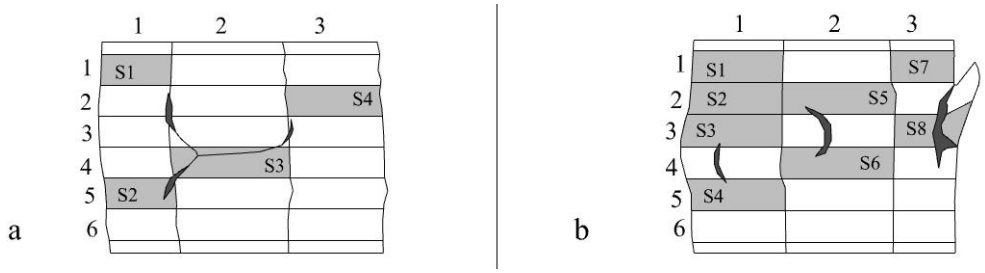

Figure 5. 20: The failure patterns of laminated bamboo under radial compression.

The analysis of the tested pieces suggests that the location of strips with irregularities can be used to predict the regions where cracks are likely to emerge. Based on the DIC and fracture analyses, a recurring fracture pattern was found:

Pattern 1: Cracking was the only type of fracture found, and it always happened in the regions placed between the strips with irregularities. If two irregular strips were placed in a staggered position, a crack appeared at the corned shared by both strips (Figure 5.21-**a**). If two irregular strips were placed in a staggered position – but there were one or two strips in-between, a crack appeared in the lines that connected the irregular strips (Figure 5.21-**b**). If irregular strips surrounded a strip with no irregularities, a crack appeared in the middle of the strip (Figure 5.21-**c**). Finally, if irregular strips surrounded a strip with no irregularities – but one of the edges was located at the edge of the specimen – a crack appeared in the middle of the strip. However, the cracks quickly extended towards the edge of the piece (Figure 5.21-**d**).

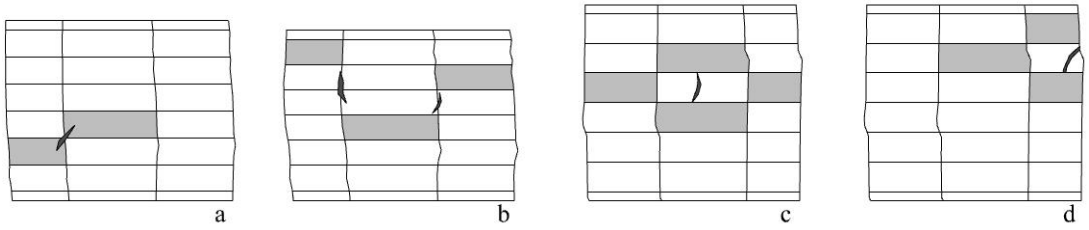

Figure 5. 21: The cracking patterns of laminated bamboo under radial compression.

5.3 Tangential deformation and failure

5.3.1 Mechanical properties and behaviour

All the pieces under tangential compression exhibited an elastic-plastic behaviour. The elastic zone of all specimens was smaller than the plastic zone. After reaching the Proportional Limit (PL), the tested pieces entered the regime of irrecoverable deformation. The average Proportional Limit of the population was 10.11 MPa. As shown in Figure 5.22, for eight of the twelve specimens, the Ultimate Compressive Strength (UCS) was the same value as the Fracture Strength (FS). However, the other specimens had different compressive and fracture values. The average Ultimate Compressive Strength was 16.60 MPa. The average Modulus of Elasticity (MOE) was 989.84 MPa. Table 5.3 summarises the strength and mechanical values of the population.

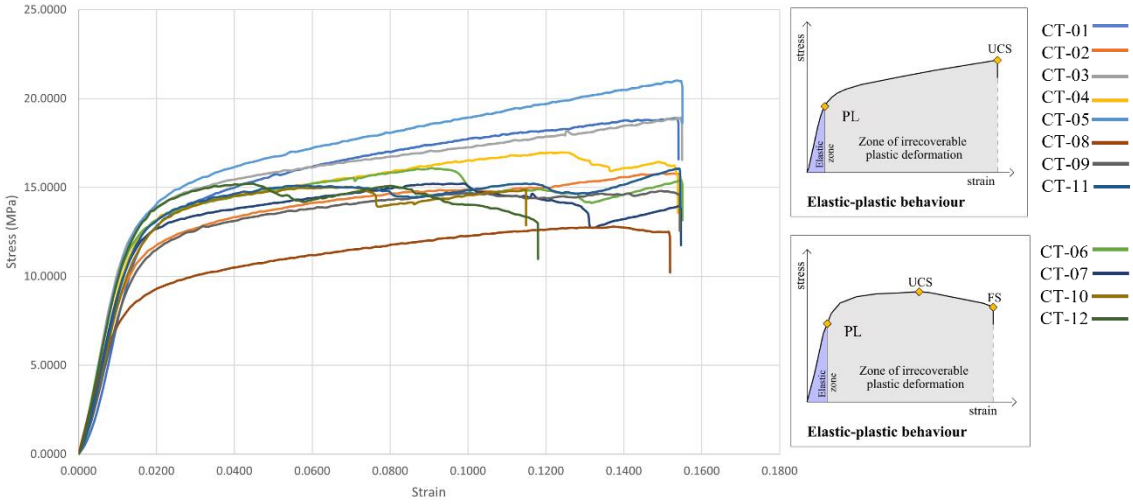

Figure 5. 22: Stress-strain curves and behaviour of the sample under tangential compression.

	Average	SD value	Characteristic value
Proportional Limit (MPa)	10.11	1.21	8.38
COV	0.12		
Ultimate Compressive Strength (MPa)	16.60	1.96	14.93
COV	0.12		
Modulus of elasticity (MPa)	989.84	119.51	813.90
COV	0.012		

Table 5. 3: Strength and mechanical properties of the sample under longitudinal compression.

The stiffness values reported in this study agree with those reported in the available literature. Sharma et al. (2017) reported an average Compressive strength of 12.00 MPa and an average Modulus of Elasticity of 1,197 MPa.

5.3.2 Deformation and failure modes

The most common fracture types were cracking due to strip delamination and shear cracking – at edges – due to uneven distribution of strain. The sample's analysis suggests that the rounded shape of bamboo culms is why these types of fractures were the most frequent. As shown in Figure 5.23-**a**, the unprocessed strips are circle segments. As such, they have curvilinear edges in the outer and inner faces. Moreover, the fibres are not aligned in straight lines; instead, they follow the circular shape of the rounded bamboo culms. When compressive loads are applied in the tangential direction, the processed strips will bend in the direction where most of the fibres are located (Figure 5.23-**b, c**). In other words, they will bend in the original direction of the outer face of the culm. The density of bamboo fibres and the arrangement of the strips are the factors that determine the failure mechanism of laminated bamboo under tangential compression.

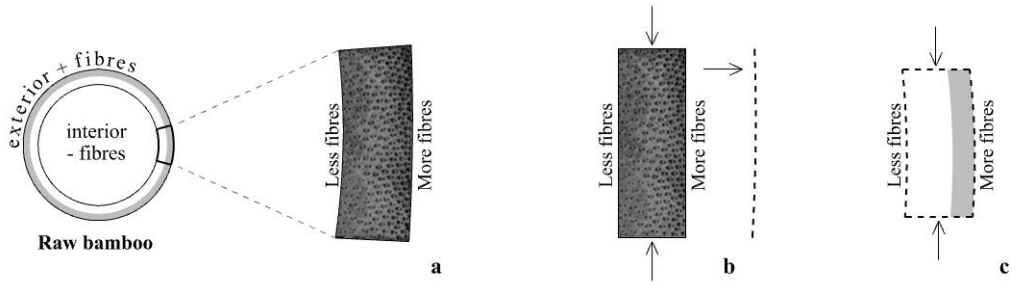

Figure 5. 23: Circular arrangement of bamboo fibres.

In total, three failure modes were found. The specimens of Failure Mode 1 cracked in the mid-section (Figure 5.24-**Mode 1**). These specimens had a compressive strength higher than the average compressive strength. The pieces of Failure Mode 2 also developed cracks in the mid-section, but in later stages, the cracks extended from the mid-section to the edges (Figure 5.24-**Mode 2**). These specimens had a compressive strength close to the average population's value. Finally, the pieces in Failure Mode 3 also developed cracks. However, the cracks appeared following a diagonal pattern. As the load increased, the energy released by the initial cracks created big cracks at the edges (Figure 5.24-**Mode 3**). These specimens had the lowest strength. Even though nodal regions did not seem to impact the failure mechanism of the tested pieces, they did seem to affect their strength properties. The pieces in Failure Mode 1 and Failure Mode 2 – with higher compressive values - had a lower node concentration than the pieces in Failure Mode 3.

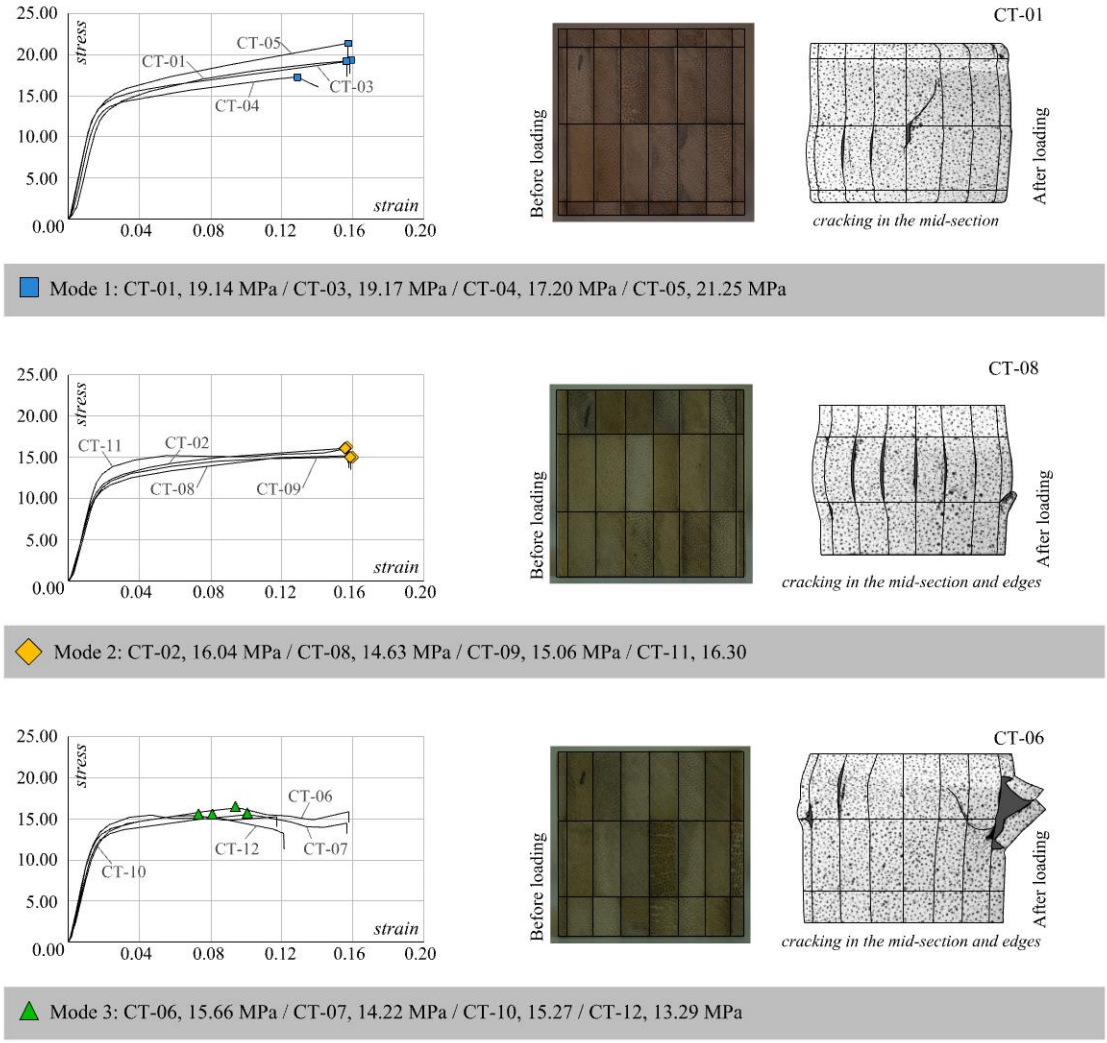

Figure 5. 24: The failure modes of laminated bamboo under tangential compression.

Failure Mode 1 happened in the specimens CT-01, CT-03, CT-04, and CT-05. As shown in Figure 5.25-**up**, the pieces had two sets of strips with a degree of inclination. S1, S2, and S3 were tilted from right to left. Whereas S4, S5, and S6 were tilted from left to right. The strips met at a central point called P1. At 10.99 MPa, yellow, orange, and red patches appeared in or near the regions where S1, S2, S3, S4, S5, and S6 were located (Figure 5.25-**PL**). At 15.58 MPa, the yellow, orange, and red patches began to be focalised in the region where S1, S2, and S3 were located (Figure 5.25-**P1**). As the load increased, the bending of the strips also increased. Strips S1, S2, and S3 bent towards the right side of the specimen. Contrary to this, strips S4, S5, and S6 bent towards the left side. The push - in opposite directions - created a strain point right at the intersection of S3 and S4. The point where the opposing forces met. For this reason, at 17.43 MPa, a red dot appeared in P1 (Figure 5.25-**P2**). At 18.32 MPa, the red dot in the mid-section began to extend towards the middle of S3 and S4 (Figure 5.25-**P3**). At the same time, strain paths began to form between S1, S2, and S3. As the fibres bent outwardly – in opposite directions – a

crack appeared between strips S1 and S2. When the specimens reached their Ultimate Compressive Strength, the red dot continued to extend towards S3 and S4. At this point, a crack began to cross the entire mid-section of S4. As shown in Figure 5.25-**UCS**, the energy released by the crack formed in the mid-region created a strain concentration in the upper left corner of the tested piece. If the load had continued, another strain concentration would likely have formed in the opposite corner, i.e., the bottom right corner.

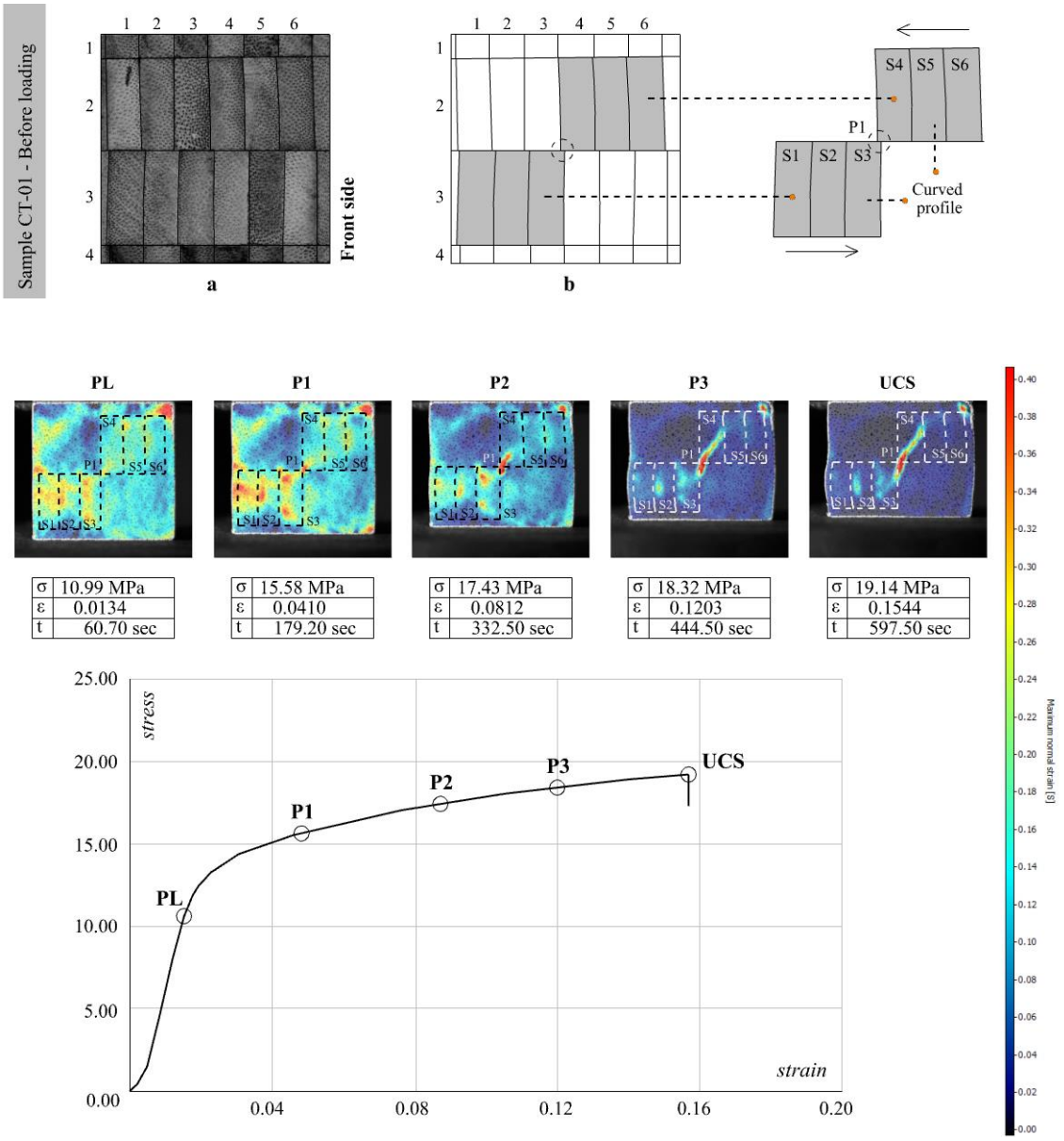

Figure 5. 25: **up**- Specimen CT-01 before loading, **down**- DIC analysis of specimen CT-01.

The process of deformation and failure of the specimens that exhibited Failure Mode 1 can be explained by identifying the location of the strips that had a tilted profile. Even though the strips were sanded into rectangular sections, the curvilinear distribution of

fibres likely made some strips retain their curved shape. As seen in Figure 5.26-**a**, the strips that had a tilted profile are the ones that experienced a higher degree of deformation. When the load increased, it is possible to see that the specimen's upper left side and bottom right side were the regions that bent the most (Figure 5.26-**b**). As the bending continued, the efforts created by the bending moments met at the intersection between strips S3 and S4. It is in this region where a crack appeared (Figure 5.26-**c**). As the loading continued, the crack in the middle grew at a faster rate. By this time, the cracks began to extend towards the S3 and S4. The energy released by the crack started to increase the deformation of the bottom right and upper left regions. As a result, the strips in the right section began to delaminate. The final geometry of the specimen – at the Ultimate Compressive Strength – was a central crack and lateral delamination in the bottom right area. It is likely that if the load continued, delamination would have also happened in the upper left side of the tested piece (Figure 5.26-**d**).

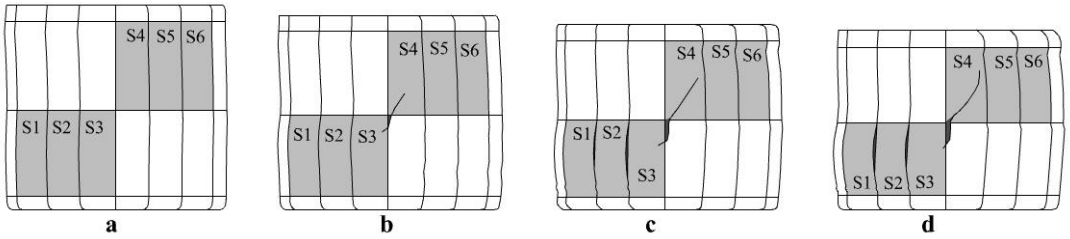

Figure 5. 26: Deformation and fracture analysis of Failure Mode 1.

Failure Mode 2 occurred in specimens CT-02, CT-08, CT-09, and CT-11. As seen in Figure 5.27-**up**, the pieces had areas with fewer fibres located horizontally across the entire section of the pieces – notice the location of A1, A2, and A3. A region with fewer fibres is created if the laminate strips are arranged following an inner-to-inner configuration. As mentioned before, the inner layer of bamboo strips has fewer fibres than the outer layer. The arrangement of strips is crucial to map out the failure mechanisms of tangential compression. At 8.97 MPa, yellow and red patches appeared in A1, A2 and A3. The maximum concentration of strain emerged in A2 (Figure 5.27-**PL**). At 12.93 MPa, red spots appeared in the bottom corners of A1 and A2. At this point, the main concentration of stress was in the middle of the specimen – right inside A2 (Figure 5.27-**P1)**. The energy concentrated in A2 began to expand laterally, creating red spots in the edges of A1, A2, and A3. These spots are clearly visible in Figure 5.27-**P2, P3**. As the load continued, the red spots became more defined, and the red zone in A2 disappeared, which means that the strain began to spread across the entire cross-section of the specimen. When the pieces reached their Ultimate Compressive Strength, cracks – by delamination – appeared in the edges between the strips forming A1, A2, and A3. At the same time, a shear crack developed in the bottom left corner of A3. Figure 5.27-**UCS** clearly shows that the central region of the tested piece – along the horizontal direction –

experienced a more significant deformation than the upper and lower sections. For this reason, the crack at the edge likely developed due to the uneven distribution of efforts across the vertical axis of the specimen.

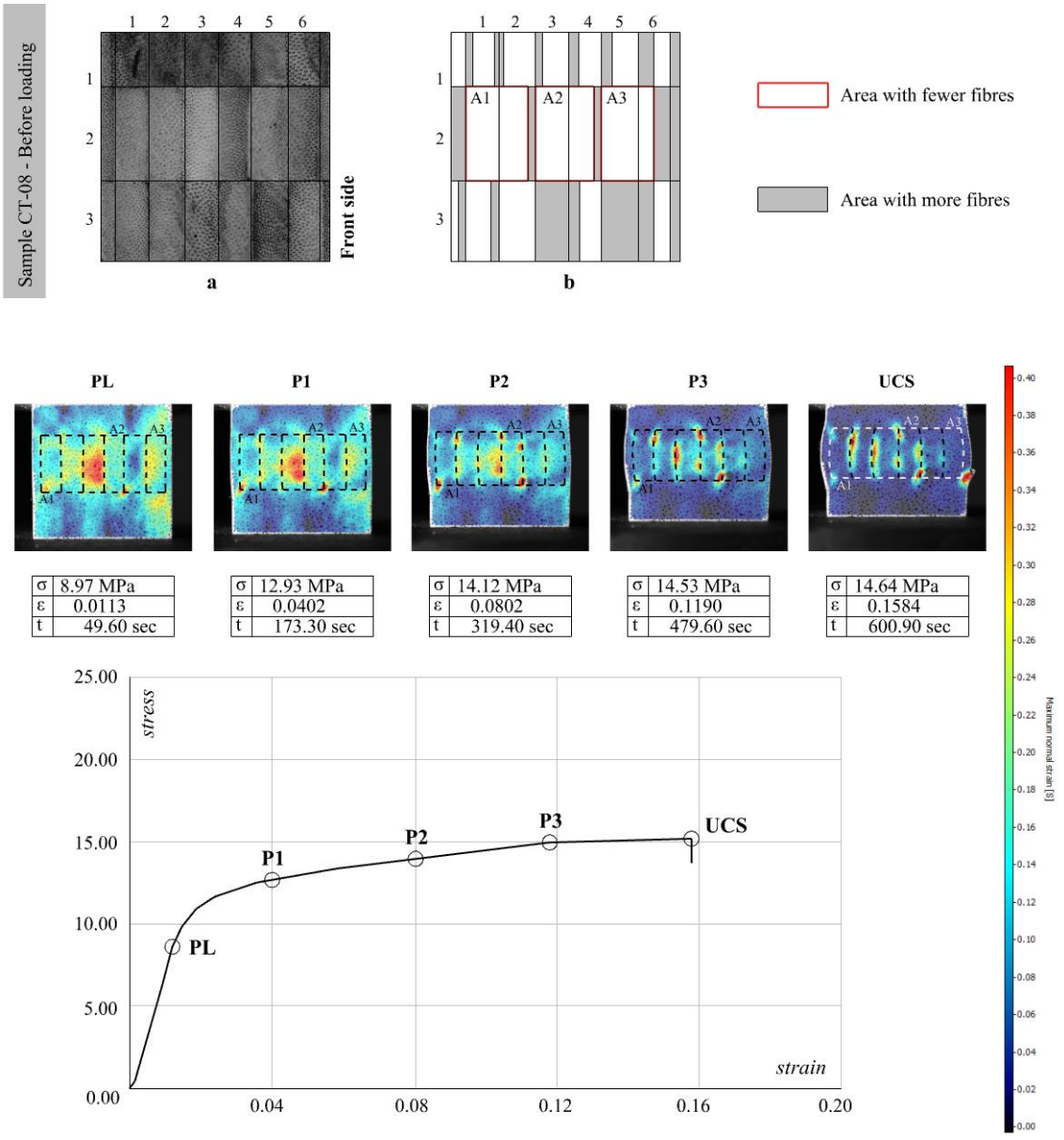

Figure 5. 27: **up**- Specimen CL-08 before loading, **down**- DIC analysis of specimen CL-08.

The deformation and fracture of specimens in Failure Mode 2 happened due to the concentration of areas with fewer fibres. As seen in Figure 5.27-**b**, these areas were in the same row, i.e., row number two. The areas had a higher concentration of parenchyma cells. The compressive load crushed the parenchyma cells, which pushed the lateral fibres outward. The fibres were arranged in concentric circular lines; hence, a curvilinear profile was created as the parenchyma cells changed their size and shape. As seen in Figure 5.28-**a, b**, the strips with fewer fibres were in the middle section of the pieces. Strips S1, S2,

and S3 curved to the right, while strips S4, S5, and S5 curved to the left. The strips continued bending to the point where delamination started to happen at the interface between the strips as the load continued. Figure 5.28-**c** shows the cracks that appeared between S1, S2, S3, S4, and S5. At the Ultimate Compressive Strength, all the strips with fewer fibres developed delamination (Figure 5.28-**d**). The higher deformation of the mid-section likely created areas of strain concentration in the outer corners of S1 and S2. For this reason, cracking began to happen in the upper and lower corners of S1 and S6.

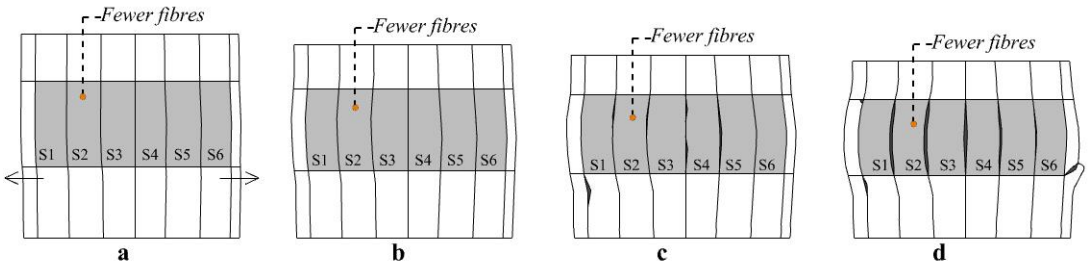

Figure 5. 28: Deformation and fracture analysis of Failure Mode 2.

Failure Mode 3 happened in specimens CT-06, CT-07, CT-10, and CT-12. Like the previous specimens, these specimens had three regions with fewer fibres (Figure 5.29-**up**). However, unlike the last group, these specimens did not have the areas in the same row. The first two areas were in row number one, while the third was in row number two. The specific arrangement of the regions with fewer fibres created a diagonal distribution of stress across the surface of the tested pieces. At 11.85 MPa, yellow and red patches appeared in A1, A2, and A3 (Figure 5.29-**PL**). As the loading continued, the patches became smaller, and the primary strain concentration began to form in the upper section of A3. At 15.49 MPa, a red patch formed in the upper area of A3 (Figure 5.29-**P1**). At 16.26 MPa, the pieces reached their Ultimate Compressive Strength. At this point, the yellow patches – in A1 and A2 – disappeared. At the same time, the red patch in the upper section of A3 began to be reduced, signalling the onset of fracture (Figure 5.29-**UTS**). After fracture began, the loading dropped to 14.59 MPa, and the crack in the upper section of A3 started to grow and extend towards the left side of the specimen (Figure 5.29-**P2**). The crack continued to grow, and 108 seconds later, the Fracture Strength was reached. At this moment, the crack pushed the lateral strips outward. In Figure 5.29-**FS**, it is possible to see the appearance of delamination cracks on the upper right side of the specimen – specifically in A1. The DIC analysis of specimen CT-06 suggests that a staggered arrangement of areas with fewer fibres creates a diagonal distribution of strain that begins in the upper section and ends in the opposite lower section. Such distribution makes the stress travel from one side to the other, and as it does so, the energy is released on one of the sides, creating big cracks on the edges.

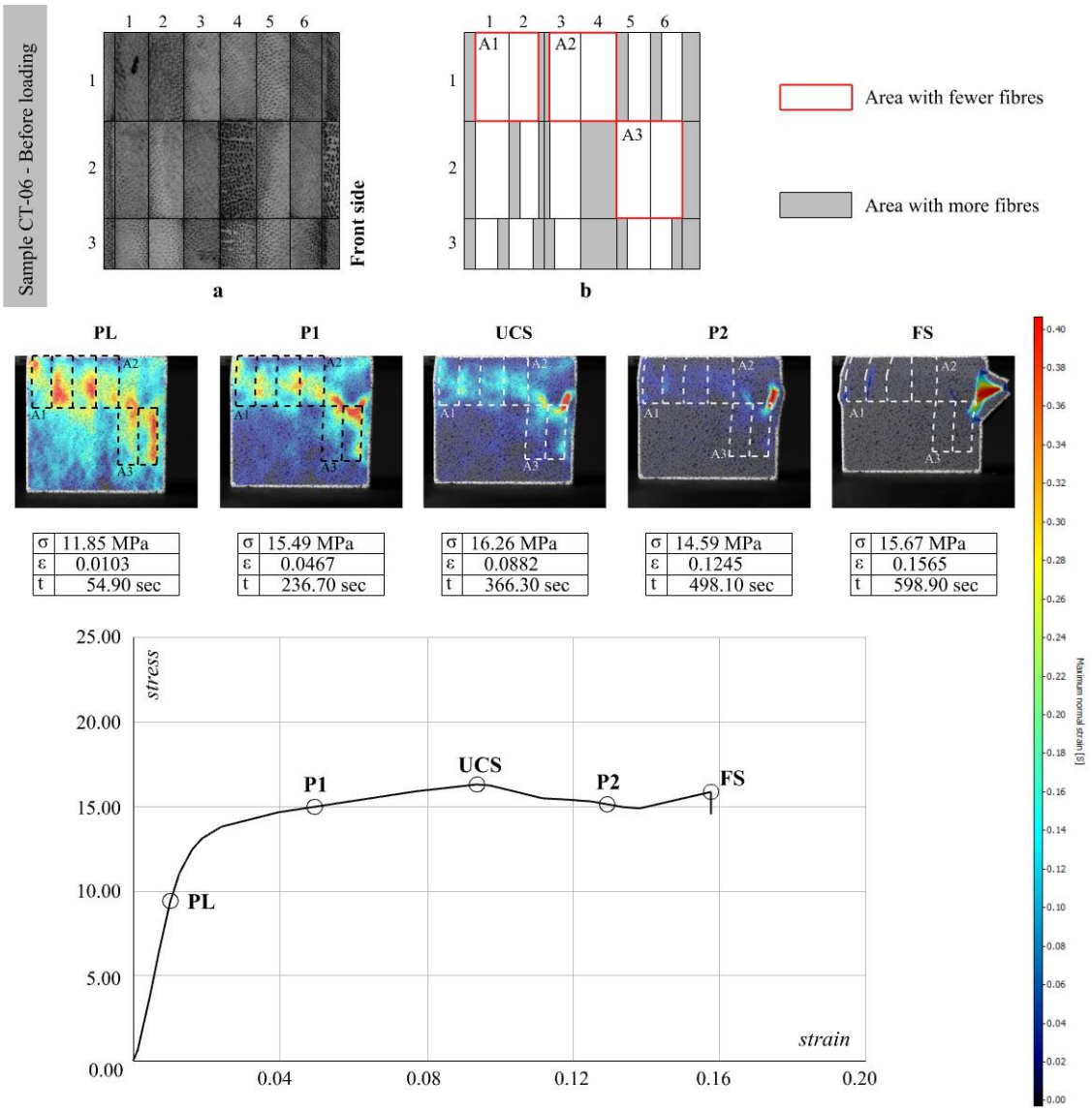

Figure 5. 29: **up**- Specimen CT-06 before loading, **down** – DIC analysis of specimen CT-06.

The failure of the pieces that exhibited Failure Mode 3 happened due to the presence of areas with fewer fibres. These areas had a low percentage of fibres which exacerbated their compressive deformation. As the load began, these areas started to push the outer fibres of the strips. At the same time, the strips started to accumulate at the lateral sides in a curvilinear arrangement – like the original circular arrangement of fibres in a bamboo culm. The higher deformation is likely to happen in the areas formed by strips with fewer fibres. In the case of specimens in Failure Mode 3, the higher concentration was located on one side of the pieces. As seen in Figure 5.30-**a**, the deformation of strips S1, S2, S3 and S4 made the strips buckle to the right side. Simultaneously, this process increased created a push in the direction of strips S6 and S6 – located on the left side. As the load continued, a crack began to form in the region above S5 and S6. These regions became particularly susceptible to deformation due to the lateral push of strips S1, S2, S3, and S4 – coming from the right and the push coming from the left side as strips S5, and S6

buckled to the left (Figure 5.30-**b**). When the tested piece reached its maximum compressive strength, the energy released by the pull and push forces, acting on the region above S5 and S6, created a crack at the intersection between S6 and the strip in the upper left corner of the specimen (Figure 5.30-**c**). Finally, the crack grew until breaking apart the strips in the left edge. As the strips broke apart, delamination cracks also appeared between S1 and S2 (Figure 5.30-**d**).

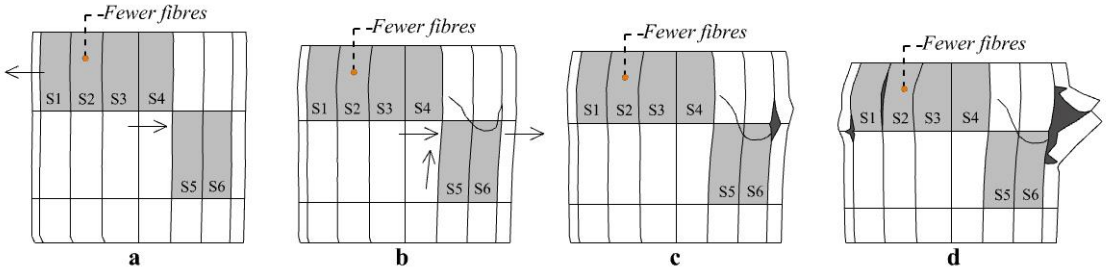

Figure 5. 30: Deformation and fracture analysis of Failure Mode 3.

5.3.3 Failure patterns in the tangential direction

The main features that determined the deformation and failure of the sample under tangential compression were the curvilinear distribution of fibres and the arrangement of bamboo strips while manufacturing the laminates. Based on the sample's analysis, these features influenced the mechanical behaviour of the specimens in the following manner:

Feature 1: Bamboo is rounded, and when strips are cut, the strips become segments of a circle. Bamboo fibres are distributed across the culm wall in a circular arrangement. They become denser near the outer layer of the culm. The cross-section becomes regular when the strips are milled into standard shapes, but the fibre distribution keeps its circular arrangement. A closer look at the strips reveals that fibres close to the outer layer create a circular boundary. When loads are applied in the tangential direction, the strips will bend in the direction of the outer layer (Figure 5.31-**a**). Depending on the arrangement of the strips, some will bow to the right, while some will bend to the left. The different bending patterns created different cracks in the tested pieces.

Feature 2: The arrangement of strips becomes critical to understand why some specimens developed cracks in the mid-region while others had cracks at the edges. Based on the research carried out by Nugroho and Ando (2001) and Mahdavi, Clouston, and Arwade (2011), the optimal way of arranging bamboo strips is to glue the inner-to-inner or the inner-to-outer faces together. Arrangement of outer-to-outer faces is not advisable. However, in practice, the outer-to-outer arrangement is likely to happen. When applying tangential compressive loads, the arrangement of fibres will become crucial. If strips have

an inner-to-outer arrangement, the strips will buckle to one side – the side with the highest percentage of fibres (Figure 5.31-**b**). If the strips have an inner-to-inner arrangement, each strip will buckle in the direction where the higher concentration of fibres is located. Hence, buckling will happen in both directions when compressive loads are applied (Figure 5.31-**c**). Finally, if the strips have an outer-to-outer configuration, the higher concentration of fibres will be in the middle. In this case, the strips will morph into a flattened rectangle when the loads are applied (Figure 5.31-**d**). In practice, the strips are arranged randomly, and the different configurations are likely to trigger different failure modes.

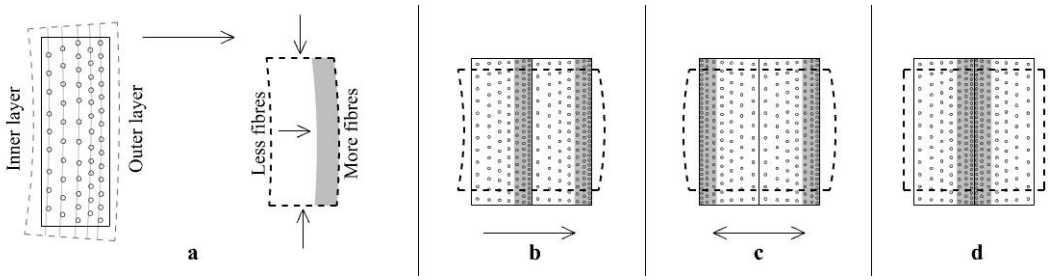

Figure 5. 31: Bamboo's features affecting compressive failure in the tangential direction.

The specimens' analysis revealed three failure mechanisms. The features mentioned above played a vital role in the mechanical response of the laminates. These were the main characteristics of the failure modes:

Failure Mode 1 happened in the specimens with strips with a pronounced circular arrangement of fibres. These strips were in opposite directions, which meant that the strips of one of the half sides of the tested piece were bending to one side, while the strips on the other half section were bending to the opposite direction (Figure 5.32-**a**). The bending moment of the upper and lower parts created a strain concentration at the point where the opposing forces met. This point was located right at the middle of the pieces in all the analysed specimens. It was at this point that cracking began.

Failure Mode 2 happened in the specimens with three zones with an inner-to-inner configuration. These zones became areas with fewer fibres, and they were in the specimen's right, middle, and left sides. More importantly, these areas were in the second row of the pieces, right in the mid-section. The mid-section buckled in both directions when the load increased, creating delamination cracks at the interface between the strips located in row number two (Figure 5.32-**b**).

Failure Mode 3 happened in specimens that had three zones with inner-to-inner configuration. Unlike Failure Mode 2, the areas with fewer fibres were not located in the

same row. Instead, they were in different rows but always in adjacent rows. The staggered arrangement of areas with fewer fibres created a diagonal path for the energy to travel across the specimen's surface. When the load increased, the energy was released at one of the edges of the pieces. The crack at the edge became more significant as the load continued, and delamination cracks appeared at the regions with inner-to-inner contact (Figure 5.32-**c**).

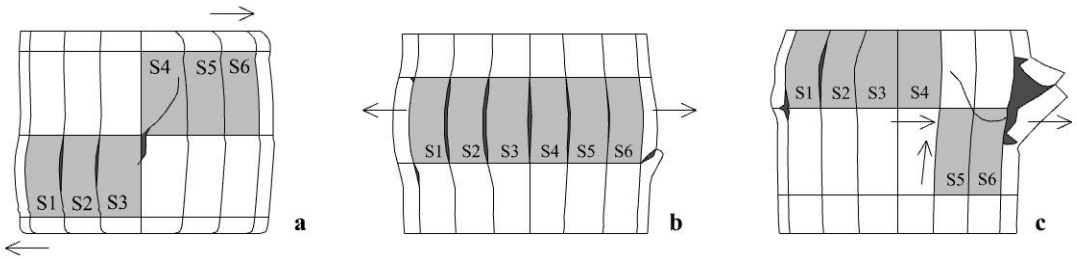

Figure 5. 32: The failure patterns of laminated bamboo under tangential compression.

Even though the cracks developed in different regions of the tested pieces, the following pattern was found:

Pattern 1: Cracking always started in the regions where opposing forces met. If two sets of strips buckled in opposite directions, but each set was in different rows, a crack appeared at the intersection point of the sets (Figure 5.33-**a**). If two sets of strips buckled in opposite directions, and both sets were in the same row, a crack appeared at the edge shared by both sets (Figure 5.33-**b**). If a third set of strips was in the row above or below two sets buckling in opposite directions, a crack appeared in the regions above set three or in the area below set 2 (Figure 5.33-**c**).

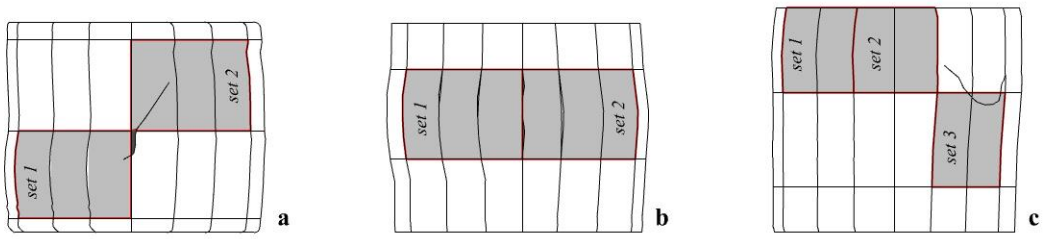

Figure 5. 33: The cracking patterns of laminated bamboo under tangential compression.

5.4 Longitudinal, radial, and tangential comparison

Based on the previous analysis, it can be concluded that the features that influenced the most the behaviour of laminated under compressive loading were the percentage of nodal regions, the geometry of nodes, the distribution of fibres – in the radial and tangential

directions, and the arrangement of strips. Unlike tensile behaviour, the pieces under compressive loading were not affected by the density of bamboo fibres. This might be because the pieces for compression were larger, which meant that the pieces had more strips with a higher percentage of bamboo fibres – reducing the likelihood of the material failing because of strips with fewer fibres.

The specimens under longitudinal loading were the pieces with the highest strength. The average compressive strength of the population was 58.43 MPa. The strength of the specimens under longitudinal loads was higher because the forces are acting in the direction of the fibres (Figure 5.34-**a**). When the load increases, the fibres exert resistance against the crushing of the parenchyma cells. The fibres do not break abruptly; instead, they will begin to buckle – which is the primary failure mechanism in the longitudinal direction. The fibres continue to resist the crushing forces even as they bend in and out. Contrary to this, when compressive loads are applied in the radial and tangential directions, the forces act in the fibres' perpendicular direction. The average compressive strength – in the radial directions – was 17.79 MPa, while the compressive strength – in the tangential direction – was 16.60 MPa. The difference can be explained by analysing the density and distribution of fibres in both directions. The fibres will be pushed down as the parenchyma cells break when loads are applied in the radial direction. The fibres will be re-distributed in the direction of the force. For this reason, as the loading continues, the fibres will act as an axial reinforcement trying to resist the compressive action of the force (Figure 5.34-**b**). Cracking is the most common type of failure of the sample under radial compression. On the other hand, when compressive loads are applied in the tangential direction, the inherent radial distribution of fibres will make the strips buckle as the parenchyma cells are crushed. The lateral push of fibres will make the strips crack by delamination. In this case, the fibres act as lateral reinforcement to counteract the horizontal expansion, but there are no fibres resisting the compressive forces trying to squeeze the piece (Figure 5.34-**c**). For this reason, the most common type of failure of the sample under tangential loading was cracking by delamination. In all cases, the percentage of nodes seemed to affect the strength of the specimens. The pieces with fewer nodes had a better performance than those with more nodes.

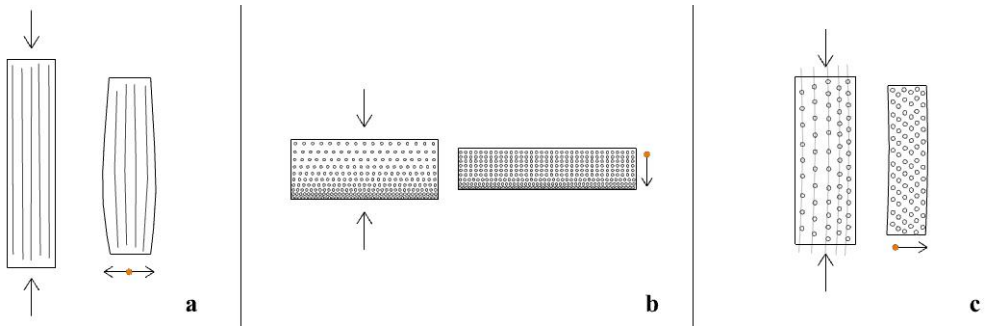

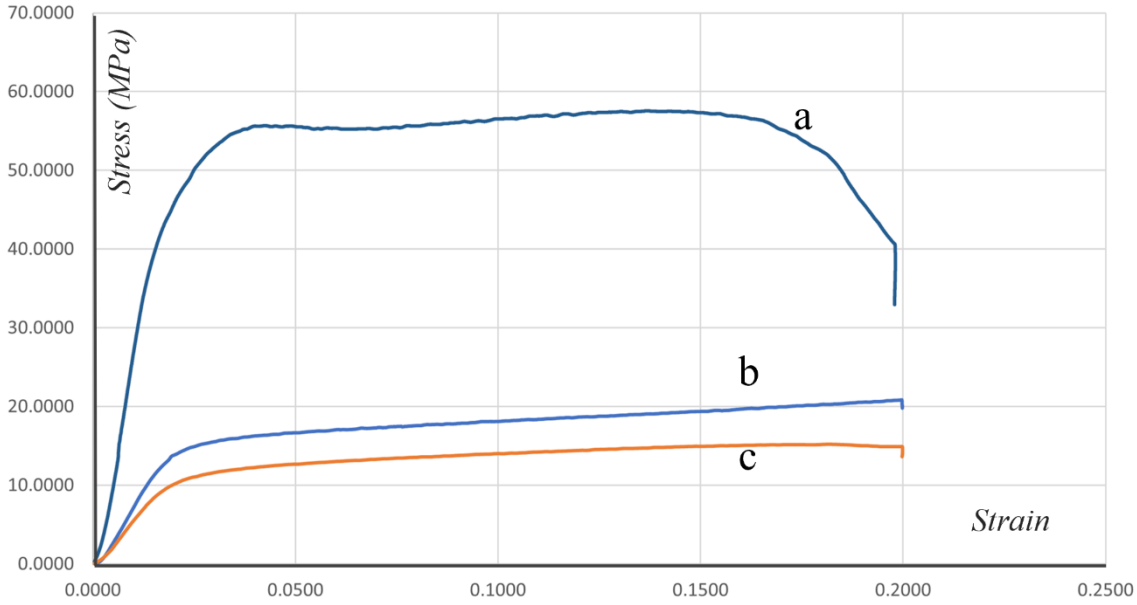

Figure 5. 34: The mechanical behaviour of the sample under compressive loading.

All the specimens had – at least – one nodal region. Nodes have different geometries in the radial and tangential faces of the strips. Depending on the geometry of the nodes and the type of loading, the nodes played a crucial role in compressive deformation and failure. The pieces under longitudinal and radial compression seemed to be more affected by the presence and geometry of nodal regions. Contrary to this, the pieces under tangential compression did not seem to be drastically affected by the presence of nodes. In the longitudinal direction, radial nodes accelerate the lateral deformation of the material. As shown in Figure 5.35-**a**, when compressive loads are applied, the already curved profile of fibres – in nodal regions – will exert more pressure on the neighbouring fibres as the parenchyma cells try to extend horizontally. In all cases, the geometry of fibres in the tangential direction always played a key role at later stages of the loading process. Every specimen with tangential nodes in one of their faces exhibited crushing as the loading increased. When pieces are subjected to longitudinal compression, the horizontal push of the fibres will easily break the strips with tangential nodes. The discontinuous and short nature of bamboo fibres - in tangential nodes – makes these regions especially susceptible to crushing (Figure 5.35-**b**). In the case of the sample under radial compression, the geometry of bamboo nodes did not play a direct role in the deformation and failure of the laminates. However, the presence of nodes means that the strips with nodes are bound to have a lower and irregular distribution of fibres. As compressive loads are applied – in the radial direction – the strips with nodes will deform faster than those without nodes (Figure 5.35-**c**). The differences in deformation rates are the main reason behind the failure mechanisms of the sample under radial compression. In many ways, though, identifying the strips with nodes is vital to predicting the failure mode likely to happen when the loading starts. Unlike the previous samples, the pieces subjected to tangential compression were not affected by the presence of node regions or

their geometric configuration. When compressive loads are applied – in the tangential direction – as the parenchyma cells push the fibres laterally, the node regions become reinforced by the adjacent fibres. Hence, the nodes do not become weak spots as the load increases (Figure 5.35-**d**).

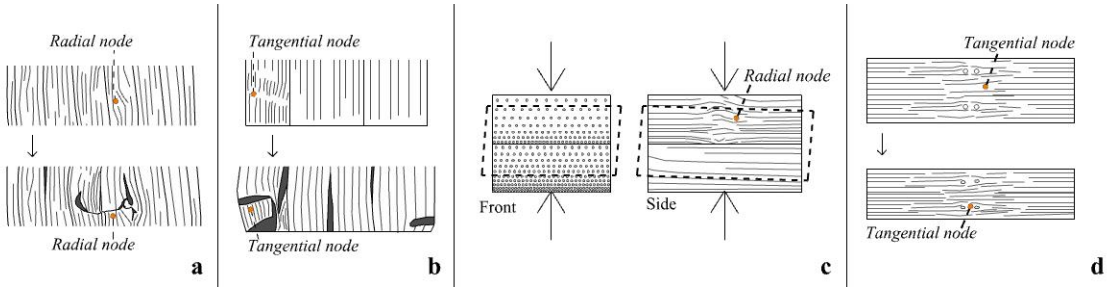

Figure 5. 35: Nodes and their effect on compressive deformation.

The arrangement of fibres plays a vital role in the deformation and failure of samples under radial and tangential compression. To a lesser degree, samples subjected to longitudinal compression are affected by this feature. As shown in Figure 5.36-**a**, when loads act in the longitudinal direction, the forces act in the direction of the fibres. The sections of the strips with more fibres are the areas with higher resistance against compressive forces. Hence, the distribution of fibres optimises the reinforcement of specimens under longitudinal compression, but it does not impact the failure modes in the longitudinal direction. Contrary to this, radial compression is affected by the monotonic distribution of fibres. The strip region with fewer fibres deforms faster than the area with more fibres. On a single strip, the different deformation rates are not significant. However, when multiple strips are assembled - and each strip is deforming at different speeds - the overall mechanical response of the material will be affected by these differences. For example, as seen in Figure 5.36-**b**, if a strip is located between two strips deforming faster, the strip is likely to develop a crack due to the pressure coming from the strips above and below. In the case of tangential compression, the arrangement of fibres will influence the direction in which the strips will bend. As the load increases, the strip will buckle in the direction that has more fibres. In other words, the strips will bend in the direction where the outer layers of the strips are facing (Figure 5.36-**c**). Overall, the direction to which a trip bends is not significant if forces are applied on a single strip. However, when multiple strips are assembled – the different bending directions will trigger different failure modes.

Strip arrangement is another factor determining the behaviour of laminated bamboo subjected to compressive loading. The pieces under longitudinal compression are not affected by the random arrangement of bamboo strips. However, the arrangement of strips is essential to determine where cracks are likely to appear – particularly in the samples under radial and tangential compression. When compressive loads are applied in the radial direction, the strips with fewer fibres will deform faster. The location of strips with

fewer fibres, hence, will determine the places where cracks will appear. If two strips with fewer fibres are located diagonally, a crack will appear at the point where both strips meet (Figure 5.37-**a**). If two strips with fewer fibres are arranged diagonally – but there are one or two strips between them – a crack will appear in the line that connects the strips with fewer fibres (Figure 5.37-**b**). Finally, if three or four strips surround a strip with fewer fibres, the strip will crack right in the middle (Figure 5.37-**c**). The arrangement of bamboo strips also orchestrates the failure modes of pieces under tangential compression. However, it does not matter the percentage of fibres that each strip has in this case. Instead, the orientation of the faces with more fibres is the factor that will determine where cracks will appear. If two strips are arranged diagonally, and one strips bends to the right and the other to the left, a crack will appear at the point where both strips meet (Figure 5.37-**d**). If two strips are arranged next two each other, and one strip bends to the right and the other to the left, a delamination crack will appear at the edge shared by both strips (Figure 5.37-**e**). Finally, if two strips are aligned diagonally, and both are bending in the same direction, a crack will appear in the area framed by the edges of both strips (Figure 5.37-**f**).

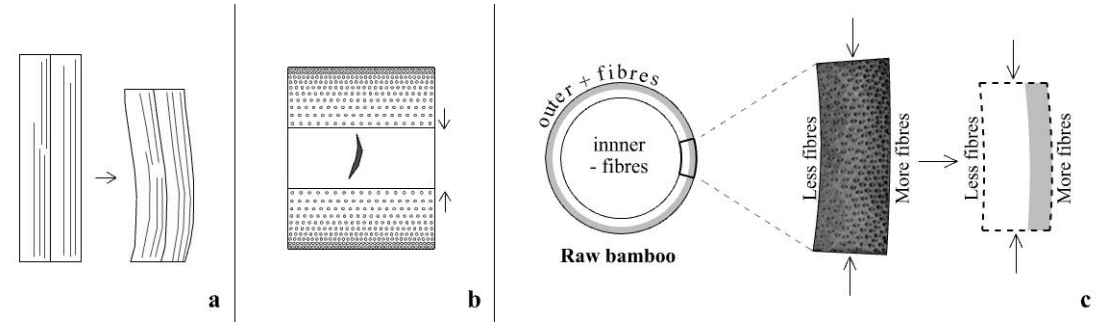

Figure 5. 36: Fibre arrangement and its effect on compressive deformation.

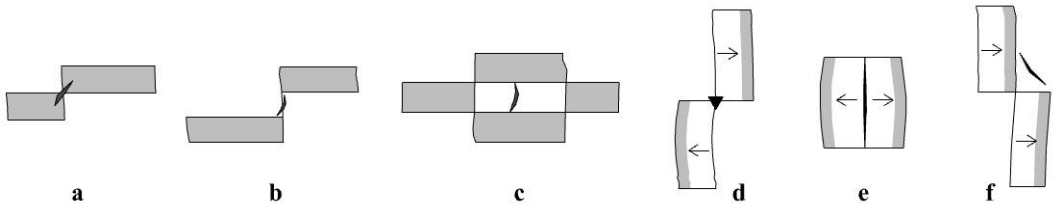

Figure 5. 37: Strip arrangement and its effect on compressive deformation.

In general, it can be concluded that the percentage of nodes affects the laminates' strength properties under compressive load. In contrast, the geometry of nodes, the distribution of fibres and the arrangement of strips are the factors that govern the failure modes of the laminates. The geometry of nodes is essential to determine the failure modes of pieces under longitudinal compression, and strip arrangement is critical to determine where cracks will develop when compressive forces are applied in the radial and tangential directions.

Chapter 6 | Uniaxial shear

| This chapter describes the results of the experiments carried out on samples subjected to longitudinal, radial, and tangential shear. The first part describes pieces' deformation and failure modes under longitudinal shear. The second part describes the results of the sample under radial shear. The third section characterises the deformation and failure patterns of laminated bamboo under tangential shear. Finally, section fourth compares the different failure modes and mechanical responses in the three directions. |

6.1 Longitudinal deformation and failure

6.1.1 Mechanical properties and behaviour

All the pieces under longitudinal shear underwent linear or elastic deformation during the first phase of the loading. However, as the load increased, the behaviour became non-linear. As shown in Figure 6.1, the Proportional Limit (PL) marked the point at which the specimens went from linear to non-linear behaviour. The average Proportional Limit of the population was 8.18 MPa. After the onset of non-linearity, the pieces reached an Ultimate Shear Strength of 9.28 MPa. Less than two seconds after reaching the maximum strength, the pieces underwent brittle and sudden failure. The behaviour described before is elastic-plastic with brittle failure. The average Modulus of Rigidity of the population was 277.83 MPa. Table 6.1 summarises the strength and mechanical values of the sample under longitudinal shear.

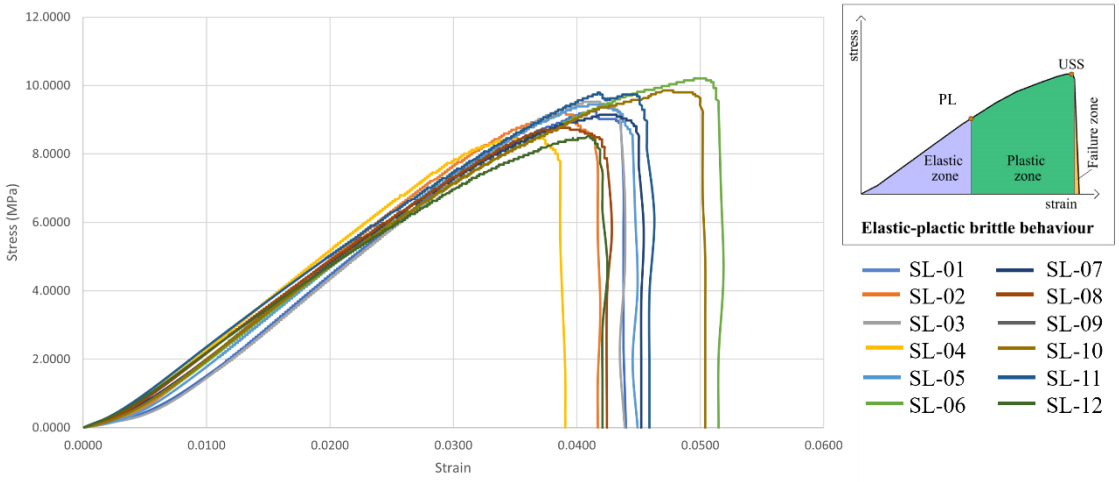

Figure 6. 1: Stress-strain curve of the sample under longitudinal shear.

	Average	SD value	Characteristic value
Proportional Limit (MPa)	8.18	0.42	7.57
COV	0.05		
Ultimate Shear Strength (MPa)	9.28	0.53	8.49
COV	0.06		
Modulus of Rigidity (MPa)	277.83	15.89	257.40
COV	0.06		

Table 6. 1: Strength and mechanical properties of the sample under longitudinal shear.

The strength value reported in this study is comparable to the values reported in the available literature. Sharma et al. (2017) registered an average Shear Strength of 7.60 MPa. Khoshbakht et al. (2018) reported an average Shear Strength of 13.15 MPa. The Modulus of Rigidity of laminates made with Moso bamboo was not reported in the literature reviewed in this study.

6.1.2 Deformation and failure modes

The results suggest that fibre distribution, fibres' density, and nodes were crucial to determining the strength properties of the specimens and determining the final fracture geometry. Overall, the area of the strips with more fibres or – generally- the strips with more fibres performed better. Hence, it can be concluded that fibres' density and distribution are the feature that determined the shear strength of the tested pieces. Fibre splitting was the only failure mechanism found in the population. However, the presence of nodes affected the final geometry of the pieces. For this reason, two failure modes were identified. The specimens that exhibited Failure Mode 1 had no nodes, and their strength properties were lower than the other specimens (Figure 6.2- **up**). Conversely, the pieces that exhibited Failure Mode 2 had nodes in the test region and better mechanical performance (Figure 6.2- **down**). The analysis of the sample suggests that nodes also improved the strength of the material under longitudinal shear. This could be because the fibres – at node regions – are not parallel. Instead, some are inclined, and some are curved.

The geometry of fibres - at nodes - diverts the load away from the central axis – which increases the material's resistance against shear.

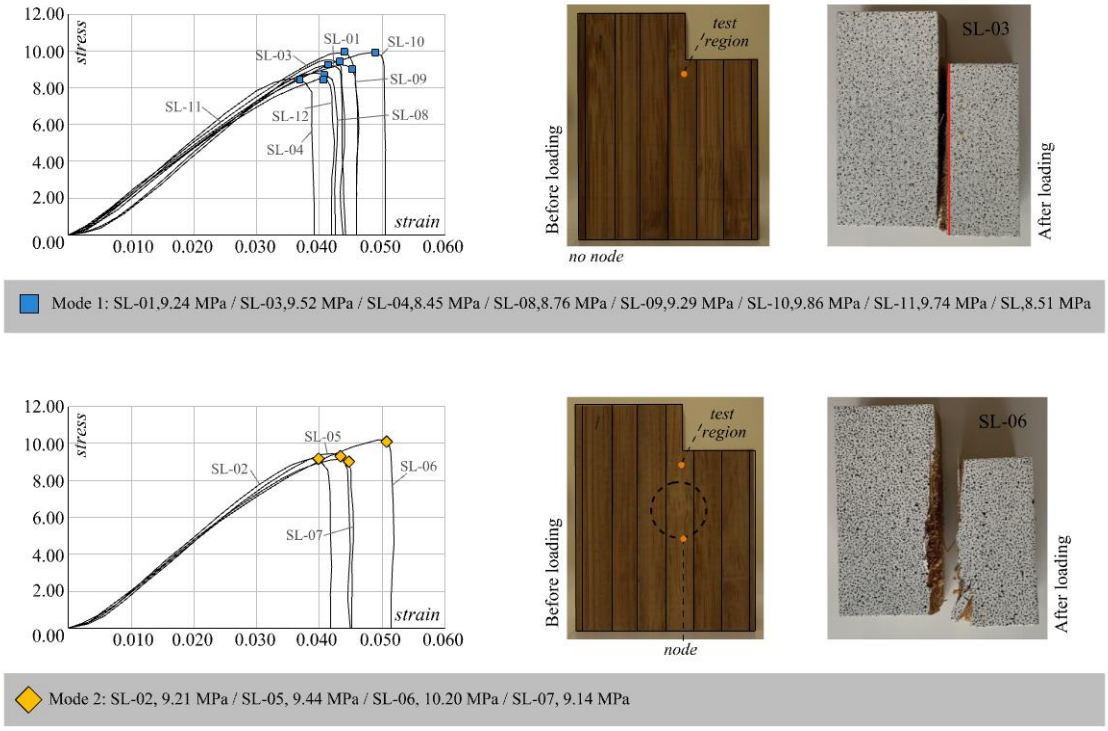

Figure 6. 2: **up**- Failure Mechanism 1, **down**- Failure Mechanism 2.

Failure Mode 1 occurred in the pieces with no nodes in the test region, and the test region was made up of two fibres arranged with the side of the strip with more fibres facing the right side (Figure 6.3-**left**). The shear line of the tested piece was located right at the middle of the strips forming the test region. AT 3.00 MPa, the main strain concentration is in the upper section of the test region. As shown in Figure 6.3- **L3.0**, a red spot is in the upper corner of the test region. At 6.00 MPa, the red area began to extend slightly to the lower part of the test region (Figure 6.3-**L.6.0**). At the same time, blue patches formed on the right side of the specimen. These patches represent the forces caused by the friction between the piece and the grip. At 8.52 MPa, the specimen reached its Proportional Limit. At this point, the area covered by the blue patches became smaller. The red dot– in the upper corner – also became smaller (Figure 6.3-**PL**). At 9.52 MPa, the specimen reached its Ultimate Shear Strength. Figure 6.3 -**USS** shows the strain field right before fracture. As seen in the figure, the red spot in the upper corner became a red line before fracture. The red line formed as a linear fracture began to extend from the upper corner to the middle of the specimen. At this point, a blue line began to appear, signalling the path of the fracture. Less than two seconds later, the piece broke in half. The final geometry of the fracture was a straight line crossing the test region from the upper corner to the bottom of the specimen (Figure 6.3-**F1**).

The fracture mechanism of Failure Mode 1 can be explained by analysing the longitudinal arrangement of fibres in the test region. As shown in Figure 6.4-**a**, the strip's fibres under shear loading were arranged linearly and without any interruptions. As loading began, the left side of the specimen started to slide down and a small notch formed in the lower side of the test region (Figure 6.4-**b**). As the loading increased, the opposite push of forces began to break apart the parenchyma cells near the grip's upper side. As shown in Figure 6.4-**c**, a crack began to develop at the upper corner of the test region. The crack quickly found a path to cross the whole section of the specimen. This path was found in-between fibres, right across the areas with no fibres. Finally, seconds after an initial crack appeared, the fracture travelled to the bottom side of the tested piece by following the channel formed in-between fibres. As a result, a vertical line cut the specimen in two. The final geometry of the fracture was a straight line formed by the straight lines of the strip's fibres (Figure 6.4-**d**).

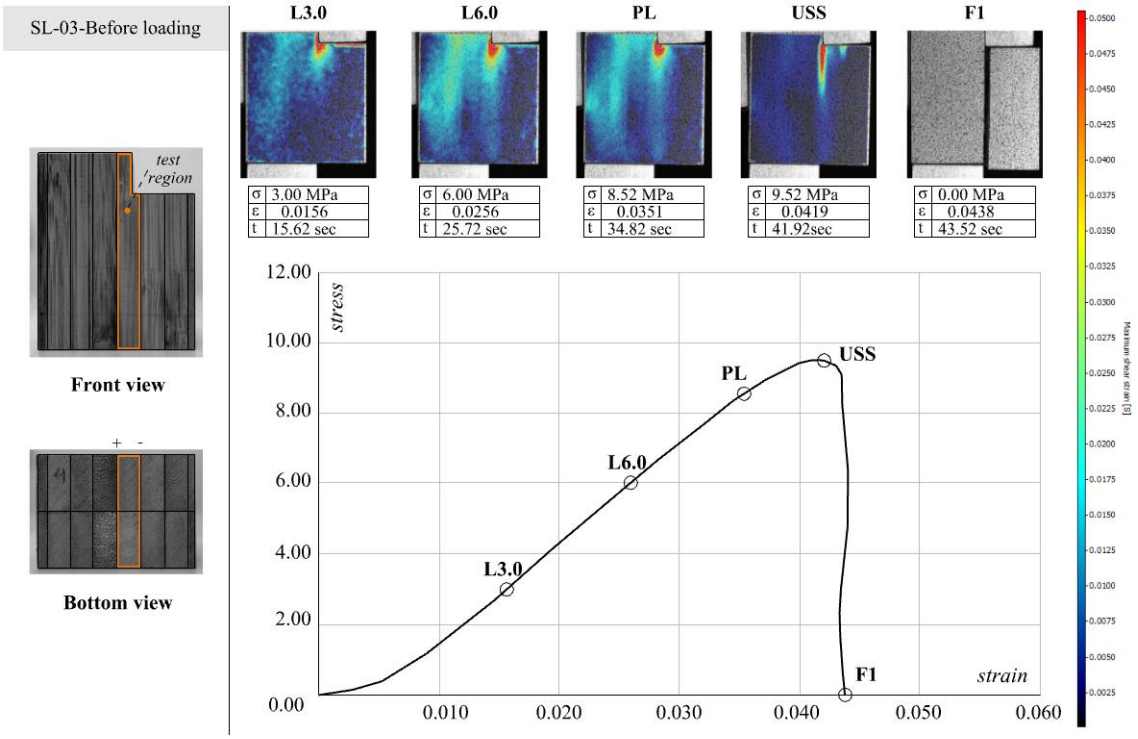

Figure 6. 3: left- Specimen SL-03 before loading, right- DIC analysis of specimen SL-03.

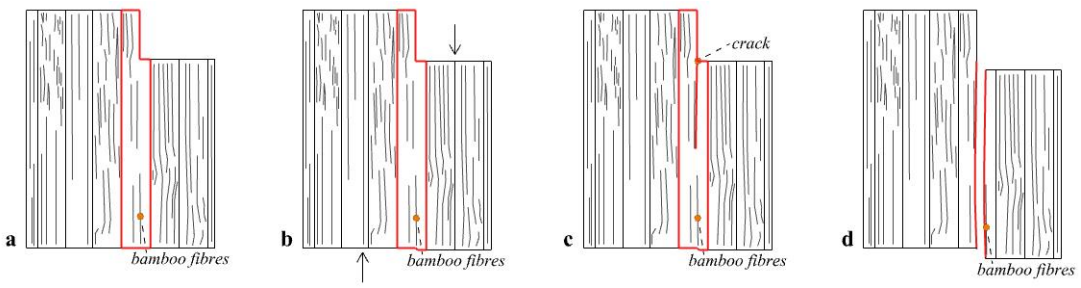

Figure 6. 4: Fracture analysis of Failure Mode 1.

Failure Mode 2 happened in the specimens with nodes. The strips forming the test region were placed in a way in which the face of the strip with more fibres was facing the right side (Figure 6.5-**left**). As with the previous pieces, the shear line was placed right in the middle of the strips forming the test region. When the loading began, small red, yellow, and blue patches appeared in the upper corner of the test region. It is essential to notice that compared to the other failure modes, the strain concentration at 3.00 MPa was lower (Figure 6.5-**L3.0**). As the load increased to 6.00 MPa, blue patches appeared in the right section of the specimen. As mentioned before, these patches appeared because of the friction exerted by the steel grips. At this point, the yellow and red patches in the upper corner became bigger (Figure 6.5- **L6.0**). When the specimen reached the Proportional Limit, the area covered by the blue patches – on the right side of the piece – became smaller. Also, another red zone appeared on the mid-right side of the tested piece (Figure 6.5- **PL**). This dot was formed due to the steel grip counteracting the rotation of the specimen. When the tested piece reached its Ultimate Shear Strength, the blue patches completely disappeared. Additionally, the rez zone on the right side also disappeared. At this point, the main strain concentration was located in the upper corner of the test region (Figure 6.5- **USS**). A red line began to extend from the upper corner of the test region to the bottom of the specimen. One second later, the piece broke apart. Unlike the pieces that exhibited Failure Mode 1, the final fracture geometry was not a straight line. Instead, the crack followed the outline of the fibres located in the node region (Figure 6.5- **F1**).

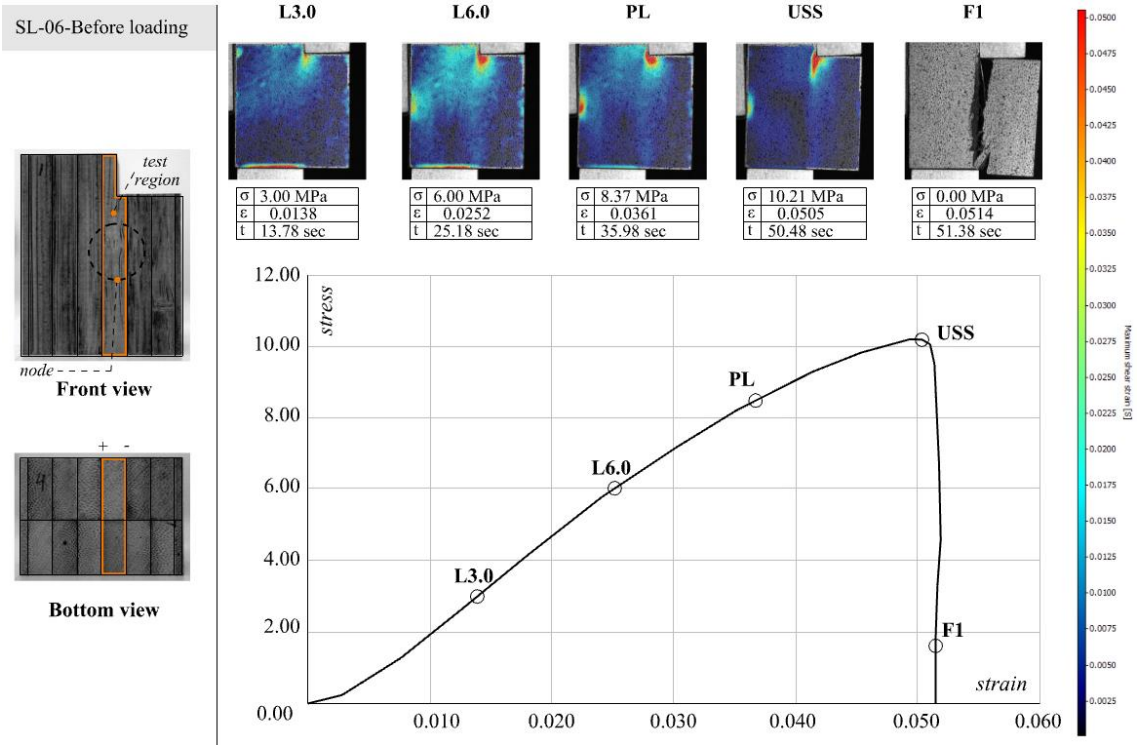

Figure 6. 5: left- Specimen SL-06 before loading, **right**- DIC analysis of specimen SL-06.

Like Failure Mode 1, Failure Mode 2 can be explained by analysing the configuration of fibres in the test zone. However, unlike the specimens in Failure Mode 1, the pieces in Failure Mode 2 had an irregular distribution of fibres in the test region. As shown in Figure 6.6-**a**, a node is located right in the middle of the strip forming the test region. For this reason, the fibres in the test region are not linear. Instead, the fibres are discontinuous and curved. As the load increased, the left side of the specimen began to slide down. While doing so, the distance between the already irregular fibres started to grow. For this reason, as seen in Figure 6.6-**b**, a crack appeared in the upper side of the test region. The crack did not follow a straight path. Instead, the crack tilted slightly to follow the curved pattern of the fibre located close to the node (Figure 6.60-**c**). As the loading continued, the crack travelled downward, following the irregular path of the fibres surrounding the node. The final fracture geometry was an irregular line with multiple angles. Figure 6.6-**d** illustrates why the pieces with nodes are likely to have a higher shear resistance than fibres with no nodes. When the shear loads are applied, the force will cross the piece straight. Without nodes, the force can easily break apart the fibres arranged linearly. Contrary to this, when fibres are placed at different angles, the force is directed off the central axis. Hence, the inherent irregularity of bamboo fibres – at nodes – counterbalances the direct shear forces acting on the tested pieces.

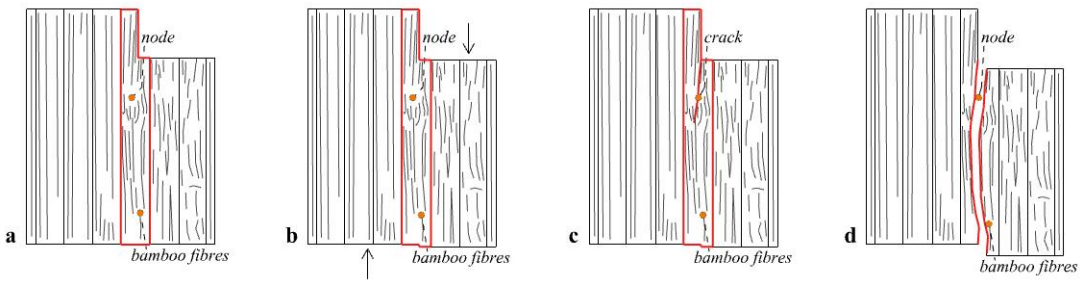

Figure 6. 6: Fracture analysis of Failure Mode 2.

6.1.3 Failure patterns in the longitudinal direction

The main features that influenced the mechanical response of laminated bamboo under longitudinal shear were the density of bamboo fibres, the monotonic distribution of fibres, and nodal regions. The way in which these features determine the behaviour of the sample is outlined below:

Feature 1: As mentioned before, bamboo species and manufacturing processes determine the percentage of fibres in a strip. The number of fibres in a strip will directly affect the material's shear strength. As shown in Figure 6.7-**a**, strips with more fibres will have more resistance against shear forces and vice versa (Figure 6.7-**b**).

Feature 2: Bamboo fibres have a section with more fibres and an area with fewer fibres. The strength of the material is affected by the location of the applied force. The shear strength will be higher if the shear forces are applied in the regions with more fibres (Figure 6.7-**c**). Conversely, if the force is applied in the part with fewer fibres, the shear strength of the pieces will be lower (Figure 6.7-**d**).

Feature 3: Uniaxial shear creates a straight line of action. If the shear line meets no resistance, the specimen will break, forming a straight line. The strips without nodes have a linear arrangement of fibres. When the shear force is applied, the force will break the parenchyma cells located in-between the fibres. The resulting fracture geometry will be a straight line (Figure 6.7-**e**). However, whenever there are nodes in the path of the shear force, the fibres surrounding the nodes will dissipate the energy in multiple directions (Figure 6.7-**f**). Much like a pebble ripping the surface tension of the water, forming circles. Strips with nodes, hence, have a higher resistance against shear deformation.

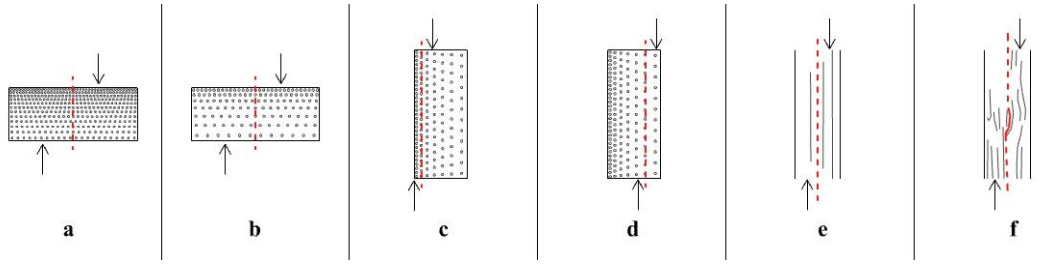

Figure 6. 7: Bamboo's features affecting shear failure in the longitudinal direction.

Based on the analysis of the population, it can be concluded that fibre density, monotonic fibre distribution and nodes affected the shear strength of the sample. However, nodes were the only features affecting the fracture geometry of the pieces. For this reason, two failure modes were found:

Failure Mode 1 happened in specimens without nodes. The shear force split the pieces by breaking the parenchyma cells located in-between fibres. The fibres of these pieces were straight and had no discontinuities. The fracture geometry of Failure Mode 1 hence was a straight line.

Failure Mode 2 happened in the specimens with nodes. Like in the previous failure mode, the shear force split the parenchyma cells located in-between fibres. However, unlike the last mode, the fibres of these pieces were not linear and discontinuous. Hence, the fracture geometry of Failure Mode 2 was a multangular line.

Overall, the results suggest that despite the final fracture geometry, all the specimens under longitudinal shear followed the same patterns:

Pattern 1: Fracture always started in the regions with no fibres. This region was always located in-between fibres.

Pattern 2: After the onset of fracture, the initial crack grew in the direction of the fibres. If the fibres were linear and continuous, the crack was linear and continuous. However, if the fibres were nonlinear and discontinuous, the crack was nonlinear and multangular.

6.2 Radial deformation and failure

6.2.1 Mechanical properties and behaviour

As shown in Figure 6.8, the sample subjected to radial shear exhibited an elastic-plastic behaviour. The pieces began their plastic deformation at an average Proportional Limit (PL) of 15.93 MPa. After reaching the Proportional Limit, the stress values increased until reaching the Ultimate Shear Strength (USS). The average Ultimate Shear Strength of the population was 23.62 MPa. The failure was ductile, and an abrupt fracture did not happen. After reaching the Ultimate Shear Strength, the tested pieces continued to deform and could still carry a load. However, the stress values did not peak after reaching the ultimate strength. For this reason, it can be assumed that failure began as soon as the Ultimate Shear Strength was reached. The average Modulus of Rigidity or Shear Modulus was 313.62 MPa. Table 6.2 summarises the strength and mechanical properties of the pieces under radial shear.

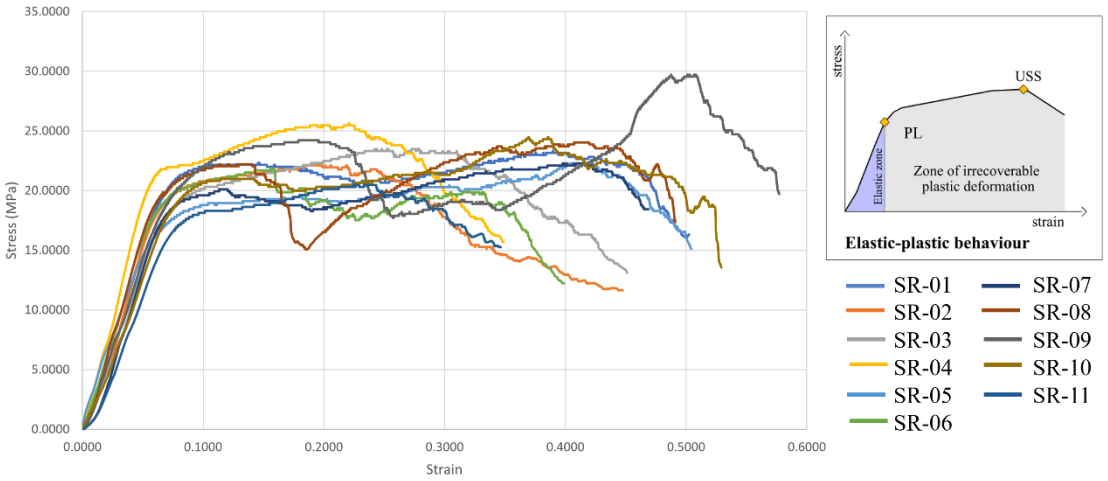

Figure 6. 8: Stress-strain curve of the sample under radial shear.

	Average	SD value	Characteristic value
Proportional Limit (MPa)	15.93	1.00	14.93
COV	0.06		
Ultimate Shear Strength (MPa)	23.62	2.46	21.17
COV	0.10		
Modulus of Rigidity (MPa)	313.62	41.84	255.43
COV	0.13		

Table 6. 2: Strength and mechanical properties of the sample under radial shear.

The studies reviewed for this research only reported the parallel shear values of laminates made with Moso bamboo. For this reason, the radial shear values calculated in this study cannot be compared against the available literature. Further research is needed to characterise the shear properties in the perpendicular direction fully.

6.2.2 Deformation and failure modes

As shown in Figure 6.9-**left**, all the tested pieces had more fibres in the upper section and fewer fibres in the lower area. The pieces had at least three fibres crossing the test regions. None of the specimens had nodes in the test region. All the samples - under radial shear - exhibited the same failure and fracture mode: fibre bending, followed by fibre ripping. As the load increased, shear bands formed due to fibre bending and ripping (Figure 6.9-**right**). This behaviour was called Failure Mode 1.

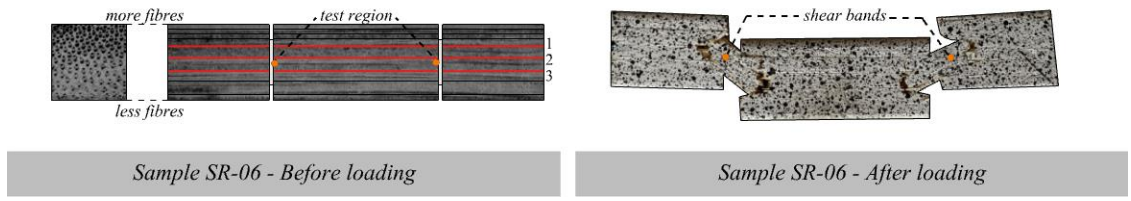

Figure 6. 9: **left**- Specimen SR-06 before loading, **right**- Specimen SR-06 after loading.

As the loading began, the main strain concentration was in the mid-section of the specimen. At 7.81 MPa, a light blue patch covered the centre of the test piece. However, it is possible to see that yellow and red patches were already visible in the test regions (Figure 6.10-**P1**). At 14.09 MPa, the strain concentration in the mid-section decreased, and the primary strain concentration became localised at the test regions. Orange and red patches formed in the test regions (Figure 6.10-**PL**). At 18.79 MPa, blue patches began

to spread towards the lateral and mid sections of the tested pieces (Figure 6.10-**P2**). At 19.12 MPa, the red patches that were previously across the surfaces of the test regions became concentrated in the lower part of the test regions (Figure 6.10-**P3**). At 20.29 MPa, the strain field in the test regions began to create a bow-tie geometry. At this time, red dots also appeared in the upper section of the test regions. Also, blue line patches extended from the test regions towards the rest of the specimen (Figure 6.10-**P4**). At 22.29 MPa, the piece reached its Ultimate Shear Strength (USS). At this point, the bow-tie geometry – formed by the strain concentration – became more extensive, and the red areas began to create a c-shaped profile (Figure 6.10-**USS**). After reaching the Ultimate Shear Strength, the load decreased. At 15.12 MPa, the strain geometry elongated at the test regions, and the c-shaped red areas also became longer (Figure 6.10-**P5**). At this point, the specimen can be considered to have failed.

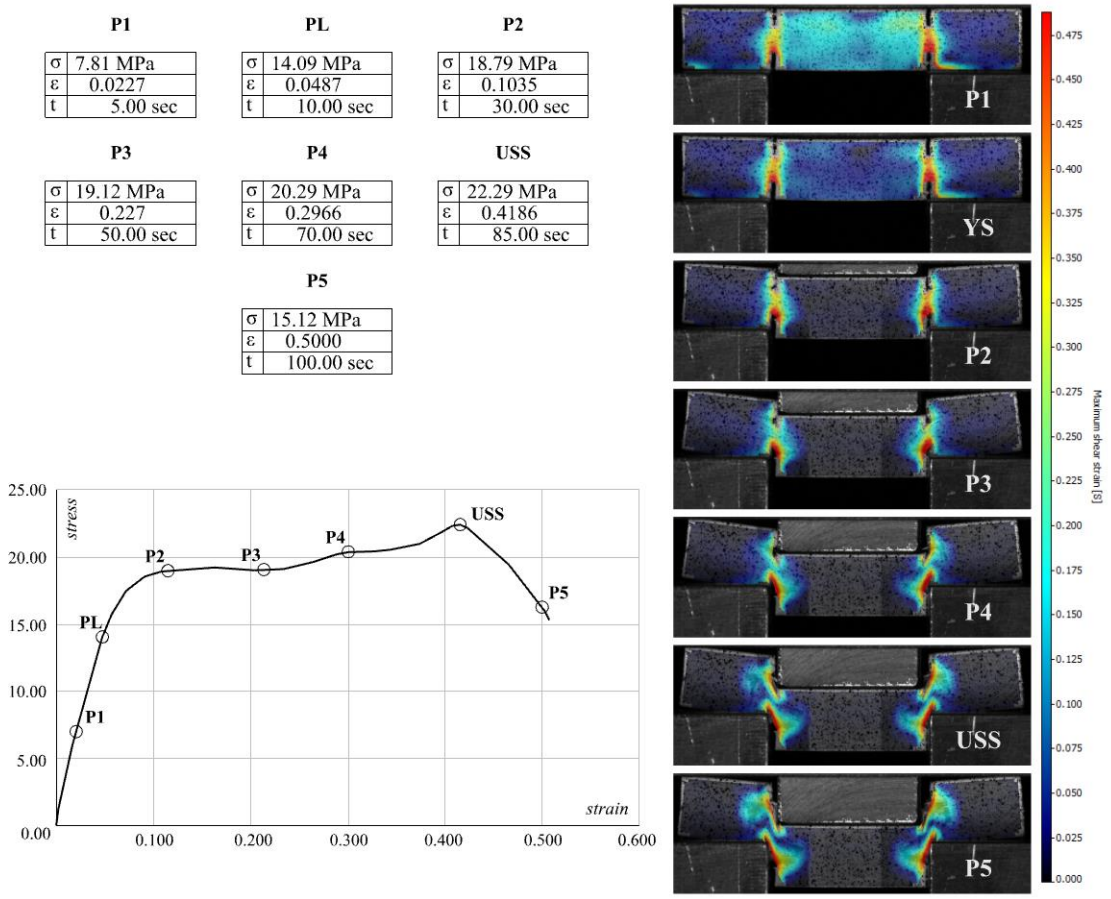

Figure 6. 10: DIC analysis of specimen SR-06.

The failure mode of specimens under radial shear can be explained by analysing the transformation of the fibres crossing the test region. Figure 6.11 illustrates the visual change of the fibres as the load increased. Time is used as a reference to map out the different stages of the radial transformation. At **0 seconds**, it is possible to see that the three fibres crossing the test region are arranged horizontally. **At 5 seconds**, the fibres began to bend towards the centre of the test piece. As they did so, the deformation of the

neighbouring fibres was minimal. At **10 and 20 seconds**, the fibres continued to tilt towards the centre of the specimen. At this point, it is possible to see how the transformation of the fibres began to push up and down the neighbouring fibres. At **30 seconds**, the rotation of the fibres changed direction as the shear movement of the test regions elongated the size of the fibres. The fibres, as mentioned before, are the strong elements of bamboo strips. By their inherent nature, bamboo fibres are made to resist lateral forces – making them highly elastic. This property explains why the fibres elongated as they bent. **At 50 seconds**, the fibres continued tilting towards the centre of the specimen. However, a closer look at the test region revealed that it is at this time that the first and third fibres broke apart. In other words, it is at this point that the fibres closer to the edges of the test region are ripped apart by the pronounced bending created by the shear forces. At **70 seconds**, the applied force continued to tilt fibre number two towards the centre of the specimen. It is at this point that the remaining fibre is ripped. At this point, the tested piece had not reached its maximum strength. That is because the rotated rectangles formed in the test regions resisted the shear forces. At **85 seconds**, it is possible to see that all the fibres – crossing the test regions – broke, forming a tilted rectangle. This is the rectangle that enabled the piece to continue resisting shear forces. However, at **100 seconds**, the specimen lost its loading capacity, and it is possible to see that the rotated rectangle morphed into a bow-tie geometry. This transformation is because as the load continued, the rectangles – in the test regions – continued to turn. Simultaneously the corners of the test piece began to squeeze the rectangles as they rotated. This process resulted in a bow-tie geometry formed by the three segments of the fibres that were initially crossing the test regions.

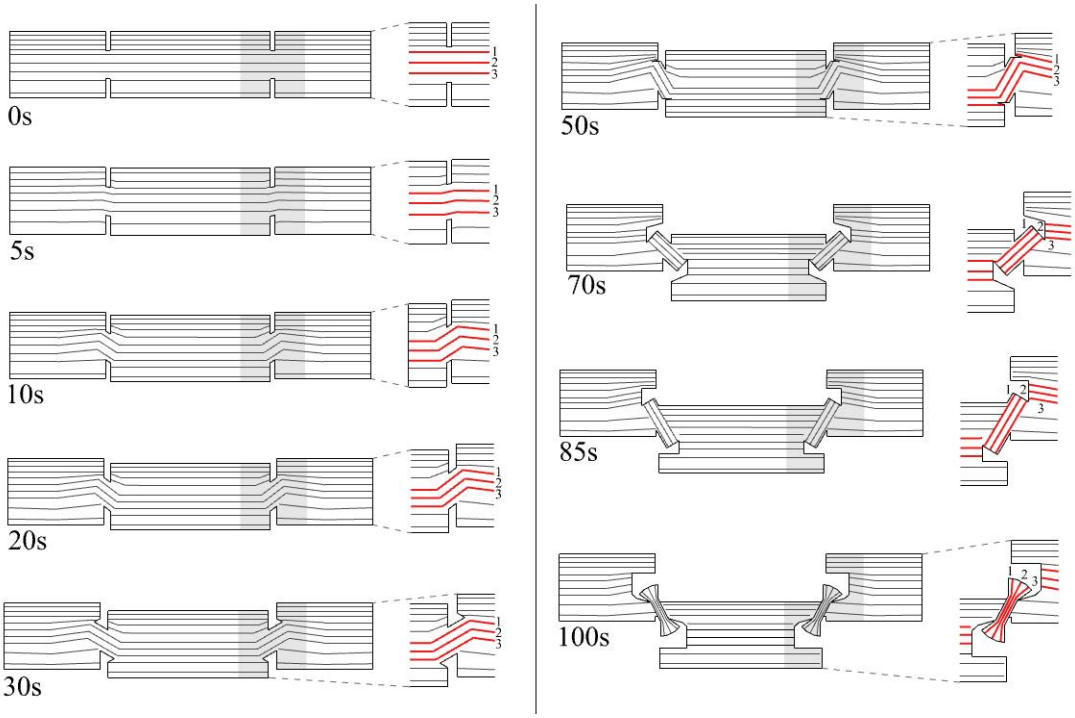

Figure 6. 11: The deformation of fibres under radial shear.

6.2.3 Failure patterns in the radial direction

In the case of radial shear, the main feature that drove the plastic deformation of the pieces was the bending capacity of the fibres located close to the central axis of the test piece:

Feature 1 – As shown in Figure 6.12-**a**, the fibres of the specimens under radial shear will undergo a higher degree of bending in the regions exposed to shear loads. As the load increases, the fibres will turn even further by rotating towards the central axis of the tested piece (Figure 6.12-**b**). Bending will continue until the bending strength of the fibres is exceeded. This will occur first in the fibres close to the edges of the test region. Notice that in Figure 6.12-**c** fibres 2 and 3 have broken. The pieces will continue to withstand loading as long as there are fibres that remain unbroken. However, at some point, all the fibres crossing the test area will break due to excessive bending. The last fibres to break will be the ones closer to the point where the opposing shear forces meet (Figure 6.12-**d**).

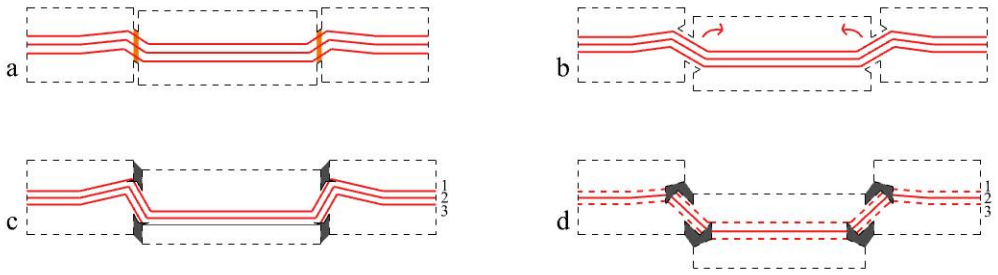

Figure 6. 12: Bamboo's features affecting shear deformation in the radial direction.

Based on the bending properties of fibres, only one failure mode was found: These are the characteristic of the failure mode:

Failure Mode 1 happened in specimens with no nodes and at least three fibres crossing the test regions of the piece. The failure mechanism followed a clear pattern. Before loading, the fibres were horizontally aligned (Figure 6.13-**a**). As the load continued, the applied shear forces in the test regions began to bend all the fibres crossing the test region. Figure 613-**b** to Figure 6.13-**e** illustrates the fibres' bending evolution before fracture. When the bending exceeded the permissible bending strength of the fibres, the fibres located near the edges were the fibres that failed first (Figure 6.13-**f**). Shortly after that, the fibre in the middle also broke (Figure 6.13-**g**). After this point, the test regions transformed into a set of tilted rectangles (Figure 6.13-**h**).

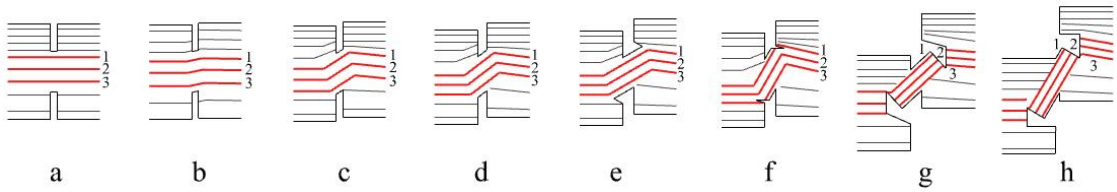

Figure 6. 13: Deformation analysis of Failure Mode 1.

As mentioned earlier, the bending strength of the fibres is the main feature affecting radial shear. In the case of radial shear, the following pattern was found in all the tested pieces:

Pattern 1: As seen in Figure 6.14, the fibre crossing the test region is entirely flat before loading. At **5 seconds**, the fibre section – in the test region – rotated 11°. At **10 seconds**, the section turned 21°. At **20 seconds**, the section rotated another 5°. At **30 seconds**, the section rotated -2.5°. Based on the analysis of the pieces, rotations with a negative sign indicate that the section of the fibre elongated or that it fractured. At **50 seconds**, the section rotated 30° from its previous position. At **70 seconds**, the section rotated -17.5°. In this case, the negative sign represents the change in direction made by the fracture of the fibre. At **85 seconds**, the segment rotated 16.5°. At this point, the segment rotation is not due to the pull of the rest of the fibre but due to the shear forces acting on the other parts of the test piece. Finally, at **100 seconds**, the segment rotated 3.5°. These parameters can be used to describe the deformation and failure of pieces under uniaxial radial shear.

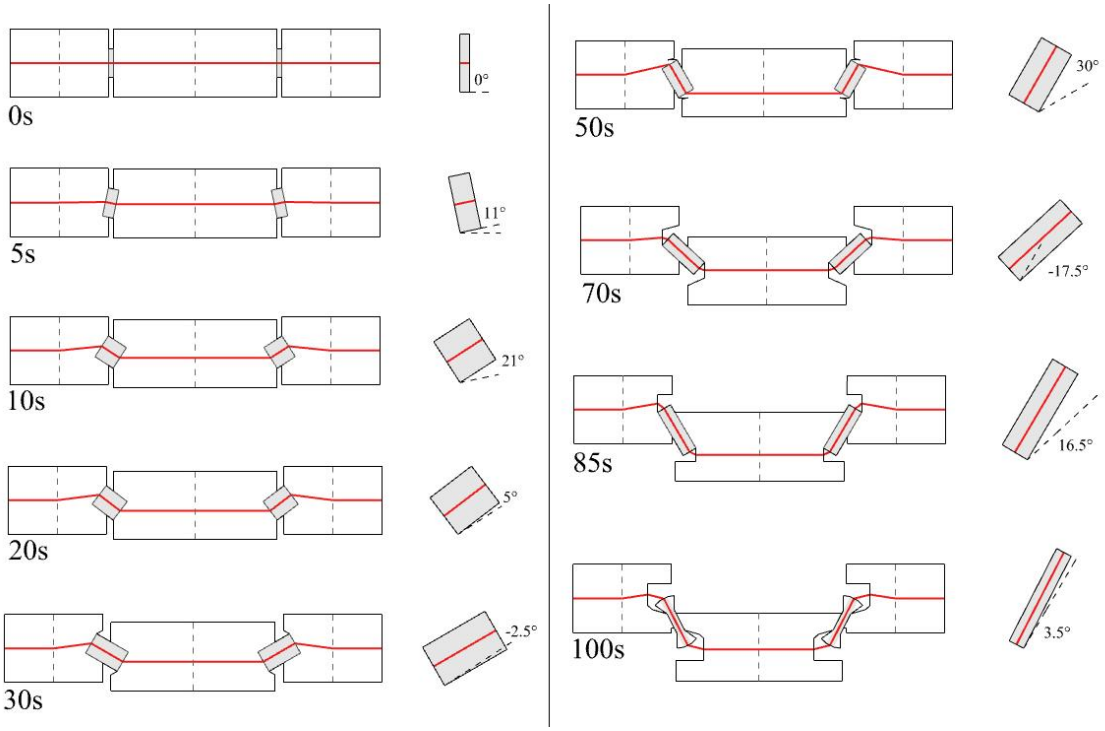

Figure 6. 14: Transformation of fibres under radial shear.

6.3 Tangential deformation and failure

6.3.1 Mechanical properties and behaviour

The sample under tangential shear had an elastic-plastic behaviour. As shown in Figure 6.15, the pieces had a short phase of linear behaviour until they reached the Proportional Limit (PL). The average Proportional Limit of the population was 19.32 MPa. After this point, the tested pieces started a phase of non-linearity. During this phase, the process of irrecoverable deformation began. The plastic deformation zone was more extensive due to bamboo fibres' plastic and malleable nature. However, after reaching the Ultimate Shear Strength (USS), the loading capacity of the pieces began to decrease. The average Ultimate Strength of the population was 41.78 MPa. The average Modulus of Rigidity was 348.86 MPa. Table 6.3 summarises the strength and mechanical properties of the sample under tangential shear.

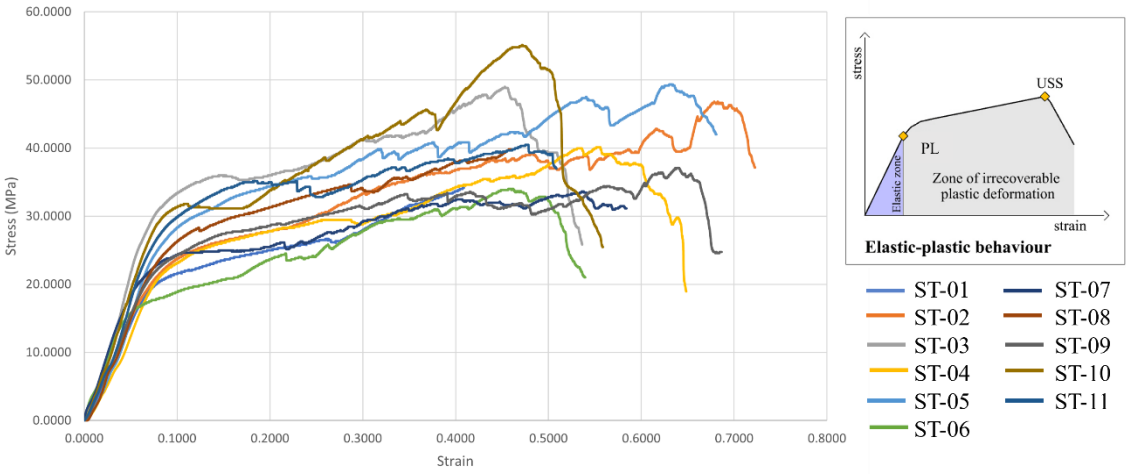

Figure 6. 15: Stress-strain curves of the sample under tangential shear.

	Average	SD value	Characteristic value
Proportional Limit (MPa)	19.32	3.04	15.28
COV	0.16		
Ultimate Shear Strength (MPa)	41.78	7.26	33.83
COV	0.17		
Modulus of Rigidity (MPa)	348.86	52.77	277.02
COV	0.15		

Table 6. 3: Strength and mechanical properties of the sample under tangential shear.

Similar to the analysis of the radial direction, the tangential shear values were not compared to the available literature. The literature reviewed for this study did not report shear value in the perpendicular direction. Overall, further research is needed to fully characterise the shear properties in the perpendicular direction.

6.3.2 Deformation and failure modes

As shown in Figure 6.16-**left**, the tested pieces had an even distribution of fibres along the vertical axis. The pieces had no nodes, and they were not affected by the monotonic distribution of fibres along the horizontal axis. All the pieces had more than three fibres crossing the test regions. All the tested pieces exhibited the same failure mode: fibre pulling and ripping due to fibre elongation. The high concentration of horizontal fibres added more strength to the test regions. Hence, instead of bending the fibres, the shear force pulled the fibres. This behaviour was classified as Failure Mode 1, and the fracture geometry is illustrated in Figure 6.16-**right**.

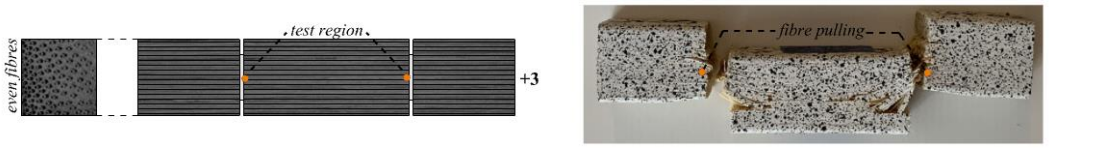

Sample ST-03 - Before loading | *Sample ST-03 - After loading*

Figure 6. 16: left- Specimen ST-03 before loading, **right**- Specimen ST-03 after loading.

The even distribution of fibres along the vertical axis enabled the specimen to have a higher loading capacity. For this reason, at 9.47 MPa, blue strain patches were only visible at the upper and lower regions of the midsection (Figure 6.17-**P1**). At 19.67 MPa, the blue patches extended across the entire surface of the section receiving the load (Figure 6.17-**PL**). Only at this point the dense pack of fibres – crossing the test region – began to fail. At 36.00 MPa, the primary strain concentration shifted to the test regions (Figure 6.17-**P2**). At this point, yellow and red patches began to appear in the test regions. At 38.50 MPa, the geometry of the strain patches – at the test regions – began to reflect the elongation forces pulling the fibres towards the upper lateral sides (Figure 6.17-**P3**). This happened because fibres highly reinforced the test region. As such, the lateral sides of the tested piece began to rotate upward. At 42.00 MPa, the primary strain continued in the test regions (Figure 6.17-**P4**). However, at this point, it is possible to observe that red zones appeared on the lower side of the test region. Some of the fibres in the test region likely began to break by this time. Because of this, the specimen started to slide further down. At 49.00 MPa, the piece reached its Ultimate Shear Strength. Figure 6.17-**USS** illustrates the strain field map as fibres continued to break in the lower side of the test region. Likely, the specimen could still carry the load because only some fibres – at the

bottom – began to fail. The upper fibres were still carrying a load. After this point, however, fibre pulling and ripping accelerated, and 15 seconds later, the tested piece completely broke apart. Figure 6.17-**F1** shows the strain field map at the moment that all fibres – in the test region – broke. Fracture happened because as the load increased, more and more fibres began to break apart until the number of fibres sustaining load was too low to withstand the shear forces.

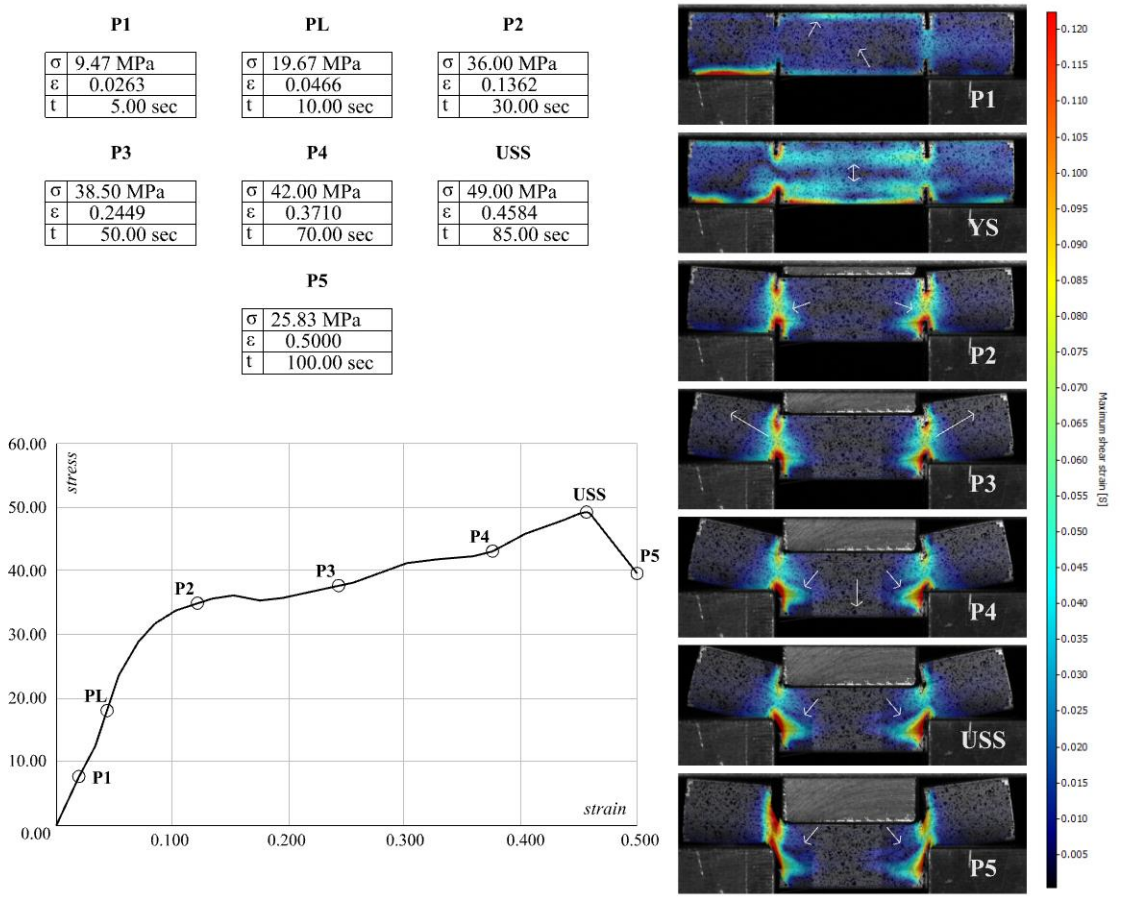

Figure 6. 17: DIC analysis of specimen ST-03.

The arrangement and density of bamboo fibres crossing the test regions explain the deformation and failure of the sample sunder tangential shear. Figure 6.18 illustrates the deformation of specimen ST-03 in 100 seconds. At **0 seconds** – before loading began – the fibres' segments in the test region are entirely flat. At **5 seconds**, no changes were recorded in the test region. Despite the initial load, the fibres remained flat. Only in the timeframe between **10** to **20 seconds** did the segments begin to deform – notice that the segments started to bend slightly towards the central axis. However, at **30 seconds**, the segments did not turn more. Instead, they became longer. Elongation happened because the lateral sides of the specimen rotated upward. The rotation pulled the fibres outward. Like the way in which a cable is pulled. At **50 seconds**, elongation continued, and the segments became even longer. At **70 seconds**, the fibres at the lower side of the test region

began to fracture. The fibres broke due to tensile forces pulling the fibres apart. At this point, elongation decreased, and fibre pulling accelerated. At **85 seconds**, more and more fibres began to break. Finally, at **100 seconds**, the shear force broke the last fibres crossing the test region. The release of energy caused the segments to spread in wing-like geometry. It is at this point that all the fibres broke apart. The tested piece could still carry some load due to the accumulation of broken fibres located in the test region.

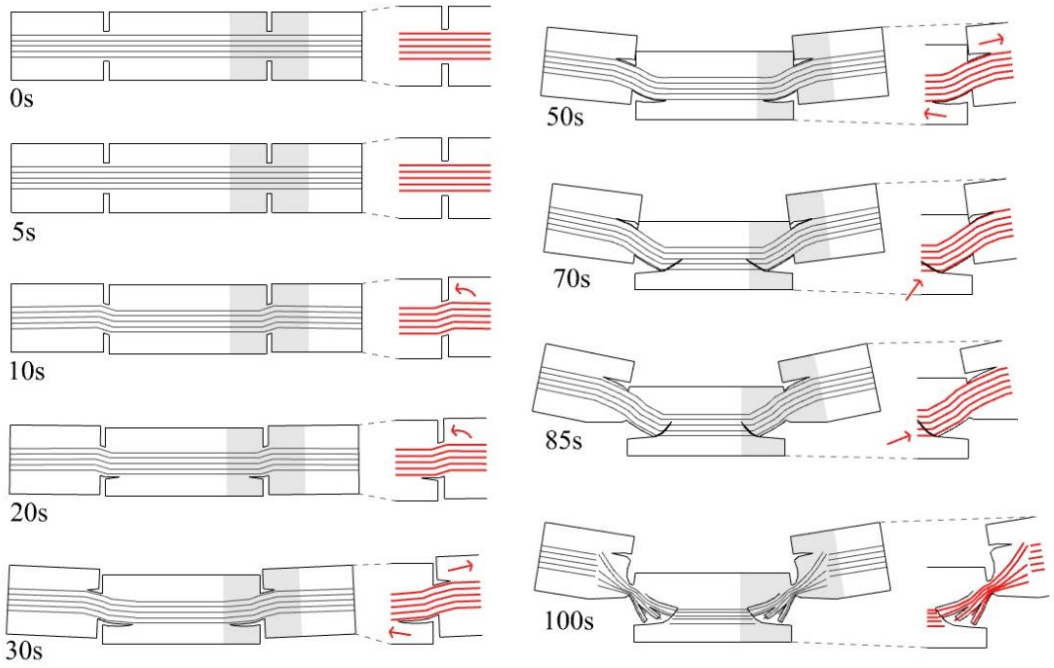

Figure 6. 18: The deformation of fibres under tangential shear.

6.3.3 Failure patterns in the tangential direction

A combination of fibre pulling, and fibre ripping were the underlying mechanisms of Failure Mode 1. This behaviour can be explained by analysing how fibre distribution, fibre density and the tensile strength of the fibres affected the mechanical response of laminated bamboo under tangential shear:

Feature 1: Fibres are equally distributed along the vertical axis in the tangential direction. The unequal distribution of fibres in the horizontal direction did not affect the response of the sample under tangential shear. As the shear force was applied, the force acted on a line of equally distributed fibres. This arrangement made the pieces withstand higher shear forces (Figure 6.19**-a**).

Feature 2: Fibre density is higher in the tangential direction. The higher the number of fibres, the higher the strength needed to deform the tested pieces. As seen in Figure 6.19**-b**, as the shear force is applied on a specimen with more fibres, the force will not be able

to break the densely packed arrangement easily. Instead, the force will travel in the horizontal direction, and as it does so, it creates a rotation movement in the extreme sides of the specimen. The rotation pulled the densely packed fibres as if they were a unit.

Feature 3: The fibres under tangential shear acted like a cable under tension. Hence, the tensile capacity of the fibres determined the moment at which fibre ripping began, the fibres close to the bottom side of the test region where the fibres with the highest tensile stress (Figure 6.19-**c**). These fibres were the first to break apart. As the load continued, fibre ripping continued.

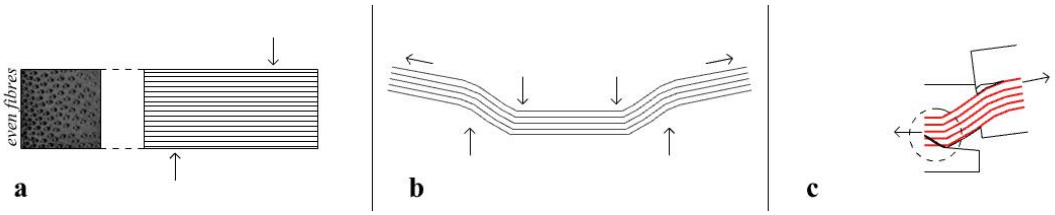

Figure 6. 19: Bamboo's features affecting shear deformation in the tangential direction.

Based on the previous analysis, these were the main characteristics of Failure Mode 1:

Failure Mode 1 happened in specimens with evenly distributed fibres – in the vertical axis – and without node regions. The failure mechanisms began with bending, followed by fibre elongation and, finally, fibre ripping. When loading began, the fibre segments remained flat in the test regions (Figure 6.20-**a**). Shortly after, the segments turned slightly towards the central axis (Figure 6.20-**b**, **c**). The densely packed fibres resisted the shear force – sending the force to the sides – where the outer parts of the specimen began to rotate. As the outer sides rotated, the fibres' segments began to elongate (Figure 6.20-d, **e**). Such transformation continued until the fibres located at the bottom started to separate. As the load increased, more and more fibres broke apart (Figure 6.20 **f**, **g**, **h**).

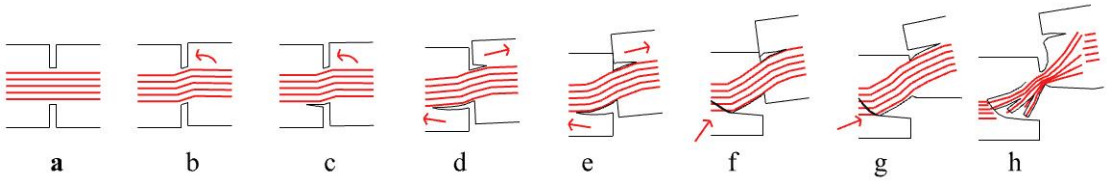

Figure 6. 20: Deformation analysis of Failure Mode 1.

Overall, the deformation and failure pattern of the sample under tangential tension is outlined below:

Pattern 1: All the tested pieces underwent a brief period of bending followed by elongation, and failure was completed by a period of fibre ripping. Figure 6.21 illustrates

the evolution of damage in the sample under tangential shear. Bending began **10 seconds** after loading started. From **20 to 50 seconds**, the fibres were elongated due to the lateral pull of the specimen as the lateral sides rotated. Finally, from **70 to 100 seconds**, the fibres started to break apart. The first fibres to break were closer to the bottom side of the test regions.

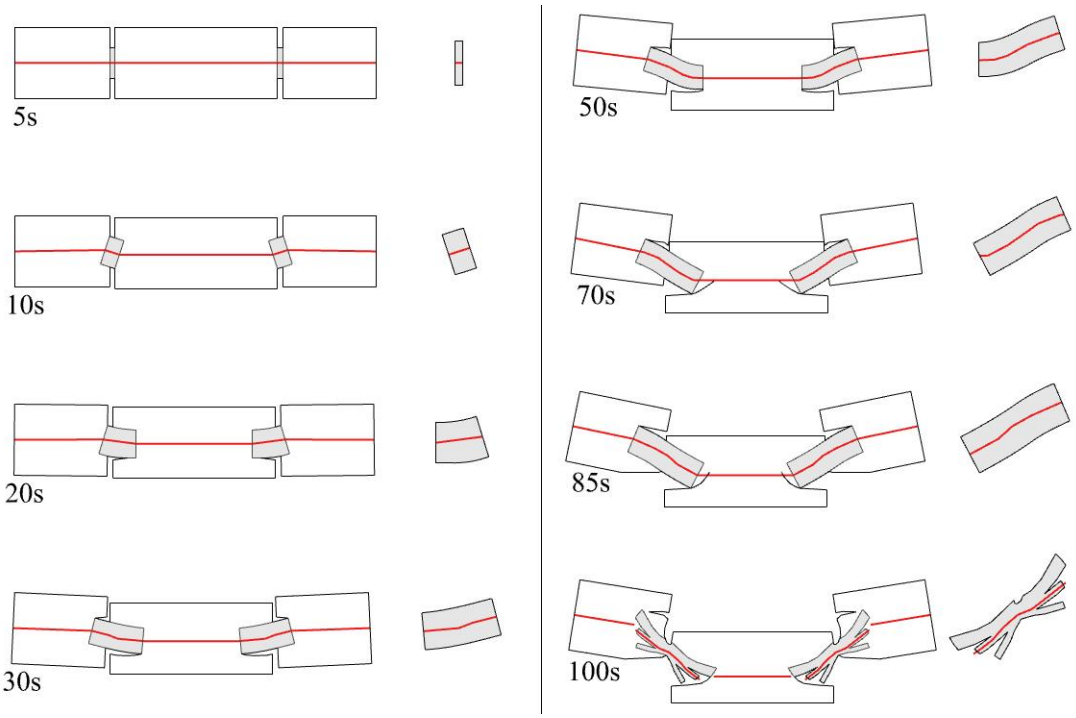

Figure 6. 21: Transformation of fibres under tangential direction.

6.4 Longitudinal, radial, and tangential comparison

Based on the previous analysis, it can be concluded that the density of bamboo fibres, the distribution of fibres and the mechanical behaviour of bamboo fibres were the features that determined the response of laminated bamboo under shear forces. Nodes also played an essential role in the fracture mechanics of the sample subjected to longitudinal shear. The pieces under radial and tangential shear did not have nodes. However, based on the analysis of other samples, it can be expected that node regions are likely to become breakpoints if they are aligned in the direction of the shear forces.

The sample under tangential shear was the population with the highest shear strength. Their average shear strength was 41.78 MPa. This can be explained by looking at the tangential distribution of fibres. As shown in Figure 6.22-**a**, when shear forces are applied, the densely packed fibres act as a unit resisting the shear forces. Contrary to this, when a shear force is applied in the radial direction, the number of fibres is not equally distributed. Hence, the reinforcement against the shear force is lower (Figure 6.22-**b**). The

average shear strength of pieces under radial shear was 23.62 MPa. The pieces with the lowest shear strength were subjected to longitudinal shear. The average shear strength of the sample under longitudinal shear was 9.28MPa. As seen in Figure 6.22-**c**, as soon as a crack developed in the parenchyma matrix, the linear arrangement of fibres put no opposition against the shear forces. Hence, the shear force was actively breaking parenchyma cells, not fibres. Instead, the fibres became channels to direct the path of the fracture. In summary, fibres are the main elements withstanding shear forces. If a specimen has many fibres, this specimen will exhibit better performance. Finally, depending on the direction of the fibres, these can act as reinforcement or as gateways to direct the energy of the fracture.

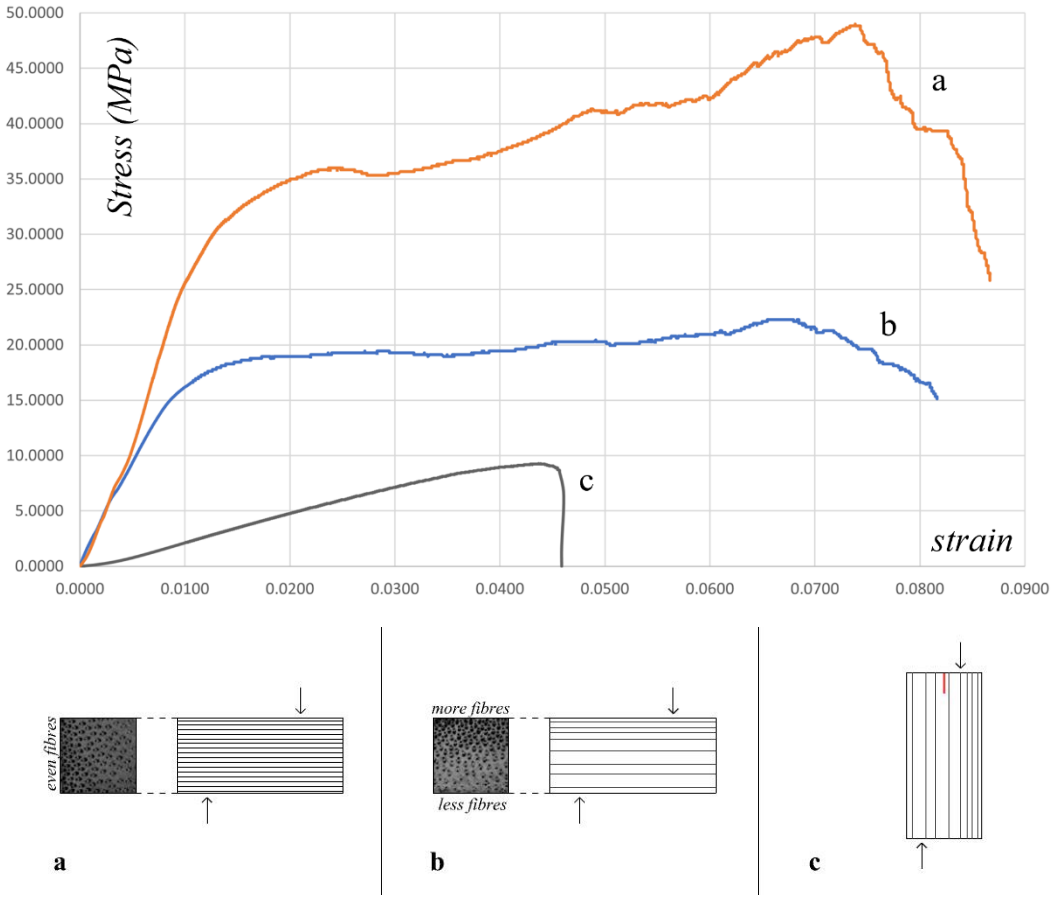

Figure 6. 22: The mechanical behaviour of samples under shear loading.

As mentioned before, the physical features of bamboo fibres are essential to determine the shear strength of laminated bamboo under shear forces. However, the mechanical properties of fibres also play a crucial role in shear deformation, particularly in the deformation of samples under radial and tangential shear. In the longitudinal direction, the mechanical properties of bamboo fibres are not directly engaged in the deformation process since the bonding strength of parenchyma cells mainly determines deformation and fracture. Contrary to this, when tangential and radial shear forces are applied, the

forces are actively trying to break the fibres apart. The fibres are the strongest elements of bamboo strips. The higher the number of fibres, the higher the resistance against shear deformation. In the case of pieces under radial shear, the number of fibres resisting deformation is limited, and the level of reinforcement is not equal across the cross-section of the strips. Because of this arrangement, the fibres will bend when the forces are applied (Figure 6.23-**a**). For radial shear, the mechanical property behind the deformation of the specimens was the bending strength of the fibres. As the load increased, the fibres bent until the push of the parenchyma cells started to rip apart the outermost fibres (Figure 6.23-**b**). Tangential deformation, unlike radial deformation, is not solely dependent on the bending properties of the fibres. When shear forces are applied in the tangential direction, the high number of fibres aligned in the tangential direction will exert an increased resistance against the forces. This resistance is constantly fighting the forces pushing the piece in opposite directions. The resistance of the densely packed fibres created a diverted energy distribution. Instead of travelling axially, the force started to travel across the horizontal direction of the fibres. At this point, two forces were acting on the tested piece: the opposite forces trying to crush the piece and the opposing forces trying to pull the fibres (Figure 6.23-**c**). As a consequence of this behaviour, the fibres began to elongate. There is only so much tensile strength that the fibres can withstand. Once the tensile strength of the fibres was ever exceeded, the fibres began to rip (Figure 2.22-**d**). The fibres with a higher concentration of tensile strength were the first to fail. Based on this analysis, it became evident that the tensile strength of bamboo fibres is a mechanical property that highly influences the shear deformation in the tangential direction.

Nodes are areas of fibre discontinuity, and as has been highlighted before, these areas are prone to failure. In the case of shear loading, nodes have a different effect on the deformation process depending on the direction in which the force is applied. In the case of pieces under longitudinal shear, nodal regions did not behave as breakpoints. Instead, they only acted as pathways to direct the fracture (Figure 6.24-**a**). It is essential to notice that - in longitudinal shear - nodal regions became spots of resistance against shear loading. The fibres surrounding the nodes are not arranged in straight lines. Instead, they are curved or inclined. The irregular arrangement of fibres made the specimens have a better performance when shear loads were applied. For this reason, the pieces with nodes had a better performance than pieces without nodes. The specimens under radial and tangential shear were very small, and to facilitate the process of cutting the pieces, nodal regions were avoided. Despite this decision, it is possible to conclude that the discontinuity of fibres – in the nodal areas – might be critical when shear loads are applied in the radial and tangential directions. As seen in Figure 6.24-**b** and **c**, be it radial or tangential direction, if a node is located in the direction of the shear forces, the discontinuity of fibres will likely accelerate the fracture of the piece. Hence, bamboo

nodes are likely to act as breakpoints when shear loads are applied in the radial and tangential directions.

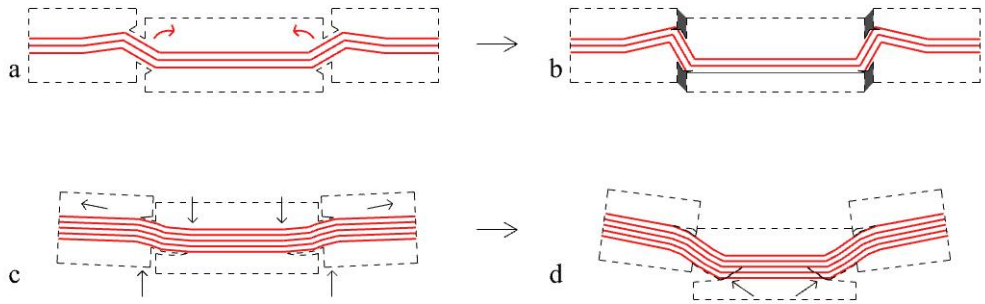

Figure 6. 23: Bamboo fibres and their effect on shear deformation.

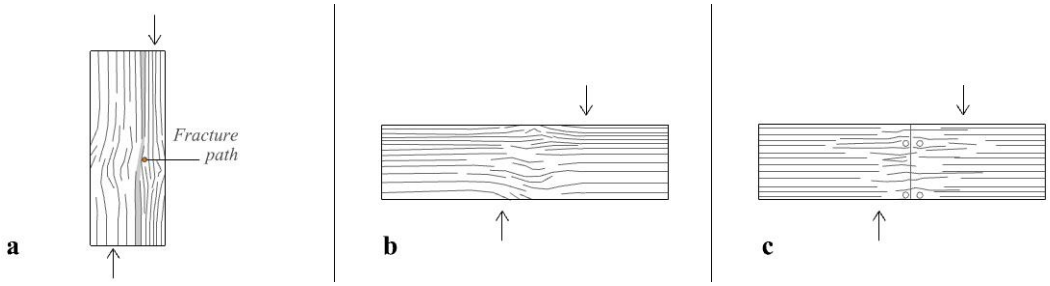

Figure 6. 24: Nodes and their effect on shear deformation.

Based on the experiments, it can be concluded that when shear forces are applied in the longitudinal direction, the parenchyma cells will be the first elements to fail. When shear forces are applied in the radial direction, the bending strength of the fibres will determine the deformation of the pieces. Finally, when shear forces are applied in the tangential direction, the tensile strength of the fibres will determine the deformation of the pieces. Overall, the previous analysis suggests that bamboo fibres' physical and mechanical properties are the main features affecting the deformation and failure of laminated bamboo under shear loading. The results also highlight the importance of identifying nodes to be able to predict the fracture geometry of pieces under longitudinal shear. Bamboo nodes are also expected to become breakpoints when radial and tangential shear forces are applied. Therefore, these should be avoided or reinforced to prevent abrupt shear failure in the radial and tangential directions.

Chapter 7 | Geometric Modelling

| This chapter describes the development of a geometric-based method to predict the deformation and failure of laminated bamboo under axial loading. The first section describes the parameters and methods used to describe deformation and fracture. The second, third and fourth parts outline the equations and algorithms developed to define tensile, compressive and shear behaviours. Finally, the fifth section illustrates the process of applying the method, compares the outcome of the method vs the results of the experiments, and discusses the limitations and applications of the method. |

7.1 Predicting deformation and fracture

Based on the experiments, laminated bamboo exhibited three types of behaviour: elastic with brittle failure, elastic-plastic with brittle failure, and elastic with plastic deformation. As shown in Figure 7.1-**a**, the samples that exhibited brittle elastic behaviour had elastic deformation all the way until reaching their Ultimate Strength (US). After this point, the pieces broke abruptly, i.e., brittle fracture ensued. The samples with elastic-plastic behaviour and brittle fracture underwent elastic and plastic deformation before reaching their Ultimate Strength (Figure 7.1-**b**). After this point, the tested pieces broke in less than two seconds. The samples with elastic-plastic behaviour had two different configurations. Those in which the pieces could still carry load after reaching their Ultimate Strength (Figure 7.1-**c**) and those that began to fracture when they reached their Ultimate Strength (Figure 7.1-**d**). In all cases, though, two stages defined the process of damage: deformation and fracture. During the deformation process, the tested pieces changed shape and size without developing cracks. Contrary to this, during the fracture process, cracks appeared on the surface of the material.

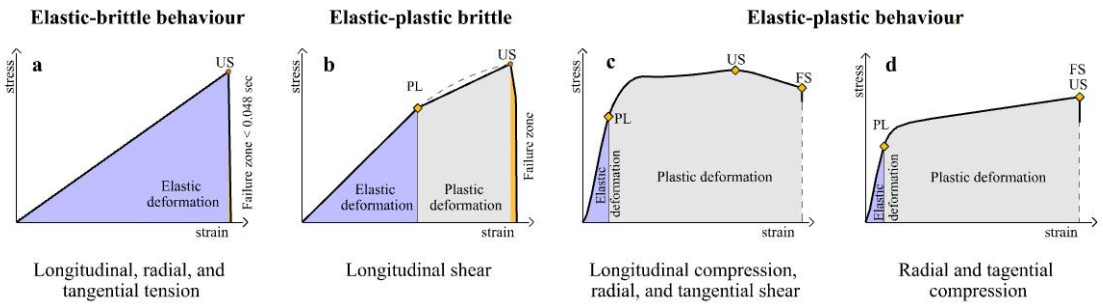

Figure 7. 1: The behaviour of laminated bamboo under axial loading.

The present study suggests two approaches to approximate damage evolution in laminated bamboo. The first approach focuses on describing the deformation of the material, both within the elastic and plastic regimes. The second approach focuses on defining where cracks are likely to appear. In other words, the second approach was developed to predict the fractured state of the material after reaching the Ultimate Strength. The following sections explain the logic and parameters behind both methods. All the geometric analysis and methods described below were implemented in Grasshopper, a generative geometric modelling tool embedded in Rhino 3D.

7.1.1 Parameters to define deformation

Retrieving deformation vector fields

A high-resolution digital camera recorded the deformation of all tested pieces. Hence, a set of photographs were used to track the morphological transformation of the pieces as the loads were applied. Within the evolution of damage, two states were used to calculate the parameters that govern the elastic and plastic deformation of laminated bamboo under axial loading. The initial state was the photograph of the piece before loading. The second state was the photograph of the piece right before the onset of fracture. The second photograph was called 'the final state', and it represented the state of the tested pieces when they reached their Ultimate Strength. The outlines of the initial and final states were retrieved from the photographs. The outlines were used as the primary input to determine the transformation of the tested pieces. Later, a set of grids were used to map out the deformation parameters, one grid represented the initial state, and the second grid represented the final or deformed state. The centroids of the grid segments were used to retrieve a series of deformation vector fields. Overall, the following steps were used to calculate the deformation vector field of the tested pieces:

Step 1: Two reference geometries or outlines were created using the initial and final pictures. As shown in Figures 7.2**-a** and **b**, Outline-00 is the shape of the tested piece before deformation, and Outline-01 is the shape of the piece after deformation.

Step 2: After defining the outlines, each geometry was divided into equal segments along the x and y directions. The resulting geometries were two grids. Grid-00 represents the initial condition, and Grid 01 represents the final condition. Finally, the centroids of every segment of the grids were calculated. The centroids are the reference points used to create the deformation vectors.

Step 3. As can be seen in Figure 7.2-**c**, in the final step, both the undeformed and deformed array of centroids were superimposed. The deformation vector fields were created by joining the initial points or 'Points 00' with the final points or 'Points 01'.

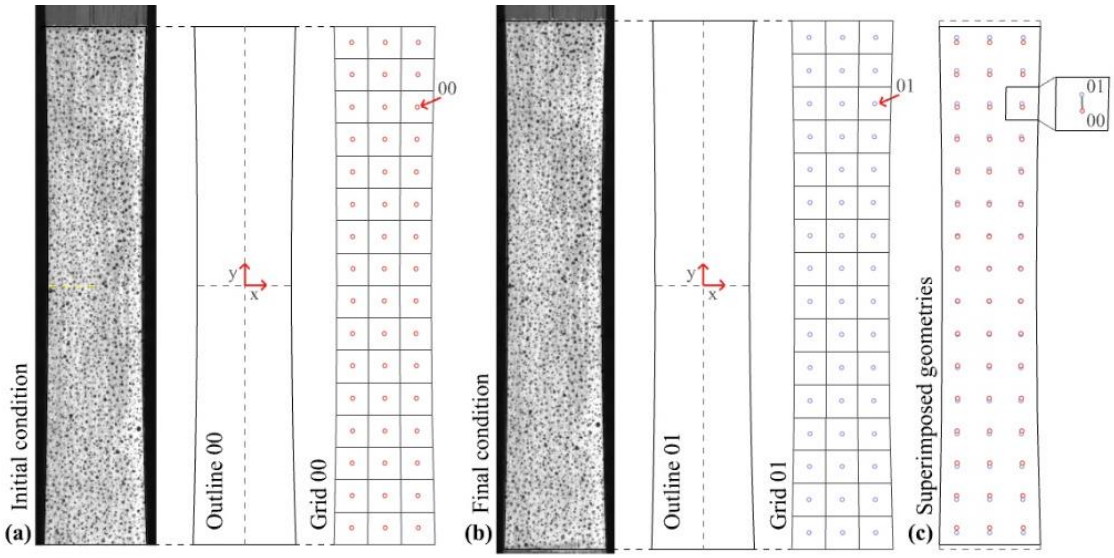

Figure 7. 2: Steps to retrieve deformation vectors.

The equations defining deformation

The vector fields were used as the parametric input to predict deformation. The mathematical relations of the deformation vectors were used to calculate equations that predict the elastic and plastic deformation of laminated bamboo under tensile, compressive and shear loads. Even though the specimens with fewer bamboo fibres had a lower performance than those with more fibres, only those with higher strength values were used to calculate the deformation vectors. The reason for doing this was because, in real-life settings, the probability of using specimens with fewer strips and fewer fibres is unlikely. Instead, mid-sized objects are likely to have a balanced number of strips with fewer fibres and strips with more fibres. Regardless of the sample and the type of loading, the overall procedure was similar. Hence, the process can be summarised as follow:

Step 1: As shown in Figure 7.3-**left**, the points calculated using the method described in the previous section were the points used to determine the mathematical relations to predict the behaviour of the material.

Step 2: The vertical transformation of points or Δy was calculated by measuring the distance from P-00 to P-01. The predicted behaviour is inferred by calculating an equation that fits the incremental data of the vector fields (Figure 7.3- **Δy**).

Step 3: The horizontal transformation of the points was defined by measuring the change in length of the horizontal lines in proportion to a reference length. In this case, the

reference length is the length of the first horizontal line or the initial transversal length (Tli). The change in length of the subsequent horizontal lines was denominated. The results of the experiments were used to calculate an equation that predicts the difference in the size of horizontal lines (Figure 7.3-**ΔTl**).

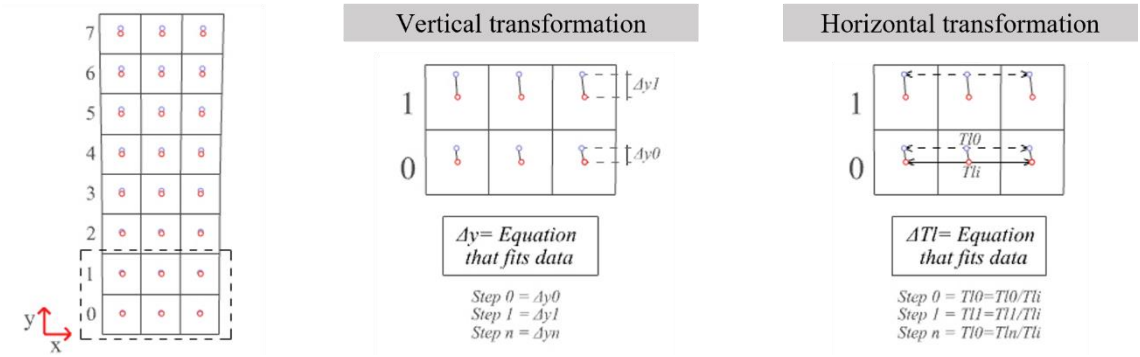

Figure 7. 3: Parameters defining deformation.

Δy and **ΔTl** represent the equations needed to predict the deformation parameters of laminated bamboo under different loading scenarios. These equations were derived from the analysis of the vector fields of the tested pieces. Section 7.2 outlines the equations to define tensile deformation. Section 7.3 describes the equations to map out the deformation of pieces under compressive load. Finally, section 7.4 lists the equation that determine shear deformation.

7.1.2 Parameters to define fracture patterns

Defining fracture geometry

Regardless of the type of loading – all the tested pieces began to fracture after reaching their Ultimate Strength. The results of Chapters 4, 5, and 6 suggest the physical characteristics of bamboo strips can be used as an input to determine the fracture geometry of laminated bamboo. In most cases – except for radial and tangential shear – fracture started in the areas of the specimens that had the lowest reinforcement. These areas were regions with fewer or no fibres, regions with a smaller cross-section, or regions with nodes. After the fracture began, the cracks propagated in the path that offered less resistance. The geometric arrangement of fibres usually defined this path. As shown in Figures 7.4 **a** to **c**, the fracture geometry of specimens that exhibited brittle fracture was a single polyline that began in the area with fewer fibres. Then it propagated across the surface of the piece following the arrangement of fibres. The fracture geometry of the samples with plastic deformation was a set of cracks that could be synthesised into geometric shapes. These cracks were always located near the strips with fewer fibres (Figures 7.4 **d** to **e**).

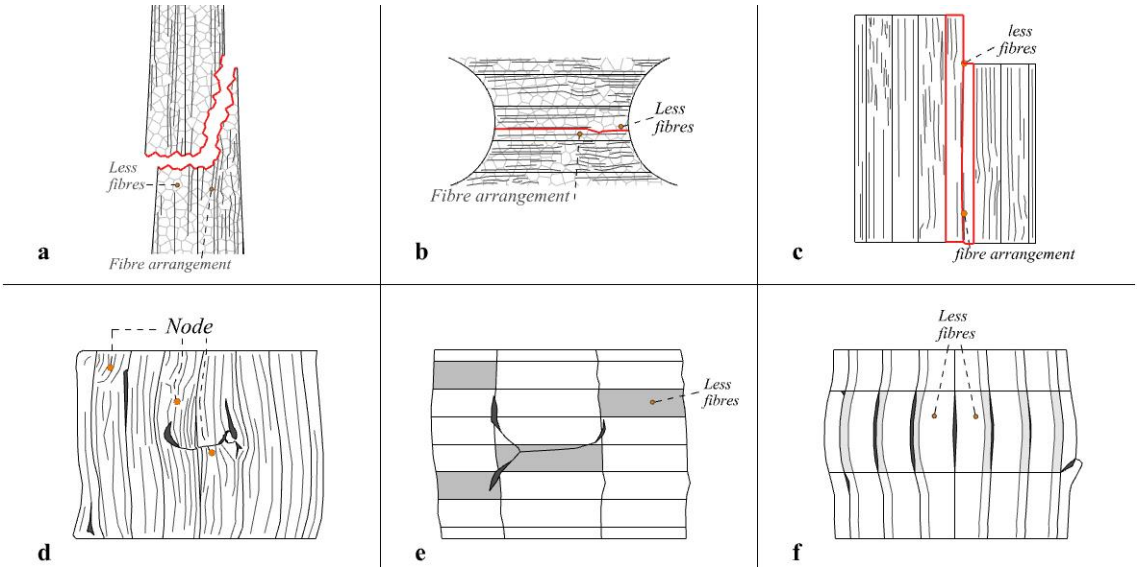

Figure 7. 4: The fracture patterns of laminated bamboo under axial loading.

Based on the analyses outlined in Chapters 4, 5, and 6, it can be concluded that a set of polygonal lines can geometrically define fracture. Hence, the criterion used to determine the final fracture geometry was to use the image of the tested piece – before deformation – as a blueprint to identify regions susceptible to failure. After these regions were identified with points, lines or polygonal shapes, a series of algorithms were developed to generate the possible fracture geometry. Depending on the type of loading, and the direction of the fibre, a series of fracture patterns were found. These patterns were used to create algorithms that predict fracture geometry by acknowledging areas prone to fail. The logic and parameters behind these algorithms are outlined in sections 7.2, 7.3, and 7.4.

Visualising fracture

To visualise the areas where fractures were likely to develop, the following process was developed:

Step 1: The polygonal lines representing the fracture geometry of the tested pieces were placed on top of the array of points representing the deformed state of the pieces (Figure 7.5-**a**).

Step 2: The points representing the deformed state were used to place polygonal shapes. The polygonal shapes represent the solid-state of the tested pieces right before fracture (Figure 7.5-**b**).

Step 3: The lines representing fracture are used to morph the polygons' scale created in the previous step. The size of the polygons is morphed by using the fracture lines as attractor fields. Hence, the polygons closer to the fracture lines will be smaller, and the polygons farthest will be bigger. As shown in Figure 7.5-**c**, this procedure creates a geometric representation of the places where the fracture is likely to happen.

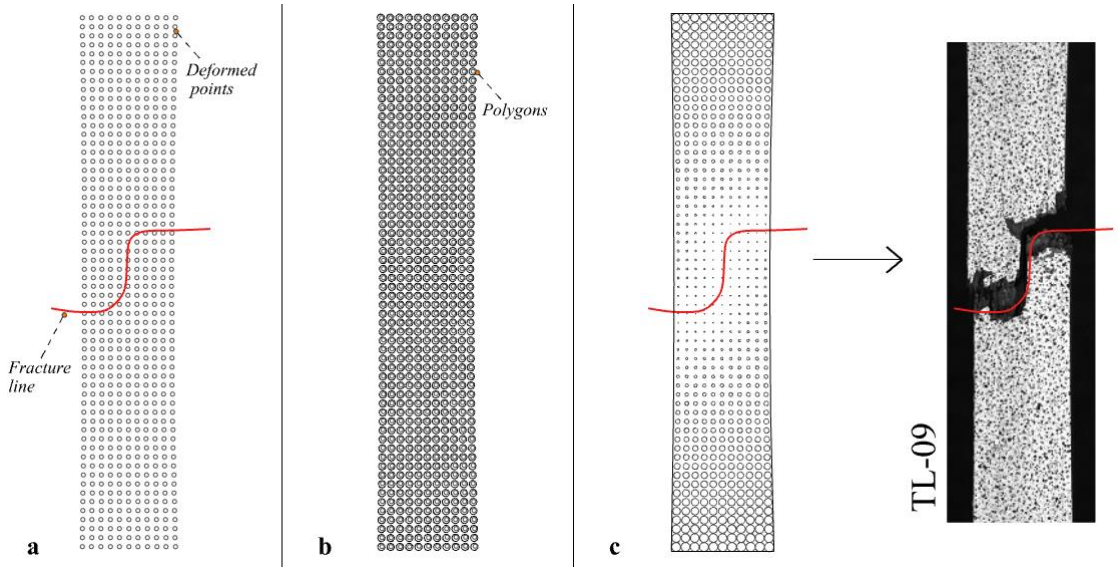

Figure 7. 5: Visualising fracture.

7.2 Tensile deformation and failure

7.2.1 Longitudinal direction

Δy and ΔTl

The Δy and ΔTl equations of tensile deformation - in the longitudinal direction - were calculated by measuring the mathematical relations of the deformation vectors of specimen TL-12, which had a higher distribution of bamboo fibres and a tensile strength higher than the average Ultimate Tensile Strength. These equations are assumed to determine the deformation of specimens with an even fibre-to-parenchyma ratio.

Figure 7.6-**left** shows the data plot used to calculate the vertical transformation (**Δy**). The equation of the fitted function is shown below:

$$y = 0.0257 * \sqrt{1 + \frac{(x-4.5047)^2}{0.1012^2}}$$

Figure 7.6-**right** shows the data plot used to adjust the length of horizontal lines (**ΔTl**). The equation of the fitted function is shown below:

$$y = 1 + \frac{1.0013\ -1}{1 + (x/4.5)^{27}}$$

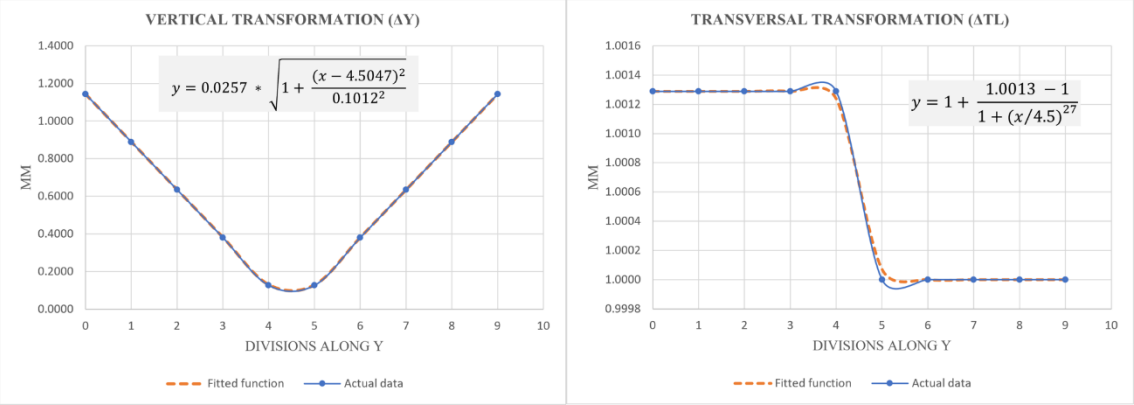

Figure 7. 6: Equations to define tensile deformation in the longitudinal direction.

For these equations and the subsequent equations, the variable x is defined by the number of segments used to divide Outline 00 and Outline 01 in the vertical direction. In other words, x is defined by the number of divisions along y.

Algorithm to define the fracture line

All the tested pieces subjected to longitudinal tension fractured abruptly after reaching their Ultimate Tensile Strength. A closer look at the specimens reveals that the fracture geometry can be anticipated by analysing the geometric configuration of bamboo fibres before loading the pieces. The results of Chapter 4 – section 4.1 - suggest that fracture can be predicted if the following patterns are acknowledged:

Pattern 1: Fracture always starts at the edges of the tested pieces. If the pieces do not have nodes, the fracture will start – simultaneously - at the edges placed along the section of the specimen with the minimal cross-section (Figure 7.7-**a**). If, however, the pieces have nodes, the fracture will start in the edge closest to the irregular distribution of fibres (Figure 7.7-**b**). In all cases, fracture always begins at the weakest region near the central axis – where the forces pulling the object apart are higher.

Pattern 2: Fracture always follows the path of least resistance. This means that fracture usually follows the parenchyma regions between bamboo fibres (Figure 7.7-**c**). For this reason, the final geometry of the fracture will depend on the arrangement and percentage of bamboo's fibres.

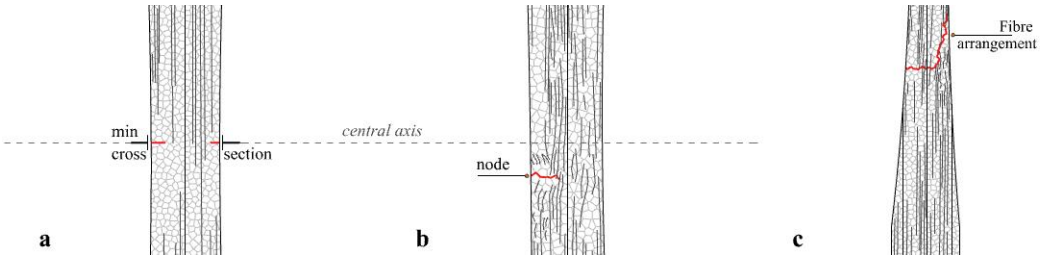

Figure 7. 7: Fracture geometry of specimens under longitudinal tension.

Based on these assumptions, the following method was developed to predict the fracture geometry of pieces under longitudinal tension. The process is described as follow:

Step 1 – The original image of the unloaded specimen is used as the basis to predict fracture. The original image is first converted to grayscale; then, the exposure is adjusted. Finally, brightness levels are modified. The result is an image where the irregularities of the tested piece and the arrangement of the bamboo fibres are highlighted (Figure 7.8-**a**).

Step 2: Then, a set of points are defined in the image. The points are placed with the following criteria in mind: if there is a node, a point is placed in the part of the node closer to the edge and at the end of the node (Figure 7.8-**b**). Subsequently, points are placed in-between bamboo fibres. Specifically in the regions where no fibres and no irregularities are found, i.e., the brighter areas of the picture (Figure 7.8-**c**). An outline is created containing the points described above to define the fracture geometry. Also, the points are randomly numbered (Figure 7.8-**d**).

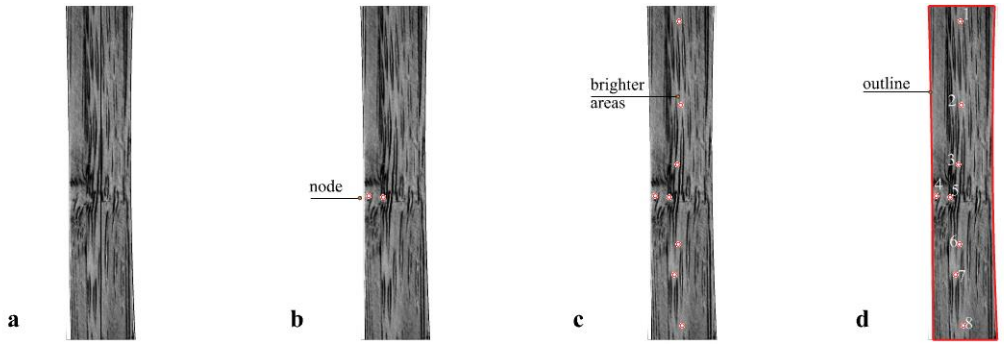

Figure 7. 8: Visual input to define the fracture polyline of samples under longitudinal tension.

Step 3: A tracking algorithm was developed in Grasshopper to define the likely path of the fracture. First, the outline is divided into two sections, and the central axis becomes the reference plane to start tracking the fracture geometry. The algorithm starts by locating the point closest to the edges and closest to the central axis. As seen in the example provided in Figure 7.9-**a**, the point with these characteristics is point number 4. Once a point is found, the algorithm will search for the closest point horizontally. The search angle is set to 30 degrees. A line is created if a point is located (Figure 7.9-**b**). If

not, the algorithm is set to rotate 30 and -30 degrees to search for the second closest point (Figure 7.9-**c**). The algorithm runs until the points closest to the upper or lower edges of the outline are found (Figure 7.9-**d**). Alternatively, the algorithm stops if the tracked points converge in the same coordinates. The resulting algorithm is a polyline representing the predicted fracture geometry (Figure 7.9-**e**). If no points are located, it is assumed that the geometry of the fracture line will be a horizontal line crossing the specimen across the section with the minimum cross-section.

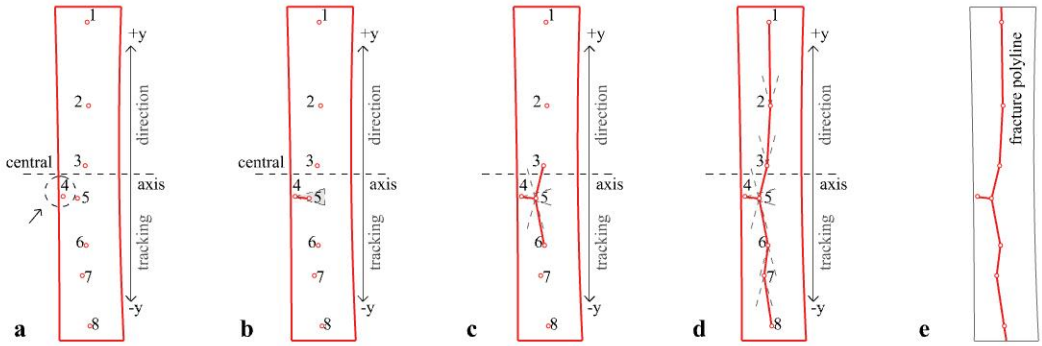

Figure 7. 9: Algorithm to define the fracture polyline of specimens under longitudinal tension.

Step 4: The polyline defined in the previous step is used to visualise the fracture of the specimen following the steps outlined in section 7.1.2 – Step 3.

7.2.2 Radial direction

Δy and ΔTl

Δy and ΔTl were calculated by measuring the proportions of the vector fields of specimen TL-12. This is the specimen that exhibited a higher tensile strength, and it is assumed better to represent the mechanical behaviour of the bulk material.

Figure 7.10-**left** shows the data plot used to calculate the vertical transformation (**Δy**). The equation of the fitted function is shown below:

$$y = 0.0164 * \sqrt{1 + \frac{(x-4.5004)^2}{0.1735^2}} - 0.0020$$

Figure 7.10-**right** shows the data plot used to adjust the length of horizontal lines (**ΔTl**). The equation of the fitted function is shown below:

$$y = 1 + \frac{1.0037\ -1}{1 + (x/4.5)^{27}}$$

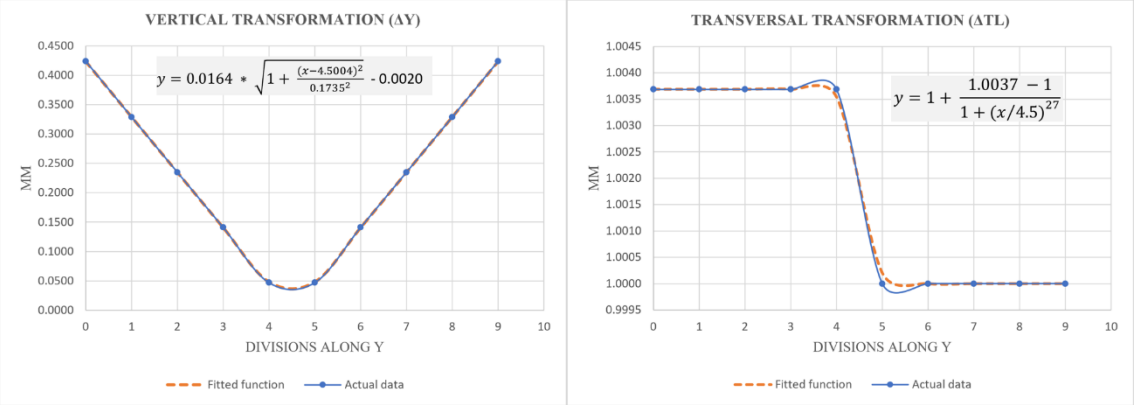

Figure 7. 10: Equations to define tensile deformation in the radial direction.

Algorithm to define the fracture line

The pieces under tangential loading underwent brittle fracture after reaching their Ultimate Tensile Strengths. The fracture geometry can be determined if the distribution of bamboo fibres and their geometric arrangement is identified. The results of Chapter 4 – section 4.2 – suggest that the fracture geometry can be predicted if the following patterns are considered:

Pattern 1: Fracture always starts in the area – within the test region – with fewer fibres (Figure 7.11-**a**). Also, fracture always begins at the lateral edges of the tested pieces (Figure 7.11-**b**).

Pattern 2: After the onset of fracture, both cracks travel towards the central axis of the specimen. The final geometry of the fracture is given by the horizontal arrangement of the fibres located near the region where the fracture started (Figure 7.11-**c**).

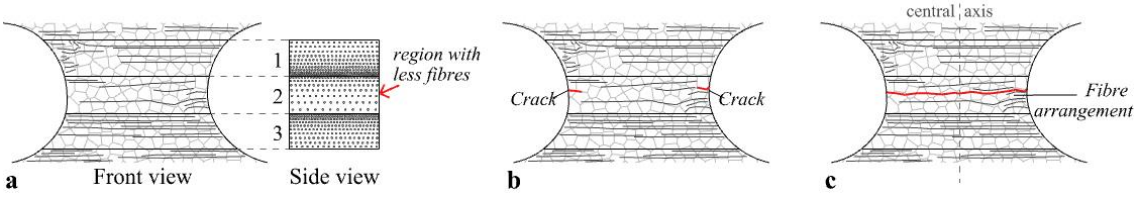

Figure 7. 11: Fracture geometry of specimens under radial tension.

Based on the patterns described above, the following procedure was developed to define the final fracture geometry of laminated bamboo subjected to radial tension:

Step 1: The front and lateral images of the tested piece – before loading – are processed. The objective of this is to highlight the areas of the strips with fewer fibres and identify the fibres' arrangement in the front view. All the images are first converted to grayscale. Then, the exposure and brightness levels are adjusted.

Step 2: After the images have been adjusted, a series of bamboo characteristics are identified. First, the sections of the strips with fewer fibres are determined using the lateral images as reference. These will be the brighter areas of the image. Then, a series of points are placed in the image of the front side. The points should be placed in the regions between the fibres located within the strip zone with fewer fibres. Figure 7.12 provides an example of the characteristics that should be acknowledged as a visual input to predict fracture geometry.

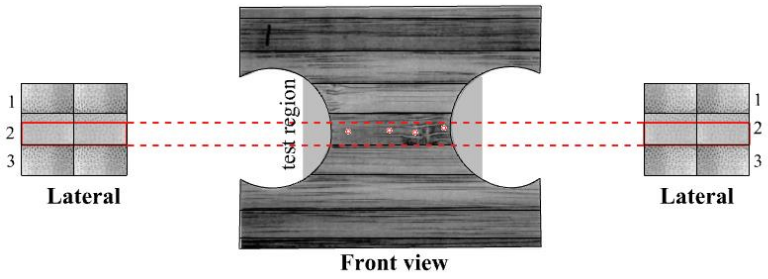

Figure 7. 12: Visual input to define the fracture polyline of specimens under radial tension.

Step 3: Once the above characteristics have been identified, an algorithm was developed to track the path of the fracture. First, the outline of the front view is created, and the points within the outline are randomly numbered. Then, the centroids of the regions with fewer fibres are identified (Figure 7.13-**a**). Then, a line is created from the centroids towards the edges of the outline that describes the tested piece. The outer points of the line are then retrieved (Figure 7.13-**b**). The points located in the outline will be the start points of the tracking algorithm. The algorithm will identify the closest point with a 30 degrees angle. The algorithm is set to look only for points located horizontally. The tracking angle is not set to rotate since the results of the experiments suggest that the fracture geometry is primarily horizontal. As shown in Figure 7.13-**c**, a line is created if a point is found. The algorithm continues until the opposing tracking algorithms converge at the same coordinate (Figure 7.13-**d**). The line created by the algorithm represents the fracture polyline. Finally, the polyline is used as the attractor point curve. As described

in section 7.1.2 - step 3, the fracture line will morph the size of the polygons representing the solid state of the deformed pieces.

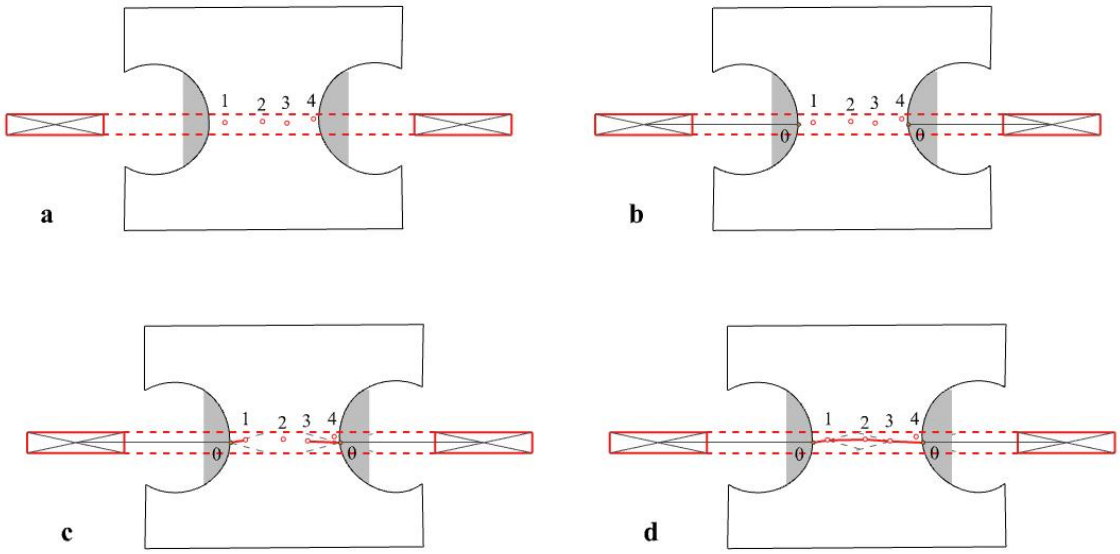

Figure 7. 13: Algorithm to define the fracture polyline of specimens under radial tension.

7.2.3 Tangential direction

Δy and ΔTl

Specimen TT-01 was used to calculate the equations Δy and ΔTl. Specimen TT-01 had a tensile strength higher than the average value. Also, the specimen had an even distribution of fibres and parenchyma cells, which is assumed to provide a better representation of laminated bamboo under tangential tension.

Figure 7.14-**left** shows the data plot used to calculate the vertical transformation (**Δy**). The equation of the fitted function is shown below:

$$y = 0.0099 * \sqrt{1 + \frac{(x-4.5002)^2}{0.2368^2}} - 0.0020$$

Figure 7.14-**right** shows the data plot used to adjust the length of horizontal lines (**ΔTl**). The equation of the fitted function is shown below:

$$y = 1 + \frac{1.0022 - 1}{1 + (x/4.5)^{27}}$$

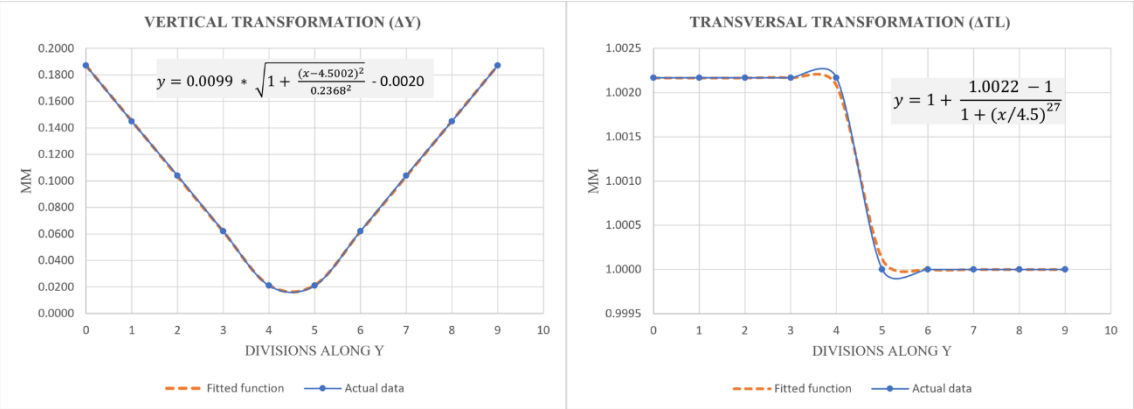

Figure 7. 14: Equation to define tensile deformation in the tangential direction.

Algorithm to define the fracture line

The pieces under tangential tension underwent rapid and abrupt brittle failure after reaching their ultimate strength. The features of bamboo that determined their fracture geometry were the density of fibres, the horizontal arrangement of fibres, and the location of nodes. Based on the results outlined in Chapter 4 – section 4.3 – the following patterns can be used to predict the fracture geometry of pieces under tangential tension:

Pattern 1: Fracture always starts in the weakest zone of the specimen. Since bamboo fibres are evenly distributed along the tangential direction, the weakest region is usually in the area of the piece with a reduced section. However, the weakest part will be located near the nodes if there are nodes.

Patterns 2: Fracture always starts at the lateral edges of the specimen. If there are no nodes, a set of cracks will develop at the edges located in the reduced section of the piece (Figure 7.15-**a**). However, if there are nodes, cracks will develop at the lateral edges - specifically, in the areas closest to the node region (Figure 7.15-**b**).

Pattern 3- After the onset of fracture, the lateral cracks travel to the central axis following the horizontal arrangement of fibres (Figure 7.15-**c**).

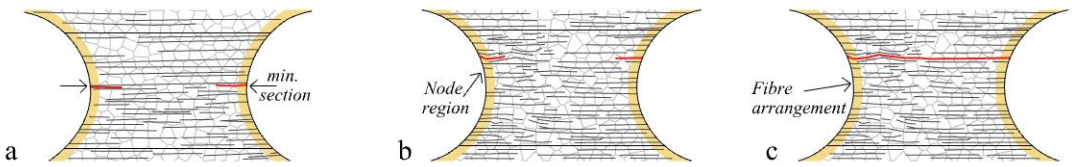

Figure 7. 15: Fracture geometry of specimens under tangential tension.

Based on these patterns, the following workflow was developed to define the geometry of the fracture polyline:

Step 1: The front image of the tested piece is used as the visual input to predict the geometry of the fracture line. The image is processed to highlight the physical features of the piece, such as node regions, fibre arrangement and fibre density. First, the images are converted to grayscale mode. Then, exposure and brightness levels are adjusted.

Step 2: The processed image is used to identify if the tested piece has nodal regions or not. If there are no nodes, no additional steps are needed since fracture is expected to occur in the reduced section of the specimen. However, if a node is identified, a series of points should be placed in the regions with fewer fibres and closer to the nodes. These regions are the brighter regions found in the space between bamboo fibres. Figure 7.16-**a** shows an example of how points are placed in a specimen with nodes.

Step 3: After placing the points, an algorithm was developed to create the final profile of the fracture polyline. The first step is to create an outline to contain the points and represent the geometry of the specimen. Also, the points within the outline are numbered. Then the points closer to the lateral edges are selected as the starting points to track the path of the fracture. As shown in Figure 7.16-**b**, the starting points would be point 1 and point 5. After identifying the starting points, the algorithm will search for the closest points. To do this, the algorithm uses a 30 degrees viewfinder to locate the following points. A line is created if a point is found within the 30 degrees range. The algorithm repeats this step until the search of both extremes converges at the same point (Figure 7.16-**c**). The final step is to use the points to create a polyline and extend it towards the edges (Figure 7.16-**d**). The line created by the algorithm is used to visualise the fracture of specimens under tangential tension. If no nodes are found, the fracture line will be a horizontal line placed at the reduced section of the piece.

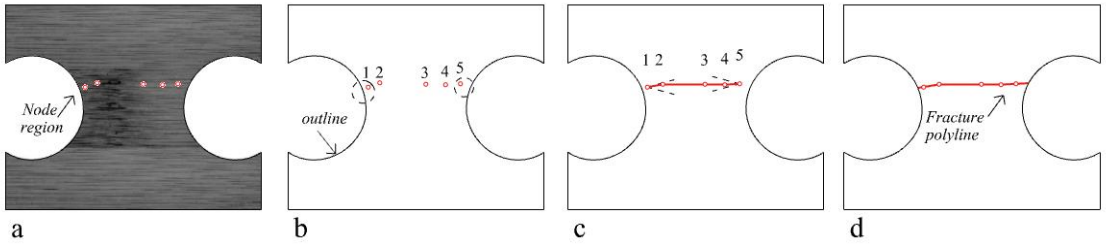

Figure 7. 16: Algorithm to define the fracture polyline of specimens under tangential tension.

7.3 Compressive deformation and failure

7.3.1 Longitudinal direction

Δy and ΔTl

Specimen CL-09 was the sample used to calculate the equations Δy and ΔTl. The piece had a compressive strength higher than the average value of the population. Additionally, the piece had a higher concentration of nodes. Based on the analysis of the sample, nodes provide more reinforcement against the compressive forces in the longitudinal direction. In a real-life scenario, the probability of using pieces with a low percentage of nodes is low. For these reasons, specimen CL-09 was used to obtain the deformation vectors and calculate the equations Δy and ΔTl.

Figure 7.17-**left** shows the data plot used to calculate the vertical transformation (**Δy**). The equation of the fitted function is shown below:

$$y = 0.0008 * \sqrt{1 + \frac{(x-4.5000)^2}{0.0012^2}} - 0.1905$$

Figure 7.17-**right** shows the data plot used to adjust the length of horizontal lines (**ΔTl**). The equation of the fitted function is shown below:

$$y = 1 + \frac{1.0395 - 1}{1 + (x/4.5)^{27}}$$

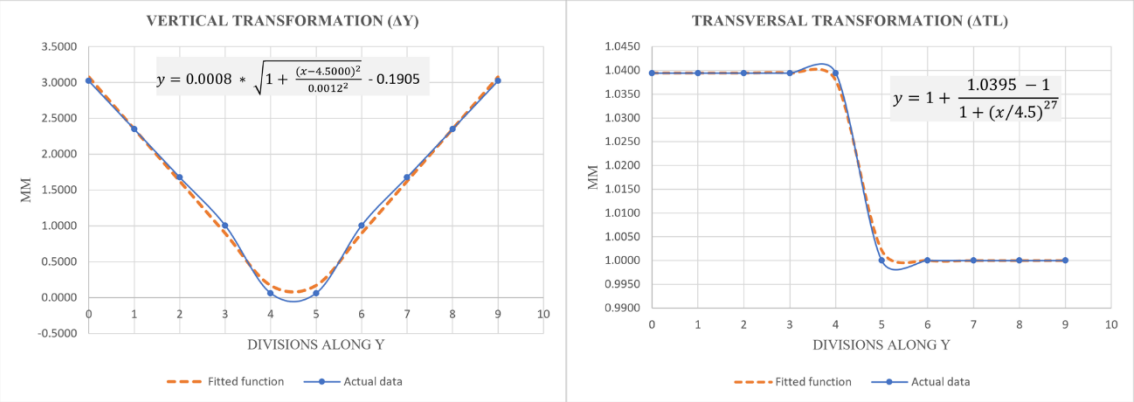

Figure 7. 17: Equations to define compressive deformation in the longitudinal direction.

Algorithm to define the geometry of cracks

The pieces under longitudinal compression had an elastic-plastic behaviour, and cracks only began to appear after the pieces reached their Ultimate Compressive Strength. The location of nodes and the arrangement of fibres near nodes were the main features that influenced the development of cracks in the pieces. Based on the findings of Chapter 5 – section 5.1 – the following patterns can be used to define the geometry of cracks:

Pattern 1: Cracking always developed in the regions with fewer, shorter or no fibres. These regions were located near nodes.

Pattern 2. The geometry of nodes in the radial direction accelerated the deformation of the tested pieces, and initial cracks always developed in the upper corners of the curved profiles of the fibres (Figure 7.18-**a**).

Pattern 3. The geometry of nodes in the tangential direction caused crushing at later stages of the plastic deformation (Figure 7.18-**b**). However, the geometry of crushing is not predicted by the algorithm. Crushing was a fracture mechanism that developed due to excessive buckling and cracking. By the time crushing began, the loading capacity of the tested pieces was already reduced by the appearance of numerous cracks. Hence, the pieces had already failed before crushing began. For this reason, the algorithm outlined below only focuses on determining the geometry and location of cracks.

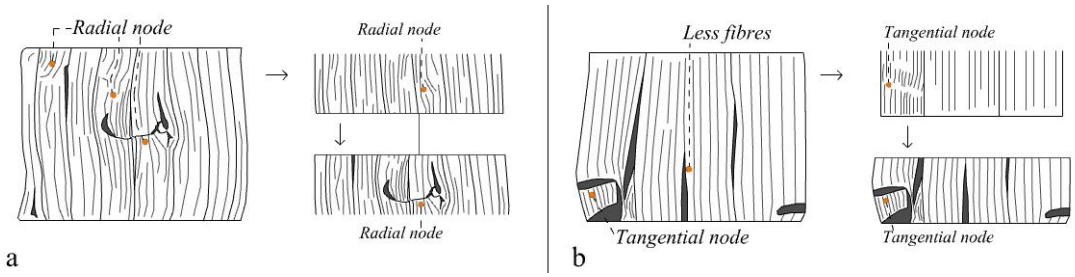

Figure 7. 18: The formation of cracks in the specimens under longitudinal compression.

Based on the patterns described above, the following procedure was developed to predict the location and shape of cracks:

Step 1: The frontal image of the specimen is used as the visual input to identify the regions where cracks are likely to appear. The image is converted to grayscale, and the exposure

and brightness levels are adjusted. Doing this increases the contrast between the regions with fibres and those with fewer fibres.

Step 2: Once the image has been edited, an algorithm was developed to determine the location and geometry of cracks. The first step is to create a polyline outlining the piece's shape (Figure 7.19-**a**). Then, a surface is made using the polyline as a boundary. Then, the surface is divided into equal segments along the x and y directions (Figure 7.19-**b**). After doing this, the centroids of the segments are retrieved (Figure 7.19-**c**). Once the centroids are placed, the following points are identified: points located near the upper corners of the curved fibres around nodes, points located near the centre of nodes, and points located near areas without fibres. Figure 7.19-**d** shows an example of how points are selected. After selecting the points, the centroids of the segments are numbered. Then the numbers that were chosen as areas prone to failure are identified. In the example shown in Figure 7.19-**e**, the selected points were points 8, 23, and 32. After this step, the algorithm shifts the points into their deformed position. The points are moved according to the deformation equations outlined at the beginning of section 7.3.1. The shifted centroids retain the same numbering sequence (Figure 7.19-**f**). In the final step of the algorithm, a set of triangles are placed in the points that were identified before (Figure 7.19-**g**). The size and rotation of the triangles are determined by the size of the strips and the angle of the curved fibres. The triangles represent the location and geometry of cracks (Figure 7.19-**h**). These triangles are used as the attractor point curves to morph the scale of the polygons used to represent the solid-state of the deformed specimen.

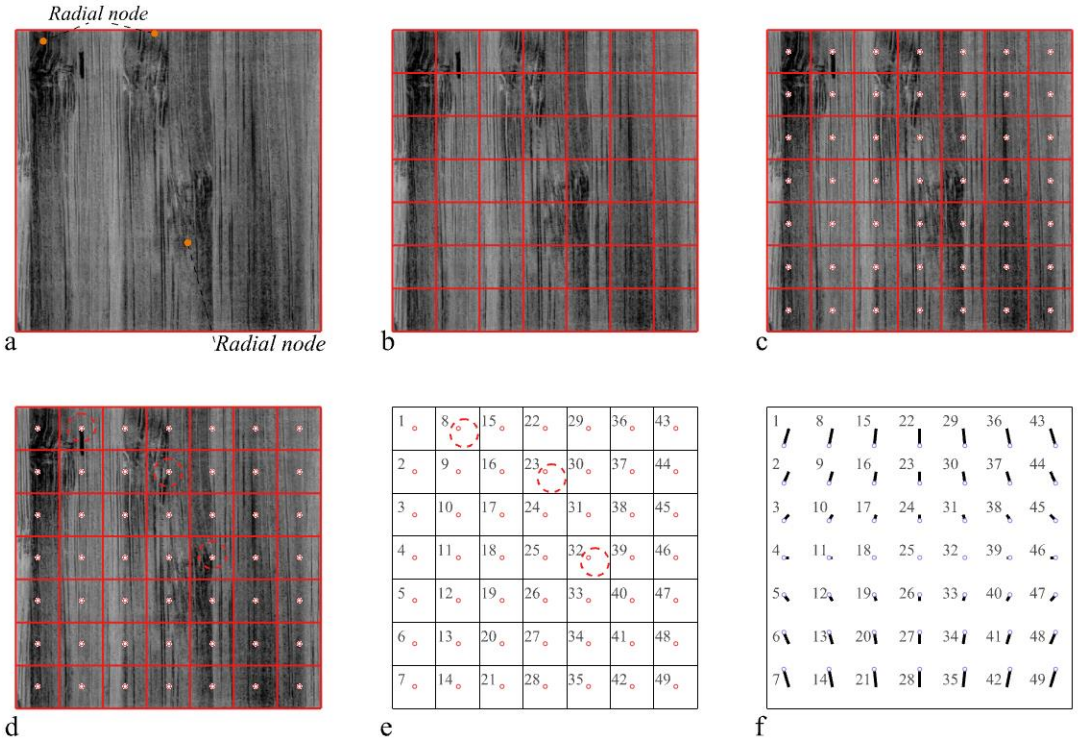

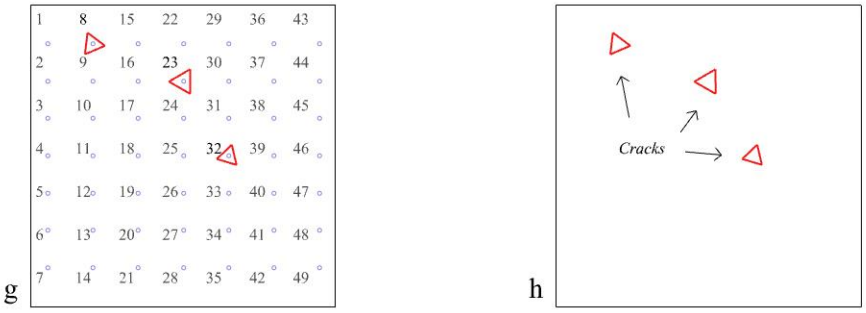

Figure 7. 19: Algorithm to define the geometry of cracks in specimens subjected to longitudinal compression.

7.3.2 Radial direction

Δy and ΔTl

Specimen CR-01 was used to calculate the equations Δy and ΔTl. The specimen had a compressive strength higher than the average compressive strength. This specimen was selected to calculate the deformation vectors of pieces under radial compression because the piece had a high number of nodes. In practice, mid to large-sized pieces are expected to have a considerable number of nodes. Specimen CR-01, hence, better represented the features of the material when used at larger scales.

Figure 7.20-**left** shows the data plot used to calculate the vertical transformation (**Δy**). The equation of the fitted function is shown below:

$$y = 0.0008 * \sqrt{1 + \frac{(x-4.5000)^2}{0.0010^2}} + 0.0002$$

Figure 7.20-**right** shows the data plot used to adjust the length of horizontal lines (**ΔTl**). The equation of the fitted function is shown below:

$$y = 1 + \frac{1.0326 - 1}{1 + (x/4.5)^{27}}$$

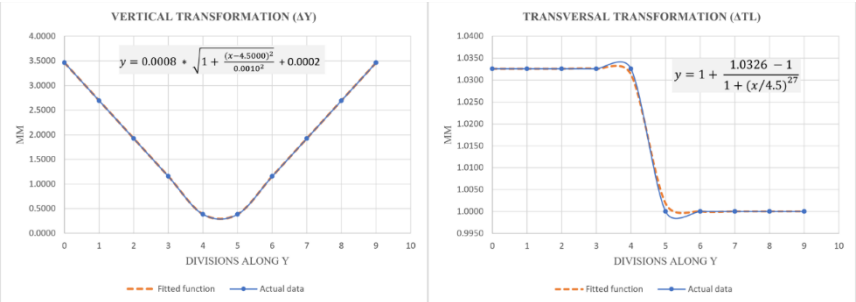

Figure 7. 20: Equations to define compressive deformation in the radial direction.

Algorithm to define the geometry of cracks

The pieces under radial compression exhibited elastic-plastic behaviour, and cracking began after reaching the Ultimate Compressive Strength. The main features that defined the location and geometry of cracks were the strips with irregular fibres, such as a lower density of fibres or irregular distribution of fibres due to nodes. The findings outlined in Chapter 5 – section 5.2 – suggest that the following patterns can be used to determine the parameters defining fracture in pieces under radial compression:

Pattern 1: Cracks always developed at the intersecting point of two strips with irregularities if these were placed diagonally (Figure 7.21-**a**).

Pattern 2: Cracks always developed in the line connecting two irregular strips if these were placed diagonally and one or two strips were placed in-between them (Figure 7.21-**b**).

Pattern 3: Cracks always developed in the centroid of a strip surrounded by 3 or 4 strips with irregularities (Figure 7.21-**c**).

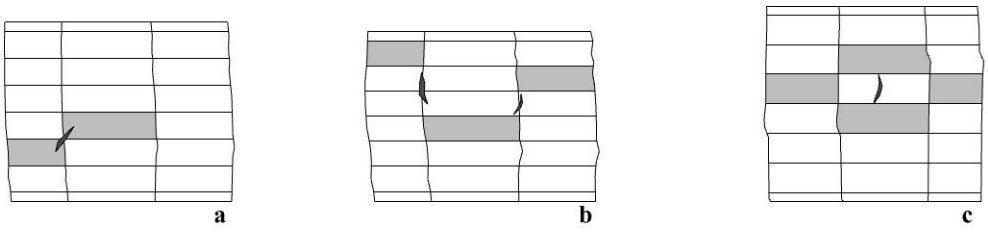

Figure 7. 21: Geometry of cracks in specimens under radial compression.

Based on the previous analysis, it is possible to conclude that the location and geometry of cracks can be determined if strips with irregularities are located. The following procedure was developed to identify the location of fibres with irregularities, as well as create the final geometry of cracks:

Step 1: The front and side pictures of the specimen are used to identify the location of strips with irregularities. The images are converted to grayscale to highlight the distribution of fibres in the piece. Then the exposure and brightness levels are adjusted. The parameters are used to identify the strips with irregularities. First, if nodes are found

in the lateral faces, the strips with the nodes are highlighted in the front view. Second, if strips with fewer fibres are located in the lateral faces, - these are also highlighted in the front view. After processing the images, the strips with fewer fibres are the brighter areas of the picture. Finally, any region with fewer fibres – located in the mid-section of the frontal view – is also highlighted. Figure 7.22 shows how the strips with fewer fibres are identified.

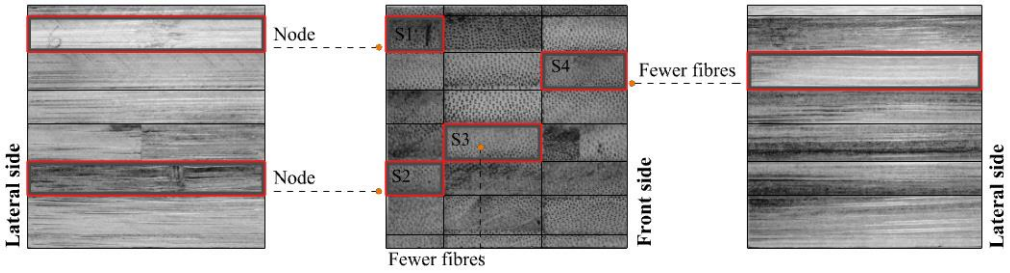

Figure 7. 22: Visual input to define the fracture patterns of specimens under radial compression.

Step 2: Once the strips with fewer fibres have been identified, an algorithm was developed to define the location and geometry of the cracks in the front view. The first step is to create an outline and hatch the areas where the strips with fewer fibres are located (Figure 2.23-**a** and **b**). After doing this, a surface is made using the outline of the specimen as a boundary. Then, the surface is divided into equal segments in the x and y directions. The edges of the segment dividing the surface are superimposed on the areas previously hatched (Figure 2.23-**c**). After this, the segments are numbered, and the segments placed over the areas that represent the strips with irregularities are identified. For example, as shown in Figures 2.23-**d** and **e**, the segments representing the strips with irregularities are segments 1, 8, 30, 37, 44, 18, 25, 5, and 12. After the areas with fewer strips have been approximated, the equations outlined at the beginning of section 7.3.2 are used to subdivide the outline of the morphed specimen. The morphed segments retain the same number sequence as the original segments. As shown in Figure 7.23-**f**, the segments representing the strips with irregularities are also highlighted in the morphed outline. Then, based on the criteria outlined in Step 1, a point or a line are placed in the regions between strips with irregularities. In the example shown in Figure 7.23-**g**, a point is placed at the intersection between irregular strips placed diagonally, and two lines are placed to connect the irregular strips placed above. The final step is to use the point and the mid-point of the lines to generate polygons representing the cracks (Figure 7.23-**h** and **i**). The geometry of the cracks is proportional to the size of bamboo strips. Finally, the polygonal shapes representing the cracks are used to visualise the fracture pattern of pieces under radial compression.

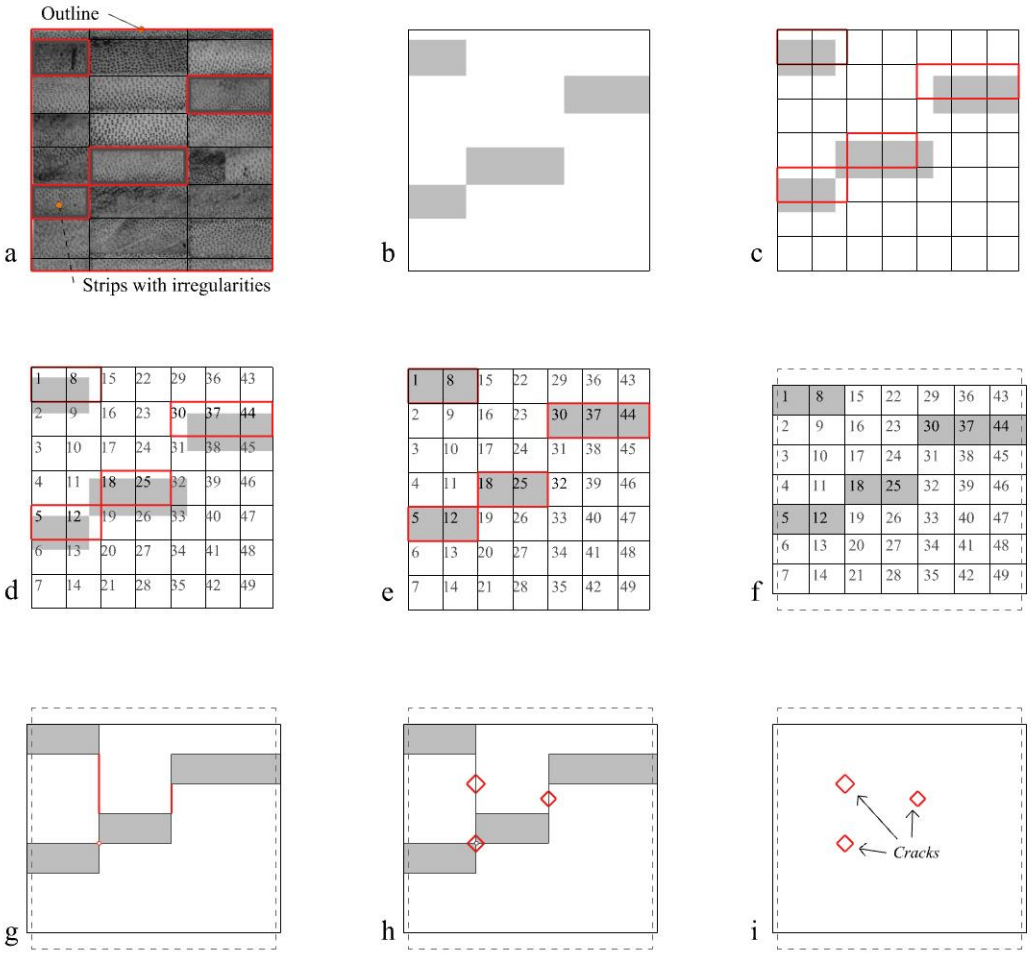

Figure 7. 23: Algorithm to define the geometry of cracks in specimens under radial compression.

7.3.3 Tangential direction

Δy and ΔTl

Specimen CT-06 was used to calculate the equations defining specimens' elastic and plastic deformation under tangential compression - Δy and ΔTl. Contrary to the pieces under longitudinal and radial compression, the results of the experiments suggest that nodes affect the performance of the sample subjected to tangential compression. Specifically, more nodes seem to reduce the material's compressive strength in the tangential direction. In a real-life setting, bamboo laminates will probably have a higher concentration of nodes. Specimen CT-06 was selected to calculate the equations Δy and ΔTl because it had a higher concentration of nodes – which was assumed to represent the behaviour of larger specimens better.

Figure 7.24-**left** shows the data plot used to calculate the vertical transformation (**Δy**). The equation of the fitted function is shown below:

$$y = 0.0002 * \sqrt{1 + \frac{(x-4.5000)^2}{0.0003^2}} + 0.0003$$

Figure 7.24-**right** shows the data plot used to adjust the length of horizontal lines (**ΔTl**). The equation of the fitted function is shown below:

$$y = 1 + \frac{1.0501 - 1}{1 + (x/4.5)^{27}}$$

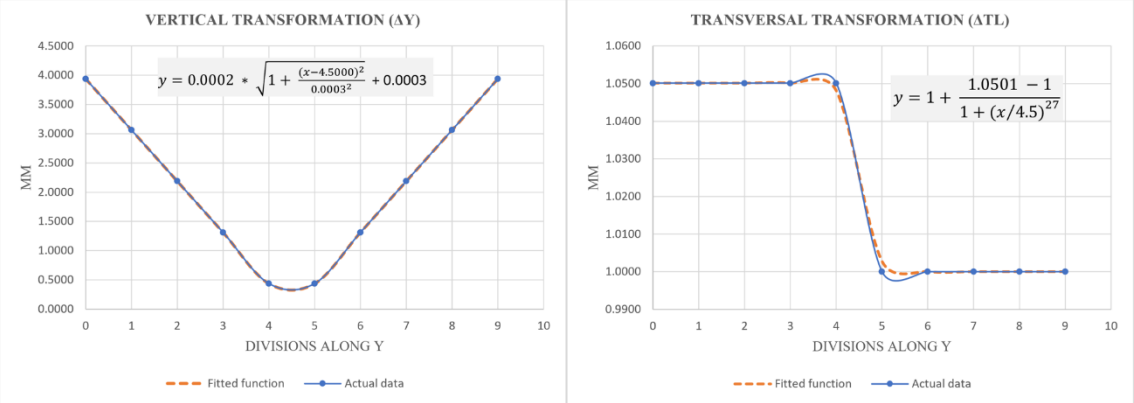

Figure 7. 24: Equations to define compressive deformation in the tangential direction.

Algorithm to define the geometry of cracks

The pieces subjected to tangential compression had an elastic-plastic behaviour, and cracking began after the pieces reached the Ultimate Compressive Strength. The curvilinear and monotonic arrangement of fibres were the main features determining the location of cracks. Bamboo strips are segments of a circle, and the strips are arranged to protect the rounded shape of bamboo culms. Hence, the fibres are densely packed towards the outer layer of the culm. When compressive forces are applied in the tangential direction, the strips tend to bend in the direction of the outer layer. The arrangement and bending directions of the strips will determine the location of cracks. The findings outlined in Chapter 5 – section 5.3 – suggest that the following patterns can be used to predict the location of cracks:

Pattern 1: If two strips are placed diagonally, and one bends to the right and the other to the left, a crack will appear at the point shared by both strips (Figure 7.25-**a**).

Pattern 2: If two strips are placed in front of each other, and one bends to the right and the other to the left, a crack will appear at the edge shared by both strips (Figure 7.25-**b**).

Pattern 3: If two strips are aligned diagonally and both bend in the same direction, a crack will appear in the corner angle formed by both strips (Figure 7.25-**c**).

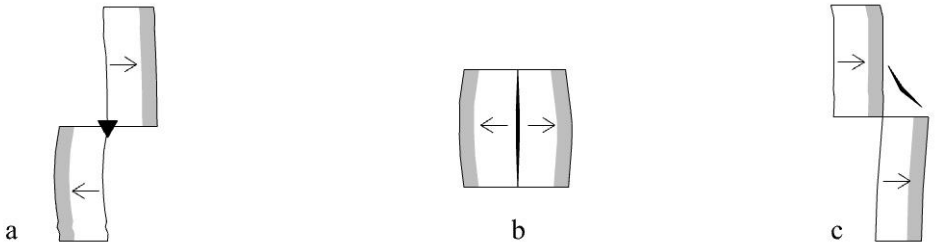

Figure 7. 25: Geometry of cracks in specimens under tangential compression.

Based on the previous patterns, it is possible to conclude that the location and geometry of cracks can be predicted if the bending direction of the strips can be anticipated. As mentioned in Chapter 5 – section 3, the bending direction can be predicted by identifying the areas of the strips with a higher volume of fibres. These areas are the sides of the strip closer to the outer layer. Also, the distribution of fibres – in these areas – is slightly curved. This criterion was used to develop a procedure to predict the location and geometry of cracks when radial compression is applied. The details of the process are outlined below:

Step 1: The frontal image of the specimen is used to identify the bending direction of bamboo strips. The image is edited to highlight the arrangement of bamboo fibres. First, the image is converted to grayscale mode. After this, the exposure and brightness levels are adjusted.

Step 2: After processing the frontal image, the outline of the specimen is created. Next, the areas of the strip with more fibres are highlighted. Figure 7.26 **a** and **b** show an example of how the areas with more fibres are identified. The next step is to determine if any of the following arrangements are found: two strips placed diagonally with opposite bending directions, two strips placed in front of each other with opposite bending directions or two steps placed diagonally and bending in the same direction. If any of these characteristics are found, a hatch is used to map the location of the arrangement (Figure 7.26-**c**). Then, a surface is created using the outline of the specimen as a boundary. The surface is subdivided into equal segments along the x and y directions. Every segment

is numbered. The edges of the segments are superimposed on the hatch area (Figure 7.26-**d**). Then, the location of the hatches is approximated using the segments of the surface, as shown in Figure 7.26-**e**. Before defining the final geometry, it is essential to consider that the hatches' segments will change shape, size, and location when the load is applied. Hence, the original segments are morphed into their deformed position using the equations Δy and ΔTl (Figure 7.26-**f**). After the segments are morphed, a point or line are placed following the previously outlined patterns. In the example shown in Figure 7.26-**g**, a point is placed at the intersection of the strips arranged diagonally. It is at this point that a crack is likely to appear. The crack is represented by a polygon proportional to the size of the strips (Figure 7.26 **h** and **i**).

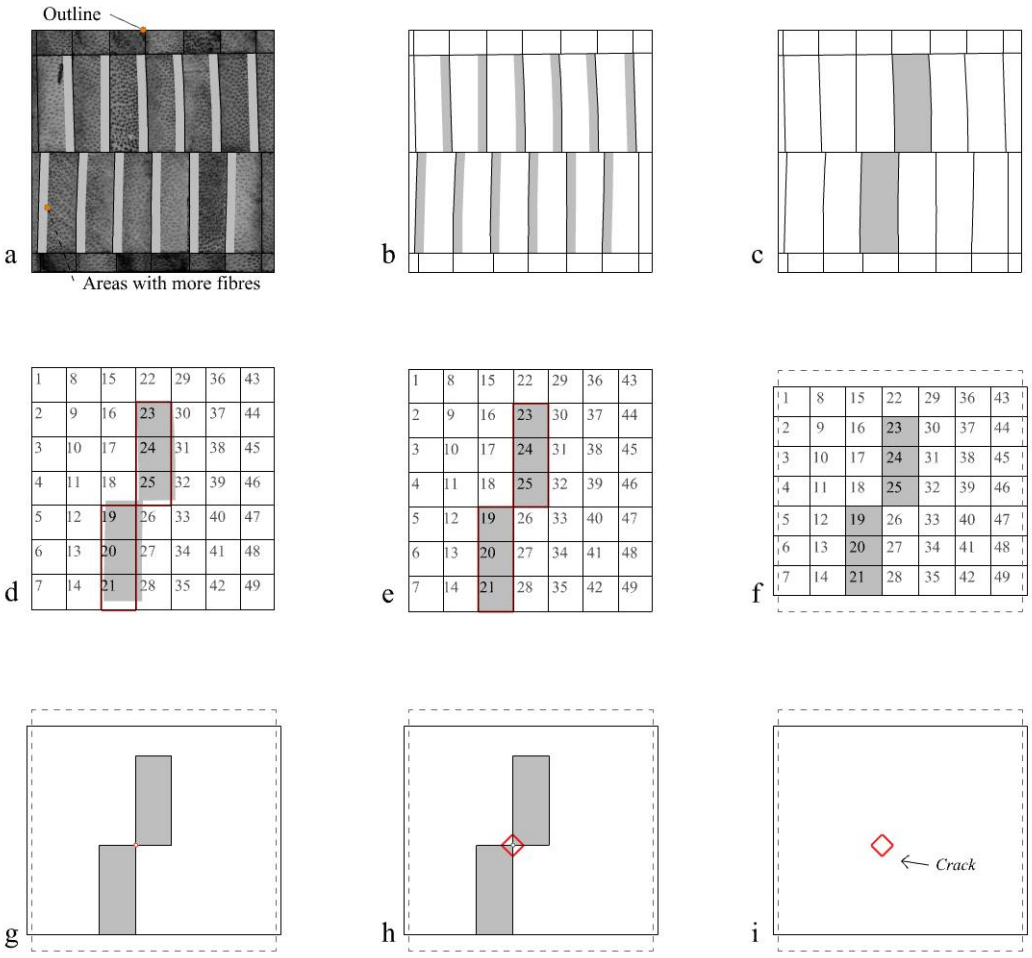

Figure 7. 26: Algorithm to define the geometry of cracks in specimens under tangential compression.

7.4 Shear deformation and failure

7.4.1 Longitudinal direction

Vertical displacement

The process outlined - in section 7.1.1 - to calculate the equations Δy and ΔTl - are not applicable to describe the deformation of specimens subjected to shear forces. The pieces do not elongate or crush when submitted to shear forces. Instead, two sections of the pieces slide in opposite directions, as shown in Figure 7.27-**a**. For this reason, the deformation of specimens under shear was calculated by determining the vertical displacement of the sliding parts. To achieve this, the displacement, and the length of the sliding portion of the specimens were measured. Then, a displacement ratio was calculated by dividing the recorded displacement between the length of the sliding part of the specimen (Figure 7.27-**b**). The displacement ratio or Δy of the samples subjected to longitudinal shear is 0.10871.

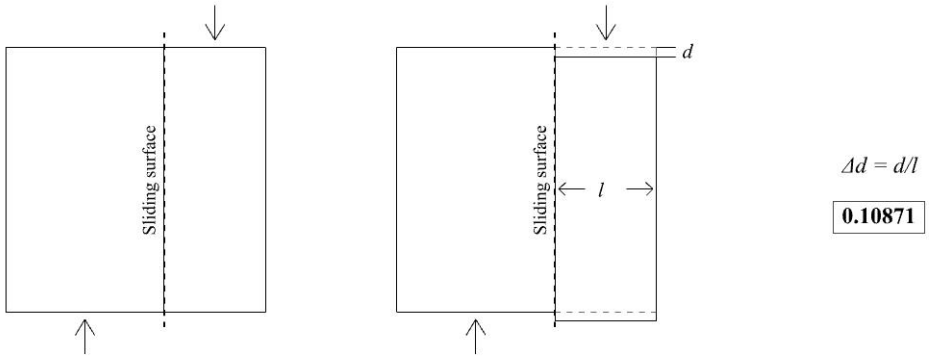

Figure 7. 27: The displacement ratio of pieces under longitudinal shear.

Algorithm to define the fracture line

The pieces under longitudinal shear exhibited an elastic-plastic behaviour with brittle failure. All pieces failed right after reaching the Ultimate Tensile Strength. The areas with fewer fibres and the linear arrangement of fibres are the features that determined the final fracture geometry of the specimens. The results of Chapter 6 – section 6.1 – suggest that the following patterns can be used to predict the shape and location of the fracture in pieces under longitudinal shear:

Pattern 1: Fracture always started in the regions with fewer fibres and closest to the edge where the load is applied.

Pattern 2: After the onset of fracture, the crack always travelled following the geometry of the fibres close to the area where the fracture began.

Based on these patterns, the following procedure was outlined to predict the location and shape of fracture produced by the application of longitudinal shear forces:

Step 1: The frontal image of the specimens is used to identify the regions with fewer fibres and the areas located in-between fibres. To highlight the physical features of the strips, the image of the specimen is converted to grayscale. Also, the exposure and brightness levels are adjusted. The first point should be located in the region closest to the edge where the load is applied. Also, it needs to be placed close to the axis crossing the sliding surface. The following points should be placed in the brighter areas between fibres. Figure 7.28 **a** and **b** show an example of identifying the areas prone to failure.

Step 2: After step 1 is completed, an outline is made to represent the specimen's shape and contain the points selected in step 1. Then, the points ate numbered. An algorithm was developed to track the likely path of the fracture. The point closest to the edge where the load is applied is the starting point of the tracking algorithm. Once the starting point has been defined, the algorithm will track the closest point vertically. The angle of search is 30 degrees. If a point is found, a line is created. The algorithm continues until reaching the opposite end of the outline (Figure 7.28-**c**). A polyline is set to cross all points selected by the algorithm. After the polyline is created, the extremes of the line are extended to the edges of the outline. The extended polyline is the predicted geometry of the fracture line (Figure 7.28-**d**).

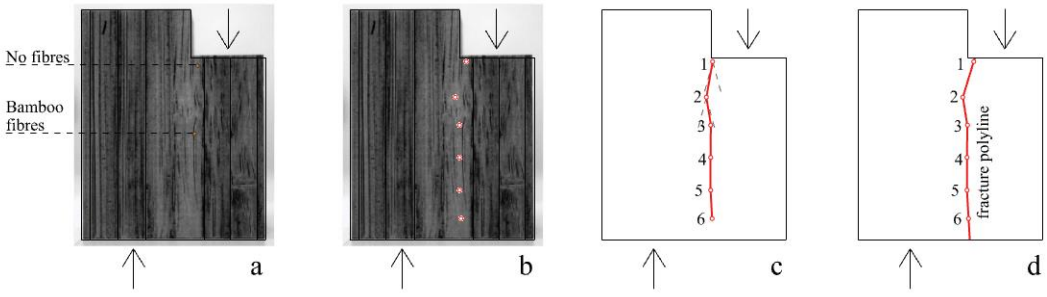

Figure 7. 28: Algorithm to define the fracture polyline of specimens under longitudinal shear.

7.4.2 Radial direction

Vertical displacement

The pieces subjected to radial shear formed shear bands as the mid-section of the piece slid downward. The shear bands were developed by the bending of fibres and the crushing of parenchyma cells. The shear bands had a bow-tie shape (Figure 7.29-**a**). However, for

predicting the failure of the material under shear loading, the main factor to consider is the displacement ratio of the pieces. To calculate the displacement ratio, the length of the midsection and its displacement along the vertical axis were measured. Then, the measured displacement was divided between the size of the midsection (Figure 7.29-**a**). The displacement ratio of the pieces under radial shear was 0.28377. This value can be used to approximate the deformation of pieces subjected to radial shear.

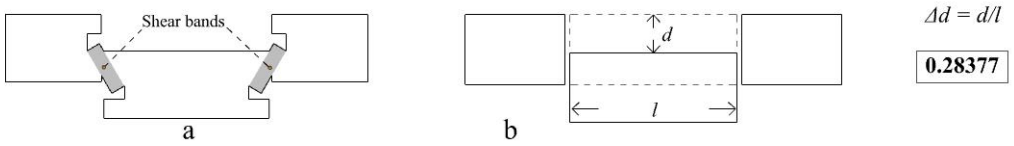

Figure 7. 29: The displacement ratio of specimens under radial shear.

The pieces underwent a high degree of deformation by the time they reached the Ultimate Shear Strength. Fracture did happen at later stages of the loading process. However, by the time that fracture happened the pieces had already failed due to excessive deformation. For this reason, predicting the fracture geometry of the pieces under radial shear is not considered essential to determine the moment at which the pieces failed.

7.4.3 Tangential direction

Vertical displacement

The pieces under tangential shear failed due to the elongation of the fibres. The highly reinforced pieces pushed the upper side of the grip as the lateral sides rotated (Figure 7.30-**a**). For this reason, the fibres elongated. However, ideally, the rotation of the pieces should have been avoided. Even though the experiment set-up forced the rotation of the pieces, the results of the experiments can be used to calculate the displacement ratio of the pieces under tangential shear. The average displacement ratio of the pieces was 0.19846 (Figure 7.30-**b**). This value can be used to approximate the behaviour of pieces submitted to tangential shear.

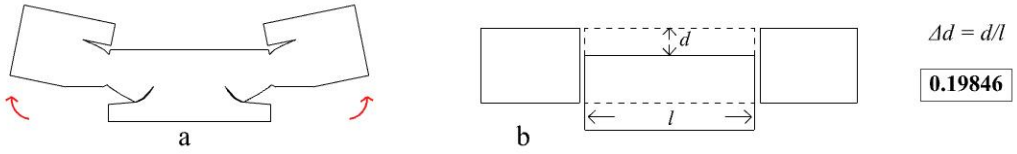

Figure 7. 30: The displacement ratio of pieces under tangential shear.

A procedure to predict the fracture geometry of pieces under tangential shear was not developed because the pieces failed long before the fracture happened. Excessive plastic deformation was the primary reason why the pieces failed.

7.5 Validation and applicability

7.5.1 Workflow

The algorithms described in the previous sections were developed in a geometric generative software called Grasshopper. The workflow to predict specimens' deformation and fracture geometry under axial loading has three components. In the first instance, a series of parameters need to be manually provided. These are the inputs to run the algorithms. Secondly, the inputs activate a series of algorithms developed in Grasshopper. Finally, an output is generated. The output is the geometric representation of the deformation of the specimen and the fracture geometry. In other words, the output is the visualisation of the vertical and horizontal transformation of the piece and the visualisation of the location and geometry of the fracture. The parameters of the three components are outlined below:

Component 1 – Manual input – First, four elements must be manually provided. The first element is a processed picture of the specimen before loading. The image needs to be edited to highlight the physical characteristics of bamboo strips. The second component is a series of points, lines, or polygons representing the areas prone to fail. The criteria to select these areas were outlined in sections 7.2, 7.3, and 7.4. Third, the number of x and y divisions to divide the surface representing the undeformed specimen's geometry need to be specified. Finally, the type of loading needs to be selected. The manual inputs are outlined in Figure 7.31-**Input**.

Component 2 – The deformation and fracture algorithms – Based on the inputs outlined before, a series of algorithms run in Grasshopper to compute the deformation and fracture geometry of the samples. Two processes run simultaneously to provide the geometric representation of the fractured piece. Figure 7.31-**Algorithm** illustrates the processes:

The ***first process*** defines the deformed state of the specimen. Five steps are followed to achieve this. In Step 1, the outline of the piece is determined. In Step 2, the shape of the specimen is divided into equal segments. In Step 3, the centroids of the segments are retrieved. In Step 4, equations Δy, ΔTl or Δd are used to move the centroids to the deformed state of the specimen. Finally, in Step 5, a series of polygons are placed in the deformed centroids to represent the solid-state of the piece.

The ***second process*** defines the location and geometry of fracture lines or cracks – depending on the type of loading and the direction of bamboo fibres. Five steps are followed to achieve this. In Step 1, the outline of the piece is defined to contain the geometric representations of areas prone to fail. These are the points, polygons or lines that were input manually to highlight the areas of the strips likely to fail first. In step 2, the outline of the piece is divided into equal segments. Then the segments are numbered, and the segments closest to the areas that have been selected as areas prone to failure are identified. In Step 3, the segments are used to approximate the location of regions prone to fail. In Step 4, the equations Δy, ΔTl or Δd are used to morph the segments into the deformed state of the specimen. Finally, the geometry and location of fractures or cracks are determined – in the deformed segments – by following the criteria outlined in sections 7.2, 7.3 and 7.4.

Component 3: The method's output is a geometric representation of the deformed and fractured specimen. The geometries determined in Steps 5 - of both processes - are superimposed to achieve the final geometric representation. Then, the fracture or crack geometries act as attractor point curves to change the scale of the polygons representing the deformed state of the specimen. The result of this process is shown in Figure 7.31-**Output**.

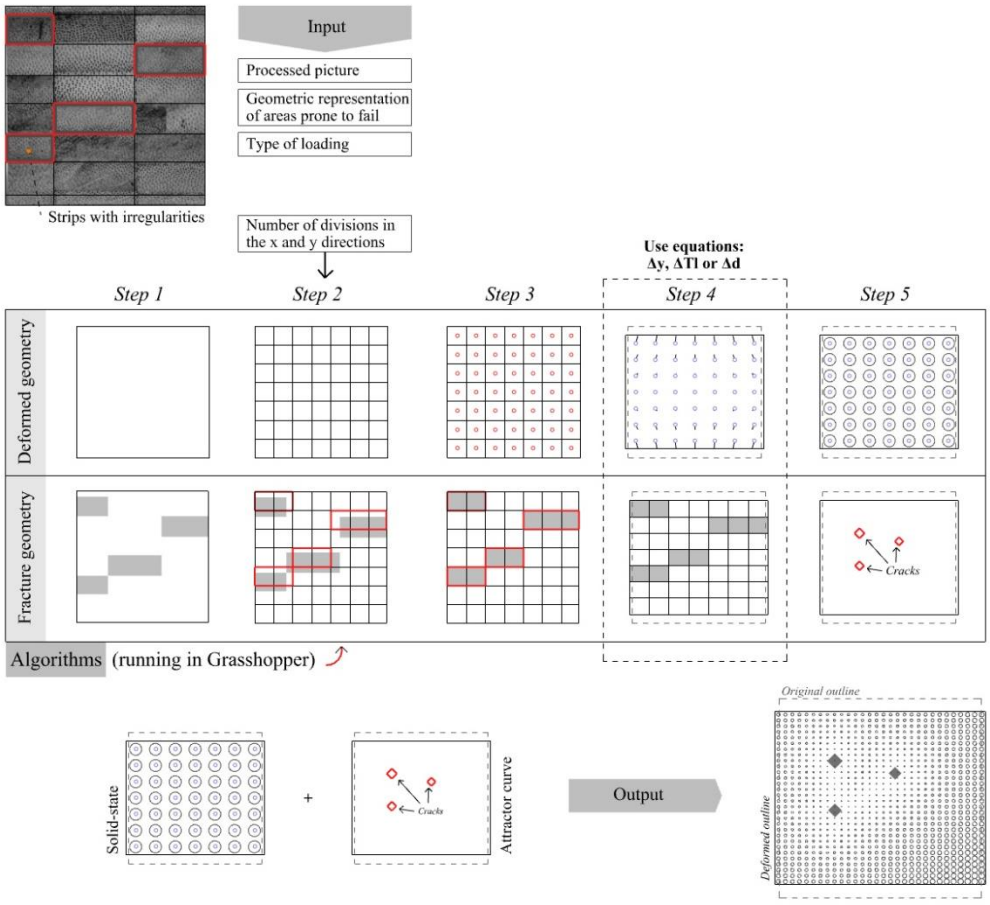

Figure 7. 31: Workflow to predict deformed state and fracture geometry.

7.5.2 Method results vs experiment results

The method was developed to predict specimens' deformation and fracture geometry under axial loading. The results of the experiments suggest that all the pieces began to fracture after reaching their Ultimate Tensile Strength. The fracture of pieces under longitudinal tension, radial tension, tangential tension, and longitudinal shear were defined with a fracture polyline. The pieces under compressive load did not have a single fracture line. Instead, a series of cracks appeared on the surface of the piece. The method also defined the location and geometry of cracks due to compressive loads. Finally, the pieces under radial and tangential shear fractured at later stages of the deformation process. By the time fracture began, the specimens had already failed due to excessive deformation. For these specimens, a fracture geometry was not defined. Instead, the displacement ratio of the pieces was used to determine the change in the shape of the specimens.

Overall, the method successfully provides a geometric representation of the deformed and fractured states of pieces subjected to uniaxial loads. As shown in Figure 7.32, the process effectively matches the deformed and fracture conditions of pieces under (**a**) axial tension and (**b**) compression. Finally, the method is also successful at approximating the deformation of pieces under radial and tangential shear (**c**).

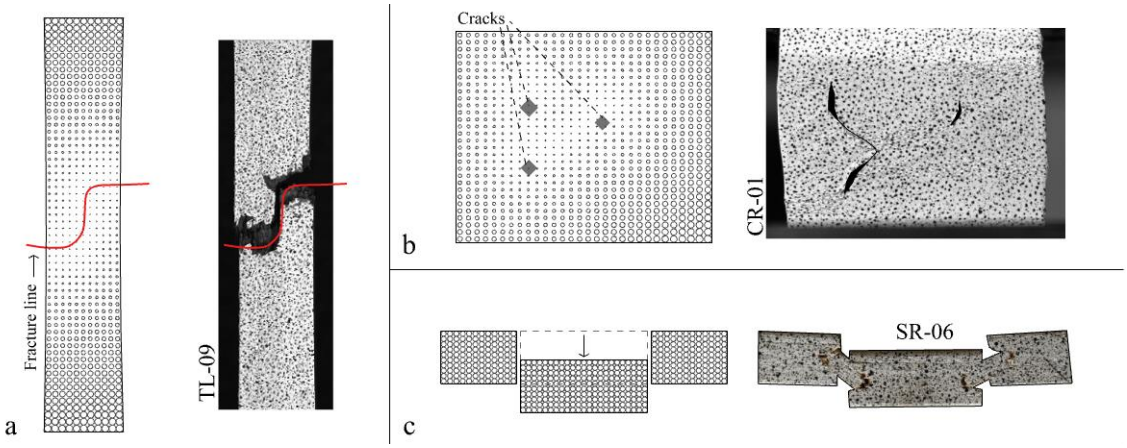

Figure 7. 32: Method vs experiments' results.

7.5.3 Limitations and applicability

The developed method provides a rapid assessment of the deformation and potential fracture of pieces submitted to tensile, compressive and shear forces by using the physical characteristics of bamboo strips as the primary input to predict the material's response. In

simple terms, the method synthesises a set of fracture patterns mapped in the three directions of the material, i.e., the longitudinal, radial, and tangential directions. Currently, the method relies on implementing guidelines – outlined in sections 7.2, 7,3, and 7.4 to select areas prone to fail using processed pictures as the templates to predict the behaviour of the material. One of the main limitations of the method is the fact that the identification of areas prone to fail is made manually. As specified in section 7.5.1, the user needs to select the specimen areas likely to fail by following a set of given criteria. In future stages, the method can be optimised by fully automating the process of identifying and selecting the areas prone to fail. Another limitation of the current approach is the fact that the efficacy of the method was not tested in larger specimens. It is possible that minor changes need to be added to account for fracture development in large scale objects. Finally, it is essential to acknowledge that the present method is only applicable for specimens subjected to uniaxial loading. In real-life settings, structures can be submitted to multiaxial loads, and different forces can act on a single structural member. Even though the current methodology cannot be applied in those cases, the procedure followed to map out the fracture patterns of uniaxially loaded bamboo laminates can also be used to map out the patterns of multiaxially loaded laminates.

To discuss the applicability of the proposed method, it is essential to highlight what the method does not do. The current procedure does not calculate the force the pieces can withstand, nor can it be used to map out the evolution of damage at a microscopic scale. Instead, the method provides a quick way of predicting the location and geometry of fracture. It does so by identifying the physical features of bamboo strips likely to influence the response and failure of the material. As seen in Figure 7.33-**a**, a simple picture of an existing structural member can be used as the primary input to predict the member's failure. Then, the characteristics of the structural member are dissected into different components. Each component represents a physical feature of the material. In the example provided in Figure 7.33-**b**, the strips with a lower concentration of fibres or with nodes have been identified as the components expected to accelerate the deformation of the structural member. The results of Chapters 4, 5, and 6 provided the basis to determine how the physical features of laminated bamboo affect the mechanical behaviour of the material. These were the guidelines used to select the laminate features likely to determine the failure modes of the material. In the example shown in Figure 7.33-**c**, failure is expected to develop in the regions located between the fibres with fewer fibres and nodes. The detection of areas prone to fail as the load increases can guide the design of strategies to reinforce and preserve the structural life of structural elements made with laminated bamboo.

As a rapid assessment tool, the method can be successfully used to quickly evaluate the likely fracture of a structural member and design strategies to reinforce and preserve its

structural life. Also, the method can be rapidly used to scan the conditions of existing structural members and prevent catastrophic failure. These preservation measures are valuable to regulate the use of a natural-based material such as laminated bamboo. Another advantage of the presented method is that the only input needed is a material picture. Overall, developing strategies to predict the mechanical behaviour and failure of laminated bamboo is a valuable contribution that can help validate the use of the material as a safe structural material. The main contribution of the research is that the method would only require the identification of the physical characteristics of the laminate as the primary input to predict failure, making the method accessible and convenient for a wide range of professionals.

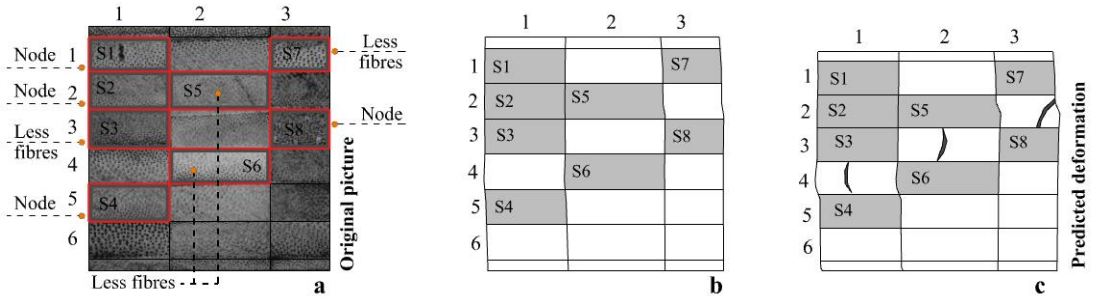

Figure 7. 33: Proposed method to predict failure.

Chapter 8 | Conclusions

| Determining how one can use bamboo strips' physical characteristics to predict the material's deformation and failure was the research question behind the present study. This chapter ponders to what extent the developed methodology answered the research question. Sections 8.1.1, 8.1.2, and 8.1.3 summarise how bamboo's physical features affect the mechanical response of laminated bamboo. The material's response under tensile, compressive, and shear loads was described. On the other hand, section 8.1.4 summarises how the physical characteristics of bamboo can be used as generative parameters to predict the material's de deformation and failure modes. The section discusses the development of geometric models and algorithms used to predict laminated bamboo composites' deformation and fracture geometries. Section 8.2 highlights the key findings of the research and addresses the literature gaps identified in Chapter 2. Section 8.3 discusses how the current research can be expanded to acknowledge the material's behaviour in three dimensions and how machine learning techniques can automate the process of predicting the material's behaviour. Lastly, section 8.4 provides a final reflection on the work done and its potential applications in the Architecture, Engineering and Construction industries. |

8.1 Summary of results

8.1.1 Tensile deformation and failure modes

This study suggests that fibre orientation and fibre density were the features that influenced the strength properties of laminated bamboo when tensile loads were applied. The orientation of bamboo fibres is essential to understand why the strength values of pieces under longitudinal tension were higher than the strength values of pieces under radial and tangential tension. When loads are applied in the longitudinal direction, the forces act in the direction of the fibres. Hence, the force is trying to pull the fibres apart. The fibres are the strongest components of the bamboo strips. However, when loads are applied in the radial and tangential directions, there are no longitudinal fibres resisting the pull of the forces. The lack of longitudinal fibres made the pieces break easily by de-bonding the interface of parenchyma cells, which are the weakest components of bamboo strips. Since bamboo fibres are the strongest elements of bamboo strips, it is reasonable

to expect that the pieces with a higher density of fibres are likely to perform better than those with fewer fibres. In all the experiments carried out, the pieces with more fibres were those with higher tensile strength.

The monotonic distribution of fibres, the presence of nodes and the arrangement of bamboo strips determined the deformation and fracture patterns of pieces under tensile loading. The fibres along the radial direction are not evenly distributed. Instead, they become smaller and denser towards the outer layer of the strip. This arrangement is monotonic since fibres' density only increases towards the outer layer. The monotonic structure of fibres influenced the fracture behaviour of pieces under longitudinal and radial tension. When tensile forces are applied in the longitudinal direction, the strip section with fewer fibres will break quicker than the section with more fibres. The distinctive failure of the areas with fewer fibres was a trimmed fracture (Figure 8.1-**a**). While the areas with more fibres create staggered patterns as the densely packed fibres rip apart (Figure 8.1-**b**). In the radial direction, the monotonic distribution of fibres played a crucial role in determining the area where fracture began. In all the samples subjected to radial tension, the onset of fracture happened at the strip section with fewer fibres (Figure 8.1-**c**).

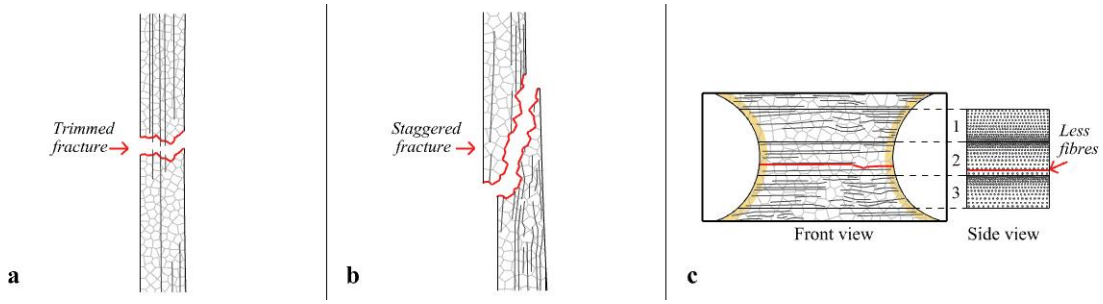

Figure 8. 1: The monotonic distribution of fibres and its influence on tensile deformation.

Nodes are the areas where bamboo fibres become irregular, discontinued, and curved. Therefore, bamboo nodes offered little to no resistance when tensile loads were applied – mainly when the loads were applied in the longitudinal direction. As shown in Figure 8.2-**a**, as the loads try to pull the fibres apart – the poorly reinforced node regions became breakpoints where fracture began. To a lesser extent, nodes also affected the fracture mode of the pieces under tangential tension. As shown in Figure 8.2-**b**, the curvilinear and discontinued distribution of fibres in nodal regions creates areas with no fibres. If any of these regions were close to the edges of the tested pieces, tangential fracture started in these regions. Nodes did not seem to influence the onset of fracture in the pieces subjected to radial tension. In this case, nodes only acted as pathways to facilitate the growth and

geometry of the fracture line (Figure 8.2-**c**). This behaviour was also observed in the pieces under tangential tension.

Finally, the arrangement of bamboo strips also played a crucial role in the development onset of fracture in the radial direction. Due to the natural characteristics of bamboo culms, the strips have an inner section with fewer fibres and an outer section with more fibres. If inner-to-inner faces were placed next to each other, the joined strips created sections with a low number of fibres (Figure 8.3-**a**). These areas became the areas less reinforced. Thus, these areas were more susceptible to trigger the onset of fracture. If outer-to-outer faces were placed next to each other, the joined strips created sections with a high number of fibres (Figure 8.3-**b**). These sections had more resistance against the pull of the tensile forces. Contrary to this, the inner-to-outer arrangement of faces created sections with a balanced number of fibres (Figure 8.3-**c**). In the case of radial tension, the areas of the laminates with inner-to-inner arrangements were the regions where fracture started.

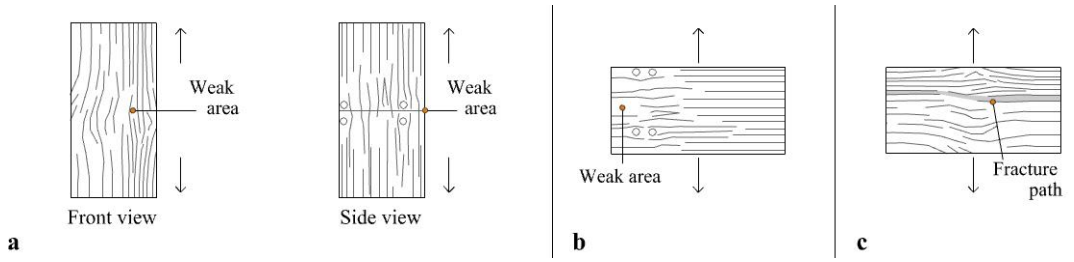

Figure 8. 2: Nodes and their influence on tensile deformation.

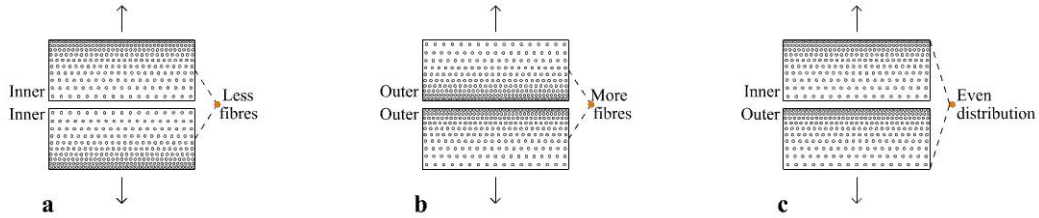

Figure 8. 3: Strip arrangement and its influence on tensile deformation.

8.1.2 Compressive deformation and failure modes

The orientation and distribution of fibres were the features that influenced the loading capabilities of the pieces under compressive loading. The specimens under longitudinal compression were the pieces with higher compressive strength. When compressive forces are applied longitudinally, the forces act in the direction of the fibres. Hence, the fibres act as vertical reinforcements, actively counteracting the crushing forces. When the load increases, the slenderness of the fibres forces them to buckle as the parenchyma cells are

horizontally displaced. Conversely, when compressive forces are applied in the radial and tangential directions, the forces act in the perpendicular direction of the fibres. When compressive forces are applied in the radial direction, the monotonic distribution of fibres will create uneven rates of deformation in a single strip. The strip section with fewer fibres will deform at a faster rate than the section with more fibres. As the fibres are pushed downward, the redistributed fibres will counterbalance the compressive push of the force. The specimens under tangential compression were the pieces that exhibited the lowest compressive strength. This can be explained due to the curved arrangement of fibres in the tangential direction. When loads are applied in the tangential direction, the strips will bend in the direction of the outer layer – where the majority of fibres are located.

The geometry of nodes, the distribution of fibres and the arrangement of strips are the features that determined the failure modes of the laminates under compressive loading. The geometry of nodes in the radial and tangential directions played a crucial role in the onset and development of fracture of the pieces subjected to longitudinal and radial compression. In the case of longitudinal compression, the curvilinear geometry of fibres – in nodal regions – exacerbated the lateral push of the parenchyma cells. Hence, neighbouring fibres bent faster than those not placed near nodes. As the bending continued, cracks developed at or near nodes (Figure 8.4-**a**). The tangential geometry of nodes also influenced the evolution of longitudinal damage – particularly at later stages. Whenever there was a tangential node, crushing happened at later stages of the loading process – precisely when the fibres underwent excessive bending (Figure 8.4-**b**). In the case of radial compression, the strips with nodes had fewer fibres. As the load increased, the strips with nodes deformed faster than the strips without nodes (Figure 8.4-**c**). The different deformation rates of the strips triggered the appearance of cracks in different locations. Contrary to this, the pieces under tangential compression were not affected by the presence of nodes.

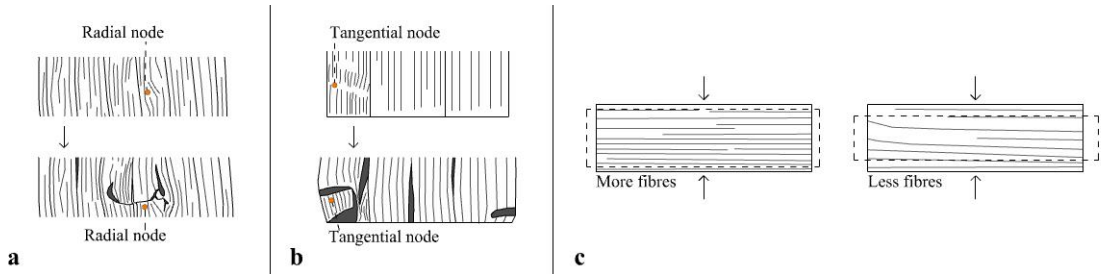

Figure 8. 4: Nodes and their influence on compressive deformation.

The distribution of fibres directly impacted the failure mechanisms of pieces under radial and tangential compression. Specimens under radial compression were particularly

affected by the monotonic distribution of fibres. The strip section with fewer fibres deformed faster than the section with more fibres. When multiple strips were joined together, the different deformation speeds of the strips determined the location and geometry of cracks. For example, if a strip was placed between two strips deforming faster, a crack appeared in the strip due to the pressure coming from the fast-deforming strips (Figure 8.5-**a**). In the tangential direction, the dense and curved nature of fibres near the outer layer of the strips determined the bending direction of the strips as the compressive loads were applied (Figure 8.5-**b**). When multiple strips were joined together, the bending directions of the strips influenced the deformation and fracture modes of the pieces (Figure 8.5-**c**).

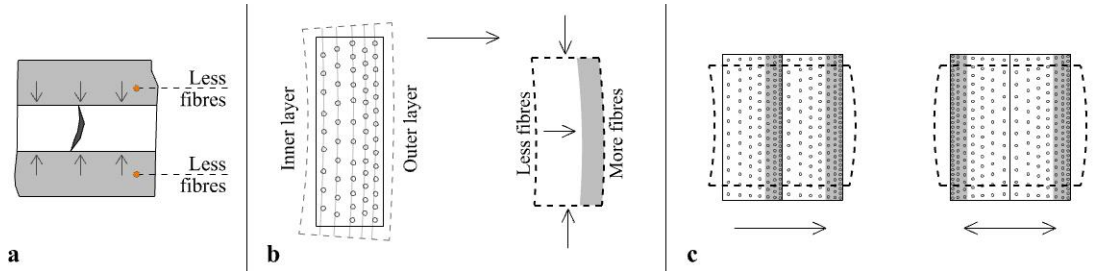

Figure 8. 5: Fibre distribution and its influence on compressive deformation.

The arrangement of bamboo strips is crucial to determine the location and geometry of cracks in the pieces subjected to radial and tangential compression. As mentioned before, the pieces under radial compression did not deform uniformly. Instead, the strips with fewer fibres deformed faster than those with more fibres. For this reason, the arrangement of strips determined the type of fracture of the pieces. Based on the analysis of the pieces under radial compression, three fracture patterns were identified: If two strips with fewer fibres were placed diagonally, a crack appeared at the point shared by both strips (Figure 8.6-**a**). If two strips were placed diagonally, but there were one or two strips between them, a crack appeared in the line connecting the strips with fewer fibres (Figure 8.6-**b**). Finally, if strips with fewer fibres surrounded a strip, a crack appeared in the middle of the strip (Figure 8.6-**c**). In the case of tangential compression, the bending direction of the strips became critical to determine the location and geometry of the cracks. In the tangential direction, the experiments also revealed three fracture patterns. If two strips were placed diagonally and each strip bend in different directions, a crack appeared at the point shared by both strips (Figure 8.6-**d**). If two strips were placed in front of each other, and each strip bend in opposite directions, a crack appeared at the edge shared by both strips (Figure 8.6-**e**). Finally, if two strips were placed diagonally and both strips bend in the same direction, a crack developed in the region formed by the edges of both strips (Figure 8.6-**f**).

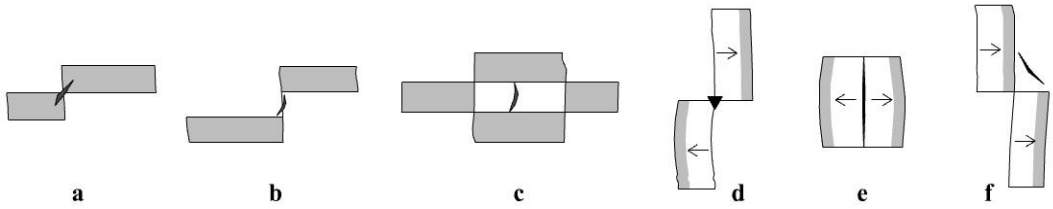

Figure 8. 6: Strip arrangement and its influence in compressive deformation.

8.1.3 Shear deformation and failure modes

The density and distribution of fibres determined the mechanical strength of pieces under shear loading. The specimens under tangential shear were the pieces with the highest shear strength. Bamboo fibres are evenly distributed in the vertical direction. As shear forces are applied, the densely packed fibres actively resist the shear forces. Contrary to this, the pieces under radial shear had fewer fibres counteracting the shear forces. The distribution of fibres in the radial direction is not even. The pieces under longitudinal shear were the specimens with the lowest shear strength. The linear arrangement of fibres can explain this. When shear forces are applied in the longitudinal direction, the areas with fewer fibres are the ones where fracture began. These areas had a low concentration of fibres and a high concentration of parenchyma cells. Hence, parenchyma bonds are the first to break when shear forces are applied. Finally, the density of fibres affected the overall performance of all the tested pieces. Those with more fibres had higher strength values and those with fewer fibres had lower strength values.

The mechanical behaviour of bamboo fibres and the location of nodes are the features that determined the fracture patterns of the pieces under shear loads. In the case of radial and tangential shear, the main properties affecting the deformation and failure of the pieces were the bending and tensile strengths of the fibres. When shear forces were applied in the radial and tangential directions, the forces acted in the fibres' perpendicular direction. Hence, the forces were actively trying to break the fibres. The fibres are the strongest components of bamboo fibres. For this reason, the pieces with more fibres put more resistance against shear forces. Contrary to this, the pieces under radial shear had a lower concentration of fibres. As the loading began, the pieces started to bend. For the sample under radial shear, the bending properties of the fibres determined the shear deformation of the specimens (Figure 8.7-**a**). In the case of tangential shear, the pieces had a high concentration of fibres. When the forces were applied, the fibres diverted the direction of the forces creating lateral elongation. Tensile forces began to pull the fibres as the lateral stretching continued. For the pieces under tangential shear, the tensile strength of the fibres became the main property determining the process of deformation (Figure 8.7-**b**).

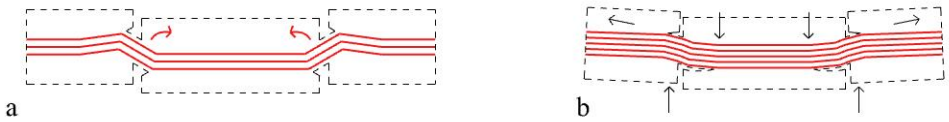

Figure 8. 7: Properties of bamboo fibres and their influence on shear deformation.

As has been mentioned before, nodes are areas of physical and mechanical discontinuity. In the case of pieces under longitudinal shear, the nodes did not influence the onset of fracture. Instead, fracture began in the regions with fewer fibres. Nodes only acted as pathways to channel the energy released by the initial crack (Figure 8.8-**a**). It is important to note that when longitudinal shear forces were applied, the pieces with nodes had more resistance against longitudinal shear forces. This can be explained by the non-linear distribution of fibres at node regions. When the shear forces were applied, the inclined or curved fibres surrounding the nodes disrupted the linear distribution of the forces. The pieces under radial and tangential shear did not have nodes. However, based on the analysis of other pieces, it is likely that nodes would act as breakpoints if shear forces were directly applied in the radial and tangential directions (Figure 8.8-**b** and **c**).

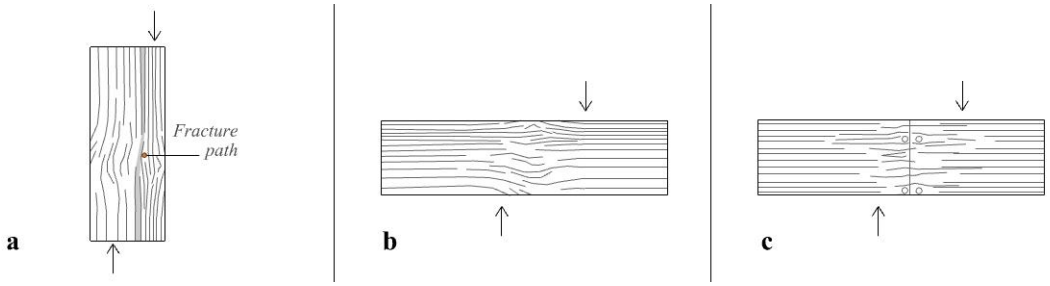

Figure 8. 8: Nodes and their influence of shear deformation.

8.1.4 Geometric modelling

Based on the analysis of how the physical features of bamboo strips affected the tensile, compressive and shear behaviour of laminated bamboo composites, a method was developed to determine the deformation and fracture of laminated bamboo. The method uses the following components to predict the deformation and fracture of the material under axial loads:

Component 1 – Deformation vectors - The deformation of the specimens was calculated with a series of equations that move an array of points from an initial position to the

deformed state of the pieces. The equations were calculated using the experiments' results.

Component 2 – Fracture geometry - A series of algorithms were developed to predict the fracture geometry of pieces under axial loads. The algorithms were created with the findings of the fracture analyses outlined in Chapters 4, 5 and 6.

To predict the deformation and fracture, the method uses a specimen picture before loading as visual input. Then, two geometric analyses and algorithms run simultaneously - in a generative geometric software called Grasshopper - to predict the specimens' deformed and or fractured states. Finally, the algorithms approximate the geometric representation of the piece after the load is applied. The method uses four steps to generate the final geometry:

Step 1 – Manual inputs – A specimen image is used as a reference to identify the areas of the specimen likely to fail. The selection criteria rely on the findings of Chapters 4, 5 and 6. In most cases, the areas with fewer fibres and the areas with nodes are the regions where the fracture is likely to start. The specimen image is edited to highlight the physical features of bamboo strips. Finally, the type of loading is determined (Figure 8.9-**a**).

Step 2 – Define deformed state – A series of geometric parameters and equations are used to calculate the transformation of the pieces from their initial state to their deformed state. The pieces are represented by a series of centroids and polygons (Figure 8.9-**b**).

Step 3 – Define fracture geometry – Using the information provided in Step 1, a series of algorithms are selected to determine the fracture geometry of the pieces. In the case of the pieces under longitudinal tension, radial tension, tangential tension and longitudinal shear, the algorithm calculates the geometry and location of a fracture polyline. For the samples subjected to longitudinal, radial, and tangential compression, the algorithms predict the location and geometry of a series of polygons representing the cracking patterns of pieces under compressive loading (Figure 8.9-**c**).

Step 4 – Visualise fracture – Finally, the fracture polylines are used as attractor point curves to morph the scale of the polygons representing the deformed state of the pieces. The polygons closer to the fracture geometries will be smaller, while the polygons further away will have a bigger size. The transformation of the polygons approximates the geometric representation of the fractured state of the pieces (Figure 8.9-**d**).

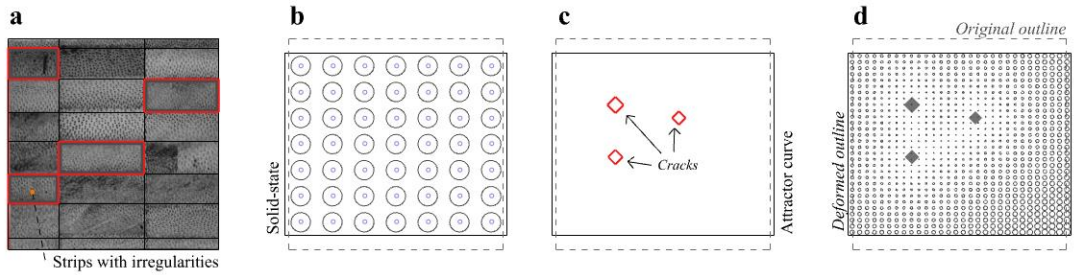

Figure 8. 9: Workflow to predict the deformation and fracture of laminated bamboo.

Overall, the method provides a novel approach to quickly assess and predict the location and geometry of failure modes in laminated bamboo composites subjected to uniaxial loads. The method successfully uses the physical features of bamboo strips as the visual input needed to predict the material's behaviour. The physical features of bamboo strips are visible on a macroscale. The findings of this study suggest that the fracture of laminated bamboo can be predicted by identifying the location of areas with fewer fibres and the geometric arrangement of fibres at node regions and the location of nodes. The method can be further optimised by automating the identification of areas prone to fail and exploring the applicability of the technique when larger specimens are submitted to uniaxial loads. Furthermore, the current method only predicts fracture in two dimensions. It is worth exploring the application of the method to predict the material's behaviour in three dimensions. Finally, the method can be adjusted to account for the cases of pieces subjected to multiaxial loading and structural assemblies.

8.2 Key findings

8.2.1 The radial and tangential directions

As stated in section 2.2.6, one gap in the literature review was the lack of studies distinguishing the mechanical performance of the radial and tangential directions. As shown in Table 8.1, the tensile and compressive strengths of the material are comparable in both directions. The difference is slight and will not significantly affect structural elements' design. The main difference was found in the shear strength of the material. The tangential direction is two times more resistant to shear loading than the radial direction. This can be explained by analysing the distribution of fibres radially and tangentially, i.e., the tangential direction has an even distribution of fibres. Shear strength is higher than this study's tensile and compressive strengths. A structural element submitted to various loading scenarios will likely fail by tension or compression before undergoing shear failure. For this reason, the different shear values - along the radial and tangential direction - are also not expected to influence the design of structures significantly.

Orientation	Tension	Compression	Shear
Radial	4.85 MPa	17.79 MPa	23.62 MPa
Tangential	5.65 MPa	16.60 MPa	41.78 MPa

Table 8. 1: The radial and tangential strength values.

The application of this study's findings can be found in the development of models and theories that accurately represent the mechanical behaviour of the material. In the first instance, the mechanical characterisation of the radial and tangential directions is essential to developing constitutive modelling theories that fully capture the orthotopic nature of the laminates. For example, Eslami, Jayasinghe, and Waldmann (2021) have developed a model to describe the orthotopic behaviour of wood. The model uses wood's strength and mechanical properties in its three directions to describe the material adequately. Future research can focus on developing similar models for laminated bamboo. Knowledge of the radial and tangential properties is critical to achieving this. Finally, the fracture patterns described in Chapters 4, 5, and 6 indicate that the different distribution of fibres - in the radial and tangential directions - plays a crucial role in determining where the fracture is likely to start. Hence, understanding the differences between the radial and tangential directions is also essential to continue developing laminated bamboo's damage and fracture theories.

8.2.2 Fibre density and fracture toughness

As stated in Chapter 2, parenchyma cells are the weakest components of bamboo cells. For this reason, the fracture of bamboo-based components happens due to the rupture of the parenchyma cells. Under this understanding, it would be expected that specimens under radial and tangential tension will have the same mechanical behaviours and failure modes. However, the findings of this research suggest that the specimens with a higher volume of fibres showed more resistance to fracture than those with fewer fibres. In other words, the specimens subjected to tangential tension had higher strength than those subjected to radial tension. The same applies to specimens subjected to shear. These findings strongly indicate that fibres are - to some extent - helping counterbalance the forces trying to rip the parenchyma bonds.

Research carried out by Habibi, and Lu (2014) suggest that the microscopic interaction of parenchyma-to-fibre bonding and the hollow nature of vessels contribute to bamboo's fracture toughness. As reported in the research, the bonding imperfections at micro and nano scales can influence the direction and speed at which cracks develop. Moreover, the hollow vessels can divert or absorb the energy caused by the initial crack. In other words, the presence of more fibres likely means that the crack is pulling apart the bondage of various structural elements and not only the parenchyma cells. Hence, in the more fibrous

specimens, the energy of the crack is breaking parenchyma-to-parenchyma bonds, parenchyma-to-fibre bonds, fibre-to-vessel bonds, and hollow vessels are popping and diverting energy in different directions. This could explain the phenomena reported in this research. However, this explanation is only speculative, and further research is needed to determine why the specimens with more fibres had a higher fracture toughness.

8.2.3 Shear testing

In this study, three out of six shear planes were tested: Planes 1, 4, and 6 (Figure 8.10). Various authors have extensively recorded the shear performance of bamboo strips and bamboo laminates along the longitudinal or parallel direction. However, the shear performance perpendicular to the fibres (in the radial and tangential directions) has not been fully characterised. This is because, as stated in section 2.2.5, the high shear resistance across the grain makes it challenging to induce pure shear forces on any given specimen. The research community has not yet identified a test suitable to record the shear properties of laminated bamboo across the radial and tangential directions. For this research, the purpose of the radial and tangential shear tests was to explore if a modified three-point short beam test could be used to induce pure shear forces in small specimens. Given the constraints of the experimental setup, the specimens could only be tested using Planes 4 and 6. The analysis of planes 3 and 5 requires the identification of another test setup, and it can be a valuable research opportunity for future investigations.

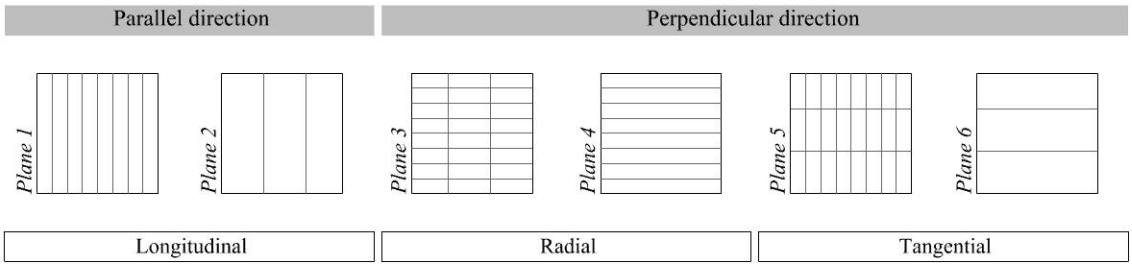

Figure 8. 10: Shear planes.

As can be seen in Figure 8.11-**a to c**, the modified three-point beam setup did not induce pure shear forces in the small specimens. Instead, the resistance of the fibres pushed the fixing plate upward. Further adjustments to the grip could help improve the results of the test. For example, the fixing plate could be secured further to avoid upward slips. Another adjustment could be to reduce the cross-section of the specimens and explore the right size and location of the indentations. The results of the experiments confirm how challenging it is to induce shear forces across the grain. Also, as stated in Chapter 6, the

results suggest that fibre density is key to determining the shear resistance of specimens when loads are applied across the grain.

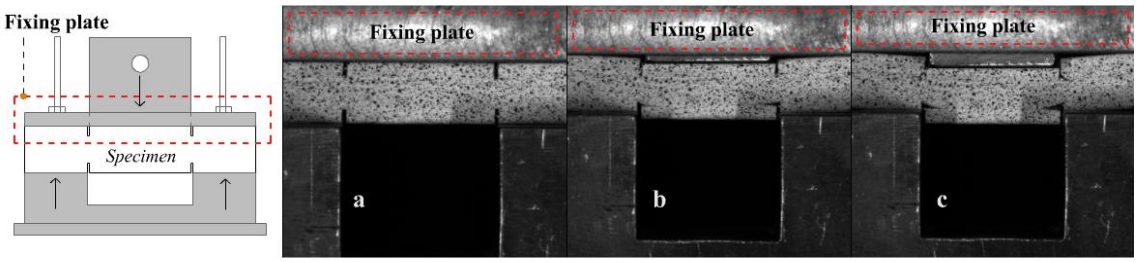

Figure 8. 11: Improvements for the perpendicular shear test.

8.2.4 Manufacturing guidelines

As outlined in section 2.1.3, manufacturing processes are expected to influence the mechanical performance of bamboo laminates. This research focused mainly on understanding how the physical characteristics of bamboo strips affect the performance of the laminates. However, the study's findings can help inform good manufacturing practices when selecting and using bamboo strips. The following manufacturing guidelines are proposed based on the key results of this research:

Fibre density matters: In all the experiments, it became evident that bamboo strips with fewer fibres were the regions where fracture began. One major step in the process of manufacturing laminates is the planning or milling of bamboo strips. Manufacturers are advised to take precautions to avoid milling off the strip area with a higher volume of fibres. A good balance of fibres and parenchyma cells is essential to minimise the number of weaker regions in the material.

Node quantity affects performance: The findings of this research suggest that, depending on the load, nodes can reduce or enhance the strength of the laminates. In tension, the nodes act as breakpoints. In longitudinal compression, the nodes reinforce the material and increase its resistance. If the loading is known before manufacturing begins, the laminates can be customised in advance to enhance resistance: more nodes in compression and fewer nodes in tension.

Location of irregularities matters: In this thesis, irregularities are those found in regions with nodes or fewer fibres. One of the key findings was that whenever an irregular area was found near the corners or boundaries of the specimens, fracture began in this area.

Minimising the number of irregularities in the exterior faces can enhance the strength of the material.

8.3 Future work

8.3.1 Research limitations

As mentioned in Chapter 3, there were some constraints while planning and conducting the methodological part of the research. Below is a list of methodological limitations that future researchers can address:

Volumetric characteristics: One of the main limitations of the research was the fact that the material was bought, and there was not a feasible way to identify the internal physical characteristics of the specimens. Instead, the methodology was carried out by analysing the specimens' outer faces. In reality, interior features are expected to play a crucial role in fracturing. Future research can address this limitation by manufacturing the specimens from scratch and recording the characteristics of the strips before laminating the pieces.

Manufacturing factors: This research focused only on understanding how bamboo strips' physical characteristics affect the laminates' mechanical behaviour. However, the experiments' results also highlight the need to analyse how manufacturing factors influence the material's performance. For example, some pieces subjected to longitudinal tension broke near nodes and then the fracture travelled along the glue line. Moreover, in reality, bamboo strips must be combined using different jointing techniques, such as finger joints, butt joints, half-lap joints, etc. Further research can be conducted to fully characterise the influence of manufacturing factors on the mechanical response of bamboo laminates.

Method validation: When this research was developed, it became difficult to have complete access to manufacturing and testing facilities. This meant that only a limited number of tests were carried out. No experiment was conducted to test the accuracy of the developed method. The next step toward developing this research is to use the technique to predict the failure modes of new experiments and compare the results.

8.3.2 Machine learning and geometric modelling

The primary input of the method is the identification of areas prone to fail using a picture of the specimen before loading. The image of the pieces acts as a map or blueprint to anticipate the onset and evolution of damage. Currently, identifying areas prone to fail is

done manually by following the parameters outlined in Chapter 7. However, this step could be fully automated using machine learning algorithms. For example, the processed images of the specimens can be used to train the computer to recognise the characteristics of bamboo fibres. Hence, the computer could determine if the load was applied in the longitudinal, radial, or tangential directions by providing an image. Then, the machine could be further trained to recognise the physical features of bamboo strips. After doing this, the machine could automatically locate the areas with fewer fibres, nodes' geometry, and the location of nodes. Finally, the computer could be trained to predict the fracture geometry of the pieces automatically.

The implementation of machine learning algorithms can enhance the applicability and easiness of assessing, predicting, and preventing the failure of structures made with laminated bamboo. In future stages, the present study can be optimised by implementing algorithms developed in Lunchbox ML, a plugin used to create machine learning algorithms in Grasshopper.

8.3.3 From 2D to 3D

The current method focuses only on the representation of deformation and fracture in two dimensions. However, the reality is that materials deform in three dimensions. The presented methodology can be further expanded to account for the three-dimensional behaviour of the material. First of all, multiple cameras can be used to record and track the deformation of the material in three dimensions. Then, similarly to the method used in this study, a series of points can be used to define the three-dimensional states of the pieces. The only difference would be that the vectors will be determined using three coordinates, the x, y and z dimensions.

The fracture of the material can also be mapped in three dimensions. The recognition of features prone to failure can be done in all the faces of the pieces. Once these areas have been recognised, three-dimensional DIC equipment can be used to track the strain maps of the pieces in three dimensions. Then the original features of all the faces are matched to the deformation strain fields recorded with the DIC equipment. Three-dimensional fracture likely follows the same patterns outlined in Chapters 4, 5 and 6. In other words, the fracture will likely begin in the specimen area with the weakest configuration. Then, the fracture will find release by following the path with less resistance. In the case of three-dimensional fractures, the path can be mapped in three dimensions. Hence, the fracture geometries will have three-dimensional shapes. Taking the current research into

three dimensions is future research that can better describe the behaviour and failure of three-dimensional structures made with laminated bamboo.

8.3.4 Multiaxial loading and structural assemblies

The current research only focuses on predicting the material's behaviour when uniaxial loads are applied. In real settings, structures can be subjected to multiaxial loading. The action of different forces on the material is likely to trigger different and more complex fracture patterns. Multiaxial testing can be done to map out the deformation and fracture patterns of the material. Such information can then be processed into geometric algorithms that can approximate the material's behaviour when multiaxial loads are applied.

Finally, the developed method can also be implemented to predict the deformation and fracture of structural assemblies. For example, experimental programs can be defined to map out the behaviour of bolted connections. Expanding the reach of the current research could help develop a series of rapid assessment tools able to predict the behaviour of laminated bamboo under a myriad of loading and structural conditions.

8.4 Final reflection

The research question of this project aimed to determine if the physical features of bamboo could be used as parameters to predict the deformation and failure modes of the material. As it was stated in Chapter 1, answering this question can help promote the use of laminated bamboo as a reliable structural material by preventing the unexpected failure of the structural members. The results of the present study strongly suggest that fibre distribution, fibre density, node regions and nodes' geometric arrangements are features that can be successfully used as visual inputs to predict the deformation and fracture of laminated bamboo composites under uniaxial loading.

The study focused on identifying how the physical features of bamboo strips influenced the deformation and failure of laminated bamboo and how to use this information to develop a workflow to predict the mechanical behaviour of the material. The proposed method used the findings of the experimental program to calculate a series of equations to predict the deformation of pieces under axial loads. Then, a series of algorithms were developed to predict the fracture patterns of the material. Based on the experiments, the fracture modes of laminated bamboo can be geometrically represented by a single

polyline or by a series of polygons. In the first instance, the method used the pictures of the specimens before loading as the visual inputs to identify the areas of the pieces prone to fail. The process of identification was informed by the fracture analysis of the pieces. The findings of the fracture analysis suggest that the areas of the strips with fewer fibres and the irregular arrangement of fibres – in nodal regions – are areas where the fracture is likely to start. After the onset of fracture, a series of patterns were identified to map out the development of cracks. The distribution of fibres and the geometry of nodes were the factors that determined the evolution of damage. Based on these findings, a series of geometric representations were used to identify areas with fewer nodes, the distribution of fibres and the location of nodes. Then, a set of algorithms used these parameters as the inputs to determine the deformation and fracture of laminated bamboo under tensile, compressive and shear loads.

As mentioned in section 2.3.5, geometric techniques have not been previously used to determine and predict the mechanical behaviour of bamboo laminates. The novelty of the method - proposed in this thesis - lies in demonstrating that geometric techniques and geometric-based software can be successfully used to analyse and predict the deformed and fractured states of laminated bamboo composites. The study's preliminary results suggest that the method is successful at geometrically representing the shape of bamboo when uniaxial loads are applied. However, the method cannot be considered an efficient procedure to determine the material's mechanical properties or to map out the evolution of damage at multiple scales. Instead, the method is a rapid assessment tool that proves that the physical features of bamboo strips can be successfully used as an input to quickly assess and determine the potential failure modes of the material. The present study provides information on how the physical features of bamboo affect the material’s mechanical response in its three directions: longitudinal, radial, and tangential. Additionally, the study 's results hint that geometric methods can be successfully used to represent the complex features of laminated bamboo. Once the features are geometrically simplified, a set of mathematical transformations can define the transformation of the geometries as the loads are applied. Furthermore, it is possible to conclude that the proposed technique can also be used to explore and predict the mechanical behaviour of other materials with visible macroscopic features, e.g., timber.

One of the main contributions of the present study was identifying how the features of laminated bamboo affect the mechanical behaviour of the material. The research findings suggest that regions with fewer fibres are critical to identifying the areas where fractures are likely to start. Moreover, the geometric arrangement of fibres is expected to determine the final fracture geometry. The physical features that influenced the fracture modes of the material are visible on a macroscopic level. If these features are recorded and

subsequently processed, a single image of the material – before loading – can be the visual input needed to predict the material's behaviour. Realising that the fracture modes of laminated bamboo are already coded in the inherent arrangement of fibres is perhaps the main contribution of the research. The development of methods that acknowledge this observation can produce several strategies to assess laminated bamboo structures' structural integrity quickly. Often, natural materials are avoided since their natural variability makes it challenging to predict their behaviour as structural materials. However, methodologies – such as the one proposed here – can help to efficiently characterise the structural capabilities of the material before accidents happen. Finally, the research suggested a novel strategy to regulate and promote the use of natural and sustainable materials. As mentioned in Chapter 1, embracing the use of sustainable materials is vital to counterbalance the impact that the building industries have on the environment. Exploring innovative and creative ways of pushing the structural limits of low-impact materials is an effort that can help secure a sustainable and resilient future for future generations.

References

[1] Akinbade, Y. et al. (2020) 'Modelling full-culm bamboo as a naturally varying functionally graded material', Wood science and technology, 55(1), pp. 155–179. doi:10.1007/s00226-020-01246-6.

[2] Amada, S. et al. (1997) 'Fibre texture and mechanical graded structure of bamboo', Composites. Part B, Engineering, 28(1), pp. 13–20. doi:10.1016/S1359-8368(96)00020-0.

[3] Ambient Bamboo Floors (2021). Prefinished Engineered Strand Woven Bamboo Flooring. Available at: https://www.ambientbp.com/pdf/MSDS_EngineeredBamboo.pdf (Accessed: 08 June 2022).

[4] Ansell, M. ed., 2015. Wood composites. Amsterdam, [Netherlands]: Woodhead Publishing.

[5] ANSI (1995) GB/T 15780-1995: Testing methods for physical and mechanical properties of bamboo. China: GB.

[6] Archila, H.F., Ansell, M.P. and Walker, P., (2015). Measurement of the in-plane shear moduli of bamboo-Guadua using the Iosipescu shear test method. In 10th World Bamboo Congress.

[7] Archila, H.F., et al., (2014). Evaluation of the mechanical properties of cross laminated bamboo panels by digital image correlation and finite element modelling. In World Conference on Timber Engineering (WCTE). Pp. 10-14.

[8] Astakhov, V.P., (2010). Surface integrity–definition and importance in functional performance. In Surface integrity in machining, pp. 1-35, London: Springer.

[9] ASTM (2014) D143-14: Standard Test Methods for Small Clear Specimens of Timber. West Conshohocken, PA: ASTM International.

[10] ASTM (2014) D3500-20: Standard test methods for wood structural panels in tension. West Conshohocken, PA: ASTM International.

[11] Bilko, P. et al. (2021) 'Determination of the shear modulus of pine wood with the Arcan test and digital image correlation', Materials, 14(2), pp. 1–18. Doi:10.3390/ma14020468.

[12] Bodig, J. and Jayne, Benjamin A (1993) Mechanics of wood and wood composites. Reprint edition. Malabar, Fla.: Krieger Publishing.

[13] British Standards Institution (1957) BS 373:1957: Methods of testing small clear specimens of timber. London: British Standards Publications.

[14] British Standards Institution (2010) BS EN 408:2010: Timber structures. Structural timber and glued laminated timber. Determination of some mechanical properties. London: British Standards Publications.

[15] British Standards Institution (2004) BS-EN 384-2004: Determination of characteristic values of mechanical properties and density. London: British Standards Publications.

[16] Broto, E. (2015) Architecture and design: bamboo construction and design: guide and 59 case study. Barcelona: Links International.

[17] Bystriakova, N., Kapos, V. and Lysenko, I. (2004). Bamboo biodiversity: Africa, Madagascar, and the Americas. UNEP-WCMC/INBAR No. 19. Cambridge: Swaingrove Imaging.

[18] Chand, N., Shukla, M. and Sharma, M.K. (2008) 'Analysis of Mechanical Behaviour of Bamboo (Dendrocalamus strictus) by Using FEM', Journal of natural fibers, 5(2), pp. 127–137. Doi:10.1080/15440470801928970.

[19] Chen, G. et al. (2019) 'Mechanical behavior of laminated bamboo lumber for structural application: an experimental investigation', European Journal of Wood and Wood Products, 78(1), pp. 53–63. Doi:10.1007/s00107-019-01486-9.

[20] Chen, H. et al. (2015) 'Tensile properties of bamboo in different sizes', Journal of wood science, 61(6), pp. 552–561. Doi:10.1007/s10086-015-1511-x.

[21] Coolidge, J.L., (2003). A history of geometrical methods. Courier Corporation.

[22] Correal, J. and Ramirez, F. (2010). Adhesive bond performance in glue line shear and bending for glued laminated Guadua bamboo, Journal of tropical forest science, 22(4), pp. 433–439.

[23] Cui, J. et al. (2020) 'Multiscale structural insights of load bearing bamboo: A computational modeling approach', Journal of the mechanical behavior of biomedical materials, 107, pp. 103743–103743. Doi: 10.1016/j.jmbbm.2020.103743.

[24] Dauletbek, A. et al. (2022) 'A review of basic mechanical behaviour of laminated bamboo lumber', Journal of renewable materials, 10(2), pp. 273–300. Doi:10.32604/jrm.2022.017805.

[25] Davis, J.R. (2004) Tensile testing [electronic resource]. 2nd ed. Materials Park, Ohio: ASM International.

[26] Deniz, I. et al. (2017) 'Kraft and modified kraft pulping of bamboo (Phyllostachys bambusoides)', Drewno, 60(200), pp. 79–94. Doi:10.12841/wood.1644-3985.224.05.

[27] Dixon, P.G. and Gibson, L.J. (2014) 'The structure and mechanics of Moso bamboo material', Journal of the Royal Society interface, 11(99), p. 20140321. Doi:10.1098/rsif.2014.0321.

[28] Eberhart, M., (2007). Why things break: understanding the world by the way it comes apart. Crown.

[29] Eslami, H., Jayasinghe, L.B. and Waldmann, D. (2021) 'Nonlinear three-dimensional anisotropic material model for failure analysis of timber', Engineering failure analysis, 130, p. 105764. doi: 10.1016/j.engfailanal.2021.105764.

[30] Estrada, M., Linero, D. and Takeuchi, C. (2019) 'Numerical model of cracking pattern in laminated bamboo specimens under tensile and shear loads', Frattura ed integritá strutturale, 13(48), pp. 348–356. Doi:10.3221/IGF-ESIS.48.33.

[31] Fang, H. et al. (2015) 'Mechanical performance of innovative GFRP-bamboo-wood sandwich beams: Experimental and modelling investigation', Composites. Part B, Engineering, 79, pp. 182–196. Doi: 10.1016/j.compositesb.2015.04.035.

[32] Gallier, J., (2011). Geometric methods and applications: for computer science and engineering (Vol. 38). Springer Science & Business Media.

[33] García, J.J., Rangel, C. and Ghavami, K. (2012) 'Experiments with rings to determine the anisotropic elastic constants of bamboo', Construction & building materials, 31(1), pp. 52–57. Doi: 10.1016/j.conbuildmat.2011.12.089.

[34] Gatóo, A. et al. (2014) 'Sustainable structures: Bamboo standards and building codes', Proceedings of the Institution of Civil Engineers. Engineering sustainability, 167(5), pp. 189–196. Doi:10.1680/ensu.14.00009.

[35] Ghavami, K., Rodrigues, C.D.S. and Paciornik, S., (2003). Bamboo: functionally graded composite material.

[36] Gibson, D.J., (2009). Grasses and grassland ecology. Oxford: Oxford University Press.

[37] Godina, M. and Lorenzo, R., (2015). Calibrating a composite material model for analysis and design of bamboo structures. World Bamboo Organization.

[38] Górszczyk, Malicki, K., & Zych, T. (2019). Application of digital image correlation (DIC) method for road material testing. Materials, 12(15), 2349. doi: 10.3390/ma12152349.

[39] Gritsch, C.S., Kleist, G. and Murphy, R.J. (2004) 'Developmental Changes in Cell Wall Structure of Phloem Fibres of the Bamboo Dendrocalamus asper', Annals of botany, 94(4), pp. 497–505. Doi:10.1093/aob/mch169.

[40] Gritsch, C.S. and Murphy, R.J. (2005) 'Ultrastructure of Fibre and Parenchyma Cell Walls During Early Stages of Culm Development in Dendrocalamus asper', Annals of botany, 95(4), pp. 619–629. Doi:10.1093/aob/mci068.

[41] Gupta, V. (2013) An introduction to mechanics of materials. Oxford, U.K: Alpha Science International.

[42] Habibi, M.K. and Lu, Y. (2014) 'Crack propagation in bamboo's hierarchical cellular structure', Scientific reports, 4(1), pp. 5598–5598. Doi:10.1038/srep05598.

[43] Haladu, A., Muhamed, F. and Moveh, S. (2016). Properties and Classification of Bamboo for Construction of Buildings. Journal of Applied Sciences & Environmental Sustainability 2(4), pp. 105-114.

[44] Harries, K.A., Sharma, B. and Richard, M., (2012). Structural use of full culm bamboo: the path to standardization. International Journal of Architecture, Engineering and Construction, 1(2), pp.66-75.

[45] Hrabovsky, G. and Susskind, L., (2020). Classical mechanics: the theoretical minimum. UK: Penguin.

[46] Huda, Z., Bulpett, Robert and Lee, K. Y. (2010) Design against fracture and failure. Stafa-Zuerich ; Enfield, New Hampshire: Trans Tech Publications Limited.

[47] ISO (2019) ISO 22157:2019: Bamboo structures – Determination of physical and mechanical properties of bamboo culms. Geneva, Switzerland: International Standards Organization.

[48] Janssen, J.J., (2005). International standards for bamboo as a structural material. Structural Engineering International, 15(1), pp.48-48.

[49] Jayanetti, D.L. and Follett, P.R., (2008). Bamboo in construction. Modern Bamboo Structures, pp. 35-44.

[50] Jones, E.M. and Iadicola, M.A., (2018). Good practices guide for digital image correlation. International Digital Image Correlation Society, 10.

[51] Kapko, V. et al. (2010) 'Flexibility of ideal zeolite frameworks', Physical chemistry chemical physics: PCCP, 12(3), pp. 8531–8541. Doi:10.1039/c003977b.

[52] Kariuki, J.K., (2018). Performance of Glue Laminated Bamboo Beams and Trusses. Doctoral dissertation: JKUAT-PAUSTI.

[53] Khoshbakht, N. et al. (2018) 'Computational Modeling of Laminated Veneer Bamboo Dowel Connections', Journal of materials in civil engineering, 30(2), p. 4017285. Doi:10.1061/(ASCE)MT.1943-5533.0002135.

[54] Klette, R. (2004) Digital geometry: geometric methods for digital picture analysis. San Francisco, Calif.: Morgan Kaufmann.

[55] LeMaître, J. (2001) Handbook of materials behavior models. Volume 1, Deformations of materials [electronic resource]. San Diego, CA: Academic.

[56] LePage, W. (2020). A practical guide to DIC. Available at: https://digitalimagecorrelation.org/ (Accessed: 13 July 2020).

[57] Li, H. et al. (2013) 'Compressive performance of laminated bamboo', Composites. Part B, Engineering, 54(1), pp. 319–328. Doi: 10.1016/j.compositesb.2013.05.035.

[58] Liese, W., (1985) Anatomy and properties of bamboo. In Proceedings of the International Bamboo Workshop, pp. 196-208.

[59] Liese, W. and Köhl, M. (2015). Bamboo. Vancouver: Springer International Publishing.

[60] Liu, X. et al. (2016) 'Nomenclature for engineered bamboo', Bioresources, 11(1), pp. 1141–1161. Doi:10.15376/biores.11.1.1141-1161.

[61] Lybeer, B. et al. (2006) 'Lignification and Cell Wall Thickening in Nodes of Phyllostachys viridiglaucescens and Phyllostachys nigra', Annals of botany, 97(4), pp. 529–539. Doi:10.1093/aob/mcl016.

[62] Mahdavi, M., Clouston, P.L. and Arwade, S.R., (2011). Development of laminated bamboo lumber: review of processing, performance, and economical considerations. Journal of Materials in Civil Engineering, 23(7), pp.1036-1042.

[63] Mannan, S., Knox, J.P. and Basu, S. (2017) 'Correlations between axial stiffness and microstructure of a species of bamboo', Royal Society open science, 4(1), pp. 160412–160412. Doi:10.1098/rsos.160412.

[64] Moso International BV (2017). MOSO ® Bamboo N-finity. Available at: https://www.moso-bamboo.com/wp-content/uploads/MOSO_Bamboo_N-finity-indoor_2019_EN_LR.pdf (Accessed: 08 June 2022).

[65] Moso ® International (2018). Moso ® product catalogue. Netherlands: Moso International.

[66] Moussady, H., Lévesque, M. and Therriault, D., (2012). Comparing finite element and analytical micromechanical modeling of randomly oriented single walled carbon nanotubes reinforced nanocomposites. Nanocomposites, American Society for composites series on advances in composite materials, Lancaster: DEStech publication, pp.153-161.

[67] Needham, T., (2021). Visual Differential Geometry and Forms: A Mathematical Drama in Five Acts. Princeton University Press.

[68] Ngudiyono et al. (2019) 'Review of creep modelling for predicting of long-term behavior of glued-laminated bamboo structures', MATEC web of conferences, 258, p. 1023. Doi:10.1051/matecconf/201925801023.

[69] Ni, L. et al. (2016) 'Manufacture and mechanical properties of glued bamboo laminates', Bioresources, 11(2), pp. 4459–4471. Doi:10.15376/biores.11.2.4459-4471.

[70] NMBA (2006). Preservation of Bamboo. TM-05. New Delhi: RSPRINTART.

[71] Nugroho, N. and Ando, N. (2001) 'Development of structural composite products made from bamboo II: fundamental properties of laminated bamboo lumber', Journal of wood science, 47(3), pp. 237–242. Doi:10.1007/BF01171228.

[72] Ogunsanwo, O.Y., Adenaiya, A.O. and Adedeji, C.A. (2019) 'Effect of adhesive quantity on selected physico-mechanical properties of bamboo glulam', Maderas, 21(1), pp. 113–122. Doi:10.4067/S0718-221X2019005000111.

[73] Osorio, L. et al. (2018) 'In-depth study of the microstructure of bamboo fibres and their relation to the mechanical properties', Journal of reinforced plastics and composites, 37(17), pp. 1099–1113. Doi:10.1177/0731684418783055.

[74] Peters, J.F., 2020. Computational geometry, topology, and physics of digital images with applications. Springer International Publishing.

[75] Ramful, R. and Sakuma, A. (2020) 'Investigation of the effect of inhomogeneous material on the fracture mechanisms of bamboo by finite element method', Materials, 13(21), pp. 1–15. Doi:10.3390/ma13215039.

[76] Ramirez, F. et al. (2012) 'Dowel-Bearing Strength Behavior of Glued Laminated Guadua Bamboo', Journal of materials in civil engineering, 24(11), pp. 1378–1387. Doi:10.1061/(ASCE)MT.1943-5533.0000515.

[77] Ramful, R. and Sakuma, A. (2020) 'Investigation of the effect of inhomogeneous material on the fracture mechanisms of bamboo by finite element method', Materials, 13(21), pp. 1–15. Doi:10.3390/ma13215039.

[78] Reynolds, T. et al. (2016) 'Dowelled structural connections in laminated bamboo and timber', Composites. Part B, Engineering, 90, pp. 232–240. Doi: 10.1016/j.compositesb.2015.11.045.

[79] Rudnev, S., Semukhin, B. and Klishin, A., (2011). Geometrical modeling of crystal structures with use of space of elliptic Riemannian geometry. Materials sciences and applications, 2(06), p.526.

[80] Rutten, D. (2011) VB Iterative Proximity (Version 1.0) [Source code]. https://www.grasshopper3d.com/forum/topics/connect-closest-points-with-lines?commentId=2985220%3AComment%3A498028.

[81] Schröder, S. (2020). The 20 Best Bamboo Species. Available at: https://www.guaduabamboo.com/blog/top-20-best-bamboo-species (Accessed: 27 June 2020).

[82] Schuler, T. A., (2016). Grandview Heights Aquatic Centre's Timber Cables [online]. Architecture Magazine. [Viewed 14 July 2018]. Available from: https://www.architectmagazine.com/technology/detail/grandview-heights-aquaticcentres-timber-cables_o

[83] Semenova, S. et al. (2021) 'Analysis of the structure formation processes of building composites by geometric methods', IOP conference series. Materials Science and Engineering, 1162(1), p. 12014. doi:10.1088/1757-899X/1162/1/012014.

[84] Semple, K.E., Zhang, P.K. and Smith, G.D. (2015). Stranding Moso and Guadua Bamboo. Part I: strand production and size classification. BioResources, 10(3), pp.4048-4064.

[85] Setaluri, R. (2015). Fast grid-based nonlinear elasticity for 2D deformations. In Proceedings of the ACM SIGGRAPH/Euro graphics Symposium on Computer Animation (pp. 67-76).

[86] Shah, D.U., Sharma, B. and Ramage, M.H. (2018) 'Processing bamboo for structural composites: Influence of preservative treatments on surface and interface properties', International journal of adhesion and adhesives, 85, pp. 15–22. Doi: 10.1016/j.ijadhadh.2018.05.009.

[87] Shao, Z. et al. (2010) Differences in structure and strength between internode and node sections of Moso bamboo, Journal of tropical forest science, 22(2), pp. 133–138.

[88] Shao, Z. and Wang, F., (2018). Mechanical characteristics of bamboo structure and its components. In The Fracture Mechanics of Plant Materials (pp. 125-146). Singapore: Springer.

[89] Sharma, B., Gatóo, A., Bock, M., Mulligan, H. and Ramage, M., (2014). Engineered bamboo: state of the art. Proceedings of the Institution of Civil Engineers-Construction Materials, 168(2), pp.57-67.

[90] Sharma, B. et al. (2015a) 'Engineered bamboo for structural applications', Construction & building materials, 81, pp. 66–73.
Doi: 10.1016/j.conbuildmat.2015.01.077.

[91] Sharma, B., Gatóo, A. and Ramage, M.H. (2015b) 'Effect of processing methods on the mechanical properties of engineered bamboo', Construction & building materials, 83, pp. 95–101.
Doi: 10.1016/j.conbuildmat.2015.02.048.

[92] Sharma, B. et al. (2017) 'Mechanical characterisation of structural laminated bamboo', Proceedings of the Institution of Civil Engineers. Structures and buildings, 170(4), pp. 250–264. Doi:10.1680/jstbu.16.00061.

[93] Sinha, A., Way, D. and Mlasko, S. (2014) 'Structural Performance of Glued Laminated Bamboo Beams', Journal of structural engineering (New York, N.Y.), 140(1), p. 4013021. Doi:10.1061/(ASCE)ST.1943-541X.0000807.

[94] Silva, E.C.N., Walters, M.C. and Paulino, G.H. (2006) 'Modeling bamboo as a functionally graded material: lessons for the analysis of affordable materials', Journal of materials science, 41(21), pp. 6991–7004. Doi:10.1007/s10853-006-0232-3.

[95] Smith, A.M. (2010) Plant biology. New York: London: Garland Science; Taylor & Francis [distributor].

[96] Smith & Fong Company (2011). Plyboo Soybond Bamboo Plywood. Available at: https://static.thermoscientific.com/images/D21098~.pdf (Accessed: 08 June 2022).

[97] Staab, G.H. and Pearson, V. (2015) Laminar composites. Second edition. Amsterdam, [Netherlands]: Butterworth-Heinemann.

[98] Sun, X., He, M. and Li, Z. (2020) 'Novel engineered wood and bamboo composites for structural applications: State-of-art of manufacturing technology and mechanical performance evaluation', Construction & building materials, 249, p. 118751. Doi: 10.1016/j.conbuildmat.2020.118751.

[99] Takeuchi, C.P., Linero, D.L. and Estrada, M. (2015) 'The Elastic Modulus and Poisson's Ratio of Laminated Bamboo Guadua angustifolia', Key engineering materials, 668, pp. 126–133. Doi: 10.4028/www.scientific.net/KEM.668.126.

[100] Takeuchi, C.P., Estrada, M. and Linero, D.L. (2018) 'Experimental and numerical modeling of shear behavior of laminated Guadua bamboo for different fiber directions', Construction & building materials, 177, pp. 23–32. Doi: 10.1016/j.conbuildmat.2018.05.040.

[101] Thomsen, O. and Kratmann, K. (2010) 'Experimental characterisation of parameters controlling the compressive failure of pultruded unidirectional carbon fibre composites', Applied Mechanics and Materials, 24-25, pp. 15–22. Doi: 10.4028/www.scientific.net/AMM.24-25.15.

[102] Tinkler-Davies, B., and Shah, D.U. (2021) 'Digital image correlation analysis of laminated bamboo under transverse compression', Materials letters, 283, p. 1-4. Doi: 10.1016/j.matlet.2020.128883.

[103] Trujillo, D.J. and López, L.F., 2020. Bamboo material characterisation. In Nonconventional and vernacular construction materials (pp. 491-520). Woodhead Publishing.

[104] Vasiliev, V.V. and Morozov, E. V. (2013) Advanced mechanics of composite materials and structural elements [electronic resource]. Third edition. Amsterdam: Elsevier.

[105] Wang, T.H., et al., (2021). Glue-laminated bamboo for dowel-type moment-resisting connections. Composite Structures, 267, p.113848.

[106] Xiao, Y., Shan, B., Yang, R.Z., Li, Z. and Chen, J., (2014) Glue laminated bamboo (GluBam) for structural applications. In Materials and Joints in Timber Structures (pp. 589-601). Springer, Dordrecht.

[107] Xiao, Y., Yang, R.Z. and Shan, B., (2013). Production, environmental impact, and mechanical properties of Glubam. Construction and Building Materials, 44, pp.765- 773.

[108] Yang, D. et al. (2020) 'Mechanical properties of laminated bamboo under off-axis compression', Composites. Part A, Applied science and manufacturing, 138, p. 106042. doi: 10.1016/j.compositesa.2020.106042.

[109] Youssefian, S. and Rahbar, N. (2015) 'Molecular origin of strength and stiffness in bamboo fibrils', Scientific reports, 5(1), pp. 11116–11116. doi:10.1038/srep11116.

[110] Zea Escamilla, E. and Habert, G. (2014) 'Environmental impacts of bamboo-based construction materials representing global production diversity', Journal of cleaner production, 69, pp. 117–127. doi: 10.1016/j.jclepro.2014.01.067.

[111] Zea Escamilla, E., Archilla, H., Nuramo, D.A. and Trujillo, D., (2019). Bamboo: An engineered alternative for buildings in the global South. In Bioclimatic architecture in warm climates (pp. 397-414). Cham: Springer International Publishing.

[112] Zhang et al. (2011). Bamboo scrimber and manufacturing method thereof. United States Patent no. US20110027529A1. Available at: https://patents.google.com/patent/US20110027529A1/en (Accessed: 08 June 2022).

[113] Zhang, L. and Yang, N. (2017) 'Evaluation of a modified Iosipescu shear test method for determining the shear properties of clear wood', Wood science and technology, 51(2), pp. 323–343. doi:10.1007/s00226-016-0888-z.